

UNIVERSITY OF SOUTHAMPTON

Faculty of Engineering, Science, and Mathematics

School of Ocean and Earth Science

Resolving phylogenetic relationships within the order
Enoplida (Phylum Nematoda)

by

Holly Marie Bik

Thesis of the degree of Doctor of Philosophy

January 2010

**Graduate School of the
National Oceanography Centre, Southampton**

This PhD Dissertation by

Holly Marie Bik

has been produced under the supervision of the following persons

Supervisors

Prof John Lambshead

Dr Lawrence Hawkins

Dr Alan Hughes

Dr David Lunt

Research Advisor

Prof W. Kelley Thomas

Chair of Advisory Panel

Dr Martin Sheader

ABSTRACT

FACULTY OF ENGINEERING, SCIENCE & MATHEMATICS

SCHOOL OF OCEAN & EARTH SCIENCE

Doctor of Philosophy

RESOLVING PHYLOGENETIC RELATIONSHIPS WITHIN THE ORDER ENOPLIDA
(PHYLUM NEMATODA)

by Holly Marie Bik

The Order Enoplida (Phylum Nematoda) has been proposed as a divergent nematode lineage—Enoplid nematodes are thought to exhibit morphological and developmental characteristics present in the ‘ancestral nematode’. However, previous molecular phylogenies have failed to unequivocally confirm the position of this group. The Enoplida is primarily comprised of free-living marine species; if these taxa represent close relatives of the nematode ancestor, this relationship would presumably imply a marine origin for the phylum. Prior to this investigation, few publically available gene sequences existed for Enoplid nematodes, and published sequences represented only shallow water fauna from Northwest Europe. This study has aimed to improve resolution at the base of the nematode tree, using drastically increased taxon-sampling within the previously neglected Enoplid clade. Morphological identifications, nuclear gene sequences (18S and 28S rRNA), and mitochondrial gene sequences (Cox1) were obtained from marine specimens representing a variety of deep-sea and intertidal habitats. Molecular data were used to assess the phylogenetic placement of the Enoplid clade, resolve internal taxonomic relationships within this group, and investigate relationships between shallow water and deep-sea fauna.

Despite rigorous empirical testing and comprehensive taxon sampling, large-scale phylogenetic analyses based on 18S rRNA sequences (using both Maximum Likelihood and Bayesian Inference methods) failed to provide added resolution at the base of the nematode tree. Molecular data from the 18S rRNA gene was unable to confirm the placement of Enoplida as a divergent lineage representing the sister taxon to all other nematodes. These findings highlight the limitations of the 18S gene for resolving the deepest evolutionary splits amongst nematode clades. Analysis of internal relationships reveals that the Enoplida is split into two main clades, with groups consisting of terrestrial and primarily marine fauna, respectively. For marine taxa, deep-sea and shallow-water specimens from the same genus consistently appear as sister taxa. Deep-sea nematode species may have arisen via several evolutionary routes; some deep-sea clades appear to represent recently derived forms, while other groups seem to have radiated much earlier. Nematodes from deep-sea sites exhibit no obvious clustering according to depth or geographic location, and specimens represent a wide taxonomic range within the Enoplida. In addition, there seems to be some molecular evidence for purportedly cosmopolitan nematode species; identical gene sequences were recorded between distant shallow water locations, as well as between deep-sea and shallow water habitats. Data from Enoplid nematodes suggests an intriguing pattern for nematode species distributions—validating these preliminary insights will require a large amount of molecular data from many additional geographic locations. Future studies will also need to incorporate data from additional genetic loci (or use phylogenomic methods) in order to build robust deep phylogenies.

Table of Contents

ABSTRACT.....	3
Table of Contents	4
List of Tables.....	6
List of Figures	8
List of Accompanying Material.....	12
DECLARATION OF AUTHORSHIP	13
Acknowledgements	14
1. Introduction.....	15
1.1 An understudied phylum.....	15
1.2 Limitations of nematode morphology and taxonomy.....	16
1.3 Molecular investigations in nematodes.....	17
1.3.1 The 18S ribosomal RNA gene.....	19
1.3.2 The 28S ribosomal subunit gene.....	21
1.3.3 The Internal Transcribed Spacer Region	22
1.3.4 Cytochrome <i>c</i> oxidase subunit I.....	22
1.3.5 Other genetic methods	23
1.4 Practical applications of molecular data.....	25
1.4.1 DNA Barcoding	25
1.4.2 Future prospects	27
1.5 Molecular evolution.....	28
1.6 Reconstructing evolution using phylogenetic methods	31
1.6.1 Alignment Construction	31
1.6.2 Phylogenetic reconstruction.....	34
1.6.3 Building molecular phylogenies.....	36
1.6.3.1 Algorithmic methods.....	37
1.6.3.2 Criterion-based methods.....	39
1.6.3.2.1 Parsimony.....	39
1.6.3.2.2 Maximum Likelihood	40
1.6.3.2.3 Bayesian Inference	41
1.6.4 Models for estimating molecular evolution	42
1.6.5 Gauging support for tree topologies.....	45
1.6.6 Choosing a phylogenetic method	48
1.7 Recent molecular phylogenies of the Phylum Nematoda	49
1.8 Unresolved questions in nematode phylogenetics	50
1.8.1 Resolving early splits amongst nematodes	50
1.8.2 Internal relationships within the order Enoplida.....	53
1.8.3 The origin of deep-sea fauna.....	64
1.9 Conclusions.....	65
1.10 Aims and Objectives.....	66
2. Materials and Methods.....	67
2.1 Sampling Regime	67
2.1.2 Collection of shallow water samples.....	67
2.1.3 Collection of deep-sea samples	68
2.1.4 Sample processing.....	68
2.2 Time Series experiments	72
2.3 Taxonomic identification and video capture of Enoplid specimens.....	73
2.4 Final protocol for DNA extraction, PCR, and sequencing	73
2.5 Attempts to amplify other informative loci	76

2.5.1 Orthologous nuclear genes.....	76
2.5.2 Long-distance PCR to amplify partial mitochondrial genomes	78
2.6 Analysis.....	82
2.6.1 Sequence alignment.....	82
2.6.2 Phylogenetic Analysis	83
3. Slide Mounting and Preservation Time Series Experiments	86
3.1 Introduction.....	86
3.2 Materials and methods	88
3.3 Results.....	90
3.4 Discussion.....	98
4. Resolving phylogenetic relationships within the basal clade Enoplida	102
4.1 Analysis of SSU data.....	102
4.2 Consistency of SSU phylogenies with previous frameworks.....	114
4.3 Phylogenetic structuring in the Enoplia according to habitat.....	122
4.4 Lower taxonomic relationships within the Enoplia	125
4.4.1 Inferences from LSU data	125
4.4.2 Inferences from cytochrome <i>c</i> oxidase subnit 1.....	138
4.5 Conclusions.....	142
5. Resolving the Basal Clade of the Phylum Nematoda.....	143
5.1 Increased taxon sampling and large-scale phylogenies.....	143
5.2 Consistency of ML topologies with previous classifications	144
5.3 Unresolved Bayesian topologies.....	146
5.4 Assessing support for tree topologies	155
5.5 Resolving earliest split in the nematode tree	158
5.5 Discussion	159
5.5.1 Problems faced in resolving the base of the nematode tree	159
5.5.2 Elucidating the habitat of the ancestral nematode	161
5.6 Conclusions.....	163
6. Geographic inferences from Enoplid Nematodes	164
6.1 Evolution of deep-sea genera.....	164
6.2 Recovery of identical gene sequences.....	173
6.3 Species distributions in the deep sea	184
6.4 Conclusions.....	191
7. Summary and Future Prospects	192
7.1 Summary of Conclusions	192
7.2 Our current understanding of evolutionary relationships amongst nematodes.....	193
7.3 Future prospects for research	194
Appendix I: Electronic Appendices on CD.....	196
Appendix II: Supplementary Tables.....	197
Appendix III: Published Manuscripts	284
Appendix IV: Recipe for DESS preservative	285
References.....	286

List of Tables

Table 1.1: Taxonomy of free-living marine nematodes within the Subclass Enoplia (after Platt and Warwick, 1983)	61
Table 2.1: Geographic data and collection depth of all sample sites used in this study. Short location codes were used to identify nematodes from different geographic locations after individual worms were digested for molecular work.....	70
Table 2.2: Nematode primers used in final PCR and sequencing protocols.	75
Table 2.3: Primers designed from protein alignments of putative orthologous genes. Ortholog names prefaced with 'TI' represent genes from the <i>Trichinella spiralis</i> genome, while names prefaced with 'XI' represent genes identified from the <i>Xiphinema index</i> genome. Ortholog gene names reflect the putative protein names assigned in the NemaLog database. Forward and reverse primers are denoted as F and R, respectively.	77
Table 2.4: Nematode mitochondrial primers tested during this study.	79
Table 2.5: Primers designed for amplifying partial mitochondrial genomes via long-distance PCR.	80
Table 2.6: Aligned rRNA sequences available for each taxonomic group in SILVA release 98. All available sequences were downloaded for each phylum, but not all were used in phylogenetic analyses.	82
Table 3.1: Sampling intervals for slide mounting experiment. All slides prepared together at the start of the experiment, and a subset of nematodes was picked out at intervals as time progressed. Specimens picked from DESS were picked from the sample extracted on the dates indicated, and genomic DNA was immediately extracted.....	89
Table 4.1: Overview of Enopliid clade topologies using different phylogenetic parameters for the small nematode dataset (Enoplia/Dorylaimia only, 563 taxa) Syringo = Syringolaimus, O = Oncholaimoidea, T = Thalassoalaimus/Litinium, Ox = Oxystomina H = Halalaimus, A = Anoplostoma, An = Anticomidae, C = Chaetonema, L = Leptosomatidae, Th = Thoracostomopsidae, E= Enoplolaimus, Ph = Phanodermopsis. Hyphens represent hierarchal derivation of clades, while slashes (e.g. A/B) denote clades appearing as sister taxa.	104
Table 4.2: Overview of Enopliid clade topologies using different phylogenetic parameters for the large nematode dataset (all nematodes, 1100-1400 taxa) Syringo = Syringolaimus, Iron = Ironidae, Alaim = Alaimina, O = Oncholaimoidea, T = Thalassoalaimus/Litinium, Ox = Oxystomina H = Halalaimus, A = Anoplostoma, An = Anticomidae, C = Chaetonema, L = Leptosomatidae, Th = Thoracostomopsidae, E= Enoplolaimus, Ph = Phanodermopsis. Hyphens represent hierarchal derivation of clades, while slashes (e.g. A/B) denote clades appearing as sister taxa. All analyses using GTR+CAT+P-Invar unless otherwise noted.	105
Table 5.1 (following page): Earliest splitting lineage recovered during various tree topology tests. Enoplida = the Enoplia represent the basal clade and all other nematode clades are derived; Dorylaimia = the Dorylaimia represent the basal clade and all other nematode clades are derived; Doryla/Enop = the Dorylaimia and Enoplia appear as sister taxa in a single basal clade, with all other nematodes forming a separate, non-derived clade.....	150
Table 5.2: Overview of clade topologies using different nematode taxa, outgroup combinations, and phylogenetic parameters. M = Microlaimoidea, C = Chromadorida, D = Desmodorida, Mo = Monhystera, ALS =	

Axonolaimidae/Linhomoeidae/Siphonolaimida. Hyphens represent hierarchal derivation of clades, while slashes (e.g. A/B) denote clades appearing as sister taxa. All analyses using GTR+CAT+P-Invar unless otherwise noted. 152

Table 6.1: Groups of shallow-water nematodes exhibiting identical ribosomal sequences. Solid boxes represent specimens that possess identical SSU and LSU gene sequences, with thick horizontal lines separating different clusters of taxa. Dotted vertical lines within boxes designate different LSU haplotypes; in these cases, all taxa possess identical SSU sequences but dotted lines separate groups of specimens according to LSU variant. In these cases, italicized text indicates the pairwise sequence identity between LSU variants; the number of differences observed between sequences is listed below in brackets. If no dotted line is present, all taxa within a box share identical copies of both LSU and SSU.	175
Table 6.2: Groups of nematodes exhibiting identical mitochondrial sequences. Solid boxes represent specimens that possess identical Cox1 gene sequences, with thick horizontal lines separating different clusters of taxa. All taxa within a box share identical copies of Cox1. Groups in bold additionally share identical SSU and LSU copies, while taxa in italics share only SSU copies	177
Table 6.3: Groups of deep-sea nematodes exhibiting identical ribosomal sequences. Solid boxes represent specimens that possess identical copies of both SSU and LSU gene sequences, with thick horizontal lines separating different clusters of taxa. Taxa within the last three boxes (denoted by italicized text) share identical SSU sequences only—these specimens all possess different LSU variants.	178
Table A2.1: List of Enoplid specimens isolated during this investigation, including alphanumeric molecular ID, taxonomic identification, sample site, and slide ID (used to label vido capture files). Parentheses indicate uncertain genus assignments. Gene sequences obtained from each specimen are listed after taxonomic information; Coloured boxes indicate sequences that were eliminated from trees, based on short length or redundancy (e.g. duplicates).....	198
Table A2.2: List of all SSU nematode sequences utilised in this study, including accession numbers, taxonomic information from EMBL, and ARB alphanumeric code used in phylogenetic trees. Colours correspond to clades in full nematode phylogenies (Chapter 5).....	210
Table A2.3: List of all LSU nematode sequences utilised in this study, including accession numbers, taxonomic information from EMBL, and ARB alphanumeric code used in phylogenetic trees.....	262

List of Figures

Figure 2.1: Visualisation of PCR products from long distance PCR. Lane numbers 1 and 2 represent <i>Oncholaimus spp.</i> , numbers 3 and 4 represent <i>Enoplolaimus spp.</i> , and number 5 represents <i>Anoplostoma sp.</i>	81
Figure 3.1: PCR amplification for unmounted nematodes preserved in 5% DMSO and 20% DMSO DESS preservative (1 week and 1 month time points). All nematodes were picked out from preserved samples and directly digested for molecular work. Plus and minus signs represent positive and negative PCR controls, respectively.	91
Figure 3.2: PCR amplification for unmounted nematodes preserved in 5% DMSO and 20% DMSO DESS preservative (3 month and 6 month time points). All nematodes were picked out from preserved samples and directly digested for molecular work. Plus and minus signs represent positive and negative PCR controls, respectively.	91
Figure 3.3: PCR amplification for unmounted nematodes preserved in 5% DMSO and 20% DMSO DESS preservative (1 year and 1.5 year time points). All nematodes were picked out from preserved samples and directly digested for molecular work. Plus and minus signs represent positive and negative PCR controls, respectively.	92
Figure 3.4: PCR amplification of slide mounted specimens at 1 day and 3 days time points. Plus and minus signs represent positive and negative PCR controls, respectively. ..	92
Figure 3.5: PCR amplification of slide mounted specimens at 1 week and 2 week time points. Plus and minus signs represent positive and negative PCR controls, respectively. PS = PCR products for unmounted nematodes amplified directly from DESS preservative, used as a comparison to mounted nematodes.	93
Figure 3.6: PCR amplification of slide mounted specimens at the 1 month time point. Plus and minus signs represent positive and negative PCR controls, respectively. PS = PCR products for unmounted nematodes amplified directly from DESS preservative, used as a comparison to mounted nematodes.	93
Figure 3.7: PCR amplification of slide mounted specimens at the 2 month time point.....	93
Figure 3.8: PCR amplification of slide mounted specimens at the 3 month time point. Plus and minus signs represent positive and negative PCR controls, respectively.	94
Figure 3.9: PCR amplification of slide mounted specimens at the 6 month time point.....	94
Figure 3.10: PCR Amplification success over time for slide mounted and unmounted nematodes. Bars represent the number of nematodes from which the 18S gene was successfully amplified. Bars for unmounted worms represent nematodes amplified directly from full strength DESS preservative (20% DMSO content). Note that unmounted worms were not amplified at the 1 day, 3 day, 2 week, or 2 month time points.....	95
Figure 3.11: Quantification of DNA content in bands appearing on gel photographs for slide mounted worms stored at room temperature. DNA content estimated per 5µl PCR product.	96
Figure 3.12: Quantification of DNA content in bands appearing on gel photographs for slide mounted worms stored at 4°C. DNA content estimated per 5µl PCR product.....	96
Figure 3.13: PCR Amplification success over time for unmounted nematodes amplified directly from DESS preservative. Bars represent the number of nematodes from which the 18S gene was successfully amplified.	97
Figure 3.14: Quantification of DNA content in bands appearing on gel photographs for unmounted nematodes amplified directly from DESS preservative. DNA content estimated per 5µl PCR product.....	97

Figure 4.1: Maximum Likelihood phylogeny displaying the major clades within the Enoplia. Tree built using 563 taxa with estimation of the P-Invar parameter, and no secondary structure gene partitions. (RAxML Job #65991)	108
Figure 4.2: Maximum Likelihood phylogeny displaying the major clades within the Enoplia. Tree built using 563 taxa with estimation of the P-Invar parameter, and using gene partitions according to rRNA stem and loop structures. (RAxML Job #66027)	109
Figure 4.3: Maximum Likelihood phylogeny displaying the major clades within the Enoplia. Variable alignment sites were trimmed using the Gblocks program prior to phylogenetic analysis. Tree built using 563 taxa with estimation of the P-Invar parameter, and no secondary structure gene partitions. (RAxML Job #547483) ..	110
Figure 4.4: Bayesian phylogeny displaying the major clades within the Enoplia. Tree built using 563 taxa using the GTR+G+I model of nucleotide substitution and no secondary structure gene partitions.....	111
Figure 4.5: Maximum Likelihood phylogeny displaying the major clades within the Enoplia, expanded to show relationships between genera. Tree built using 563 taxa with estimation of the P-Invar parameter, and no secondary structure gene partitions. (RAxML Job #65991)	112
Figure 4.6: Bayesian phylogeny displaying the major clades within the Enoplia, expanded to show relationship between genera. Tree built using 563 taxa using the GTR+G+I model of nucleotide substitution, and no secondary structure gene partitions	113
Figure 4.7: Maximum Likelihood Phylogeny displaying separation of marine (blue) and terrestrial (brown) taxa within the Enoplida. Tree Built using 563 taxa with estimation of the P-Invar parameter, and no secondary structure gene partitions (RAxML Job #65991).....	123
Figure 4.8: Bayesian Phylogeny displaying separation of marine (blue) and terrestrial (brown) taxa within the Enoplida. Tree Built using 563 taxa using the GTR+G+I model of nucleotide substitution, and no secondary structure gene partitions. ...	124
Figure 4.9: Maximum Likelihood phylogeny built using sequences from the D2/D3 region of the LSU gene. Variable alignment regions were excluded from the analysis. Tree built using 1062 taxa, with estimation of P-Invar parameter. (RAxML Job #400) ..	127
Figure 4.10: Maximum Likelihood phylogeny built using sequences from the D2/D3 region of the LSU gene. No alignment regions were excluded from the analysis. Tree built using 433 taxa, with estimation of P-Invar parameter. (RAxML Job #643538)	128
Figure 4.11: Maximum Likelihood phylogeny built using SSU sequences, showing the separation of genera within the Tripyloididae. Tree Built using 563 taxa with estimation of the P-Invar parameter, and no secondary structure gene partitions (RAxML Job #65991).....	130
Figure 4.12: Maximum Likelihood phylogeny built using LSU sequences, showing the separation of genera within the Tripyloididae (RAxML Job #643538).	130
Figure 4.13: Maximum Likelihood phylogeny built using LSU sequences, showing the separation of genera within the Oncholaimoidea (RAxML Job #643538).	131
Figure 4.14: Maximum Likelihood phylogeny built using LSU sequences, showing the separation of genera within the Oncholaimoidea (RAxML Job #643538).	132
Figure 4.15: Maximum Likelihood phylogeny built using SSU sequences, showing the separation of genera within the Oncholaimoidea. Tree Built using 563 taxa with estimation of the P-Invar parameter, and no secondary structure gene partitions (RAxML Job #65991).....	132
Figure 4.16: Maximum Likelihood phylogeny built using SSU sequences, showing the separation of genera within the Phanodermatidae, Thoracostomopsidae, and Enoplidae. Tree Built using 563 taxa with estimation of the P-Invar parameter, and no secondary structure gene partitions (RAxML Job #65991).	134

Figure 4.17: Maximum Likelihood phylogeny built using LSU sequences, showing the separation of genera within the Phanodermatidae, Thoracostomopsidae, and Enopliidae (RAxML Job #643538).	135
Figure 4.18: Maximum Likelihood phylogeny built using SSU sequences, showing the separation of genera within the Phanodermatidae. Tree Built using 563 taxa with estimation of the P-Invar parameter, and no secondary structure gene partitions (RAxML Job #65991).	136
Figure 4.19: Maximum Likelihood phylogeny built using LSU sequences, showing the separation of genera within the Phanodermatidae (RAxML Job #643538).	137
Figure 4.20: Bayesian phylogeny built using Cox1 gene sequences. Tree constructed using a 3 alignment partitions according to codon positions, using 2 million generations, and chain heating temperature of 0.1. Final average standard deviation = 0.014216	140
Figure 4.21: Maximum Likelihood phylogeny built using Cox1 gene sequences. Tree constructed using a 3 alignment partitions according to codon positions, and using estimation of the P-Invar parameter.	141
Figure 5.1: An example of a Maximum Likelihood topology which recovered the Enoplia as the earliest splitting lineage (RAxML Job #830526). Tree built using 1336 nematode taxa, all four outgroup phyla, estimation of the P-Invar parameter, and no secondary structure gene partitions.	147
Figure 5.2: An example of a Maximum Likelihood topology which recovered the Dorylaimia as the earliest splitting lineage (RAxML Job #830467). Tree built using 1336 nematode taxa, the Nematomorpha as a single outgroup phylum, estimation of the P-Invar parameter, and no secondary structure gene partitions.	148
Figure 5.3: An example of a Maximum Likelihood topology which recovered the Dorylaimia/Enoplia as sister taxa which split early from all other nematodes (RAxML Job #884354). Tree built using 1336 nematode taxa, the Tardigrada as a single outgroup phylum, no estimation of the P-Invar parameter, and no secondary structure gene partitions.	149
Figure 5.4: A Bayesian tree built using 1336 nematode taxa and all four outgroup phyla. Analysis was run for 2,000,000 generations using the GTR+I+G model of nucleotide substitution, 4 MCMC chains, and a heating temperature of 0.06.	150
Figure 5.5: Maximum Likelihood topology showing the typical clustering of <i>Brevibucca</i> , <i>Cuticularia</i> , and <i>Steinernema</i> species. (RAxML Job #830526)	157
Figure 5.6: Maximum Likelihood topology showing clade topologies when of <i>Brevibucca</i> and <i>Cuticularia</i> split from the main clade containing and <i>Steinernema</i> species. (RAxML Job #992781).	157
Figure 6.1: Maximum Likelihood phylogeny based on SSU data displaying the habitats of marine nematodes within the Enoplida. Red clades indicate deep-sea species, blue clades represent shallow water species, and yellow clades contain species from both environments. (RAxML Job #65991).	167
Figure 6.2: Maximum Likelihood phylogeny based on SSU data displaying the habitats of marine nematodes within the Enoplida, expanded to show all taxa (next 5 pages). Black taxa = shallow-water, red taxa = deep-sea sub-Antarctic (CROZET), blue taxa = deep-sea Pacific, and yellow taxa = deep-sea Antarctic shelf. Collection depths listed after all deep-sea specimens. (RAxML Job #65991).	168
Figure 6.3: Maximum Likelihood phylogeny built using SSU sequences, showing the collection depths of deep-sea specimens within the Phanodermatidae (RAxML Job #65991). Colours equate to collection location of samples: Blue = deep-sea Pacific, Red = deep-sea sub-Antarctic (CROZET project), Yellow = Antarctic shelf, Purple = deep-sea Atlantic.	185

- Figure 6.4:** Maximum Likelihood phylogeny built using SSU sequences, showing the collection depths of deep-sea specimens within the genus *Oxystomina* (RAxML Job #65991). Colors equate to collection location of samples: Blue = deep-sea Pacific, Red = deep-sea sub-Antarctic (CROZET project), Yellow = Antarctic shelf. 186
- Figure 6.5:** Maximum Likelihood phylogeny built using SSU sequences, showing the collection depths of deep-sea specimens within the genus *Halalaimus* (RAxML Job #65991). Colors equate to collection location of samples: Blue = deep-sea Pacific, Red = deep-sea sub-Antarctic (CROZET project), Yellow = Antarctic shelf. 187

List of Accompanying Material

Supplementary CD-ROM contains the following files:

FASTA file containing all SSU sequences amplified during this study:

<Enoplid_SSU_sequences.FASTA>

FASTA file containing all LSU sequences amplified during this study:

<Enoplid_SSU_sequences.FASTA>

FASTA file containing all Cox1 sequences amplified during this study:

<Enoplid_Cox1_sequences.FASTA>

ARB Database used to build large nematode tree (1438 taxa), containing SSU gene alignment: <ARB_LargeDB.arb>

ARB Database used to build small Enoplid/Dorylaimid tree (563 taxa), containing SSU gene alignment: <ARB_SmallDB.arb>

ARB Database used to build LSU phylogeny (433 taxa), containing LSU gene alignment:

<ARB_LSU_DB.arb>

Cox1 gene alignment:

<Cox1_alignment.FASTA>

Taxa list and ARB codes used to build smaller Enoplid/Dorylaimid phylogenies:

<EnopTree_TaxaList.xls>

Best scoring maximum likelihood trees obtained during topological tests: unannotated tree files (text files) and annotated tree graphics (.PNG files) included in folders named according to RAxML job number.

DECLARATION OF AUTHORSHIP

I, Holly Marie Bik,

declare that the thesis entitled

“Resolving phylogenetic relationships within the order Enoplida (Phylum Nematoda)”

and the work presented in the thesis are both my own, and have been generated by me as the result of my own original research. I confirm that:

- this work was done wholly or mainly while in candidature for a research degree at this University;
- where any part of this thesis has previously been submitted for a degree or any other qualification at this University or any other institution, this has been clearly stated;
- where I have consulted the published work of others, this is always clearly attributed;
- where I have quoted from the work of others, the source is always given. With the exception of such quotations, this thesis is entirely my own work;
- I have acknowledged all main sources of help;
- where the thesis is based on work done by myself jointly with others, I have made clear exactly what was done by others and what I have contributed myself;
- parts of this work have been published as: Bik, H. M., Hawkins, L., Hughes, J. A. & Lamshead, P. J. D. (2009) Rapid decline of PCR amplification from genomic extracts of DESS-preserved, slide-mounted nematodes. *Nematology*, **11**, 827-834.

Signed:

Date:.....

Acknowledgements

This thesis is a culmination of a dream I've held for a long time. My science career has progressed from excavating 'dinosaur bones' in the back garden (at the age of five) to something entirely more sophisticated and refined. All science is collaborative, and I could not have submitted this thesis without help and guidance from many people (even my father who buried those 'dinosaur bones'). I am eternally indebted to you all.

Immense thanks goes out to my supervisors, Professor John Lambhead (Natural History Museum, London and National Oceanography Centre, Southampton), Dr David Lunt (University of Hull), Dr Alan Hughes (National Oceanography Centre, Southampton), and Dr Lawrence Hawkins (National Oceanography Centre, Southampton), as well as Professor Kelley Thomas (University of New Hampshire) who acted as a research advisor—your advice and support was invaluable during this whole process. I was very lucky to end up with such a wonderful supervisory team. I learned so much about the world of research, and I was presented with some amazing travel opportunities over the last three years. John—as your last PhD student, I hope I let you go out with a bang!

Thank you to past and present members of the 'worm group' at the NHM—Margaret, Natalie, Tim, Adrian, Kirsty, Lenka, Nick and everyone else who was transiently in the 6th floor labs. I could not have survived this process without your sympathetic ears and the occasional pub lunch! Special thanks goes to Margaret, who toiled many hours preparing gallons of DESS and was always on hand to transport me around the UK.

I am privileged to have been a part of the NHM student council during my PhD, and I would like to thank Eileen, Elliott, Scott, Chris, Linda, Lydia, Claire, Siobhan, Rosie, Nick, and everyone else who was involved with our activities at some point. Thank you for listening to me rant about my PhD on many, many occasions (and then handing me wine).

Thank you to all my other friends in the UK and USA who have always been there to listen to me when I was stressed, and then distract me with inane conversations. There are too many of you to name individually, but I am especially grateful to Emily, Sarah, and Anita who probably got the brunt of it. Emily—you're now officially obliged to reciprocate my acknowledgement in print!

Thank you to my partner Tom who has provided endless support (and occasional distractions to take my mind off things)—your encouragement has largely helped to keep me sane, especially during this final year. Thanks for also looking impressed when I show you big trees and DNA alignments!

Finally, I cannot thank my parents and family enough. Without their love and support (especially financially), I would not be where I am today. They read everything I publish, even though my mother openly admits that she never gets past the title. I hope I've made you proud!

1. Introduction

1.1 An understudied phylum

Purported to be the most abundant metazoan group, nematodes can be found in every habitat on earth, from alpine soils to the deepest ocean trenches. There are many examples of well-studied species: *Caenorhabditis elegans* is a ubiquitous name in genetic research, *Ascaris* species infect millions of humans worldwide, and plant parasitic nematodes such as *Meloidogyne javanica* are notorious agricultural pests. While these nematodes may be well known and well-studied, free-living marine species rarely warrant attention or funding. Yet, nematodes are integral to ecosystem functioning—they facilitate basal process such as nutrient cycling, sediment stability, and even pollutant distribution in marine systems (Snelgrove *et al.* 1997). The global richness of nematode species has been estimated between 10^6 and 10^8 (Lambshead 2004), but the majority of free-living species are unknown. Nematodes possess the lowest ratio of known to unknown taxa for all animal groups (Malakhov 1994)—overall estimates for the phylum suggest that a mere 0.3% to 5.3% of the world's nematode fauna has been described (Hugot *et al.* 2001; Meldal 2004). Hugot *et al.* (2001) counted 26,646 described nematode species out of potentially 1,000,000 that exist; this known fauna comprises 4,070 free-living marine species, 6,611 free-living terrestrial species, 4,105 plant parasitic nematodes, and 11,860 animal parasitic nematodes. Taxonomic knowledge is greater amongst the insects, a group whose estimated diversity far exceeds that of nematodes; around 950,000 insect species have been described out of an estimated 10 million total, representing 9.5% of taxa within this group (Hugot *et al.* 2001).

For free-living marine species, the described fauna is highly biased towards Northwest Europe; study sites with close geographic proximity to this region tend to report the highest percentage of known taxa. For example, a 65% of specimens recovered from the Clyde Estuary (Lambshead 1986) and 38% of specimens from the Irish Sea (Lambshead & Boucher 2003) represented previously described nematode species. This is a stark contrast to species collected from more remote geographic locations, particularly in regards to the deep-sea; 4% of specimens recovered from the Norwegian sea (Jensen 1988) and only 1% of specimens from the Venezuelan Basin (Tietjen 1984) correlated with previously described nematode species. Most investigations typically report between 30-99% of the studied nematode taxa as new, undescribed species (Lambshead 2004).

1.2 Limitations of nematode morphology and taxonomy

With the unaided eye, the visual appearance of nematodes, or 'roundworms', can be compared to thin piece of thread or a speck of dust (depending on the size of the species being viewed). Parasitic nematodes can grow quite large; the size record is held by *Placentonema gigantissima*, a species which inhabits the placenta of sperm whales and can grow up to 8 metres in length (Gibbons 2001). Free-living species tend to be smaller in size compared to their parasitic counterparts, and this factor no doubt contributes to the limited taxonomy in this group. Typical free-living nematodes obtained from deep-sea sediments average between 0.5-0.75mm in length (Lambshhead 2004). Specimens from intertidal sediments are generally between 1-2mm in size, but some species have been known to grow larger (Platt & Warwick 1983). Members of this phylum are said to exhibit pseudocoelomate body plans, consisting of an ectoderm (the exterior cuticle), mesoderm (muscle layer), endoderm (digestive tract) and a fluid-filled pseudocoelom (Gibbons 2001). The pseudocoelom and surrounding longitudinal muscles act as a hydrostatic skeleton and facilitate sinusoidal locomotion. Male and females generally exhibit sexual dimorphism; species can often be distinguished according to the morphology of spicules, a reproductive structure found in male nematodes. Nematodes do not have a circulatory system, although they do possess a complex nervous system and a secretory-excretory system.

Nematodes are typically studied using light microscopy, where features of the head, tail, cuticle, and reproductive organs are observed, measured and drawn. The shape, size and relative position of features such as the amphids (pores on the lateral surface of the head), setae, buccal cavity, genital spicules (in males), vulva (in females), and tail shape are used to narrow an unknown specimen into a known genera using pictorial and dichotomous keys (e.g. Platt & Warwick 1983; Abebe *et al.* 2006). Species are then identified or delineated using the same characters on a finer scale. Specific features are weighted heavier in certain genera and serve as the primary means for separating species; for example, two species could be distinguished based on the measured distance between rows of setae present on the head capsule.

Nematodes are inherently small animals, and specimens that are fixed and mounted are identified at settings approaching the resolution limits of light microscopy. Artefacts from preservation in the specimens, bad optics in the microscope itself, and environmental conditions which affect microscopy may plague the process of identification (Coomans 2002). Electron microscopy can reveal much more detailed morphology, but its

use is impractical for all but the most painstaking taxonomic investigations (De Ley 2000). Furthermore, inexperience may lead to observational flaws through improper use of the microscope, or identification mistakes through misinterpretation of nematode characters (Coomans 2002). Experienced taxonomists learn to cope with many of these problems and limitations, yet, nematology is often perceived as an inaccessible field due to the depth of training needed to interpret anatomical features.

Nematode taxonomy has been historically rooted in morphology; some recent revisions of morphological classifications include those of Andr  ssy (1976) and Lorenzen (1981). Meldal (2004) provides a comprehensive overview detailing nematode taxonomy from start to present. The field of nematology has made vast strides in the 200 years since its inception, but the current state of morphological classification is by no means coherent. The nature of many nematode descriptions is highly subjective; many species are poorly known and poorly described, with some genera needing complete revision for any hope of correctly identifying the species (Coomans 2002). Redundant species names and *nomina dubia* (names of doubtful or unknown application) are particularly pervasive in nematodes, where specimens are comparatively small and diverse compared to other taxonomic groups (Dayrat 2005). More worrying is the fact that nematode species descriptions are overwhelmingly dependent on physical characters and morphometrics; there exists a huge knowledge gap concerning the biology and reproduction of most specimens, and the number of existing nematode species remains unknown (Lambshhead 1993). Identification of newly collected specimens is difficult because of these scanty descriptions and is further complicated by the loss of many type specimens which would be useful for comparison in cases where the literature is ambiguous (Lambshhead 2004). De Ley *et al.* (2005) note that in their experience, voucher specimens are often lost or destroyed within 5-15 years of preservation, despite protocols which are supposed to offer protection for over a hundred years in storage. Given the above impediments, we cannot hope to claim that the current state of nematode systematics is clear or concise by any means.

1.3 Molecular investigations in nematodes

For nematodes, there is a pressing need for coherent taxonomy. The application of molecular tools in nematodes has been slow compared to other phyla; molecular investigations in other animal groups are moving towards whole-genome analysis (Saccone *et al.* 1999), whilst most free-living nematode studies still focus on one or two genetic loci.

Several molecular evolutionary frameworks for nematodes have been published to date, by Blaxter *et al.* (1998), Aleshin *et al.* (1998), De Ley and Blaxter (2002), Holterman *et al.* (2006), Meldal *et al.* (2007) and most recently Van Megen *et al.* (2009). These studies have primarily focused on resolving deep phylogenetic relationships using sequence data, although this has mainly been limited to terrestrial and parasitic nematode groups. Only Meldal *et al.* have provided insight into any free-living marine taxa, sequencing shallow water species from Northwest Europe. A comprehensive molecular investigation of deep-sea nematode assemblages has not yet been undertaken.

Genetic data obtained to date has not been consistent with morphological classifications (Coomans 2002). Selection pressures can drive morphological change, and in nematodes especially this has resulted in convergent evolution of anatomy (Van Megen *et al.* 2009). Most morphological characters cannot be considered homologous, making it extremely difficult to reconstruct an accurate evolutionary history of nematodes from morphology alone (Meldal 2004). Groups with highly similar morphology have been demonstrated as quite diverse at the genetic level, and vice versa (Blaxter *et al.* 1998). Such cryptic diversity has now been found in many nematode genera, including *Caenorhabditis* (Butler *et al.* 1981), *Meloidogyne* (Esbenshade & Triantaphyllou 1987), *Globodera* and *Heterodera* (Bakker & Bouwman-Smits 1988), *Anguina* (Riley *et al.* 1988), *Acrobelloides* (De Ley *et al.* 1999), *Cylicostephanus* (Hung *et al.* 1999), *Panagrolaimus* (Eyualem & Blaxter 2003), *Pellioiditis* (Derycke *et al.* 2005), and *Geomonhystera* (Derycke *et al.* 2007). In comparison, nucleotide sequences at informative loci usually follow a neutral mode of evolution. In this sense, nematode classifications based on DNA sequence data provide an ideal template for studying the evolution of morphological characters across taxa (Meldal 2004).

Molecular investigations in nematodes have primarily focused on using direct sequencing methods to obtain gene sequences from individual specimens, usually in combination with morphological identification. The choice of genetic loci depends on the focus of the study; conserved loci such as the 18S ribosomal RNA gene are well suited for uncovering deep phylogenetic relationships (Blaxter *et al.* 1998), while more variable loci such as the Internal Transcribed Spacer Region or Cox1 are more useful for investigations centred on a single species or genus (Derycke *et al.* 2005). Other molecular methods have aimed at quantifying whole nematode communities present in environmental samples. The most recent work in this area has focused on so-called 'next-generation' sequencing

methods (Porazinska *et al.* 2009), although the utility of older techniques such as denaturing gradient gel electrophoresis has also been investigated (Cook *et al.* 2005).

1.3.1 The 18S ribosomal RNA gene

The nuclear gene encoding the small ribosomal subunit (referred to as 18S rRNA or SSU) has been the most frequently sequenced locus. The popularity of this gene grew as a result of its easy amplification, its prospective applications in both phylogenetics and routine diagnostics, and the growing availability of SSU sequences in public databases (De Ley *et al.* 2005). This gene has been shown to work especially well for reconstructing deep phylogenetic relationships (particularly at the family and order level), and all molecular evolutionary frameworks have based their phylogenies on SSU sequence data (Aleshin *et al.* 1998; Blaxter *et al.* 1998; Meldal 2004; Holterman *et al.* 2006). Despite the recommendations for higher level taxonomic designations, SSU has been observed to have a high success rate for genus and species-level assignments (Bhadury *et al.* 2006) and has also been used to identify reproductively isolated populations within a species (Eyualem & Blaxter 2003). However, such species assignments using SSU are more resolved in some groups than in others (De Ley *et al.* 2005); there is evidence to suggest that the SSU gene displays accelerated rates of evolution for taxa that exhibit short generation times or parasitic lifestyles (Holterman *et al.* 2006). Small subunit sequences are the most ubiquitous nematode sequences available in public databases (e.g., GenBank), and this library representing identified specimens (although far from complete) provides an ideal starting point for phylogenetic studies and diagnostic identifications of unknown specimens. The presence of highly conserved regions within the SSU gene has allowed for the development of robust, nematode-specific primers (Blaxter *et al.* 1998; Floyd *et al.* 2005; Bhadury *et al.* 2006). Some primer optimisation may be required for SSU in some nematode groups (De Ley *et al.* 2005), but in general, the existing primer sets can be used to successfully amplify the SSU gene across a wide range of taxa.

The appeal of SSU as a diagnostic and phylogentic locus can be attributed to the conserved nature of the gene; sequences are highly informative and not subject to high amounts of polymorphism. SSU is typically arranged in repetitive tandem arrays, and individual nematodes may possess between 50-100 gene copies (Floyd *et al.* 2002). The genome of *Caenorhabditis elegans*, for example, features one such array containing approximately 55 copies of the SSU gene (Ellis *et al.* 1986). This high copy number

contributes greatly to the high success rates of SSU amplifications, but it also raises concerns of variation between copies in an individual. The SSU gene is subject to processes of concerted evolution that tend to homogenize gene arrays, effectively minimizing variation amongst copies within an individual (Hillis & Dixon 1991). Widespread divergence between copies has not been observed and is not likely in nematodes (Floyd *et al.* 2002). However, evidence from new high-throughput technologies indicates that nematode specimens may actually carry a suite of minor 18S variants within their genome, at least transiently (Porazinska *et al.* 2009). Currently, such variation is only detectable when using next-generation sequencing platforms that return sequences from single DNA strands. Most phylogenetic and barcoding studies of nematodes rely on automated Sanger sequencing methods to obtain SSU sequences from single worms; these sequences effectively represent a consensus sequence of all the 18S copies present within an individual. The signal from any minor 18S variants present within a genome is likely to be lost amongst the overwhelming signal from the dominant 18S copy, meaning it is still possible to obtain a unique SSU sequence (representing the dominant 18S variant) for each nematode species. Nevertheless, the apparent presence of minor 18S variants presents an intriguing challenge for identifying species using new high-throughput technologies.

Although not subject to the same functional (and thus mutational) restrictions as protein coding genes, ribosomal genes are also marked by conserved and variable regions reflecting hairpins and loops, respectively, present in the folded ribosomal structure (Kjer 1995). Nucleotide sequences are more conserved in hairpins (also known as stem or helix regions), where the ribosomal structure requires complementary base pairing to occur between nucleotides. Loop regions tend to be more divergent at the sequence level, as they represent unpaired expansion segments in the folded ribosome that are not subject to the same base pairing constraints. Secondary structure information can be used as a guide for nucleotide alignments (Kjer 1995), and in phylogenetic reconstructions where stem/loop regions can be used to model different structural constraints that may affect molecular evolution (Holterman *et al.* 2006). A continued focus on the SSU gene is likely to result in more sophisticated tools to analyse divergence based on ribosomal structure. In the future, programs may be developed specifically to apply differential weighting of substitutions occurring in more informative sites, such as residues important to maintaining secondary or tertiary protein structure (Blaxter *et al.* 2005).

Small subunit DNA is typically obtained via direct sequencing from individual nematodes or clonal isolates, but several studies have investigated the use of denaturing gradient gel electrophoresis (DGGE) to evaluate diversity (Waite *et al.* 2003; Foucher *et al.* 2004; Cook *et al.* 2005). This method simultaneously extracts and amplifies 18S DNA from an entire nematode community in a given sample and applies the product to a gel containing DNA denaturants, urea, and formamide. Each resulting band on the gel represents an operational taxonomic unit (OTU), and the overall number of OTUs present can be used to ascertain the diversity of a sample (Foucher *et al.* 2004). Although this method is quicker than morphology or direct sequencing, DGGE fails to amplify all nematode groups within a sample and under-reports biodiversity by failing to identify rare taxa that may be present in a sample (Cook *et al.* 2005). The resulting sequences lack any morphological information as a comparison, limiting inferences regarding how well operational taxonomic units define species boundaries. However, Cook *et al.* (2005) recommended the use of DGGE as a potentially useful method for detecting changes in the most abundant taxa within nematode communities.

1.3.2 The 28S ribosomal subunit gene

The gene encoding the large ribosomal subunit (known as 28S rRNA or LSU) is more variable in its nucleotide sequence, and compared to SSU, it shows different rates of evolution across its structural domains (Hillis & Dixon 1991). The gene region spanning the D2 and D3 expansion segments of LSU (600-1000 bps in length, close to the 5' end of the gene) provides a particularly robust signal and is most commonly used in nematode studies (Thomas *et al.* 1997; De Ley *et al.* 1999; Yoder *et al.* 2006). Primer pairs available for LSU are reported to have the broadest application and highest success rate across different nematode groups; conservation in these D2D3 regions is even consistent across several metazoan phyla (De Ley *et al.* 2005). However, the LSU gene is too variable overall to be informative for inferring deep phylogenetic relationships, and is generally used for small-scale studies aimed at resolving relationships below the family level. De Ley *et al.* (2005) further note that species assignments using LSU sequences do not always correspond to accepted boundaries.

1.3.3 The Internal Transcribed Spacer Region

Sequences from the Internal Transcribed Spacer Region (ITS) represent the second most abundant in databases after SSU. Structurally, ITS is comprised of two variable spacer regions situated between the 28S, 18S, and 5.8S loci in the repeated ribosomal gene arrays (De Ley *et al.* 2005). Although formerly hailed as a good taxonomic marker (Powers *et al.* 1997), subsequent studies demonstrated the existence of highly polymorphic haplotypes (Hugall *et al.* 1999). Some ITS sequences are so divergent that it is impossible to infer species boundaries, and gene variation can even prevent direct sequencing in some cases (De Ley *et al.* 2005). The ITS region is highly variable (sometimes even within individual nematodes), and this variation between sequences presents enormous difficulties for constructing homologous alignments (Hugall *et al.* 1999). De Ley *et al.* (2005) note that one primer set is unlikely to be applicable across all nematode groups, and predict the focus of ITS will be shifted to population genetics rather than deep phylogeny or species identification. To date, ITS sequences have been successfully used to study phylogenetic relationships between close taxa (Chilton *et al.* 2001; Subbotin *et al.* 2001), to elucidate potential hybridization events between taxa (Hugall *et al.* 1999), to assess intraspecific molecular variation (Kaplan *et al.* 2000; Elbadri *et al.* 2002; Ye *et al.* 2004) and to detect cryptic speciation (Hung *et al.* 1999; Derycke *et al.* 2005; Derycke *et al.* 2007).

1.3.4 Cytochrome c oxidase subunit I

Mitochondrial genes are usually the preferred markers for population genetic studies in animal taxa. Mitochondrial DNA is present in a high copy number in animal tissue, and universal primers exist that allow easy amplification of several informative genes such as cytochrome c oxidase subunit 1 (Cox1) and 16S rRNA. The utility of mitochondrial genes stems from their supposed uniparental mode of inheritance, lack of recombination, and effectively neutral selection (Beebe & Rowe 2003). Typically maternal inheritance means that the effective population size of mitochondrial DNA (mtDNA) is one-quarter that of nuclear genes; thus, a gene in any given individual had only a single ancestor in the previous generation. Genetic variation can therefore accrue over

relatively short time scales, and the distribution of haplotypes across populations is considered to reflect demographic rather than selective events (Beebe & Rowe 2003).

Mitochondrial loci have not been widely applied in molecular studies of nematodes, although fragments of Cox1 have been successfully amplified from a limited number of species (Kanzaki & Futai 2002; Derycke *et al.* 2005; Derycke *et al.* 2007). So-called 'universal' primer binding sites that allow robust amplification of Cox1 in many other taxa (Wilcox *et al.* 1997; Hebert *et al.* 2004; Smith *et al.* 2005; Gómez *et al.* 2007) are notably absent in many orders of nematodes and tardigrades (Blaxter 2004). Because of this, it is likely that Cox1 primers sets will need to be specifically developed for different families or genera, according to the requirements of a particular investigation. Even studies with a specific focus on one genus have required multiple primer sets for adequate amplification of short Cox1 sequences (Derycke *et al.* 2005). These persistent difficulties in amplification have resulted in a notable lack of Cox1 data in online sequence databases; molecular investigations in nematodes have instead focused on other informative loci which can be robustly amplified using existing primer sets.

1.3.5 Other genetic methods

Restriction enzymes and cloning methods have been used to amplify stretches of the mitochondrial genome in nematodes such as *Globodera pallida* (Armstrong *et al.* 2000), *Meloidogyne spp.* (Harris *et al.* 1990; Okimoto *et al.* 1991) and *Romanomermis culicivora* (Hyman & Slater 1990). These genomic methods have been successful in differentiating closely related species and providing insight into the structural organisation of mitochondrial genes. However, restriction enzymes slice DNA only at specific nucleotide 'words'; thus, products amplified from genomic methods are comprised of random segments of varying length dependent on the number and position of restriction sites present. Analysis of restriction fragments is based on the different fragment profiles obtained after genomic DNA has been sliced by restriction enzymes. The nucleotide sequence of any given fragment is not phylogenetically informative, as there is no indication as to whether it derives from a functional gene or a non-transcribed region.

Several other genes have been sequenced in nematodes, including heat shock protein gene Hsp90 (Skantar & Carta 2004) and cytochrome *b* oxidase (Vanfleteren & Vierstraete 1999). Such studies usually represent isolated efforts, however, and the overwhelming majority of molecular investigations focus on ribosomal genes (SSU, LSU, or

ITS). Various other molecular techniques have been tested in nematodes, including restriction fragment length polymorphism (RFLP) (Powers *et al.* 1997; Szalanski *et al.* 1997; Elbadri *et al.* 2002), amplified fragment length polymorphism (AFLP) (Folkertsma *et al.* 1996; Semblat *et al.* 1998), random amplified polymorphic DNA (RAPD) (Da Conceição *et al.* 2003), and single-stranded conformational polymorphisms (SSCP) (Derycke *et al.* 2007). These alternative techniques represent 'molecular fingerprinting' methods, and have often been used in combination with direct sequencing for selected taxa (Floyd *et al.* 2002; Derycke *et al.* 2007). However, use of these methods alone offers limited information compared to direct sequencing of specific genes. Some may offer only very limited information from certain taxa (as in the case of RFLP), while other methods deliver copious amounts of data that cannot be placed into an informative context (e.g. RAPD and AFLP) (Floyd *et al.* 2002). There is particular concern about using fingerprints from RAPD and AFLP studies to make species delimitations from nematode community samples; it is unclear what banding patterns represent real species differences, and what patterns instead represent novel intraspecific diversity (Floyd *et al.* 2002). Many concerns have been raised about the reproducibility of RAPD markers; existing protocols are extremely sensitive to minute variation, and many labs have found it difficult to reliably duplicate RAPD marker profiles (Jones *et al.* 1997). Despite these drawbacks, more robust methods (e.g. AFLP) are highly informative for studying the population genetics and biogeography of a specific species; this technique is routinely applied in this context in other phyla (Meudt & Clarke 2007).

One drawback of direct sequencing is most often related to the high cost of processing a large number of specimens; in such cases, methods such as single-strand conformational polymorphism (SSCP) can be valuable analyses that minimize costs by reducing the total amount of sequencing required (Sunnucks *et al.* 2000). In SSCP methods, a gene of interest (either a nuclear or mitochondrial marker) is amplified from a target population, labelled with radioisotopes, and run on non-denaturing polyacrylamide gels. Under these conditions, DNA fragments will physically contort and fold, and the resulting structures will migrate on the gel according to their shape; different haplotypes will exhibit different 'fingerprints' when visualised on a gel. To characterise the nucleotide sequence of a given haplotype, investigators can choose a small subset of specimens to undergo direct sequencing. Such SSCP methods have been successfully applied to population genetic studies in nematodes (Derycke *et al.* 2005; Derycke *et al.* 2007).

1.4 Practical applications of molecular data

1.4.1 DNA Barcoding

There has been much discussion about barcoding methods in nematodes, such as the Molecular Operational Taxonomic Unit (MOTU) concept outlined by Floyd *et al.* (2002) and Blaxter *et al.* (2005). Although barcoding itself has been subject to intense controversy (Sperling 2003), preliminary work in nematodes shows promise for its use in routine identifications and biodiversity investigations. Robust primers are first used to amplify a short sequence of a chosen gene (generally ~500 bps of SSU for nematodes); sequences are subsequently analysed and clustered by similarity, according to a user-defined cut-off value. These sequence clusters represent MOTUs, and are defined by an algorithm that separates species based on pairwise distances; the authors use cut-offs which represent 2 or 3 base pair differences to assign divergent sequences into different MOTUs. Assigning such a cut-off value is dependent on the genes being examined—the level of intraspecific variability may require a higher or lower cut-off value to obtain MOTUs which correlate with biological assemblages. Blaxter *et al.* (2005) empirically demonstrated the application of varying cut-off values to a dataset of SSU sequences. Higher cut-off values result in lower numbers of MOTUs with higher sequence diversity per cluster; there still remains some structure, although this structure becomes increasingly ‘fuzzy’. Delimitation of sequence clusters is also contingent on the order in which sequences are presented to the algorithm, as this can determine MOTU membership and overall number of units. Blaxter *et al.* (2005) do not see this as a shortcoming, but rather as a tool which allows “exploration of the ‘clouds’ of taxa which are closely related” (Blaxter *et al.* 2005). MOTUs representing robust biological species are likely to be distinct from other sequence clouds and consistently comprised of the same member sequences. Conversely, if MOTUs seem to be unstable and swap member sequences between analyses, this could represent population structuring within a species, or recently diverged taxa which still share gene polymorphisms. Repeated analysis can be undertaken if the investigator remains unconvinced, but data from SSU sequences suggests that MOTU clusters are likely to represent real biological assemblages.

Bhadury *et al.* (2006) further tested barcoding methods in free-living nematodes, sequencing a 345 bp segment of the SSU gene from individually identified nematodes. Results indicated that approximately 98% of barcodes were correctly assigned to genus

and species level; this success rate of SSU sequences in nematodes is akin to that of Cox1 barcodes employed in other taxa. Despite the promising outlook for barcoding applications in nematodes, the authors stress that accuracy and efficiency of barcoding is dependent on several factors. Firstly, extensive sequence databases are needed in order to ensure accurate species assignments using barcodes of unknown specimens. Secondly, continuing work is needed to ensure congruence between molecular and morphologically defined species assemblages. Finally, single-worm methods in nematodes are inherently time consuming; development of high-throughput methods is needed if nematode barcoding is to be used for routine surveys and monitoring.

Opponents often condemn barcoding studies for their use of arbitrary divergence ranges and cut-off values to separate species based on short DNA sequences. Investigations in nematodes have acknowledged this limitation; studies often compare morphological and molecular methods to assess the reliability of sequence analysis. Floyd *et al.*'s (2002) initial attempt at defining MOTUs from soil nematodes indicated a strong correlation with morphological identifications; MOTUs were defined from sequence data and taxa 'clouds' were identified via comparisons with online databases. Those sequences which did not match exactly with previously sequenced species could instead be assigned to genera, potentially representing unknown cryptic diversity at the sample site. In the case where a defined MOTU matched with multiple genera, as with *Acrobeloides* and *Cephalobus* in Floyd *et al.*'s (2002) study, it may represent an area which requires further taxonomic investigation to resolve ambiguous and difficult groups. Eyualem and Blaxter (2003) added a further dimension by conducting a breeding trial alongside taxonomic identification and sequence analysis of *Panagrolaimus* cultures. The results of this experiment showed that the two distinct MOTU clusters derived from sequence analyses accurately represented reproductively isolated populations; morphological characters showed only the slightest variation in one culture, and this did not correspond with the sequence data or breeding results. Many other nematode investigations have used integrative methods to verify conclusions from molecular results (De Ley *et al.* 1999; Felix *et al.* 2001; Bhadury *et al.* 2006; Griffiths *et al.* 2006; Fonseca *et al.* 2008) and some species descriptions have even begun to include molecular characterisations (Sommer *et al.* 1996).

Molecular analyses serve to highlight areas requiring further work utilising integrated methods; it is anticipated that continuing analysis of sequence data will reveal many morphological groups that are misrepresented by current taxonomy. A jump to barcoding methods has been suggested in nematodes, but our current understanding of

nematode biodiversity is still rudimentary at best. Even in well-studied terrestrial groups, the focus remains on amassing sequence data and developing comprehensive, integrated databases (Powers 2004). One such example is the push for morphological vouchers using video capture, whereby anatomical features can be recorded and stored before a specimen is destroyed for molecular analysis (De Ley & Bert 2002; De Ley *et al.* 2005). The information can be linked with any molecular data obtained, thus providing a valuable reference in the case of ambiguous results. Online databases have since emerged to curate both sequence data and morphological vouchers from nematode specimens, such as the NemaTol website hosted at the University of New Hampshire (<http://nematol.unh.edu/>).

1.4.2 Future prospects

With the advent of new high-throughput, 'next-generation' sequencing technologies, the future of nematode molecular studies is evolving. Despite this promise, the field of metagenomics is still in its infancy. Ribosomal data obtained from next-generation sequencing platforms (e.g. the GS FLX by 454 Lifesystems) is inherently different from data obtained using traditional automated sequencing methods; this is a consequence of repeated ribosomal gene arrays and concerted evolution within individual nematodes. Automated Sanger sequencing essentially returns a consensus sequence representing all the 18S copies within an individual; the resulting chromatogram is obtained from a huge pool of PCR amplicons and the consensus sequence represents the most dominant 18S variant. In comparison, a sequence obtained from a next-generation platform represents a single PCR amplicon from a single 18S copy found in an individual. Intraspecific variation exists between gene copies (at least transiently) and in this case, individual nematodes could be represented by several gene sequences. This fundamental difference means that more complex analyses are needed to define species using next-generation techniques—instead of obtaining one diagnostic 18S sequence (as in automated Sanger Sequencing), high-throughput methods produce 'clouds' of 18S variant sequences for any given nematode species (Porazinska *et al.* 2009).

The current challenge is developing robust analytical methods that can be applied to such high-throughput, or 'metagenomic' datasets. The OCTUPUS pipeline (Sung *et al.* in preparation) has recently been assembled as a computational tool for processing the large amount of 18S rRNA sequence data generated from a typical nematode metagenomic

dataset (up to 400,000 sequences per run on the GS FLX platform). OCTUPUS processes raw data, performs quality checks on all sequences, and subsequently uses several algorithms to delineate sequence 'clouds' as biological species. These clouds are similar to the MOTU clusters obtained in single-worm barcoding approaches (Blaxter *et al.* 2005); they may represent intraspecific variation between 18S gene copies within an individual, or shared polymorphisms between recently diverged taxa.

Preliminary work on control samples indicates that metagenomic methods work relatively well at estimating species richness from short ribosomal gene fragments (Porazinska *et al.* 2009); data from two genetic loci may be more effective at accurately estimating species richness within a sample, as opposed to data from a single locus. However, control studies have not been able to obtain accurate abundance estimates of individual species, suggesting that further methodological refinement is needed. Another problematic issue is the identification of closely related sister species (which may be biologically distinct species but share copies of 18S rRNA variants). Metagenomic techniques developed using artificial control samples will need to be further tested using real environmental samples from a variety of habitats. Much more data is needed in order to validate conclusions from control studies and address unresolved issues.

In studies of microbes, metagenomic investigations have expanded known diversity by several orders of magnitude (Edwards *et al.* 2006; Sogin *et al.* 2006), and studies focused on nematodes are likely to have similar results. High-throughput methods will facilitate attempts to accurately estimate global nematode biodiversity. Molecular data also indicates that some shallow-water nematode species may be cosmopolitan (Bhadury *et al.* 2008; Derycke *et al.* 2008). These new sequencing methods will allow for much broader comparisons across many taxa, perhaps shedding light on the true extent of 'cosmopolitan' nematode species.

1.5 Molecular evolution

The study of molecular evolution is inherently based on the sporadic imperfections that occur during the replication of DNA. Mutations that arise in gene sequences provide primary information that can be used to reconstruct the evolutionary history of a species. The functional implication of mutations depends on where they occur within a gene. In protein coding genes, changes in single nucleotides (point mutations) can either be synonymous or non-synonymous with respect to the resulting protein's primary structure;

in either case, variation at a single site within a gene is known as a single nucleotide polymorphism (SNP). Because most amino acids are encoded by several triplet nucleotide codons, mutations can occur within gene sequences (particularly at third codon positions) and the translated amino acid sequence can be synonymous with respect to the pre-mutational sequence. In non-synonymous mutations, a nucleotide change produces a codon that encodes a different amino acid, resulting in a substitution within the translated amino acid chain. At the protein level, changes in the amino acid sequence are likely to be highly debilitating if the given residue possesses a key structural or enzymatic function. However, the mutation may not affect the protein structure or function if the residue is in a less crucial position; this 'milder' form of amino acid substitution may be subsequently incorporated into the genetic code of future offspring.

Mutations that occur in the sequences of non-coding genes such as 18S rRNA are subject to different constraints. Ribosomal genes are not transcribed into proteins; instead, the gene sequence itself is directly folded into a complex secondary structure displaying paired stem (helix) regions and unpaired loop expansions (Noller 1984). The effect of nucleotide substitutions that occur within this gene sequence depends on whether a given base is normally incorporated into a stem or loop regions. Substitutions in loop regions are likely to have little effect on overall structure, while substitutions in stem regions are more crucial because bases in this region are paired with a complementary string of nucleotides. In stem regions, paired nucleotides may undergo compensatory changes in order to circumvent potentially lethal mutations—in this scenario, a substitution in one nucleotide also causes a substitution to occur at the complementary paired base (Page & Holmes 1998). This dual nucleotide substitution effectively serves to maintain structural stability in the stem regions of ribosomes. The functional implications of rRNA mutations are still not fully understood; contrary to traditional views, there is evidence that points to conserved bases in rRNA loops (potentially retained because of functional constraints) (Hickson *et al.* 1996) and hypervariable nucleotide sites in paired stem regions (Kjer 1995).

Any given SNP may represent a single substitution or a multiple substitution; two sequences may possess different nucleotides at the same homologous alignment site, but the data itself gives no further information regarding the number of historical mutational steps that have resulted in the observed change (Page & Holmes 1998). Observed substitutions are likely to represent single events if the taxa are closely related or if the gene being studied evolves at a very slow rate. If the studied taxa are very distantly

related, or a given gene shows a rapid rate of evolution, than the observed substitutions may actually represent multiple events. Sites can also exhibit homoplasious similarities; in this case, the same base is present at a homologous site but the observed similarity has not been inherited from the same ancestral sequence. If the same nucleotide change has occurred independently in different lineages, it is said to be a parallel substitution. Convergent substitution is when multiple changes in multiple lineages have resulted, by chance, in the same base at a homologous position. Back substitutions may also occur if repeated substitution events at a given position ultimately result in a nucleotide representing the ancestral state. Because phylogenetic methods depend on homologous similarity, the choice of genetic marker is crucial. Conserved, slowly evolving genes such as 18S rRNA are generally recommended for deep phylogenies involving distantly related taxa. Rapidly evolving genes are not useful for deep phylogenies because they exhibit site saturation; multiple substitutions have probably occurred at most nucleotide positions, confounding any phylogenetic signal. However, for studies of closely related taxa (e.g. at the level of genus or species), conserved genes would not exhibit enough variation between individuals; quickly evolving genes such as ITS or Cox1 are more suited for this purpose. Another way to classify substitutions is based on the chemical nature of the original and replacement base. There are two chemical classes of nucleotides, pyrimidines (cytosine and thymine) and purines (adenine and guanine). Substitution within one chemical class (e.g. purine → purine) is known as a transition, while substitutions between chemical classes (e.g. purine → pyrimidine) are known as transversions. Mutations are often biased in favour of transitions—base changes within a class will retain a similar chemical structure and are also more likely to be synonymous (or have less severe consequences) at the amino acid level (Turner *et al.* 2000).

It is often assumed that the evolutionary steps inferred from a gene sequence represent the actual evolutionary path of a particular species. In reality, this is not always the case; populations undergoing speciation may still exhibit sporadic reproduction, hybridization, and gene flow (Nichols 2001). Such processes may affect certain genes more than others, leading to separate evolutionary histories at different genetic loci which may not independently reflect the historical trajectory of the species. Lineage sorting may also contribute to alternative gene histories, for example, if alleles of a given gene show differential survival rates or retain ancestral polymorphisms (Page & Holmes 1998). Coalescence time is the amount of evolutionary time observed since orthologous genes last shared a common ancestor (e.g. since the lineages coalesced). It is generally thought

that gene lineages tend to diverge long before speciation occurs at the population level (Nei 1987), and calculations concerning the timing of past speciation events are likely to be biased in this respect. Molecular phylogenies actually reconstruct the evolutionary history of the gene—this may or may not accurately reflect the evolutionary history of species. Thus, the choice of genetic loci is critical for phylogenetic studies. Genes are said to be orthologous if a particular locus (present across many taxa) has arisen from a single gene present in the nearest common ancestor. Paralogous genes, on the other hand, have arisen following a gene duplication event in an ancestral lineage. A third and less common situation is xenology, where a gene has been directly copied from the genome of one species to another as a result of horizontal gene transfer (Page & Holmes 1998). Accurate phylogenies can only be inferred from orthologous genes; the evolutionary history of these genes is most likely to correspond to evolution at the species level. Ribosomes are critical components for cellular protein synthesis, and thus rRNA genes are universally present in all living organisms. Ribosomal genes such as 18S have long been recommended for molecular phylogenies (Hillis & Dixon 1991)—the ubiquity and conserved nature of these genes makes them ideal molecular markers for accurately inferring the evolutionary history of species.

1.6 Reconstructing evolution using phylogenetic methods

1.6.1 Alignment Construction

Alignment construction is perhaps one of the most contentious steps in the overall process of building molecular phylogenies. Alignment of protein-coding genes can be relatively straightforward for a conserved gene amongst closely related taxa. Hall (2005) recommends the alignment of translated protein sequences when constructing alignments for protein coding genes, noting that aligning translated sequences (and backtranslating to nucleotides after alignment) resulted in more accurate phylogenies compared to those built from directly aligned nucleotide sequences. Aligning sequences at the protein level avoids the risk of introducing gaps within codons, thus eliminating any potential frameshift artefacts in the resulting alignment (Hall 2008). Risks of protein alignment only increase when aligning distantly related homologs found in highly divergent taxa. The accuracy of resulting phylogenetic trees falls sharply if there is under 20% amino acid identity in

pairwise comparisons between sequences (Thompson *et al.* 1999); in this scenario, less than 50% of amino acid residues are correctly aligned. Above this threshold identity value, there appears a 'twilight zone' between 20-30% where approximately 80% of amino acids are correctly aligned; at levels exceeding 30% average identity, one can expect over 90% of residues to be accurately aligned (Thompson *et al.* 1999).

Non-coding DNA sequences (such as rRNA genes) are notoriously more difficult to align, due to the increased presence of insertions/deletions. In addition, difficult decisions must be made regarding the placement of gaps in less conserved alignment regions. Nevertheless, it has been suggested that phylogenetic methods can produce robust tree topologies as long as sequence alignments are more than 50% accurate (Ogden & Rosenberg 2006). Non-coding genes such as 18S rRNA normally exhibit a mixture of conserved and variable sequence regions. For non-coding sequences, Kumar and Filipowski (2007) recommend a minimum threshold of 66% sequence identity using pairwise comparisons to ensure that alignments maintain at least 50% overall accuracy. As long as 60% of bases are accurately aligned, further improvements to alignment accuracy result in little difference for tree-building programs. Even if a sequence alignment displays near perfect alignment, the quality of resulting phylogenetic trees can vary substantially—tree accuracy is highly contingent on the chosen method of phylogenetic analysis (Ogden & Rosenberg 2006).

For highly similar sequences exceeding 80% sequence identity, most sites in the resulting alignment (>99%) would represent homologous positions (Rosenberg 2005), with alignment homology declining with decreasing identity. For nematodes, most phylogenetic reconstruction is based on the 18S rRNA gene, a loci which is slowly evolving and thus highly conserved across nematode taxa. A BLAST comparison of two divergent nematode sequences (an Enoplid nematode, *Viscosia* sp. [Acc. No. FJ040494] and a Rhabditid nematode, *Cruznema tripartitum* [Acc. No. EU196012]) reveals that the two 18S rRNA sequences maintain 77% sequence identity, despite these two species being placed at opposite ends of the nematode tree (Meldal *et al.* 2007)—this value is well within the recommended threshold of sequence identities. Although some manual alignment editing is necessary to confirm the homology of alignment positions, it is likely that the resulting nematode alignments for such conserved, noncoding genes will be highly accurate.

To avoid any potential problems in aligning non-coding genes such as 18S rRNA, another method is to use secondary structural information, where available. The small ribosomal subunit is organised into paired stem regions and loop expansions; although

bacteria and archaea exhibit some specific structural features, a core section of the small subunit is highly conserved and found across all domains of life (Wuyts *et al.* 2002).

Theoretical models have proven immensely useful for predicting and inferring secondary structure features from a variety of taxa (Wuyts *et al.* 2000), and empirical data from X-ray crystallography has confirmed the existence (and usefulness) of many ribosomal structures (Ban *et al.* 1999; Cate *et al.* 1999; Clemons *et al.* 1999). Previous studies have found that secondary structure information can aid decisions regarding homologous alignment positions and improve the resulting phylogeny (Kjer 1995). The large ribosomal subunit (28S rRNA) exhibits similar structural features, although variable regions in this subunit's gene sequence are much less conserved—producing accurate alignments in such variable gene regions represents one of the major hurdles for molecular evolutionary studies (Lee 2001).

One of the main concerns for multiple sequence alignments is dealing with the placement of gaps. Gaps represent valid evolutionary events—insertions or deletions (indels) that have historically occurred within nucleotide sequences (Kumar & Filipski 2007). Automated alignment programs such as ClustalX (Thompson *et al.* 1997) aim to accurately infer where these indel events occurred by assigning certain costs to the opening and extension of gaps in nucleotide sequences. The 'optimal' alignment is the one with the lowest overall score, theoretically representing the best inference of homology. Placing gaps may not be much of a problem for closely related sequences, where homology can be easily inferred for most alignment sites. In contrast, alignments containing distantly related taxa or highly divergent sequences may exhibit ambiguously aligned regions containing many gapped sites. It is impossible to guarantee that alignments have inferred the exact place and length of historical indel events—thus, homology of alignment sites cannot be guaranteed. The most conservative solution would be to remove all alignment sites containing gaps. However, strict exclusion of gapped alignment sites may result in a loss of phylogenetic information. Some authors argue that only fully ambiguous positions need be excluded (Smith 1994), while other authors object to removing any gapped positions at all (Phillips *et al.* 2000; Lee 2001), arguing that alignment sites are not independent of each other and gapped sites play an important role in positional homology assessments. Alignment sites that contain gaps may still be useful for elucidating phylogenetic relationships amongst a subset of closely related taxa. Finally, excluding heavily gapped regions may artificially homogenize evolutionary rates within an alignment, preventing comparisons of evolutionary rates across a gene sequence or set of

taxa (Lee 2001). Despite the concern regarding gaps, alignment accuracy can be drastically improved by adding intermediate sequences that represent 'stepping stones' between distantly related taxa (Kumar & Filipowski 2007).

1.6.2 Phylogenetic reconstruction

The goal of molecular phylogenetics is to use information from DNA sequences to reconstruct a taxon's evolutionary history in the form of a phylogenetic tree. Phylogenetic methods implicitly assume that all gene sequences in a given dataset are homologous and orthologous, that is, they share common descent from an ancestral sequence that has not undergone a gene duplication event. Two sequences can be similar (but not necessarily homologous) if they share a proportion of identical nucleotide sites when aligned. The homology and phylogenetic utility of ribosomal gene sequences is now widely accepted, so this question of homology is not particularly relevant to molecular studies of nematodes. However, the issue becomes pertinent when investigating new gene families; for example, cases where enzymes show similar catalytic properties but their genes have not derived from a single common ancestor (Hall 2008).

A tree is a mathematical structure whose topology models the evolutionary history of a given group of gene sequences (with each sequence representing a specific taxon) (Page & Holmes 1998). A phylogeny, or evolutionary tree, is an accepted tree topology that is thought to represent the historical relationships between species, and (if a sufficiently conserved gene is used) deeper relationships between major clades. When visually represented, a tree is comprised of branches and nodes. Nodes can either be external (also known as terminal nodes, representing present-day taxa or gene sequences) or internal (points representing hypothetical ancestral lineages). Branch lengths reflect the amount of observed divergence between nodes, and in the case of sequence data, the actual genetic difference that separates extant taxa from ancestral lineages. Most phylogenetic analyses will return numerical values to represent branch lengths; this value reflects the amount of genetic change that has occurred per alignment site, and such trees are referred to as 'weighted trees'. Trees can be rooted or unrooted. If a root is specified, the tree topology will signify a directional path which has led to the evolution of present-day taxa; this root also represents the common ancestor of all sequences within a tree. Divergent, extant lineages that split off closest to the root of the tree are often thought to

represent the most ancestral taxa. Unrooted trees do not imply evolution from any given direction, and only demonstrate relationships between extant taxa. Rooted trees provide more information about evolutionary relationships, as they allow for inferences of older lineages and more recently derived taxa. Nodes can be described as bifurcating or multifurcating. A bifurcating node is one that has only two descendent lineages; that is, speciation of one ancestral taxon resulted in two daughter lineages. A multifurcating node, or polytomy, is where more than two species simultaneously arose from an ancestral node (a 'hard' polytomy), or alternatively, a node that lacks enough data to sufficiently elucidate historical events (a 'soft' polytomy) (Page & Holmes 1998; Hall 2008). Hard polytomies probably do not represent real evolutionary events, but instead reflect scenarios where the evolutionary rate of phylogenetic characters was too slow to infer the true relationship (Maddison 1989).

A number of terms can be used to describe the layout and information contained in tree topologies. A cladogram is the most basic way to display evolutionary relationships; it shows lineage descent and common ancestry of taxa, but offers no other information (Page & Holmes 1998). Additive trees (also known as metric trees or phylograms) contain additional information about branch lengths as well as displaying evolutionary relationships. A tree is said to be 'additive' if the sum of the branch lengths between any two nodes is equal to the distance between them. In reality, this is unlikely to be the case because multiple substitutions may have occurred at any given alignment position, but certain phylogenetic methods do not account for this possibility (Hall 2008). An 'ultrametric' tree (also known as a dendrogram) is a special type of additive tree where all terminal nodes are equidistant from the root of the tree (Page & Holmes 1998). Depending on the algorithm, phylogenetic methods may return trees in the form of a strict consensus tree or majority-rule consensus. In a strict consensus tree, the topology represents only those nodes and splits present in all trees considered by the chosen phylogenetic algorithm. A majority-rule consensus tree represents a more relaxed topology, displaying all nodes and splits present in over half the trees considered.

The evolutionary history displayed by given phylogeny can be analysed in terms of character state changes observed in a set of taxa (Page & Holmes 1998). For sequence data, a character is one of four possible nucleotides (A, C, T, or G). A plesiomorphy (or plesiomorphic character state) represents an ancestral trait that is retained in extant taxa. Characters which have changed between ancestral and terminal nodes are said to represent apomorphic, or derived character states. For example, an ancestral lineage may

have possessed an 'A' in certain nucleotide position, but mutational change over time changed this nucleotide to a 'T' in extant taxa. Derived character states may only be observed in only one extant lineage (autapomorphies), or shared between several terminal taxa (synapomorphies). Synapomorphies only refer to homologous derived characters—that is, the character state arose from the same mutational event in a common ancestral lineage. Shared character states which arose independently in different taxa are known as homoplasies. Homoplasy presents a particularly difficult challenge for inferring evolutionary relationships, and it may appear through several different processes. In parallel evolution, separate events produce homoplasies in multiple terminal taxa, from the same ancestral character state. In convergent evolution, the ancestral nodes possessed different character states, but mutational changes led to extant taxa possessing the same character state. Secondary loss results when a synapomorphic character reverts back to an ancestral state.

Closely related groups of taxa on a phylogenetic tree are known as clades. A clade is said to be monophyletic if all its taxa are derived from the same common ancestor. Taxa which do not group into a monophyletic clade are said to be either paraphyletic or polyphyletic. Paraphyletic clades are groups of taxa that share plesiomorphies, and exclude related taxa which exhibit unique autapomorphies. Such excluded taxa may actually be closely related certain members of a paraphyletic clade; for example, birds are closely related to crocodiles, but crocodiles are instead classed with their more distant relatives of the Reptilia based on primitive, shared traits (Page & Holmes 1998). Polyphyletic taxa are those which have been grouped together based on homoplasious characters. Before the advent of molecular phylogenies, many nematode groupings were polyphyletic; taxa were organised according to morphological structures which exhibited convergent evolution, and such classification did not represent the true evolutionary history of most species.

1.6.3 Building molecular phylogenies

A variety of phylogenetic methods exist which can be differentially applied depending on the scope and focus of a given investigation. These methods can be divided into two main types of analysis: algorithmic methods and criterion-based methods (Swofford *et al.* 1996). In algorithmic methods (such as Neighbour Joining), the input data is analysed using a specific set of steps (an algorithm), and once completed, these steps

determine a tree topology. Criterion-based methods (such as Maximum Likelihood or Bayesian Inference) instead use a standard guideline, known as an optimality criterion, to compare different trees and choose the best scoring topology that is produced by a given algorithm. Algorithmic methods tend to be fast, since they infer and choose trees in a single step. Criterion-based methods are much slower because tree inference and tree choice represent separate, discrete tasks; searching for the best tree requires significant computing power, especially for large datasets. These two methods often implement the same algorithms for different purposes; an algorithmic method may use a given algorithm as the primary means to construct and output a tree, while a criterion-based method may use the same algorithm as a preliminary step during tree topology searches (Swofford *et al.* 1996). Algorithmic methods produce only one tree from the data, whereas criterion-methods can return many different versions of the 'best' tree (Hall 2008).

1.6.3.1 Algorithmic methods

The two most widely applied algorithmic methods (also known as distance methods) are Unweighted Pair-Group Method with Arithmetic Mean (UPGMA) and Neighbour Joining (NJ). These methods measure the divergence between sequences in a dataset by calculating a matrix of pairwise distances; this matrix is then used to compute branch lengths and order and output a tree topology (Hall 2008). UPGMA uses a clustering method to sequentially reduce a dataset into a set of matrices; it first calculates pairwise distances between the most closely related sequences and collapses these into single nodes. Pairwise differences are calculated between the closest nodes, and so on, until the dataset is represented by a matrix with a single entry. The final set of matrices (representing nodes at different levels) is then used to construct the tree starting at the root and moving outwards until it reaches the terminal branches (representing the sequences with the lowest pairwise distance). UPGMA assumes that the final tree topology is additive and ultrametric (e.g. it relies on molecular clock assumptions with a constant rate of evolution); it incorrectly assumes that all taxa are equally distant from the base of the tree, and uses this reasoning to root the tree. Because of this, UPGMA is now viewed as an outdated and unreliable method and is rarely used in modern phylogenetic studies (Hall 2008).

Neighbour Joining is considered a more robust distance method, as it does not suffer from the same incorrect assumptions as UPGMA (Hall 2008)—NJ instead relies only

on tree additivity. Tree construction is similar to UPGMA in that NJ sequentially reduces and creates a set of distance matrices, but NJ analyses construct unrooted trees. NJ does not cluster sequences but instead directly computes pairwise differences to internal nodes. NJ calculates a distance matrix that represents net divergence; this represents a sum of the distances observed between each individual sequence and all other taxa within the dataset. The two sequences with the lowest net distance in the dataset are collapsed into a single node, and a new matrix is built following this reduction. As in UPGMA, this continues until a matrix is obtained with a single datapoint, and the calculated set of matrices is used to construct a final tree topology. NJ analyses do not utilise an optimality criterion and thus topologies only represent approximate solutions; the final output does not represent the best or even optimal tree, and thousands of alternate, better topologies can typically be found using an optimality criterion (Hillis *et al.* 1996). As a result, several authors have recommended the use of Neighbour Joining only as a fast, preliminary method to test tree topologies before subjecting datasets to more robust phylogenetic methods (Hillis *et al.* 1996; Swofford *et al.* 1996). Neighbour Joining is used frequently in barcoding studies, where investigators are required to match unknown barcode sequences with the closest identified relative (Hebert *et al.* 2003; Bhadury *et al.* 2006; Hajibabaei *et al.* 2006). NJ methods fare quite well for such studies where the group of choice has been thoroughly sampled; the more representative sequences in a tree, the more likely that an unknown sequence will exhibit a low pairwise distance to the query dataset.

Two main criticisms of distance methods entail their inherent tendency to lose information through use of a distance matrix and the limited evolutionary interpretations possible from the branch lengths of resulting trees (Page & Holmes 1998). Algorithmic methods essentially 'summarise' sequence data by comparing sequences in terms of overall relatedness; in comparison, criterion-based methods examine datasets using every nucleotide site in a multiple sequence alignment. While distance methods report how much change has occurred between two sequences, criterion-based methods allow us to additionally infer the exact location of this change in the gene sequence. For distance methods, the value of branch lengths on a tree cannot be biologically interpreted as the actual number of nucleotide substitutions that have occurred over time. The total tree length (representing the total number of substitutions) resulting from distance methods may be less than the minimum amount of nucleotide substitutions actually observed in the data (Page & Holmes 1998). Despite this, the branch lengths of distance trees are

internally consistent, and they can be used as a general guide to demonstrate which sequences are more or less divergent from other taxa.

1.6.3.2 Criterion-based methods

Criterion-based methods tend to be very computationally expensive; the total number of possible tree combinations increases exponentially with greater numbers of taxa present in a dataset. Even for a dataset containing only 20 sequences, there are a total of 8.2×10^{21} possible tree topologies (Page & Holmes 1998). Because of the huge amount of possibilities in 'tree space', phylogenetic methods need to employ heuristic methods in their search for the best possible tree—this searching method examines a small subset of trees (out of millions of possibilities) in hopes of finding an optimal topology.

1.6.3.2.1 Parsimony

Parsimony analyses aim to find the most parsimonious tree—that is, the topology that requires the minimum number of evolutionary changes. There are two types of Parsimony: generalised parsimony and weighted parsimony. Both of these methods increase the flexibility and accuracy of parsimony analyses by allowing users to specify additional criteria for analysing sequence data. Generalised parsimony allows the incorporation of basic nucleotide substitution models (in the form of step matrices), while weighted parsimony assigns weights to alignment sites according to their information content. In weighted parsimony, conserved, slowly evolving sites are considered phylogenetically informative—these sites are more valuable because they provide better evidence for reconstructing evolution. Informative sites are assigned more weight in comparison to phylogenetically uninformative sites which may be invariable, highly conserved, or exhibit site saturation. Parsimony analysis evaluates tree topologies for each informative site, scoring the number of evolutionary steps required in each tree; the topology with the lowest total score is accepted as the best reconstruction of evolutionary history (Hall 2008).

There has been much debate regarding the use of parsimony for phylogenetic reconstructions of sequence data (Page & Holmes 1998). Supporters of the method argue that parsimony is, by definition, aimed at maximising the homologous similarity displayed

by a given tree topology; parsimony assumes that homoplasies are rare, and that shared characters are more likely to be derived from a common ancestor (Hall 2008). Secondly, parsimony assumes that mutational change is rare, and thus the resulting tree topology is likely to be an accurate reflection of evolutionary history. Critics of parsimony state that this phylogenetic method often recovers the wrong tree under certain conditions, even if more data is added to reduce this possibility (Hendy & Penny 1989). Parsimony can be especially inconsistent within the so-called 'Felsenstein zone' (Felsenstein 1978) where heterogeneous evolutionary rates result in some taxa displaying long branches on the true tree topology. Because parsimony aims to reconstruct the shortest possible tree (e.g. the one requiring the fewest evolutionary changes), long branches attract under this scenario and Parsimony consistently infers the wrong tree topology. Using longer gene sequences only increases the likelihood of incorrect trees. Thorough empirical tests by Meldal *et al.* (2007) demonstrated the inaccuracy of parsimony methods for reconstructing evolutionary history of nematodes using the 18S rRNA gene.

1.6.3.2.2 Maximum Likelihood

The principle of likelihood suggests that the most probable explanation for a given scenario is likely to be the correct one. In Maximum Likelihood (ML) methods, the 'best' tree is the one whose topology maximises the likelihood of observing the dataset (Hall 2008). For a given dataset, ML methods will compute a likelihood value for all possible tree topologies; the tree that recovers the greatest likelihood value is chosen as the 'best tree'. Such likelihood searches are computationally intensive, and this has limited the application of maximum likelihood analyses in the past. However, increasing computational power and faster algorithms such as RAxML (Stamatakis 2006) have contributed to the widespread use of ML in recent years.

One advantage of ML is the ability to apply detailed models of molecular evolution in the analysis of sequence data. Model parameters are either predefined or estimated from the dataset during analysis—in practice, parameters such as base frequency estimates, proportion of invariable sites, and the gamma distribution parameter are usually estimated from the dataset (Hall 2008). Although ML is generally accepted as a robust phylogenetic method, its dependence on an explicit nucleotide substitution model presents an inherent dilemma. Since we do not possess the true evolutionary tree of any given dataset, the parameter values of nucleotide models represent assumptions regarding the probability

that certain evolutionary events will occur. One argument suggests that ML methods should simultaneously search for both the best model as well as the best tree in order to obtain the most accurate topology (Page & Holmes 1998). However, recent studies have shown that model choice does not significantly affect evolutionary inferences from tree topologies; alternate models only appear to differ in their arrangements of poorly supported nodes (Ripplinger & Sullivan 2008). Phylogenetic methods that require a model choice (e.g. ML) usually outperform other methods that do not utilise evolutionary models (e.g. Parsimony)—maximum likelihood methods in particular display less variance in response sampling error and can withstand repeated violations of model assumptions (Swofford *et al.* 1996).

1.6.3.2.3 Bayesian Inference

Bayesian inference (BI) represents a variation of maximum likelihood. Whereas ML chooses the tree that maximises the likelihood of observing the dataset, Bayesian inference chooses the tree with the greatest likelihood, given the dataset. Instead of assessing trees based on likelihood values, BI utilises posterior probabilities and seeks to find the best tree from the dataset by searching for the topology with the highest probability value (Hall 2008). Maximum Likelihood analyses return one 'best' tree, while Bayesian methods instead return the best set of trees (in the form of a consensus tree) that can be found at the top of a 'hill'. In this 'hill-climbing' strategy, Bayesian algorithms choose a random tree and rearrange the topology; if this new topology scores higher than the original tree, then this tree is retained and used as a new starting point. If the new tree has a significantly worse score, the topology is rejected and the search re-commences using original tree. In this sense, the range of tree scores represent the 'hill' and trees with sequentially higher scores represent 'steps' leading to the optimal tree (the highest point of the hill). There is a difference between the 'locally optimum tree' and the 'globally optimum tree' (Page & Holmes 1998). The locally optimum tree may represent the best scoring tree (or highest point of a hill) that exists within the sampled subset of tree space. However, because not all possible tree topologies were examined, there may be a better scoring tree (on a higher hill) within the unsampled tree space that is the best tree to represent the data—the global optimum. Since true Bayesian algorithms are too computationally expensive, current programs implement the Metropolis-coupled Markov Chain Monte Carlo (MC)³ approximation method to efficiently search tree space

(Huelsenbeck & Ronquist 2001). This method involves simultaneous, independent Bayesian searches (chains) that exchange information at specified intervals, preventing independent chains from becoming trapped on suboptimal hills; chains are thus able to jump valleys and reach increasingly higher hills. The (MC)³ approximation method uses several 'heated' chains and one 'cold' chain to further improve tree searches. Heated chains are more effective at climbing hills and crossing valleys to find optimal tree topologies, but trees are only empirically sampled from cold chains. During (MC)³ analysis, heated and cold chains will change states, helping the cold chain to reach higher hilltops—the final tree outputs represent the highest hill (and ideally the global optimum) found during the analysis. Bayesian methods are said to have found the highest possible hill when the differences amongst a given set of trees is no longer statistically significant; choosing the 'best tree' from within a set essentially becomes a random choice, and the algorithm is said to have reached convergence. In practise, it is usually acceptable to say convergence has occurred when the average standard deviation of split frequencies falls below 0.05 (although much more confidence is placed in values <0.01) (Hall 2008). The average standard deviation measures the similarity of tree samples between independent Bayesian runs, and lower values correlate to more stable tree topologies.

1.6.4 Models for estimating molecular evolution

Criterion-based methods of phylogeny reconstruction rely on models of nucleotide substitution to estimate actual evolutionary distances. Models are implemented as distance correction measures, in order to account for the potential of multiple substitutions occurring at homologous sites in sequence data. Otherwise, methods that strictly measure observed base differences at homologous sites are likely to underestimate the actual amount of historical change. The six most common models are known as Jukes-Cantor (JC), Kimura 2 parameter (K2P), Felsenstein (F81), Hasegawa, Kishino and Yano 1985 (HKY85), and the General Time Reversible (GTR or REV) (Page & Holmes 1998). The GTR model (Rodríguez *et al.* 1990; Yang *et al.* 1994) is considered the most complex and is also the most widely used in current phylogenetics investigations; all other models represent more simple incarnations of GTR. The 'time reversible' nature of this model refers to nucleotide substitutions—there is no favoured directionality of mutational change over time, and all substitutions are fully reversible (and thus, equally likely). The main differences amongst these models relates to the anticipated base frequencies and

substitution patterns likely to be observed in real datasets. The JC and K2P models are the only ones to assume that equal base frequencies are likely across datasets; all other models assume that base frequencies are likely to vary. With regard to substitution rates, JC and F81 models assume that all types of substitutions are equally likely. The K2P and HKY85 models expect more variance in substitution patterns, and both specify different rates for transitions and transversions. The GTR model uses a much more complicated probability matrix, assuming that there are six different classes of substitutions, all with different rates. Although the ultimate goal of choosing a model is to incorporate biological factors which affect the evolution of gene sequences, the addition of more parameters increases the chance of sampling error—each parameter must be estimated from the dataset itself (Page & Holmes 1998). However, simpler models may inaccurately estimate biological processes, and opting for fewer parameters may not be the best solution. There has been much discussion and debate about model choice in phylogenetic methods (Yang *et al.* 1994; Liò & Goldman 1998; Ripplinger & Sullivan 2008). The MODELTEST program (Posada & Crandall 1998) is often used to determine the best fitting model for a particular dataset; this software uses the Akaike information criterion and likelihood ratio tests to choose amongst substitution models. In practise, many single and multi gene phylogenies use the GTR model in combination with other parameters (e.g. for invariant sites or rate variation) (e.g. Holterman *et al.* 2006; Meldal *et al.* 2007; Hunt & Vogler 2008), although newer models (e.g. CAT) are being specifically utilised in phylogenomic analyses (Philippe *et al.* 2009). The GTR+I+ Γ model is especially well suited for large-scale phylogenies, where the inclusion of many taxa permits precise estimation of model parameters (Hunt & Vogler 2008).

All models used to estimate molecular evolution in phylogenetic analyses make implicit assumptions about the processes that effect sequence data. They assume that: all nucleotides within a sequence change independently of each other, substitution rates do not vary through time or between taxa, all base compositions are at equilibrium, and substitution probabilities are equal at all sites and do not vary through time (Page & Holmes 1998). From a biological point of view, it is probable that any given dataset is likely to violate at least one of these assumptions. In ribosomal genes, compensatory changes in stem regions ultimately mean that changes at one nucleotide position directly influence subsequent changes at another site. However, this compensatory process may not be overly rapid; ribosomal stem regions can maintain mismatches for millions of years (Page & Holmes 1998). If a subset of sequences exhibits base compositions that deviate from the

expected equilibrium (e.g. a high G + C content), model assumptions may cause such sequences to cluster together instead of grouping each sequence with its closest relative in the tree. In this case, alternate models such as the LogDet transformation can be used to correct for potential biases in base composition (Lockhard *et al.* 1994; Steel *et al.* 1994); this method recovers the additive distances of sequences, which can be effectively utilised even when base compositions vary.

Substitution probabilities are most certainly not equal at all sites within a nucleotide sequence. For both non-coding and protein coding genes, functional and structural requirements effectively restrict mutation at certain nucleotide positions, while other sites are less constrained. For third codon positions of protein-coding genes, fourfold degenerate sites evolve twice as rapidly as twofold degenerate sites, and nearly four times more quickly than non-degenerate sites (Gaur & Li 1991). Thus, synonymous mutational changes are the most frequently observed, as they have the least functional impact. Over time, rapidly evolving genes actually show less divergence than those that evolve more slowly, due to the effects of site saturation in the rapidly evolving gene (Palumbi 1989; Janecek *et al.* 1996).

To account for among-site rate variation (ASRV), phylogenetic studies commonly utilise estimation of invariant sites and/or a gamma distribution. Invariant-site models assume that a proportion of nucleotide sites do not vary at all, or undergo a constant rate of substitution (Hasegawa *et al.* 1985; Churchill *et al.* 1992; Reeves 1992; Sidow *et al.* 1992). The gamma distribution (represented by Γ) models rate variation across nucleotide sites as a continuous distribution (Steel *et al.* 1993; Yang 1993); this model is comprised of a shape parameter (α) and a scale parameter (β). Implementation of the full gamma distribution is very computationally expensive—a more feasible option is the discrete gamma model (Yang 1994), an approximation which separates the continuous distribution into several rate categories. Data from nuclear and mitochondrial genes suggests that rate variation under the discrete gamma model (estimated according to the gamma shape parameter α) usually falls between 0.16 and 1.37, meaning that rate variation in most datasets is most often represented by an ‘L-shape’ gamma distribution (Yang 1996). At such levels, most sites within a sequence will show no variation in substitution rates (e.g. they are practically invariable), while a few sites display very high rate variation. Some authors have recommended using the discrete gamma model in combination with estimation of invariant sites (Gu *et al.* 1995). This common implementation identifies invariant sites, and estimates rate variation for the remaining alignment positions. For

large-scale phylogenies, even the discrete gamma parameter approximation becomes computationally expensive; thus, some phylogenetic software programs use the CAT approximation as a replacement model (Stamatakis 2006). The CAT model uses a set number of rate categories to estimate individual per-site evolutionary rates; in the maximum likelihood program RAxML, rate categories are optimised by maximizing individual per-site likelihood values. The use of GTR+CAT model implemented in RAxML results in likelihood values that are comparable to GTR+ Γ (Stamatakis 2006), and this model choice is currently one of the most robust methods for computing large-scale phylogenies.

1.6.5 Gauging support for tree topologies

The accuracy of phylogenies can be assessed according to overall tree topologies, as well as confidence values for internal nodes. A robust tree topology is one that is consistently supported using different phylogenetic methods, model choices, and parameter values. If a given topology is observed to stay intact despite such rigorous assessment, it is likely that this tree represents the true evolutionary history of the dataset—e.g. it contains an unambiguous phylogenetic signal. For molecular phylogenies, careful consideration must be given to the choice of genetic loci, in order to ensure that the gene tree (represented by the phylogenetic topology) is close to the actual species tree (See Section 1.5). Additionally, the use of different character sets (e.g. different genetic loci) can provide independent support for the hypothesized evolutionary history of a given set of taxa (Page & Holmes 1998).

Bootstrapping represents a method for assessing confidence values of nodes within a given tree topology; use of the non-parametric bootstrap in phylogenetics was first proposed by Felsenstein (1985). Bootstrapping essentially estimates parameter values by producing a set of pseudoreplicates from a given dataset (Page & Holmes 1998). As a result of subsampling the datapoints with replacement, the pseudoreplicates represent slightly modified datasets with different frequencies amongst alignment sites (referred to as ‘sampling with replacement’). These pseudoreplicates are then used to construct tree topologies, and the congruence between topologies is assessed across all pseudoreplicates sampled (typically 100 to 1000 replicates). Parametric bootstrapping represents a modified method that also models the evolution of a given dataset during phylogenetic analysis; certain parameters are estimated from the dataset itself, including the resulting

tree (Page & Holmes 1998). However, most bootstrapping methods in current phylogenetic algorithms generally utilise non-parametric methods. The bootstrap value assigned to a given node represents the recovery rate of that node across all pseudoreplicates sampled, expressed as a percentage of total topologies. Bootstrap values above 85% generally indicate strongly supported clades, while values between 65-85% only suggest moderate support (Hillis & Bull 1993). Many authors have debated the true meaning of bootstrap values. Some suggest that support values indicate repeatability (Felsenstein 1985; Sanderson 1989)—the consistent recovery of a group from independent samples. Other authors maintain that bootstraps represent accuracy (Felsenstein & Kishino 1993)—the likelihood that a given clade exists in the true evolutionary phylogeny. Alternatively, Hillis & Bull (1993) argue that bootstrap values only support the recovery of a given clade using a specific phylogenetic method. Regardless of this debate, bootstrap values provide useful information when used in conjunction with other topological tests (outgroup comparison, use of multiple phylogenetic methods, etc.). Low bootstrap values can result from low taxon sampling within a given clade, the presence of unstable 'rogue' taxa, or 'fast' bootstrapping algorithms (Sanderson & Shaffer 2002). Bootstrapping hundreds of taxa can be extremely time consuming, and many programs such as RAxML have incorporated rapid bootstrap heuristics (Stamatakis *et al.* 2008) to accommodate large-scale phylogenies. Such 'fast' algorithms can result in much lower support values (Debry & Olmstead 2000; Mort *et al.* 2000), although bootstraps for strong clade groupings (e.g. >80-90% support) do not seem to be affected by heuristic search strategies.

Insufficient taxon sampling can often result in low support values or incorrect tree topologies (e.g. the 'Felsenstein Zone'). Graybeal (1998) recommends the addition of more taxa over the addition of more characters, noting that a large, well-sampled dataset can effectively break up any potential long branch artefacts. Thorough taxon sampling has been repeatedly cited as the most important factor for constructing accurate phylogenies (Omeland *et al.* 1999; Brinkmann & Philippe 2008; Heath *et al.* 2008). Heath *et al.* (2008) note that a small dataset with large number of characters can introduce systematic bias—this scenario can produce highly supported and repeatable (but inaccurate) phylogenies. The inclusion of few taxa can mean that phylogenetic algorithms do not have enough information to accurately estimate the parameters of evolutionary models; phylogenetic relationships may thus reflect homoplasies rather than true evolutionary relationships. There is some disagreement regarding the effect of taxon sampling on bootstrap values; some studies report decreasing support values with an increasing number of taxa (Bremer

et al. 1999; Sanderson *et al.* 2000), while Omland (1999) reported higher bootstraps with increased taxon sampling at the species level. Increased taxon sampling can also greatly reduce the computing time for large phylogenies (Soltis *et al.* 1998; Savolainen *et al.* 2000), returning a better tree topology in a shorter amount of time. There do not appear to be any strong arguments against dense taxon sampling, except the computational power needed to build large trees. Given the recent advances in computing power and phylogenetic algorithms, even this argument is no longer valid—the RAxML program has been used to build maximum likelihood trees containing upwards of 50,000 taxa (Stamatakis 2006).

Molecular phylogenies are rooted according to outgroup taxa—closely related sequences that represent species outside the primary group of interest. The choice of outgroup taxa can significantly impact the overall tree topologies (Smith 1994). By default, outgroups allow inference of ancestral character states as well as shared, derived characters for the entire ingroup—thus, the choice of outgroup taxa will significantly impact the interpretation of how such character states evolved (Nixon & Carpenter 1994). Ingroup topology can be affected by outgroup choice, even impacting nodes that are far from the inferred root (Milinkovitch & Lyons-Weiler 1998; Tarrío *et al.* 2000). Outgroups whose sequences are very divergent or exhibit widespread site saturation can introduce long-branch attraction artefacts (Wheeler 1990; Maddison *et al.* 1992; Johnson 2001); in these cases, the root placement is likely to be incorrect. To ensure accurate rooting, many authors advocate using the closest related sister taxon as an outgroup (Mayden & Wiley 1992; Smith 1994; Sanderson & Shaffer 2002). Alternatively, including a mixture of close relatives and more distantly related species (Maddison *et al.* 1984; Sanderson & Shaffer 2002) can allow for accurate phylogenetic inference. A combination of outgroup taxa may be necessary if the closest sister taxon has undergone a severe rate speedup (Lyons-Weiler *et al.* 1998); other taxa may be more distantly related but less divergent with respect to the ingroup. There are clearly many different recommendations for rooting trees, but most authors agree that outgroup choice should be empirically tested and rigorously evaluated. Outgroup taxa can be rotated, to determine whether root placement changes using different, divergent taxa (Hutcheon *et al.* 1998; Tarrío *et al.* 2000; Dalevi *et al.* 2001). Variable alignment sites or rogue taxa can also be removed in order to reduce the possibility of long-branch attraction between the outgroup and ingroup (Hendy & Penny 1989; Smith 1994). Any observed changes in rooting or ingroup topology can elucidate uncertain relationships within the phylogeny.

The Gblocks program (Castresana 2000) is one method that is often used to remove variable positions that may be subject to site saturation or exhibit dubious homology. Trimming alignment sites is generally useful for multi-gene phylogenies or phylogenomic methods that include rapidly evolving genes (Rodriguez-Ezpeleta *et al.* 2007; Brinkmann & Philippe 2008); SSU alignments contain mostly conserved or constant sites, and few (if any) hypervariable positions. The full gene sequence of 18S rRNA is only ~1600 base pairs, and trimming alignment positions of comparatively short gene sequence (versus multi-gene or phylogenomic alignments) may result in a loss of information. Fewer alignment sites have been linked to phylogenetic error and decreased resolution (Lecointre *et al.* 1993; Hillis *et al.* 1994; Hillis *et al.* 2003), so trimming of sites should only be undertaken if absolutely necessary.

Visual inspection can often determine inaccuracies in tree topologies, especially in regards to long-branch taxa. Other, more subtle inaccuracies can only be revealed by assessing phylogenies in regards to the above-outlined criteria. Data from large-scale phylogenomic methods indicates that accurate trees are obtained by using: 1) dense taxon sampling, 2) complex evolutionary models that mirror biological reality, and 3) removing data (species and alignment sites) that exhibit accelerated evolutionary rates (Brinkmann & Philippe 2008). Thus, solid sampling methodology and rigorous phylogenetic tests are the best guarantee for accurate tree topologies.

1.6.6 Choosing a phylogenetic method

With so many different phylogenetic methods available, it can be difficult to decide which one is likely to recover the most accurate tree topology for any given dataset. Early attempts to validate phylogenetic methods utilised data from real evolutionary trees to evaluate reconstructions. UPGMA, Neighbour-joining, and Parsimony methods were able to successfully reconstruct the real evolutionary history of T7 bacteriophage cultures (Hillis *et al.* 1992). However, in this case the real evolutionary tree was relatively easy to infer because of the balanced tree topology and the abundance of informative character changes (Page & Holmes 1998). More stringent trials have utilised artificial phylogenies to test the accuracy of different methods in reconstructing datasets with deviant tree topologies and abnormal nucleotide substitution parameters. Such studies have revealed the inaccuracies of UPGMA and Parsimony under certain conditions. For datasets with small numbers of taxa, the effect of long-branch attraction can potentially lead to

inaccurate tree topologies using Parsimony. Although UPGMA can accurately infer tree topologies when evolutionary rates are constant, its accuracy is significantly reduced as rate variation (and thus branch length) differs amongst taxa; Parsimony methods offer greater capability to cope with rate variation, but only to a certain point. The effect of different branch lengths is especially significant in the 'Felsenstein zone' where the presence of a short internal edge and two long terminal edges misleads the parsimony algorithm into inferring the wrong tree topology (Huelsenbeck & Hillis 1993). For small datasets, the effects of long-branch attraction for Parsimony reconstruction cannot be overcome simply by adding more alignment sites per taxon (Huelsenbeck *et al.* 1996). The effect of long-branch attraction becomes much less of a problem with increased taxon sampling, as a large dataset reduces the chance of covarying homoplasies which can result in incorrect tree inferences with a small set of taxa (Hillis 1996). As molecular research moves toward multi-gene phylogenies (sometimes encompassing hundreds of loci) and phylogenomic methods, the need for rigorous empirical tests becomes even clearer. Phylogenetic studies currently utilise several methods (typically maximum likelihood and Bayesian inference), combined with rigorous topological tests to validate evolutionary inferences.

1.7 Recent molecular phylogenies of the Phylum Nematoda

The first molecular phylogeny was produced by Blaxter *et al.* (1998) and proposed three fundamental clades for the Phylum Nematoda: the Dorylaimia, Enoplia, and Chromadoria. De Ley and Blaxter (2002) suggested a new classification scheme for the Nematoda based on this original molecular phylogeny. Phylogenies by Aleshin *et al.* (1998), Holterman *et al.* (2006), Meldal *et al.* (2007), and Van Megen *et al.* (2009) have continued to expand this framework with additional molecular data. The most recent phylogeny by Van Megen *et al.* (2009) represented the first large-scale nematode tree, incorporating 1215 taxa and subdividing nematodes into 12 major clades. Further details of these various phylogenies are discussed in Section 1.8.

1.8 Unresolved questions in nematode phylogenetics

Our understanding of evolution within the Phylum Nematoda has improved drastically since the first molecular phylogeny by Blaxter *et al.* (1998), but many relationships remain unresolved. A number of longstanding questions have yet to be answered: 1) Which nematode taxa split first from all other groups? (and, consequently, how does this information contribute to our knowledge regarding the habitat of the ancestral nematode)? 2) What are the internal relationships within the basal clade Enoplia? 3) What evolutionary patterns can be observed for deep-sea nematodes?

1.8.1 Resolving early splits amongst nematodes

Our understanding of evolution within the Phylum Nematoda has improved drastically since the first molecular phylogeny by Blaxter *et al.* (1998), but many questions remain. Phylogenetic analyses have so far failed to answer the longstanding question surrounding the ancestral nematode—was the first nematode a marine or terrestrial species? The marine ancestry of nematodes was first proposed by Filipjev (1929; 1934), and the idea has garnered widespread support and acceptance amongst the scientific community (Lambshhead & Schalk 2001). A marine ancestry for nematodes would be plausible, based on the supposed evolution of metazoan life during the Precambrian and molecular clock rates that place nematodes diverging from the Metazoa circa 1000 Mya—pre-dating any known life on land (Meldal *et al.* 2007). However, divergence times based on molecular clock estimates are not entirely reliable, and the lack of a nematode fossil record further complicates attempts to characterise the lifestyle of the ancestral nematode. Marine ancestry has at least been proposed for some nematode groups, such as the Chromadorea and Rhabditida (Meldal *et al.* 2007). The mainly terrestrial Rhabditid clade is shown to be derived from the Monhysterida or Araeolaimida—clades that both contain predominantly marine species.

An alternate view suggests that nematodes could have first arisen and diversified in terrestrial habitats. De Ley and Blaxter (2004) argue that our knowledge of the early earth is not sufficient to presume a marine ancestry for nematodes, and it is plausible that the Cambrian explosion may simply reflect a mass migration from land to sea. There is some evidence to support the existence of productive terrestrial habitats during the Precambrian period when the Nematoda first appeared (Kenny & Knauth 2001), as well as

other hypotheses which envision the early ocean as harsh and inhospitable. One theory proposes that the marine environment was characterised by especially high salinity and low oxygen levels, and metazoan life was only able to invade the oceans once conditions had become more amenable (Knauth 1998). The widely publicized 'snowball earth' theory suggests several potential scenarios leading up to the Cambrian (Runnegar 2000). In the first, persistent oceanic glaciations and anoxic marine conditions resulted in an evolutionary bottleneck: only a few eukaryotic lineages were able to persist in isolated terrestrial refugia. Even if the early ocean was chemically suitable for life, metazoans may have first evolved in continental oases during such periods of global glaciation. However, other snowball earth scenarios propose that animal taxa could have instead survived in marine refugia—thus, this theory does not necessarily exclude a marine origin for nematodes.

Analysis of the Chromadorea reveals that transitions between terrestrial and marine habitats are surprisingly common amongst nematodes (Holterman *et al.* 2008). Marine sediments represent physically and chemically disparate environments—switches between terrestrial and marine environments are much more physiologically demanding, compared to switches between terrestrial and freshwater habitats. Freshwater nematodes can essentially be considered terrestrial species; the microenvironments of wet soil and freshwater sediments are nearly identical, and many terrestrial species can also be found in aquatic habitats (Abebe *et al.* 2006). Despite these physical differences between marine and terrestrial environments, habitat transitions have occurred at least 16 times within the Chromadorea (Holterman *et al.* 2008). It appears that nematodes are able to adjust to new habitats with relatively simple adaptations, potentially controlling osmoregulation through glycerol synthesis and breakdown (Lamitina *et al.* 2004; Huang *et al.* 2007). It is plausible that this ecological flexibility helped nematodes expand into diverse habitats early in their evolutionary history. However, the direction of this expansion—whether the first nematodes migrated from marine to terrestrial environments or *vice versa*—remains a mystery.

Recent phylogenies have utilised gene sequences from the small ribosomal subunit (SSU or 18S) to reconstruct ancient splits amongst nematode lineages. Early molecular frameworks did not offer any insight regarding the earliest branching taxa, but were able to separate nematodes into three main clades: the Enoplia, Dorylaimia and Chromadorea (Blaxter *et al.* 1998; De Ley & Blaxter 2002). This division roughly agreed with past morphological classifications set forth by Pearse (1942) and Inglis (1983) which also

proposed three main lineages (Abebe *et al.* 2006). The most recent phylogenies have found little support for De Ley and Blaxter's suggestion of a Chromadorid clade, but the Dorylaimia and Enoplia are consistently well-supported (Holterman *et al.* 2006; Meldal *et al.* 2007). These molecular frameworks have routinely placed both the terrestrial Dorylaimid clade and the primarily marine Enoplid clade towards the base of the nematode tree. Meldal *et al.* (2007) expanded the nematode tree to include representative marine taxa, but were unable to confirm the earliest branching lineage; the authors suggested that the SSU gene potentially lacked sufficient phylogenetic signal to pinpoint the ancestral nematode group. Using secondary structure information from SSU genes, Holterman *et al.* (2006) further divided the nematode tree into 12 clades, recovering the Enoplida as the earliest branching clade. However, this study reported low support values for this position of the Enoplia (posterior probabilities of 0.81 from Bayesian analyses). The authors noted that taxa in clades 9-12 appear to have increased rate of sequence evolution for the SSU gene. Differential rates of evolution may explain the difficulties in resolving deep relationships at the base of the nematode tree, as gene sequences from older lineages seem to possess less phylogenetic signal compared to more recently derived clades. Despite the suggestion of the Enoplida as the earliest branching nematode clade, all molecular phylogenies published to date have so far failed to unequivocally resolve the most ancestral group within the phylum.

Morphological and developmental data may support the early split of the Enoplida from all other nematodes. Members of the Enoplid clade seem to be unique amongst nematodes; developmental pathways in Enoplid species deviate substantially from the 'standard' development patterns observed in most other nematodes groups (Holterman *et al.* 2006). Embryo development in Enoplids shows no bilateral symmetry during early embryogenesis, lacks an asymmetrically dividing germ line, and exhibits only a weakly centralized nervous system (Malakhov 1994; Voronov *et al.* 1998; Schierenberg 2005). Blastomeres from the Enoplid nematodes *Enoplus brevis* and *Pontonema vulgare* exhibit a distinct lack of organisation in cell-lineage pattern, compared to nematodes in other clades where blastomeres can be distinguished even after the first division (Voronov *et al.* 1998). From these data it appears that Enoplid embryos retain a greater flexibility regarding which cells can contribute to particular body structures, compared to development in *C. elegans* where cell fate appears pre-programmed and much more deterministic. Developmental studies of *Tobrilus diversipapillatus* show a similar lack of distinct cell lineages, no asymmetric cleavages in early embryogenesis, and the formation of a

prominent coeloblastula which resembles 'classical' gastrulation seen in myriad animal taxa but not generally observed in nematodes (Schierenberg 2005). Morphological evidence suggests that Enoplids retain the ancestral trait of a nuclear envelope present in mature spermatozoa, compared to all other nematode groups which lack this anatomical feature (Baccetti *et al.* 1983; Justine 2002; Yushin 2003).

Previous phylogenies utilised small sequence datasets to represent the huge diversity of nematode taxa; the first molecular phylogeny utilised 53 gene sequences (Blaxter *et al.* 1998), while more recent phylogenies have included up to 350 nematode taxa (Holterman *et al.* 2006; Meldal *et al.* 2007). Increased taxon sampling has been shown to greatly improve phylogenetic resolution and aid recovery of accurate tree topologies (Lecointre *et al.* 1993; Zwickl & Hillis 2002; Philippe & Telford 2006), but computational limitations have previously hindered the analysis of larger datasets. Recent advances in computing power and phylogenetic algorithms have facilitated a move towards large-scale phylogenies (e.g. Robertson *et al.* 2005; Stamatakis 2006; Stamatakis *et al.* 2008); however, exhaustive analyses of nematodes have been hindered by the scarce availability of gene sequences for many taxonomic groups. Published nematode phylogenies have included only a few representatives from some highly diverse and ubiquitous marine taxa, such as the Enoplida and Microlaimoidea. Previously sparse representation within the Enoplida may have contributed to the uncertain placement of this clade—to date, ribosomal phylogenies have so far failed to unequivocally resolve the base of the nematode tree.

1.8.2 Internal relationships within the order Enoplida

The order Enoplida is an early splitting group of nematodes comprising many marine representatives. This taxon is thought to represent a state closest to the ancestral nematode, with all other nematode groups exhibiting derived and complexified forms. The phylogenetic topology of the Enoplida is not well resolved, and previous molecular frameworks have failed to firmly elucidate internal relationships amongst taxa (De Ley & Blaxter 2002; Holterman *et al.* 2006; Meldal *et al.* 2007). The Enoplids represent the largest marine nematodes in terms of physical size, and can reach up to several millimetres in length. Members of the Leptosomatidae represent the largest species (growing up to 30-50mm in length), while species from the Anticomidae are among the smallest observed Enoplids (measuring only 7-8mm in length) (Platonova & Gal'tsova 1985). Many groups

are thought to be active predators due to the complex array of teeth and mandibular structures exhibited in several families. Little is known about the biology or reproduction of most Enoplids, although species have been reported to exhibit both short and long generation times (Platt & Warwick 1983).

The most recent molecular frameworks currently classify the order Enoplida within the subclass Enoplia (class Enoplea) (De Ley & Blaxter 2002; De Ley & Blaxter 2004). De Ley and Blaxter's class Enoplea also encompasses terrestrial Dorylaimid nematodes within the subclass Dorylaimia. Morphological classifications had previously grouped the terrestrial order Triplonchida within the Dorylaimia, but these molecular frameworks have now placed this taxon within the subclass Enoplia. Despite molecular advances, Lorenzen's (1981) framework remains the currently accepted classification system for marine nematodes within the order Enoplida (Table 1.1), and has been used as the basis for Platt & Warwick's (1983) ubiquitous illustrated keys for identifying genera. Abebe *et al.* (2006) provide the most recent classification and key to the Dorylaimia, which has been completely updated to reflect inference from molecular data. Historical classification schemes of the Enoplia and Dorylaimia were based solely on morphology and often disagreed on the organisation and placement of taxa within this group. A number of taxonomic frameworks have attempted to classify the huge morphological diversity found within these groups, with previous systems primarily differing in their placement of the Tripyloididae, Alaimidae, Ironidae (all currently grouped in the Enoplia), and the Mononchoidea (now grouped under the Dorylaimia).

Filipjev (1934) was the first author to produce a comprehensive morphological classification of free-living nematodes. Species within the current Enoplia and Dorylaimia were all grouped within the order Enoplata, with this taxon containing four families: the Enoplidae, Trilobidae, Dorylaimidae, and Mermitidae. The Enoplidae contained nine subfamilies, the Leptosomatinae, Enoplinae, Oxystominae, Phanodermatinae, Thoracostomopsinae, Oncholaiminae, Rhabdodemaniinae, Eurystominae, and Enchelidiinae. The Leptosomatinae was a combination of Lorenzen's (1981) Anticomidae and Leptosomatidae, while Lorenzen's Enchelidiidae was split between Filipjev's Eurystominae and Enchelidiinae. Filipjev's Enoplinae also contained several genera (e.g. *Enoplolaimus*, *Enoploides*) which Lorenzen grouped within his Thoracostomopsidae. Filipjev's Trilobidae contained the subfamilies Trilobinae (containing the modern Tripylidae and Prismatolaimidae), Mononchinae, and Tripyloidinae (containing the modern Tripyloididae and Trefusiidae). The Alaiminae and Ironinae were grouped as separate

subfamilies within Filipjev's Dorylaimidae; members of the modern Diphtherophoridae and Trichodoridae were also contained in this family, classed under the Tylencholaiminae and Dorylaiminae, respectively.

Chitwood and Chitwood (1950) defined the order Enoplia within the class Aphasmidia, with this group containing the suborders Enoplina and Dorylaimina. The Enoplina consisted of the superfamilies Enoploidea (divided into the families Enoplidae and the Oncholaimidae) and Tripyloidea (containing the Tripylidae, Alaimidae, and Ironidae). The family Enoplidae contained the subfamilies Enoplinae, Leptosomatinae, Phanodermatinae, and Oxystomininae, while the Oncholaimidae contained the subfamilies Oncholaiminae, Eurystomininae, and Enchelidiinae. The suborder Dorylaimina contained the superfamilies Dorylaimoidea (containing the families Dorylaimidae, Leptonchidae, Diphtherophoridae and Belondiridae), Mermithoidea (containing the families Mermithidae and Tetradonematidae), and Trichuroidea (containing the families Trichuridae, Trichinellidae, and Cystoosidae).

Clark (1961) heavily revised previous classification schemes, using the position of the oesophageal glands and ducts as a basis for his new arrangement of taxa. Clark's system outlined five suborders: the Enoplina, Alaimina, Dorylaimia, Trichosyringina, and Dioctophymatina. The Enoplina contained the superfamilies Enoploidea (including families Enoplidae, Lauratonematidae, and Oncholaimidae) and Tripyloidea (including families Tripylidae and Ironidae). The family Enoplidae contained the equivalent of modern-day superfamily Enoploidea (Lorenzen 1981) plus the Oxystominidae. Clark was the first to classify the superfamily 'Diphtherophoroidea' as comprising the Diphtherophoridae and Trichodoridae; he placed this group within the Dorylaimina along with the Campydoridae. However, Clark later moved the Diphtherophoroidea into the suborder Alaimina (Clark 1962). Clark's classification followed on from Chitwood (1937) and Filipjev (1934), whose classifications were primarily based on parasitic and terrestrial species. Alternative classification of marine nematode species regarded all subfamilies within Clark's Enoplidae as families (e.g. Wieser 1953); this marine nomenclature later gained wide acceptance and is reflected in the most recent taxonomic revisions (Lorenzen 1981).

De Coninck (1965) proposed a similar classification to Clark. He defined the Subclass Enoplia containing two orders: the Enoplida (containing suborders Enoplina and Oncholaimina) and Dorylaimida (containing suborders Dorylaimina and Alaimina). The suborder Enoplina was further divided into the superfamilies Tripyloidea and Enoploidea; the Oncholaimina was split into the families Oncholaimidae and Eurystominidae. De

Coninck's Tripyloidea contained the Tripylidae (including the modern Tobrilidae) and the Ironidae. The Enoploidea was split into the families Leptosomatidae (containing the modern Anticomidae), Oxystominidae (containing the modern Trefusiidae), Lauratonematidae, Phanodermatidae, Thoracostomopsidae, and Enoplidae (containing genera such as *Mesacanthion* and *Enoploides*). The suborder Dorylaimina contained the superfamilies Mononchoidea (containing families Mononchidae and Bathyodontidae), Nygolaimoidea (containing families Nygolaimidae and Campydoridae), Dorylaimoidea (containing families Dorylaimidae, Actinolaimidae, Longidoridae, Belondiridae, Leptonchidae and Opailaimidae) and Diphtherophoroidea (containing only the family Diphtherophoridae).

Andrassy (1976) defined the Enoplida and Dorylaimida as two separate orders within the class Penetrantia. The Enoplida contained the suborders Enoplina, Oncholaimina and Tripylina, while the Dorylaimida contained the suborders Mononchina, Dorylaimina, Diphtherophorina, and Mermithina. The Enoplina contained superfamilies Leptosomatoidea (containing families Leptosomatidae and Thoracostomatidae) and Enoploidea (containing families Phanodermatidae, Enoplidae, and Thoracostomopsidae). The suborder Oncholaimina consisted of the Pelagonematoidea (containing only the family Pelagonematidae), Enchelidioidea (containing the families Eurystominidae, Enchelidiidae, and Belbollidae), and Oncholaimoidea (containing the families Mononcholaimidae and Oncholaimidae). Finally, the Tripylina contained the Oxystominoidea (containing the families Paroxystominidae, Oxystominidae and Alaimidae), Tripyloidea (containing the families Lauratonematidae, Tripylidae, and Prismatolaimidae) and Ironoidea (containing the families Cryptonchidae and Ironidae). The Tripylidae also contained the subfamily Tobrilinae, containing genera from the modern Tobrilidae. Andrassy followed on from previous classifications, and continued to lump several of Lorenzen's (1981) families within other groups; the Anticominae was considered a subfamily within the Leptosomatidae, and the Trefusiidae and the Bastianiidae were both grouped within the Oxystominidae. Andrassy raised both the Enoplinae and Thoracostomopsinae (Filipjev 1934) to the rank of family, but did not reorganise the member taxa. Most of the genera classed within Lorenzen's Thoracostomopsidae were retained alongside *Enoplus* in the Enoplidae—Andrassy designated the Thoracostomopsidae as having only two member genera, *Euthoracostomopsis* and *Thoracostomopsis*.

In contrast to other authors, Maggenti (1982) defined the subclass Enoplia within the class Adenophorea. Maggenti raised the rank of several taxa, and denoted the Enoplia

as containing seven orders: the Enoplida, Isolaimida, Mononchida, Dorylaimida, Trichocephalida, Mermithida and Muspiceida. The Enoplida was divided into three suborders: the Enoplina, Oncholaimina, and Tripylina. The Enoplina contained two superfamilies, the Enoploidea (containing the families Enoplidae, Lauratonematidae, Leptosomatidae, Phanodermatidae, and Thoracostomopsidae) and the Oxystominoidea (containing the families Paroxystominidae and Oxystominidae). The Oncholaimina contained only the superfamily Oncholaimoidea, which was divided into the families Oncholaimidae, Eurystominidae, and Symplocostomatidae. The suborder Tripylina included the superfamilies Tripyloidea (containing the Tripylidae and Prismatolaimidae) and the Ironoidea (Ironidae only). Under Maggenti's classification scheme, the Diphtherophorina and Alaimina were included as suborders within the Dorylaimida.

Lorenzen (1981) considerably rearranged the classifications of nematodes—within the class Adenophorea he defined the subclass Enoplia. He divided the Enoplia into three orders: the Enoplida (containing the suborders Enoplina and Tripyloidina), the Trefusiida, and Dorylaimida (containing the suborders Dorylaimina, Mononchina, and Bathyodontina). The Enoplina was further divided into the Enoplacea and the Oncholaimacea, and the classification of taxa within the Enoplina was mostly consistent with that of Filipjev (1934) and Chitwood & Chitwood (1950). The Enoplacea contained the superfamilies Enoploidea (including families Enoplidae, Thoracostomopsidae, Anoplostomatidae, Phanodermatidae, and Anticomidae), and Ironoidea (containing families Ironidae, Leptosomatidae, and Oxystominidae). The Oncholaimacea contained only the superfamily Oncholaimoidea (including families Oncholaimidae and Enchelidiidae). The suborder Tripyloidina consisted of the families Tripyloididae, Tobrilidae, Tripylidae, Triodontolaimidae, Rhabdodemaniidae, and Pandolaimidae. Lorenzen's classification made some notable alterations. The Anticomidae were separated from the Leptosomatidae and elevated to the rank of family, in contrast to previous classifications where the 'Anticominae' had been considered a subfamily within the Leptosomatidae (e.g. De Coninck 1965). Lorenzen rearranged the membership of the Enoplidae and the Thoracostomopsidae; *Enoplus* was retained as the only genus within the Enoplidae, while all other species were divided amongst three subfamilies in the Thoracostomopsidae (the Thoracostomopsinae, Trileptiinae, and Enoplolaiminae). The genera *Anoplostoma* and *Chaetonema* were placed into their own family, the Anoplostomatidae, based on buccal cavity morphology and the consistent arrangement of gonads to the left of the intestine within these taxa. Previously, *Chaetonema* had been grouped within the Enoplidae and *Anoplostoma* was associated

with the Oncholaimids (Andrássy 1976). In addition, the formerly separate family Eurystominidae was reduced to a subfamily within the Enchelidiidae. Within the Tripyloidina, the Tobrilidae and the Tripylidae were placed into separate families for the first time. Furthermore, Lorenzen drastically changed the placement of Bastianiidae and Pristomatolaimidae—he moved them out of the Enoplida completely and placed within the Leptolaimina (Chromadorida) based on amphid shape.

Lorenzen designated the order Trefusiida as containing the families Simpliconematidae, Trefusiidae, Onchulidae, Laurathonematidae, and Xenellidae. The Trefusiidae and Laurathonematidae were separated from their former place within the Enoplida and placed into their own order, the Trefusiida. Lorenzen viewed the presence of metanemes within the Enoplia as a synapomorphy for this group; all taxa which did not exhibit this morphological feature were placed within other groups. The Trefusiida was created as a paraphyletic grouping to hold the outliers from the Enoplia that did not easily fit into other groups, and he argued that its creation was necessary to ensure the monophyly ('holophyly') of the Enoplia. Molecular frameworks now firmly place the Triplonchida and Trefusiidae, two groups which lack metanemes, within the Enoplia (De Ley & Blaxter 2002; Holterman *et al.* 2006; Meldal *et al.* 2007). Although this placement appears contrary to Lorenzen's criteria for classification, De Ley and Blaxter (2002) uphold metanemes as a synapomorphy for Enoplids, proposing that this feature was secondarily lost in some groups.

Lorenzen established the monophyly of the Dorylaimia based on the posterior opening of the pharyngeal glands in comparison to the nerve ring. Taxa which did not fit this criterion were placed into the Bathyodontina, another non-monophyletic suborder created to hold outlier groups. This Bathyodontina contained seven families: the Bathyodontidae, Cryptonchidae, Mononchulidae, Diphtherophoridae, Trichodoridae, Isolaimiidae, and Alaimidae. The rank of the Alaimidae was substantially reduced compared to previous classifications that placed this group within its own suborder (Clark 1961). Lorenzen also did not agree with the superfamily Diphtherophoroidea, and separated the member taxa back into separate families within the Bathyodontina (Diphtherophoridae and Trichodoridae).

Malakhov (1994) recently argued that the true classification of the subclass Enoplia most likely agrees with that outlined by Pearse (1942). Under this system, the Enoplia contained seven orders: Enoplida, Marimermithida, Mononchida, Dorylaimida, Mermithida, Trichocephalida, and Dioctophymida. The Enoplida contained the suborders

Enoplina, Oncholaimina and Tripyloidina. Furthermore, the Diphtherophorina was recognized as a valid taxon and grouped within the Dorylaimida.

De Ley and Blaxter (2002) proposed the first comprehensive classification of the phylum Nematoda based on SSU sequence data, following on from the first groundbreaking molecular phylogeny by Blaxter *et al.* (1998). De Ley and Blaxter designated the higher taxon names according to Inglis (1983) and Pearse (1942), denoting the class Enoplea as containing the subclasses Enoplia and Dorylaimia. De Ley and Blaxter outlined three orders within the Enoplia (the Enoplida, Triplonchida and Trefusiida) and eight orders within the Dorylaimia (the Dorylaimida, Mononchida, Isolaimida, Dioctophymatida, Muspiceida, Marimermithida, Mermithida, and Trichinellida). The order Enoplida comprises the suborders Enoplina, Oncholaimina, Ironina, Tripyloidina, and Alaimina. De Ley and Blaxter's classification of the suborder sEnoplina (containing only the superfamily Enoploidea), Ironina (containing only the superfamily Ironoidea), and Oncholaimina (containing only the superfamily Oncholaimoidea) is consistent with morphological groupings according to Lorenzen (1981). Sequence data indicated that the Alaimidae belonged in its own suborder within the Enoplida, contrary to many morphological classifications. De Ley and Blaxter's Triplonchida consisted of the suborders Diphtherophorina, Tobrilina, and Tripylina. Molecular data indicated that Lorenzen's Tripyloidina was actually a paraphyletic grouping; phylogenetic relationships indicated that the Tripyloididae belonged within the Enoplida (suborder Tripyloidina), while other families showed a closer association with the Triplonchida. The Tobrilidae, Triodontolaimidae, Rhabdodemaniidae, and Pandolaimidae were classed together under the suborder Tobrilina (forming the superfamily Tobriloidea) within the Triplonchida, while the Tripylidae was separately placed within the suborder Tripylina. Membership within the Trefusiida was consistent with Lorenzen's classification, with the exception of the Onchulidae which De Ley and Blaxter moved into the Tripylina. Phylogenetic relationships did not support Lorenzen's classification of the Prismatolaimidae within the Chromadorida. Molecular evidence supported earlier morphological classifications which placed this group within subclass Enoplia; De Ley and Blaxter grouped the Prismatolaimidae within the order Triplonchida (suborder Tobrilina) based on SSU data.

Despite this comprehensive molecular framework proposed by De Ley and Blaxter, molecular phylogenies have so far been unable to resolve internal relationships within the order Enoplida—this is primarily because few SSU gene sequences were available for inclusion in past phylogenetic analyses. In an updated version of their classification

scheme (De Ley & Blaxter 2004), De Ley and Blaxter revised the internal structure of the Enoplida. The Trefusiida was moved into the Enoplia and lowered to the rank of suborder and the suborder Campydorina was moved from the Dorylaima into the Enoplida. In a more recent phylogeny, Meldal *et al.* (2007) noted that the monophyly of some Enoplid families was highly supported (e.g. the Oncholaimoidea and Tripyloididae), whilst other families were suspected to be paraphyletic (e.g. the Ironidae). Holterman *et al.* (2006) and Van Megen *et al.* (2009) also recovered the Bastianiidae and the Rhabdolaimidae within the Enoplida, despite De Ley and Blaxter's suggestion that they belonged in the order Plectida (subclass Chromadoria). Van Megen *et al.* (2009) utilised more Enoplid sequences compared to any other investigation (including 39 taxa in their analysis), but the placement of many major clades was still not well resolved. Many more gene sequences from Enoplid specimens will be required to clarify evolutionary relationships at lower taxonomic levels within the Enoplida

Table 1.1: Taxonomy of free-living marine nematodes within the Subclass Enoplia (after Platt and Warwick, 1983)

Order	Suborder	Superfamily	Family	Genus
Enoplida	Enoplina	Enoploidea	Enoplidae	<i>Enoplus</i> Dujardin, 1845
Enoplida	Enoplina	Enoploidea	Thoracostomopsidae	<i>Enoploides</i> Ssaweljev, 1912 <i>Enoplolaimus</i> De Man, 1893 <i>Epacanthion</i> Wieser, 1953 <i>Mesacanthion</i> Filipjev, 1927 <i>Mesacanthoides</i> Wieser, 1953 <i>Oxyonchus</i> Filipjev, 1927 <i>Paramesacanthion</i> Wieser, 1953 <i>Thoracostomopsis</i> Ditlevsen, 1918 <i>Trileptium</i> Cobb, 1933
Enoplida	Enoplina	Enoploidea	Anoplostomatidae	<i>Anoplostoma</i> Bütschli, 1874 <i>Chaetonema</i> Filipjev, 1927
Enoplida	Enoplina	Enoploidea	Phanodermatidae	<i>Crenopharynx</i> Filipjev, 1934 <i>Micoletzkyia</i> Ditlevsen, 1926 <i>Phanoderma</i> Bastian, 1865 <i>Phanodermella</i> Kreis, 1928 <i>Phanodermopsis</i> Ditlevsen, 1926
Enoplida	Enoplina	Enoploidea	Anticomidae	<i>Anticoma</i> Bastian, 1865 <i>Anticomopsis</i> Micoletzky, 1930 <i>Cephalanticoma</i> Platonova, 1976 <i>Odontanticoma</i> Platonova, 1976 <i>Paranticoma</i> Micoletzky, 1930

Order	Suborder	Superfamily	Family	Genus
Enoplida	Oncholaimina	Oncholaimoidea	Oncholaimoidea	<i>Adoncholaimus</i> Filipjev, 1918 <i>Filoncholaimus</i> Filipjev, 1927 <i>Metaparoncholaimus</i> Filipjev, 1918 <i>Metoncholaimus</i> Filipjev, 1918 <i>Meyersia</i> Hopper, 1967 <i>Oncholaimellus</i> De Man, 1890 <i>Oncholaimus</i> Dujarkin, 1845 <i>Pontonema</i> Leidy, 1855 <i>Prooncholaimus</i> Micoletzky, 1924 <i>Viscosia</i> De Man, 1890
Enoplida	Oncholaimina	Oncholaimoidea	Enchelidiidae	<i>Bathyeurystomina</i> Lamshead and Platt, 1979 <i>Belbolla</i> Andrassy, 1973 <i>Calyptonema</i> Marion, 1870 <i>Ditlevsenella</i> Filipjev, 1927 <i>Eurystomina</i> Filipjev, 1921 <i>Pareurystomina</i> Micoletzky, 1930 <i>Polygastrophora</i> De Man, 1922 <i>Symplocostoma</i> Bastian, 1865
Enoplida	Ironina	Ironoidea	Ironidae	<i>Dolicholaimus</i> De Man, 1888 <i>Parironus</i> Micoletzky, 1930 <i>Pheronus</i> Inglis, 1966 <i>Syringolaimus</i> De Man, 1888 <i>Thalassironus</i> De Man, 1889 <i>Trissonchulus</i> Cobb, 1920

Order	Suborder	Superfamily	Family	Genus
Enoplida	Ironina	Ironoidea	Leptosomatidae	<i>Cylicolaimus</i> De Man, 1889 <i>Deontosoma</i> Filipjev, 1916 <i>Leptosomatides</i> Filipjev, 1918 <i>Leptosomatum</i> Bastian, 1865 <i>Metacylicolaimus</i> Stekhoven, 1946 <i>Platycoma</i> Cobb, 1894 <i>Platycomopsis</i> Ditlevsen, 1926 <i>Pseudocella</i> Filipjev, 1927 <i>Synonchus</i> Cobb, 1894 <i>Thoracostoma</i> Marion, 1870
Enoplida	Ironina	Ironoidea	Oxystominidae	<i>Halalaimus</i> De Man, 1888 <i>Litinium</i> Cobb, 1920 <i>Nemanema</i> Cobb, 1920 <i>Oxystomina</i> Filipjev, 1921 <i>Paroxystomina</i> Micoletzky, 1924 <i>Thalassolaimus</i> De Man, 1893 <i>Wieseria</i> Gerlach, 1956
Enoplida	Tripyloidina	Tripyloidoidea	Tripyloididae	<i>Bathylaimus</i> Cobb, 1894 <i>Gairleanema</i> Warwick and Platt, 1973 <i>Tripyloides</i> De Man, 1886
Trefusiida			Trefusiidae	<i>Cytolaimium</i> Cobb, 1920 <i>Halanonchus</i> Cobb, 1920 <i>Rhabdocoma</i> Cobb, 1920 <i>Trefusia</i> De Man, 1893 <i>Trefusialaimus</i> Riemann, 1974
Trefusiida			Lauratonematidae	<i>Lauratonema</i> Gerlach, 1953
Trefusiida			Xenellidae	<i>Xenella</i> Cobb, 1920

1.8.3 The origin of deep-sea fauna

Another longstanding question concerns the evolution of deep-sea nematode fauna. There is some evidence to suggest the existence of novel deep-sea nematode taxa (J. Lamshead, unpublished data); such novel taxa may be a product of the deep-sea's unique evolutionary trajectory and the influence of historic fluctuations in oxygen availability. Expansion and contraction of anoxic zones in the deep-sea would have likely resulted in waves of extinction and radiation, respectively, for deep-sea fauna (Rogers 2000). As a dominant abyssal group with limited dispersal capabilities, past nematode faunas would theoretically be at the mercy of climatic events and fluctuations in physical conditions. Fossil evidence (Jablonski & Bottjer 1988; Sepkoski 1991) and biogeographic data (Rex *et al.* 2005) from other taxa suggest that deep-sea species represent radiations from shallow-water taxa. It is unknown whether the current deep-sea nematode fauna represent relatively recent radiations or much older lineages; different depths (e.g. abyssal versus bathyal) may have acted variably as source or sink habitats following historical fluctuations in anoxic zones (Rogers 2000). Many deep-sea genera are cosmopolitan in their occurrence, but it is not known if nematode species exhibit similar widespread distribution. Data from shallow water species indicates that the same species can span vast geographical distances (Bhadury *et al.* 2008; Derycke *et al.* 2008), raising questions about the long-distance dispersal capabilities of nematode taxa. Only a limited amount of molecular data has previously been obtained for deep-sea taxa, and these nematode specimens have not been subject to phylogenetic analysis. Future investigations will need to incorporate the deep-sea nematode fauna into existing molecular frameworks.

1.9 Conclusions

The increasing sophistication of molecular analyses has dramatically improved our understanding of evolutionary relationships within the Phylum Nematoda. Nematode investigations have addressed questions ranging from populations genetics to deep phylogeny, using a wide breath of genetic loci, molecular techniques, and analysis methods. Past molecular frameworks were able to define phylogenetic relationships and provide new insight on the evolution of morphological characters, despite the comparatively limited computational power available for these studies. Recently, increases in computing power and the development of efficient phylogenetic algorithms have helped to usher in a new era of large-scale phylogenetics.

This chapter has reviewed the scope of molecular investigations in nematodes, providing insight on future prospects and unanswered questions. Nematode studies need to address several important questions, particularly in regard to the evolutionary origin of nematodes and radiation of deep-sea fauna. Taxon sampling is one of the most important considerations in phylogenetic studies. Future investigations will need to incorporate dense sampling methodology, in combination with multiple genetic loci and rigorous empirical test—such comprehensive studies will be necessary to address longstanding evolutionary questions.

1.10 Aims and Objectives

This thesis aims to resolve the phylogenetic status of the Order Enoplida using sequence data from multiple genes, as well as elucidate relationships between shallow-water and deep-sea nematodes. Prior to this investigation, few publically available full-length SSU sequences were available for Enoplid nematodes; no deep-sea nematode sequences had yet been published. Morphological data and at least two gene sequences were each collected from over 200 Enoplid nematodes (representing approximately 30 genera), with specimens obtained from a variety of deep-sea and intertidal marine habitats. This study aimed to obtain a wide taxonomic breadth within the Enoplida, but this goal was sometimes hindered by the availability of specimens from sediment cores. Some families were well represented (e.g. the Oncholaimidae, Oxystominidae), while other families were represented by only one or two specimens (e.g. the Leptosomatidae).

Structural alignments were utilised to reconstruct phylogenies from the 18S and 28S ribosomal rRNA genes, and a range of phylogenetic methods and parameters were used to test hypotheses of tree topology. Previous phylogenies of the Phylum Nematoda had utilised only a small subset of taxa for analyses. This investigation has taken advantage of recent advances in computing power and phylogenetic algorithms, aiming to build a large-scale, comprehensive phylogeny of the Phylum Nematoda, with drastically increased taxon-sampling within the largely understudied Enoplid group.

Molecular data from multiple genes were analysed in order to resolve the phylogenetic placement of higher clades within the Enoplida, and also to investigate lower taxonomic relationships between approximately 30 Enoplid genera. Additionally, sequence data from different geographic locations were compared in order to shed light on evolutionary relationships between shallow water and deep-sea nematode fauna, as well as assess genetic divergence for shallow-water genera found in disparate locales.

2. Materials and Methods

2.1 Sampling Regime

Samples for this investigation were collected from a variety of shallow-water and deep-sea locations (refer to Table 2.1 for detailed geographic information). Shallow-water sample sites were specifically chosen to represent locations on the Eastern and Western shores of the Atlantic, with additional samples collected from a volcanic island (Azores) and along the coast of South Africa. East/West Atlantic samples were used to compare species in similar habitats that were separated by large geographic distances; other shallow water samples (Azores and South Africa) were included in this study because of their availability, and not for testing any particular geographic hypothesis. Deep-sea sample sites were not chosen based on any geographic pattern; samples were analysed based on the availability of material. Deep-sea cores were obtained from molecular samples currently available in museum collections (NHM), and additional arrangements were made to collect fresh material from several research cruises.

2.1.2 Collection of shallow water samples

Fresh estuarine sediment was collected from all sites delineated as 'intertidal' in Table 2.1; sediment types ranged from coarse sand to fine mud, depending on sampling site. Non-quantitative samples were collected from most intertidal sites, with the exception of the two sites in South Africa, where samples represented quantitative cores. For non-quantitative samples, sediment was collected at the low water mark using a spade (utilising a sampling depth of approximately 5cm) and material was immediately fixed in DESS preservative. DESS preservative is a dimethyl sulphoxide (DMSO)/EDTA solution saturated with sodium chloride, and is the currently recommended solution for preserving both morphology and DNA in nematode specimens (Yoder *et al.* 2006); the full recipe for DESS preservative used in this study is outlined in Appendix IV. An equal ratio of preservative to sediment was used for each sample, and all samples were thoroughly shaken after collection to distribute the preservative. Quantitative samples were collected using a Perspex hand corer pushed into the sediment; the top 5cm of sediment was sliced off and immediately preserved in DESS, using the same procedure as non-quantitative

samples. All intertidal samples were kept at room temperature whilst being transported to the Natural History Museum. Upon arrival at the NHM, preserved samples were placed into cold storage at 4°C.

2.1.3 Collection of deep-sea samples

Deep-sea samples were collected from the seabed using a Megacorer, consisting of a large metal frame equipped with a ring of Perspex tubes (each 10cm in diameter). Sediment from the top 1-3 centimetres of deep-sea cores (representing either a full core tube or a subsample within a core) was sliced off and immediately preserved in DESS. With the exception of the CROZET samples, deep-sea cores collected during this study are not quantitative. Equal ratios of sediment to preservative were used for all samples, and each sample was shaken thoroughly after collection in order to distribute the DESS preservative. For the quantitative CROZET samples, the top centimetre of each core was removed and washed with filtered seawater on a 45µm sieve to remove as much sediment as possible. All material retained on the sieve was then transferred to DESS preservative. All deep-sea samples were kept at room temperature whilst being transported to the Natural History Museum. Upon arrival at the NHM, preserved samples were placed into cold storage at 4°C.

2.1.4 Sample processing

The meiofauna fraction of all samples was extracted *via* decantation and floatation in Ludox[®] colloidal silica (W.R. Grace & Co.-Conn.) using a 45µm sieve according to the methods of Somerfield *et al.* (2005). For decantation, sediment samples were transferred to a 2 liter graduated cylinder, and filtered tap water was added until a final volume of 2 liters was reached. This mixture was inverted 10 times and then set down and allowed to settle for 30 seconds; after this time, the supernatant was poured over a 45µm sieve. This process was repeated 10 times in order to fully separate the meiofauna fraction from sediment particles. For samples containing muddy or clay sediments, the entire sediment sample was pre-washed on 45µm sieve before decantation (using filtered tap water), in order to remove as much fine sediment as possible. All meiofauna fractions and sediment residues were returned to DESS preservative solution following extraction.

The meiofauna fraction of certain samples retained a high proportion of sediments after decantation. These particular samples were subsequently processed using flotation in Ludox, in order to further separate meiofauna from sediment particles. Ludox (a mixture of colloidal silica and water, prepared at a specific gravity of 1.16) was used to wash meiofauna fractions into 100ml plastic centrifuge tubes, and tubes were filled until each was approximately three-quarters full. Tubes were thoroughly shaken and then centrifuged at 4000 RPM for five minutes, using a Hermle Z323 centrifuge (Hermle Labortechnik, Wehingen, Germany). During centrifugation, heavy sediment particles settle out of the Ludox mixture, but the meiofauna fraction remains in suspension. The resulting supernatant was then poured over a 45 μ m sieve and washed with filtered tap water to remove any remaining Ludox; this centrifugation process was carried out ten times per sample. At the end of the flotation process, all extracted meiofauna fractions were returned to DESS solution, with sediment residues archived separately in DESS. All extracted meiofauna fractions were placed into storage at 4°C; sediment residues from decantation and flotation in Ludox were archived at room temperature.

Table 2.1: Geographic data and collection depth of all sample sites used in this study. Short location codes were used to identify nematodes from different geographic locations after individual worms were digested for molecular work

Location	Coded As	Latitude	Longitude	Depth	Collected
Appledore, Torridge Estuary, UK	AUK/BAUK	51° 1' 54" N	4° 12' 12" W	Intertidal	19-Feb-08
Llansteffan, Towy Estuary, UK	LUK	51° 47' 18" N	4° 22' 15" W	Intertidal	20-Feb-08
All Hallows, Thames Estuary, UK	HUK	51° 28' 52.56" N	0° 38' 47.58" E	Intertidal	21-Jun-08
Shoebury Ness, Thames Estuary, UK	SBN	51° 31' 40.32" N	0° 48' 43.44" E	Intertidal	18-Jun-08
Helensburgh, Clyde Estuary, UK	HCL	56° 0' 10.97" N	4° 44' 12.87" W	Intertidal	30-Aug-08
Lunderston, Clyde Estuary, UK	LCL	55° 55' 15.27" N	4° 52' 38.51" W	Intertidal	30-Aug-08
Barnstable, Massachusetts, USA	BUS	41° 50' 35.48" N	69° 57' 4.62" W	Intertidal	28-Mar-08
Nauset, Massachusetts, USA	NUS	41° 42' 19.70" N	70° 18' 5.87" W	Intertidal	28-Mar-08
Narragansett, Rhode Island, USA	NAR	41° 26' 5.96" N	71° 27' 19.43" W	Intertidal	27-Jun-08
Scarborough, Rhode Island, USA	SUS	41° 23' 26.35" N	71° 28' 16.52" W	Intertidal	27-Jun-08
Odiorne Point, New Hampshire, USA	OUS	43° 2' 54.62" N	70° 43' 47.0" W	Intertidal	19-Jun-08
Wallis Sands State Beach, New Hampshire, USA	WUS	43° 1' 37.44" N	70° 43' 41.82" W	Intertidal	19-Jun-08
Porto Pim, Faial island, Azores	PPA	38° 31' 25" N	28° 37' 32" W	Intertidal	13-Sep-08
Dolphin Beach, Cape Agulhus, South Africa	DBA	33° 48' 44.02" S	18° 28' 10.73" E	Intertidal	26-Jan-07
Struis Bay, South Africa	SBA	34° 47' 24.82" S	20° 2' 51.29" E	Intertidal	23-Jan-07
Erosional Fairway, Seine Abyssal Plain, Atlantic Ocean, JC27-22#1	JCC	35° 33' 16.8" N	9° 41' 55.2" W	4321 m	15-Aug-08
Inside Scour, Seine Abyssal Plain, Atlantic Ocean JC27-25#2	JCC	35° 44' 45" N	9° 59' 16.2" W	4630 m	16-Aug-08
Sao Vicente Canyon Mouth, Atlantic Ocean, JC27-29	JCC	36° 13' 3.6" N	10° 1' 49.2" W	4878 m	17-Aug-08
Cascais canyon mouth, Atlantic Ocean, JC27-43	JCC	38° 21' 39.6" N	9° 59' 4.8" W	4572 m	22-Aug-08
Cascais canyon, Atlantic Ocean, JC27-45	JCC	38° 23' 18" N	10° 24' 7.8" W	4835 m	23-Aug-08
Off coast California, Thistle Cruise, 112 Nem	TCR	43° 59' 49.98" N	130° 23' 36" W	3260 m	16-Sep-08
Off coast California, Thistle Cruise, 221 Nem	TCR	42° 33' 28.32" N	132° 0' 40.2" W	3605 m	18-Sep-08
Off coast California, Thistle Cruise, 312 Nem	TCR	39° 59' 58.2" N	125° 52' 27.24" W	3673 m	20-Sep-08
Off coast California, Thistle Cruise, 418 Nem	TCR	39° 59' 52.86" N	125° 26' 36.06" W	2730 m	21-Sep-08
Off coast California, Thistle Cruise, 518 Nem	TCR	36° 47' 17.28" N	123° 41' 28.86" W	3673 m	23-Sep-08
Off coast California, Thistle Cruise, 617 Nem	TCR	36° 40' 52.2" N	122° 49' 36.6" W	2692 m	24-Sep-08
Off coast California, Thistle Cruise, 712 Nem	TCR	32° 52' 39.42" N	120° 36' 30.84" W	3855 m	27-Sep-08

(Continued)

Location	Coded As	Latitude	Longitude	Depth	Collected
Off coast California, Thistle Cruise, 817 Nem	TCR	32° 47' 49.14" N	120° 22' 16.02" W	2720 m	28-Sep-08
Off coast California, Thistle Cruise, 856 Nem	TCR	32° 47' 54.24" N	120° 22' 20.7" W	2694 m	30-Sep-08
Off coast California, Thistle Cruise, 861 Nem	TCR	32° 47' 52.32" N	120° 22' 18.36" W	2695 m	1-Oct-08
Bellinghausen Sea, Shelf N' Alexander Island, off Antarctica, Biopearl II BC 470	BCA	69° 05' 18" S	76° 23' 21" W	670 m	29-Feb-08
Pine Island Bay, inner shelf basin, off Antarctica, Biopearl II BC 476	BCA	74° 29' 00" S	104° 25' 00" W	1120 m	6-Mar-08
Pine Island Bay, inner shelf basin, off Antarctica, Biopearl II BC 477	BCA	74° 21' 47" S	104° 40' 19" W	1406 m	6-Mar-08
Southern Indian Ocean, off Crozet islands, CROZET core 15772#2	Cr	44° 29' 40" S	50° 0' 54" E	2908 m	8-Dec-05
Southern Indian Ocean, off Crozet islands, CROZET core 15773#18	Cr	45° 52' 57" S	56° 23' 46" E	4186 m	15-Dec-05
Southern Indian Ocean, off Crozet islands, CROZET core 15773#21	Cr	45° 53' 40" S	56° 24' 23" E	4193 m	15-Dec-05
Southern Indian Ocean, off Crozet islands, CROZET core 15773#27	Cr	45° 53' 33" S	56° 25' 1" E	4210 m	18-Dec-05
Southern Indian Ocean, off Crozet islands, CROZET core 15773#31	Cr	45° 53' 48" S	56° 25' 46" E	4200 m	20-Dec-05
Southern Indian Ocean, off Crozet islands, CROZET core 15775#3	Cr	49° 3' 38" S	51° 14' 12" E	4202 m	27-Dec-05
Southern Indian Ocean, off Crozet islands, CROZET core 15775#25	Cr	49° 4' 31" S	51° 13' 7" E	4202 m	3-Jan-06
Southern Indian Ocean, off Crozet islands, CROZET core 15775#32	Cr	49° 2' 30" S	51° 12' 50" E	4197 m	4-Jan-06
Southern Indian Ocean, off Crozet islands, CROZET core 15775#33	Cr	49° 1' 58" S	51° 13' 58" E	4192 m	4-Jan-06
Southern Indian Ocean, off Crozet islands, CROZET core 15775#37	Cr	49° 1' 52" S	51° 14' 5" E	4192 m	5-Jan-06

2.2 Time Series experiments

The original aim of this PhD project was to construct the first molecular phylogeny of deep-sea nematodes, utilising abyssal plain samples (4000m depth) collected during the Benthic CROZET project. Lengthy attempts were made to isolate nematode DNA and obtain reliable sequence data from this material, but continued problems resulted in a decision to abandon work on the CROZET samples. Persistent contamination was an ongoing issue that often prohibited any PCR amplification whatsoever; in cases where PCR products were obtained, sequence results were mostly bad quality or matched to fungal sequences after BLAST searches.

Previous work suggested that the traditional preparation of nematodes for taxonomic identifications could be adversely affecting DNA preservation (Meldal 2004), and further enquiry revealed that other labs were experiencing similar problems (Simon Creer, personal communication). Taxonomic methodology dictates nematodes must be picked out of preservative solution and desiccated overnight in dehydrating solution (water, alcohol, and glycerol) in order to harden anatomical structures and ease visualisation under the light microscope. Desiccated nematodes are then transferred to a drop of 100% glycerol within a wax ring on a glass slide and heated to melt the wax, thus securing the coverslip. Meldal (2004) noted that this methodology of mounting nematodes in glycerol seemed to affect subsequent success of PCR amplification depending on the length of time specimens were stored in slide mounts before being removed for DNA extraction. Although Meldal's results were not conclusive, it was decided that DNA degradation could be an important factor in the original failure of the CROZET specimens; nematodes were often left mounted for months at a time before the slides were broken open and DNA extracted. Additionally, the amplification failure of the CROZET samples may have been related to the method of preservation. The standard DESS protocol calls for a final 20% DMSO content, but it was discovered that the DESS preserving the CROZET samples had been incorrectly prepared with a final DMSO content of only 5%.

To determine the true cause of the recurrent molecular problems in the CROZET samples, two time series experiments were designed: one to test the effect of the slide mounting process, and another to assess the effect of preservative strength.

2.3 Taxonomic identification and video capture of Enoplid specimens

For each sample site, nematodes were removed from preserved meiofauna fractions and picked into dehydrating solution (water, glycerol, and molecular grade ethanol) using a fine wire instrument. Specimens were desiccated at room temperature for a maximum of 24 hours before being mounted on slides. After desiccation, nematodes were mounted in a drop of anhydrous glycerol on glass slides (up to 3 specimens per slide) and sealed with a wax ring. Due to the apparent degradation of DNA over time for slide mounted nematodes, specimens intended for DNA sequencing were stored for no longer than 3 days in slide mounts before being removed for molecular analyses. Generally, it was possible to process one sample per day, and most nematodes sequenced in this study were kept in slide mounts for less than 24 hours.

Slide mounted nematodes were examined under a light microscope (Olympus BH-2) using differential interference contrast; all Enoplid nematodes encountered were identified down to genus level. High-definition video capture images were recorded as a morphological voucher for all Enoplid specimens, using a Canon HG10 HD camcorder (Canon Inc., Tokyo, Japan). For each nematode, separate video files were recorded to detail the head/buccal cavity features, tail shape, overall body shape, and male reproductive structures (if present). Additional features were recorded for specific genera, for example, the presence of oesophageal bulbs in *Syringolaimus* specimens.

After identification, Enoplids were removed from slide mounts, washed in distilled water, and transferred to a 1.5ml microcentrifuge tube containing molecular-grade distilled water. At this stage, samples were typically frozen overnight at -20°C. The number of Enoplid nematodes per sediment sample could vary widely, and time constraints meant it was easier to extract DNA in batches after a few samples had been processed. This temporary freezing was also used to physically disrupt the tough nematode cuticle and ease extraction of genomic DNA.

2.4 Final protocol for DNA extraction, PCR, and sequencing

Frozen microcentrifuge tubes containing individual Enoplids in 25µl sterile water were thawed in preparation for molecular work. Genomic DNA of all nematodes was extracted *via* proteinase K digestion following the methodology of Holterman *et al.* (2006). An equivalent volume (25µl) of lysis buffer (containing 0.2 M NaCl, 0.2 M Tris-HCl (pH 8.0),

1% β -mercaptoethanol and 800 $\mu\text{g/ml}$ proteinase K) was added to microcentrifuge tubes containing individual nematodes. The final reaction volume was incubated for 2 h at 65°C and 750 rpm in an Eppendorf Thermomixer (Eppendorf, Hamburg, Germany), followed by a final 5 min at 100°C and 750 rpm to inactivate the proteinase K enzyme. Final lysates were stored at -20°C.

All PCR reactions were conducted using a DyNAzyme EXT PCR kit (New England Biolabs, Ipswich, MA, USA), with a final reaction volume of 25.75 μl . Each reaction contained 2 μl of nematode genomic DNA, 18.25 μl sterile water, 0.4 μM of each primer (Integrated DNA technologies, Coralville, IA, USA) 2.5 μl 10X DyNAzyme EXT Buffer containing MgCl_2 (final reaction concentration 1.5mM MgCl_2), 0.5 μl dNTP mix containing 10 μM of each nucleotide, and 0.5 μl DyNAzyme EXT DNA polymerase (0.5 enzyme units in final reaction volume). The DyNAzyme polymerase was chosen based on its ability to proofread DNA during PCR; such proofreading enzymes reduce the risk of incorrect bases being incorporated during gene amplification, resulting in high fidelity sequences. This study attempted to amplify three genes from each Enoplid nematode, encompassing two nuclear genes and one mitochondrial locus: the entire 18S rRNA gene (~1650bps), the D2/D3 expansion segment of the 28S rRNA gene (~650bps) and a segment of the mitochondrial Cox1 gene (~400bps). Both 18S and 28S genes were successfully amplified from a total of 256 Enoplid nematode specimens; Cox1 was additionally amplified from a subset of these nematodes (85 specimens in total).

The following PCR profile was used to amplify all primer sets for all three genes: 94°C for 5 min followed by 35 cycles of denaturation at 94°C for 30 seconds, annealing at 54°C for 45 seconds, and extension at 72°C for 2 minutes, with a final extension of 72°C for 10 min. Table 2.2 lists all primers used in this study. The 18S rRNA gene was amplified in three fragments using primer sets G18S4 and 26R, 22F and 13R, and 24F1 and 18P. The D2/D3 expansion segment could be fully amplified in one reaction, using primers D2A and D3B. Cox1 was also amplified as a single fragment using primers JB3 and JB5. Positive and negative controls were used for all reactions to confirm successful PCR, and all reactions were stored at 4°C once completed. All PCR products were visualized by running 4 μl of completed reactions on a 1.5% agarose gel containing ethidium bromide (final concentration 0.5 $\mu\text{g/ml}$).

Successful PCR reactions were purified using a QIAquick PCR purification kit (QIAGEN, Valencia, CA, USA), using the manufacturer's protocol for purification using a microcentrifuge. Steps were carried out according to the manufacturer's instructions,

apart from final elution of DNA which was completed using 30 μ l molecular-grade distilled water. The manufacturer recommends eluting DNA in 50 μ l of its own Buffer EB, but personal experiences suggested that this buffer can potentially interfere with downstream sequencing reactions. Thus, during this study it was more reliable to store purified PCR products in water alone. Furthermore, single-nematode PCR reactions generally do not produce overwhelming amounts of amplified DNA; eluting in a smaller volume of water further concentrated the PCR amplicons and improved the quality of sequencing reactions.

Sequencing reactions were carried out using a BigDye Terminator v3.1 cycle sequencing kit (Applied Biosystems, Foster City, CA, USA), with individual sequencing reactions having a final volume of 10 μ l. Each reaction contained 3 μ l 5X ABI sequencing buffer, 2 μ l of 2 μ M forward or reverse primer, 1 μ l BigDye Terminator v1.1, and either 2 μ l or 4 μ l of purified PCR product. The amount of PCR product to use in sequencing reactions was based visual inspections of gel photographs; 2 μ l of purified PCR product was used for reactions displaying strong, bright bands, while a larger volume of purified DNA (4 μ l) was used for fainter bands. For sequencing reactions containing only 2 μ l of purified PCR product, an additional 2 μ l of molecular grade water was added in order to reach the final reaction volume. The same primers were used for both PCR and sequencing reactions, and all PCR products were sequenced in both forward and reverse directions. Sequencing reactions were carried out using the following thermal profile: 96°C for 1 minute followed by 25 cycles of 96°C for 10 seconds, 50°C for 5 seconds, and 60°C for 4 minutes. Completed reactions were wrapped in aluminium foil (to prevent light-induced degradation of cycle-sequencing product), and stored at 4°C.

Table 2.2: Nematode primers used in final PCR and sequencing protocols.

Primer Name	Gene Amplified	Primer Sequence (5' → 3')	Reference
G18S4	18S rRNA	GCT TGT CTC AAA GAT TAA GCC	(Blaxter <i>et al.</i> 1998)
26R	18S rRNA	CAT TCT TGG CAA ATG CTT TCG	(Blaxter <i>et al.</i> 1998)
22F	18S rRNA	TCC AAG GAA GGC AGC AGG C	(Blaxter <i>et al.</i> 1998)
13R	18S rRNA	GGG CAT CAC AGA CCT GTT A	(Blaxter <i>et al.</i> 1998)
24F1	18S rRNA	AGA GGT GAA ATT CTT GGA TC	(Meldal <i>et al.</i> 2007)
18P	18S rRNA	TGA TCC WKC YGC AGG TTC AC	(Blaxter <i>et al.</i> 1998)
D2Ab	28S rRNA	ACA AGT ACC GTG AGG GAA AGT TG	(De Ley <i>et al.</i> 1999)
D3B	28S rRNA	TCG GAA GGA ACC AGC TAC TA	(De Ley <i>et al.</i> 1999)
JB3	COX1	TTT TTT GGG CAT CCT GAG GTT TAT	(Derycke <i>et al.</i> 2005)
JB5	COX1	AGC ACC TAA ACT TAA AAC ATA ATG AAA ATG	(Derycke <i>et al.</i> 2005)

Prior to sequencing, all products from dye-terminator sequencing reactions were purified via ethanol precipitation. Reaction products were initially centrifuged at 100 *g* for 60 seconds, followed by an addition of 5 μ l 125mM EDTA and 60 μ l 100% ethanol to each reaction. Reaction plates were sealed and inverted four times before being incubated at room temperature for 15 minutes. Plates were then centrifuged at 3000 *g* for 30 minutes at a temperature of 4°C, causing the cycle-sequencing products to form a pellet at the base of each reaction tube. Immediately following centrifugation, plates were immediately inverted onto tissue paper and centrifuged at 100 *g* for 60 seconds to remove ethanol from the pelleted reaction product. Pellets were cleaned by adding 60 μ l 70% ethanol to each reaction, followed by centrifugation at 1650 *g* for 15 minutes at a temperature of 4°C. Plates were again inverted on tissue paper and centrifuged at 100 *g* for 60 seconds, and then subjected to a final incubation at 55°C for 2 minutes in order to remove all excess ethanol. Purified PCR pellets were stored at -20°C, and were resuspended in 10 μ l formamide immediately before being loaded for automated capillary sequencing. All DNA sequencing during this study was carried out at the Hubbard Centre for Genome Studies (University of New Hampshire, USA) using an ABI 3130 genetic analyzer. Before alignment, the identity of all gene sequences were compared against online sequence databases using BLAST. Any suspected contaminant or non-nematode sequences (e.g. fungi) were discarded from subsequent analyses.

2.5 Attempts to amplify other informative loci

2.5.1 Orthologous nuclear genes

At the start of this investigation, several attempts were made to identify and amplify additional genes that could be informative for phylogenetic analysis in nematodes. The NemaLogs database (<http://nematol.unh.edu/ortholog/index.php>) on the University of New Hampshire's NemaTol website was used to identify potentially orthologous genes in Enoplid nematodes. This database uses reciprocal best BLAST (RBB) (following the methods of Blair *et al.* 2005) and non-reciprocal best BLAST (non-RBB) (following the methods of Lerat *et al.* 2003) bioinformatics methods to mine complete nematode genome sequences for conserved putative protein sequences. Such predicted proteins are likely to function in integral cellular processes, exhibiting conserved structural regions that

would be ideally suited for primer design. The genomes of two Dorylaimid nematodes, *Trichinella spiralis* and *Xiphinema index* (the only genomes currently published from this nematode group; no Enoplid genomes are currently available) were searched for putative protein sequences using both RBB and non-RBB methods with maximally stringent parameters. Several sets of orthologs from both analyses were chosen for further investigation and primer design. Protein sequences were downloaded from the NemaLog database, sets of orthologs from the two nematode species were aligned in MEGA version 4.0 (Tamura *et al.* 2007), and primers were designed according to conserved alignment regions containing amino acids encoded by only one or two codons. All primers were designed to have melting temperatures as close as possible to 65°C; a high T_m is required for long-distance PCR, and a matching T_m between primer pairs was used to increase the likelihood of successful amplification. All primers designed in this study are listed in Table 2.3.

Table 2.3: Primers designed from protein alignments of putative orthologous genes. Ortholog names prefaced with 'TS' represent genes from the *Trichinella spiralis* genome, while names prefaced with 'XI' represent genes identified from the *Xiphinema index* genome. Ortholog gene names reflect the putative protein names assigned in the NemaLog database; NemaLog mines published nematode genome sequences, and thus listed protein names reflect arbitrarily assigned codes. Forward and reverse primers are denoted as F and R, respectively.

Ortholog set	Primer position in protein alignment	Primer Name	Primer Sequence (5' → 3')
TS00978 / XI00621	8-15	TS978 3F	CCN CAY YTN CAY AAY GGN TGG CA
TS00978 / XI00621	78-85	TS978 78F	TAY GAY CCN TGY ACN ACN ATG TT
TS00978 / XI00621	126-133	TS978 133R	DAT NAC NAR NCC NCK NCC YTT
TS00978 / XI00621	74-81	TS978 80R	RCA NGG RTC RTA NAR YTC RTA CAT
TS00806 / XI00904	10-19	TS806 1F	ATG GCN GAY CAR YTN ACN GAR GAR CA
TS00806 / XI00904	129-136	TS806 130R	DAT CAT YTC RTC NAC YTC YTC RTC
TS00806 / XI00904	135-142	TS806 135R	RTC DAT RTC NGC YTC NCK DAT CAT
TS01137 / XI01062	4-12	TS137 1F	ATG GCN YTN AAR MGN ATH CAR AAR GA
TS01137 / XI01062	31-37	TS137 30F	GAY GAY YTN TTY CAY TGG CA
TS01137 / XI01062	35-42	TS137 35F	CAY TGG CAR GCN CAN ATH ATG GG
TS01137 / XI01062	144-150	TS137 140R	CAT NGC RTA YTT YTG NGT CCA
TS00838 / XI00569	1-7	TS838 1F	ATG GGN AAR CCN AAR GGN AT
TS00838 / XI00569	31-37	TS838 35F	CAY YTN GGN CAN MGN TGG AA
TS00838 / XI00569	132-139	TS838 130R	YTT YTT NCC YTT RTA NAR NGC CCA

Attempts were made to amplify the chosen orthologous genes from control nematode DNA (*C. elegans* N2 genomic extracts), as well as from genomic extracts of

freshly collected estuarine nematodes. All possible combinations of primer sets were tested for each of the four target orthologous genes, with no successful PCR amplification observed. Methodological variations of PCR protocols were tested for all primer combinations, such as gradient PCRs to observe the effect of different annealing temperatures, and the use of PCR additives such as DMSO to increase the potential for primer binding. Despite repeated efforts, PCR amplification consistently failed. Lack of success was most likely related to the failure of primers to bind correctly to the target gene. Designing primers from protein alignments is notoriously difficult, given that each amino acid is normally encoded by multiple codons; it was unlikely that the degenerate primers designed in this study reflected the true nucleotide sequences encoding the target genes.

2.5.2 Long-distance PCR to amplify partial mitochondrial genomes

It was noted that primers JB3 and JB5 were not able to universally amplify Cox1 from all Enoplids; furthermore, the resulting amplicon represented only a short gene fragment (~400bps). Initial attempts to amplify larger fragments of Cox1 with other primer pairs were unsuccessful, and most other 'universal' or nematode-specific primers for other mitochondrial genes also failed to amplify the target loci. Table 2.4 lists all mitochondrial primers sets initially tested on Enoplid nematodes. Four cytochrome *b* primers were designed during this study. Primers prefaced with 'Thor' were Enoplid-specific primers designed using aligned nematode sequence data from *Thoracostoma* sp. (Kelley Thomas, unpublished data), while primers prefaced with 'Invit' were designed using cytochrome *b* sequences mined from published nematode mitochondrial genomes.

Most primer sets were unsuccessful in amplifying the target loci from Enoplid nematodes. Along with primers JB3 and JB5, the only other successful mitochondrial primer set was the universal primer set of CytbF and CytbR that amplified (~400bps) of cytochrome *b* oxidase (CytB). However, successful amplification of cytochrome *b* was only obtained from a limited number of Enoplids (approximately 30 specimens), and not enough sequences were acquired for use in phylogenetic analyses. These data were used to design an investigation using long-distance PCR methods, with the aim of amplifying partial mitochondrial genomes from certain Enoplid genera found in specific intertidal samples. If partial mitochondrial genomes could be obtained from multiple Enoplid

genera, the resulting gene sequences could be aligned and used to design taxon-specific mitochondrial primers.

Long-distance PCR efforts were focused on three genera where Cox1 and CytB were easily amplified: *Anoplostoma* (specimens collected from sample site OUS), *Enoplolaimus* (specimens collected from sample site SUS), and *Oncholaimus* (specimens collected from sample site BUS). Gene sequences from both loci were aligned separately for each genus; conserved regions within each gene alignment were used to design specific primers for long-distance PCR (Table 2.5). One forward and one reverse primer were designed for each gene alignment, and primer pairs consisted of one directional primer from the Cox1 gene and the reverse directional primer from the CytB gene. The aim of long-distance PCR was to amplify part of the mitochondrial genome (aiming for fragments ~4kb in length) that lay between these two genes. If amplification was successful, DNA sequencing would be completed by primer walking, following the methodology of Hu *et al.* (2007).

Table 2.4: Nematode mitochondrial primers tested during this study.

Primer Name	Loci	Primer Sequence (5' → 3')	Reference
JB3	COX1	TTT TTT GGG CAT CCT GAG GTT TAT	(Derycke <i>et al.</i> 2005)
JB5	COX1	AGC ACC TAA ACT TAA AAC ATA ATG AAA ATG	(Derycke <i>et al.</i> 2005)
CytbF	CytB	GGW TAY GTW YTW CCW TGR GGW CAR AT	(Boore & Brown 2000)
CytbR	CytB	GCR TAW GCR AAW ARR AAR TAY CAY TCW GG	(Boore & Brown 2000)
Thor_CytB_137F	CytB	CAT GAT CAA ACA GGG CAT TA	Present Study
Thor_CytB_565R	CytB	ACC TCA AGT ACG TAG TCG GC	Present Study
Invit_CytB_65F	CytB	AGA AGA TGG ACG GGA TCC TT	Present Study
Invit_CytB_511R	CytB	TTT TGG CCT TGA AGG ATG AC	Present Study
16SarL	16S	CGC CTG TTT AAC AAA AAC AT	(Palumbi <i>et al.</i> 1991)
16SbrH	16S	CCG GTC TGA ACT CAG ATC ACG T	(Palumbi <i>et al.</i> 1991)
Meld_16S_F1	16S	AAW RGC ASY YTT AGC GTG AK	(Meldal 2004)
Meld_16S_R1	16S	AAT TTC YRA AGA CTT WTC TTW G	(Meldal 2004)
Meld_16S_F2	16S	ACW AAG AWA AGT CTT YRG	(Meldal 2004)
Meld_16S_R2	16S	GAA YTA AAC TAA TWT CAM G	(Meldal 2004)

Table 2.5: Primers designed for amplifying partial mitochondrial genomes via long-distance PCR.

Primer Name	Primer Sequence (5' → 3')
Anoplostoma_cox1_F	GGG GGA GTY ACT GGK ATT RTT TTA TC
Anoplostoma_cox1_R	TAA ACC CYA TAC ACC ACC TTA TTG
Anoplostoma_cytb_F	GCA GTT TTR CAC TTT TAY GGR AGA TCC
Anoplostoma_cytb_R	ATW AGT ATY TCC CCY ACC CC
Enoplolaimus_cox1_F	TTY ACM GTT GGG ATA GAC ATT GA
Enoplolaimus_cox1_R	GCT CGR GTR TCA ATG TCT ATC CCA AC
Enoplolaimus_cytb_F	CGA TTT TTC WTC YTC YCC YGC
Enoplolaimus_cytb_R	CAA AAA ART GAA TMG CWA AYA ART GG
Oncholaimus_cox1_F	GGA TGT TGA TAC TCG GGC TTA TTT TAC
Oncholaimus_cox1_R	CAG TAA AAT AAG CCC GAG TAT CAA CAT C
Oncholaimus_cytb_F	GTT TGA AGA AGA TTT AGA GTT GGG G
Oncholaimus_cytb_R	CCC CAA CTC TAA ATC TTC TTC AAA CTC

Genomic DNA of all nematodes was extracted *via* proteinase K digestion following the methodology of Holterman *et al.* (2006). For nematodes used in long-distance PCR, genomic extracts were purified using a DNeasy Blood and Tissue Kit (QIAGEN, Valencia, CA, USA). The kit protocol was modified to exclude initial steps for proteinase K digestion (as this had already been carried out), but all remaining steps were completed according to manufacturer's instructions; final extracts of nematode DNA were eluted in 50 μ l water. A test PCR was run to confirm successful elution of nematode DNA, using primers G18S4 and 22F (refer to Section 2.4 for PCR reaction conditions). Long-distance PCR was conducted using an Expand 20kb^{PLUS} PCR System (Roche Applied Science, Mannheim, Germany), with a final reaction volume of 50 μ l. Each reaction contained 18 μ l genomic DNA, 500 μ M PCR Grade Nucleotide Mix (Roche Applied Science), 0.4 μ M of both Forward and Reverse primers (Sigma-Aldrich Ltd, Dorset, UK), 1X Expand 20kb^{PLUS} reaction buffer (including a final concentration of 2.75 mM MgCl₂), and 1 μ l Expand 20kb^{PLUS} enzyme mix (5 enzyme units in final reaction volume). Positive and negative controls were amplified alongside nematode samples; control reactions were conducted using human β -globin control primers and human genomic DNA included with the kit. Two primer set combinations were tested for nematode extracts from each genus, using a forward primer designed from either Cox1 or CytB and a reverse primer from the remaining gene; the aim was to amplify a part of the circular mitochondrial genome which lay between the two genes. The following PCR profile was used to amplify all fragments: 94°C for 2 minutes followed by 35 cycles of denaturation at 94°C for 20 seconds, annealing at 62°C for 30 seconds, extension

at 68°C for 11 minutes, with a final extension of 68°C for 7 minutes. All PCR products were subsequently visualized on a 1% agarose gel containing Ethidium Bromide (Figure 2.1).

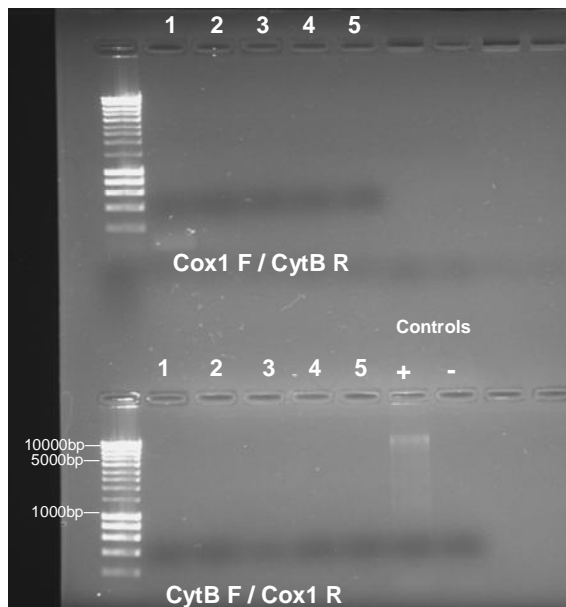


Figure 2.1: Visualisation of PCR products from long distance PCR. Lane numbers 1 and 2 represent *Oncholaimus spp.*, numbers 3 and 4 represent *Enoplolaimus spp.*, and number 5 represents *Anoplostoma sp.*

Long distance PCR was unable to amplify any large mitochondrial fragments, despite the use of several different primer combinations from multiple genera. It is unlikely that amplification failure was related to ineffective thermal cycling conditions, given that the positive control confirmed the success of the PCR reaction. The problems were most likely a result of sub-optimal primer design or mitochondrial genome organization which hindered PCR amplification from nematode templates. Long-distance PCR is especially sensitive to inequalities in melting temperatures of primer pairs; although primers sets were designed to match as closely as possible, small differences in melting temperatures could have played a role. Sub-optimally designed primers may have also failed to bind to template DNA during PCR. Furthermore, long distance PCR tends to be more successful for shorter genome fragments. The Cox1 and CytB genes could be situated on opposite sides of the circular mitochondrial genome for the chosen nematode genera; this situation would reduce the likelihood that the intermediate genome sequence would be successfully amplified, compared to a scenario where these genes were only located a few kilobases apart.

2.6 Analysis

2.6.1 Sequence alignment

Ribosomal gene alignments (18S and 28S) were constructed using template alignments obtained from the SILVA rRNA database (Pruesse *et al.* 2007). This online resource provides curated structural alignments for both the 18S and 28S rRNA genes in Eukaryotes, Bacteria, and Archaea. Releases of the SILVA database are synched with release numbers for the EMBL database; new rRNA sequence submissions in each EMBL release are detected and incorporated into the SILVA database. Alignments for this project were constructed using nematode and outgroup sequences contained in SILVA release 98 (March 2009). All SILVA sequences obtained from EMBL are first subjected to quality checks before being incorporated into the database; sequences will only be accepted if they are above 300bps in length, are comprised of less than 2% ambiguous bases, are not comprised of more than 2% homopolymer stretches, and have less than 5% identity to common vector sequences. Accepted sequences ('seeds') are then aligned to secondary structure motifs in a manually curated set of reference sequences, using a dynamic incremental profile sequence aligner (SINA). The SINA aligner continually 'jumps' between structural motifs in different reference sequences, resulting in optimal alignments over the whole length of a seed sequence. The graphical layout of the SILVA website allows for users to browse available taxa and download customized structural alignments based on their chosen groups. All downloaded sequences retain their taxonomic information (where available) and EMBL accession numbers, for reference. Table 2.6 outlines the number of sequences downloaded from SILVA for this investigation.

Table 2.6: Aligned rRNA sequences available for each taxonomic group in SILVA release 98. All available sequences were downloaded for each phylum, but not all were used in phylogenetic analyses.

Taxa	SSU Sequences	LSU Sequences
Nematoda	5265	1544
Nematomorpha	19	6
Kinorhyncha	10	4
Priapulida	23	4
Tardigrada	723	48

Alignments downloaded from SILVA were then imported into the ARB software suite (Ludwig *et al.* 2004). This program functions as a complementary tool to SILVA; it allows users to import downloaded secondary structure alignments, which can then be used as references for aligning user-generated sequences. Enoplid sequences generated during this investigation were incorporated into nematode secondary structure alignments using the Positional Tree (PT) Server function. The PT server is a fast method for aligning imported sequences to their nearest relatives in the alignment database. Of course, neither the SILVA databases nor the PT server function result in perfect alignments for all sequences; manual editing of both the 18S and 28S alignments were necessary to ensure that all secondary structure motifs were properly aligned.

The quality of manual alignment edits was assessed by building Neighbour-Joining trees in the ARB program. Although Neighbour-Joining is not a robust method for constructing final phylogenies, it is a useful tool for identifying misaligned taxa during alignment manipulation. Oftentimes, taxa with incorrect alignments would be placed into the wrong taxonomic group (for sequences whose identity could be trusted), or potentially problematic sequences could be singled out by their long branches in the Neighbour-Joining tree. When the EMBL information was checked for such long branch taxa, it was often found that they were of dubious quality (e.g. sequences resulting from whole-genome shotgun studies where sequences may contain many errors or gene assignment may be incorrect). Long branch problems were also encountered with very short sequences (<500bps), and a decision was made to remove these sequences from the alignment.

2.6.2 Phylogenetic Analysis

Previous phylogenetic analyses had noted that parsimony methods are not useful for building trees based on SSU data, nor do they produce robust large-scale phylogenies (Meldal *et al.* 2007). Thus, a decision was made to restrict phylogenetic reconstruction methods in this study to more informative methods, such as Maximum Likelihood (ML) and Bayesian Inference (BI). ML and BI are currently the two most widely utilised and accepted methods for building accurate phylogenies; published ribosomal phylogenies typically use both analyses as independent methods to assess evolutionary relationships (e.g. Cannon *et al.* 2009; Tsagkogeorga *et al.* 2009). Both methods are also ideal for constructing large-scale phylogenies, due to recent algorithm improvements.

Large-scale ML trees (containing upwards of 1000 taxa) were constructed using Randomized Axelerated Maximum Likelihood (RAxML) version 7.04 (Stamatakis 2006; Stamatakis *et al.* 2008). This program implements a rapid bootstrapping algorithm using the original alignment file, and, in addition to standard ML tree searches, allows users to conduct full maximum likelihood analyses within a single program run (as opposed to other programs which require that bootstrapping is completed separately). All sequence data was submitted to RAxML using either of two web servers: the RAxML Blackbox hosted at the Vital-IT unit of the Swiss Institute of Bioinformatics (<http://phylobench.vital-it.ch/raxml-bb>), or the CIPRES project cluster hosted at the University of California, San Diego (<http://8ball.sdsc.edu:8889/cipres-web/Bootstrap.do>). RAxML uses the General Time Reversible model in conjunction with a CAT approximation that estimates rate variation (GTR+CAT) to implement Maximum Likelihood searches, allowing for faster searches of large datasets (in contrast to the slower GTR+ Γ algorithm). The author of RAxML only offers ML analyses under the GTR model of nucleotide substitution, citing that it is the most widely used and biologically relevant model for reconstructing molecular evolution (Stamatakis 2008). Most alternative models only represent special cases of GTR—based on experience, the author of RAxML notes that the GTR model returns a slightly better likelihood compared to other simpler models. Furthermore, the rapid search mechanisms implemented in RAxML reflect the author's belief that thoroughly searching of tree space is much more important for building robust trees than minute details of nucleotide substitution models. Thus, RAxML offers an efficient and highly optimised platform for building large maximum likelihood trees.

The discrepancies between SSU and LSU datasets made it impossible to include both genes in a single phylogenetic run. For nematodes, there were far fewer LSU sequences available in SILVA, compared to the relatively large SSU database. Both gene alignments contained a different assemblage of taxa, and only a limited number of species were represented by both gene sequences. Furthermore, linking LSU and SSU sequences for database species would introduce empirical discrepancies—sequences would have derived from different individual nematodes, and this may adversely impact phylogenetic inference. Although SSU and LSU sequences were both collected from individual nematodes in this study, it would not have been informative to construct a combined gene analysis in the absence of other taxa. Furthermore, some authors have actually argued against combined gene alignments, noting that corroboration between independent gene

analyses provides more definitive evidence of evolutionary relationships (Miyamoto & Fitch 1995).

Separate alignment files representing SSU and LSU nematode datasets were exported from ARB in PHYLIP file format and submitted to RAxML via online web servers. The best scoring ML tree with bootstrap values was analysed from each run. Problematic taxa were identified in the tree topology and alignments for these taxa were re-evaluated and edited in ARB databases; many topological anomalies were simply related to misaligned sequences. Repeated analyses of SSU trees found that short sequences (<1000 bps) were consistently destabilising tree topologies, with correctly identified taxa being placed in the wrong clades or continually changing position within the tree. It was decided to remove all sequences less than 1000 bps in length, as alternative full-length SSU sequences representing most of the same genera were present within the ARB database.

Bayesian phylogenies were constructed on Portal version 2.0 of the CIPRES web server (http://www.phylo.org/sub_sections/portal/) hosted at the University of California, San Diego. Like RAxML, the CIPRES project focuses on the inference of large phylogenetic trees. The Portal v2.0 provides users with an online workbench, comprising a data storage area access to a suite of phylogenetic analysis tools. Ribosomal alignments were exported from ARB databases in NEXUS format and run on MrBayes version 3.2 using the GTR+I+G model of nucleotide substitution. Jobs were run for up to 4 million generations, using 2 independent Bayesian runs (4 chains per run), and chain heating temperatures of 0.06 - 0.2; all other parameters were set as default values. Due to time constraints (maximum job run times were imposed by the CIPRES administrators) and problems with tree convergence (particularly in larger phylogenies), Bayesian analysis was only carried out for SSU alignments representing the full nematode phylogeny (>1000 taxa) and a smaller Enoplid/Dorylaimid phylogeny (563 taxa). Because of these restrictions, it was also unfeasible to carry out any rigorous empirical tests using Bayesian methods. Bayesian trees were used to assess the robustness of clade placement and relationships between taxa that were recovered in maximum likelihood topologies.

3. Slide Mounting and Preservation Time Series Experiments

(This chapter was published in modified form in *Nematology*; Appendix III contains the published manuscript)

3.1 Introduction

The use of molecular data in nematode studies is now ubiquitous, yet it is still routine for researchers to corroborate DNA sequences with morphology in order to assess the biological relevance of molecular patterns (Griffiths *et al.* 2006; Stock & Nadler 2006). DNA barcoding studies promote visual identification of specimens as well as the retention of 'morphological voucher images' to record taxonomic features before nematodes are destroyed for DNA extraction (De Ley *et al.* 2005). These barcoding studies have also provided empirical evidence concerning the resolution of different genetic loci used in species identification, with the nuclear 18S ribosomal subunit gene currently recommended as the ideal barcoding locus for nematodes (Bhadury *et al.* 2006).

Despite the frequent integration of morphological and molecular protocols in nematode studies, there is little published information to suggest how these two disparate approaches might best be optimised to obtain the most robust data. Taxonomic protocols are designed to maximise the clarity of specimens viewed under a microscope—preservatives and mounting methods are determined based on the resulting physical effects, ideally 'hardening' nematode anatomy and not introducing any preservation artefacts. In contrast, the success of molecular techniques hinges on the chemistry of reactions; PCR reactions are only successful if the concentrations of different ingredients are balanced at specific ratios. For reagents that are added to enhance reactions (such as formamide or MgCl_2), there is usually only a narrow concentration range within which any given substance can aid DNA amplification, with excess amounts of such substances becoming inhibitory (Saunders & Parkes 1999). Taxonomic protocols are quite 'dirty' in comparison to most molecular protocols, which aim for purity and strict control of all reaction components. The ideal taxonomic protocol will provide unambiguous presentation of morphology and will cater for long-term storage of nematode specimens, regardless of the molecular impacts effected during this process.

For nematode studies, the currently favoured preservative is DESS, a dimethyl sulphoxide (DMSO)/EDTA solution saturated with sodium chloride. DESS offers the

advantage of preserving both morphology and DNA with one solution, as opposed to previous sampling methodology which required collection of separate subsamples in ethanol and formalin for integrative studies (Yoder *et al.* 2006). The latter situation could lead to potential discrepancies if species assemblages in subsamples differed, as well as preventing analysis of both morphology and DNA sequences from single nematodes. Although several studies have successfully amplified DNA from formalin-fixed samples (Thomas *et al.* 1997; Rubtsova *et al.* 2005), formalin is neither recommended nor widely used as a preservative when fresh material is being collected for molecular work. This study was aimed at optimising protocols for DESS-preserved material, and does not encompass the separate problems encountered with amplifying DNA from formalin-fixed samples—other published works have already approached this topic (Bhadury *et al.* 2007).

The adoption of DESS preservative facilitates and encourages the collection of morphological and molecular data from individual nematodes. However, this approach may be problematic; the most sensitive molecular procedures are situated furthest downstream in the overall process. Nematodes are exposed to many compounds during extraction and slide mounting, including colloidal silica (Ludox), ethanol, paraffin, glycerol and filtered tap water (non-distilled). Any of these compounds may subtly interact with nematode tissue and affect the chemistry of subsequent molecular reactions.

Previous work suggested that standard taxonomic slide preparations of nematodes mounted in glycerol could be adversely affecting DNA integrity, thus reducing subsequent PCR success (Meldal 2004; Cook *et al.* 2005). We have also encountered frequent problems in obtaining reliable and consistent PCR results from DESS-preserved specimens stored in slide mounts and determined that a formal study was needed to assess the impact of standard methodology. To determine the true cause of the recurrent molecular problems, a time series experiment was designed to test the effect of the slide mounting process and account for any preservative effects.

3.2 Materials and methods

Fresh estuarine sediments were collected in February 2008, at the mouth of the River Torridge in Devon, southwest England (51°1'54"N, 4°12'12"W) and immediately fixed in DESS preservative. All samples were collected using an equal ratio of preservative to sediment. Each sample was thoroughly shaken after collection to distribute the preservative. The meiofauna fraction was extracted *via* decantation and floatation in Ludox using a 45 μm sieve according to the methods of Somerfield *et al.* (2005). All collected sediments and extracts were stored at 4°C when not needed.

Freshly collected material was used to conduct two separate time series experiments: one to test the effect of the slide mounting process, and another to assess the effect of preservative strength. In order to test whether weak strength DESS had degraded the nematode DNA in the CROZET samples, fresh material was collected and preserved in DESS with both 5% and 20% DMSO content. The aim of this experiment was to compare the preservation quality of nematode DNA in weak versus full-strength DMSO concentrations. DMSO acts in the DESS preservative to increase tissue porosity and allow diffusion of EDTA and NaCl into cells; the high cellular concentration of EDTA and NaCl inactivates nucleases that would otherwise shear DNA (Yoder *et al.* 2006); a decreased concentration of DMSO may thus decrease the efficiency of this process.

For the slide mounting time series, nematodes were individually picked out of the extracted meiofauna fraction (preserved in full strength, 20% DMSO DESS) under a dissecting microscope and transferred to a watch glass containing dehydrating solution (90% distilled water, 5% molecular grade glycerol and 5% molecular grade ethanol) before being placed into a desiccator for 48 h. Specimens were subsequently mounted on glass slides in anhydrous glycerol and sealed with a wax ring. Two test groups were set up to examine whether the storage temperature of slide-mounted specimens would impact PCR success. Longevity of molecular samples is known to be affected by temperature (e.g. PCR products can be stored for a short time at 4°C, or for longer periods at -20°C), and the 4°C treatment was designed to test whether the integrity of nematode DNA could be maintained for longer simply by using a lower storage temperature. Desiccation and slide storage were both carried out at 4°C for one set of nematodes and these processes were conducted at room temperature for a second set of nematodes. Picking and slide mounting of all specimens took place at room temperature as these procedures could be completed relatively quickly.

At each predetermined interval in the time series (Table 3.1), ten slide-mounted nematodes from each temperature treatment were removed from slides and transferred into 1.5 ml microcentrifuge tubes containing 25 μ l sterile water. To test preservative strength at each time interval (Table 3.1) ten nematodes were picked straight out of 5% and 20% DMSO content DESS, and directly transferred to 1.5 ml microcentrifuge tubes containing 25 μ l sterile water. At each time point, genomic DNA was extracted from individual nematodes and PCR was conducted. Genomic DNA of all nematodes was extracted *via* proteinase K digestion following the methodology of Holterman *et al.* (2006). An equivalent volume (25 μ l) of lysis buffer (containing 0.2 M NaCl, 0.2 M Tris-HCl (pH 8.0), 1% β -mercaptoethanol and 800 μ g/ml proteinase K) was added to microcentrifuge tubes containing individual nematodes. The final reaction volume was incubated for 2 h at 65°C and 750 rpm in an Eppendorf Thermomixer (Eppendorf, Hamburg, Germany), followed by a final 5 min at 100°C and 750 rpm to inactivate the proteinase K enzyme. Final lysates were stored at -20°C.

Table 3.1: Sampling intervals for slide mounting experiment. All slides prepared together at the start of the experiment, and a subset of nematodes was picked out at intervals as time progressed. Specimens picked from DESS were picked from the sample extracted on the dates indicated, and genomic DNA was immediately extracted.

Sampling time series										
	1 day	3 days	1 week	2 weeks	1 month	2 months	3 months	6 months	1 Year	1.5 Years
Room Temperature	✓	✓	✓	✓	✓	✓	✓	✓	X	X
Cold Treatment	✓	✓	✓	✓	✓	✓	✓	✓	X	X
Picked from DESS	X	X	✓	X	✓	X	✓	✓	✓	✓

To test preservation of DNA, the metazoan specific primers G18S4 (5'-GCTTGCTCAAAGATTAAGCC-3') and 22R (5'-GCCTGCTGCCTTCCTTGGA-3') (Blaxter *et al.* 1998) were used to amplify a *ca* 400 bp product of the nuclear 18S rRNA gene under the following profile: 94°C for 5 minutes followed by 35 cycles of denaturation at 94°C for 30 seconds, annealing at 54°C for 45 seconds, extension at 72°C for 2 minutes, with a final extension of 72°C for 10 minutes. The PCR reaction was conducted using a DyNAzyme EXT PCR kit (New England Biolabs, Ipswich, MA, USA), with a final reaction volume of 25.75 μ l.

Each reaction contained 2 μ l of genomic DNA, 18.25 μ l sterile water, 0.4 μ M of each primer (Integrated DNA technologies, Coralville, IA, USA) 2.5 μ l 10X DyNAzyme EXT Buffer containing MgCl₂ (final reaction concentration 1.5mM MgCl₂), 0.5 μ l dNTP mix containing 10 μ M of each nucleotide, and 0.5 μ l Dynazyme EXT DNA polymerase (0.5 enzyme units in final reaction volume). The varying sizes of individual nematodes presumably resulted in different amounts of starting template in individual PCR reactions. In order to save costs and emulate standard protocols, no attempt was made to measure the DNA content of nematode genomic templates. Positive and negative controls were amplified alongside all reactions containing experimental samples. Samples were subsequently visualised by running 5 μ l PCR product on a 1.5% agarose gel containing ethidium bromide. The same volume of a quantitative ladder, Hyperladder V (Bioline Ltd., London, UK), was run alongside all samples in order to estimate the amount of amplified DNA based on the resulting gel photographs. To compare gel band intensity, PCR products from nematodes picked straight from DESS preservative were occasionally run on gels alongside PCR products from slide mounted nematodes (indicated by the code 'PS' on gel photos).

3.3 Results

Results clearly demonstrate reduced PCR success over time for preserved nematodes mounted in glycerol, with eventual failure of PCR amplification. Figures 3.1 to 3.3 display results obtained from unmounted nematodes amplified directly from DESS preservative. Successful amplification can be observed at all time points with no obvious decrease in band intensity, and no large discrepancy between nematodes preserved in DESS containing 5% versus 20% DMSO content. An overview of PCR amplification success is illustrated in Figure 3.14; even weak-strength DESS appears to maintain DNA preservation 1.5 years after collection

For slide mounted nematodes, gel band intensity is noticeably weaker for nematodes amplified after 1 day in slides (Figure 3.4), compared to PCR products from individuals picked straight out of DESS. Similar band intensities are seen for PCR products of specimens mounted for 3 days (Figure 3.4), 1 week and 2 weeks (Figure 3.5). After 1 month and 2 months in slide mounts, PCR amplification of 18S almost fails completely, apart from a few weak bands still visible on the gel photograph (Figures 3.6 and 3.7). A sudden, universal, low-level amplification is seen in all slide-mounted specimens extracted at a time point of 3 months (Figure 3.8). This anomalous result was initially suspected to be

laboratory contamination, yet the negative control shows no sign of any contaminant and the positive control confirms success of the PCR reaction. At 6 months (Figure 3.9), only one very faint band is visible amongst 20 specimens amplified.

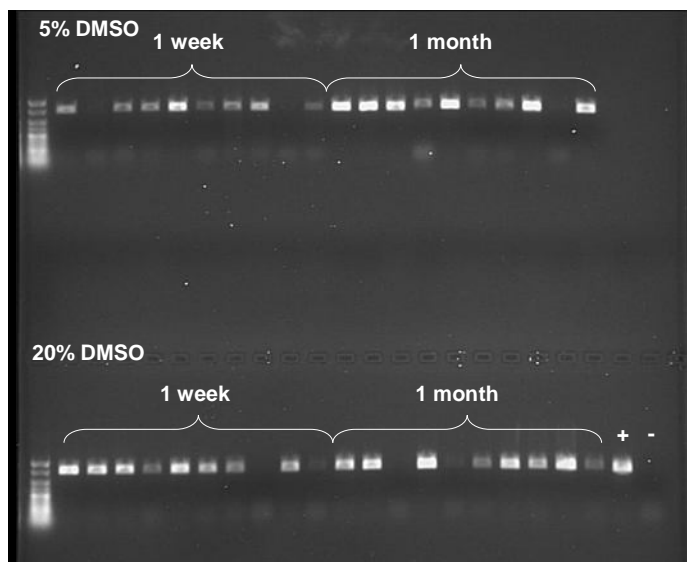


Figure 3.1: PCR amplification for unmounted nematodes preserved in 5% DMSO and 20% DMSO DESS preservative (1 week and 1 month time points). All nematodes were picked out from preserved samples and directly digested for molecular work. Plus and minus signs represent positive and negative PCR controls, respectively.

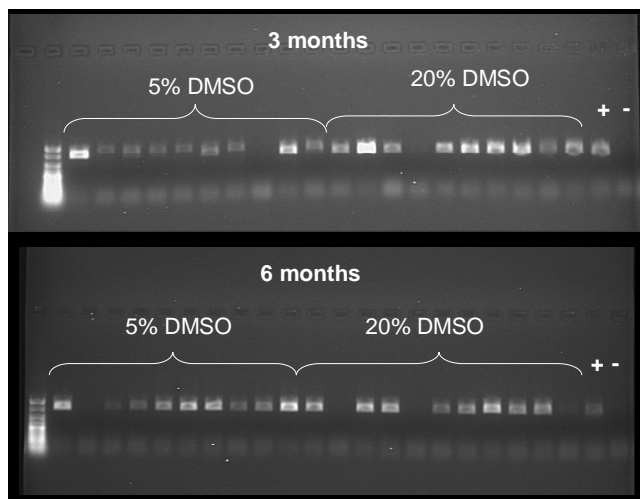


Figure 3.2: PCR amplification for unmounted nematodes preserved in 5% DMSO and 20% DMSO DESS preservative (3 month and 6 month time points). All nematodes were picked out from preserved samples and directly digested for molecular work. Plus and minus signs represent positive and negative PCR controls, respectively.

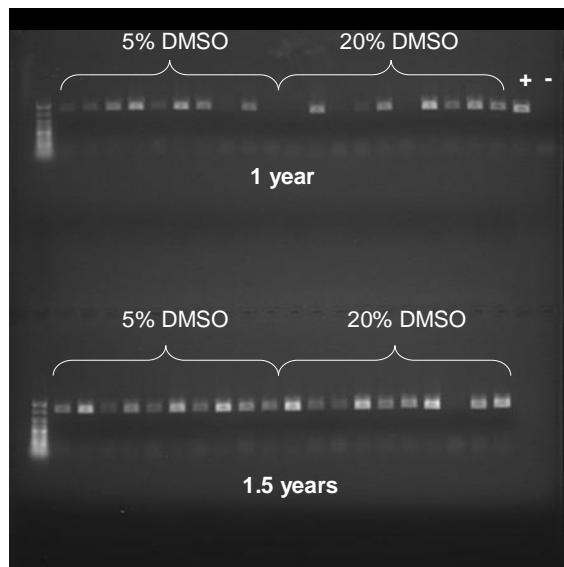


Figure 3.3: PCR amplification for unmounted nematodes preserved in 5% DMSO and 20% DMSO DESS preservative (1 year and 1.5 year time points). All nematodes were picked out from preserved samples and directly digested for molecular work. Plus and minus signs represent positive and negative PCR controls, respectively.

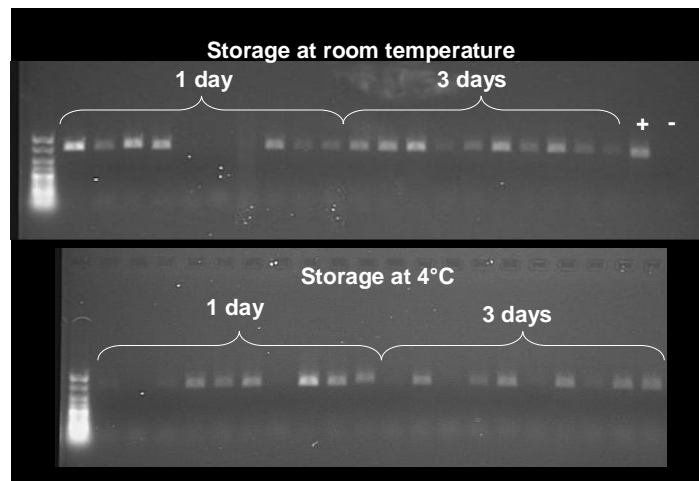


Figure 3.4: PCR amplification of slide mounted specimens at 1 day and 3 days time points. Plus and minus signs represent positive and negative PCR controls, respectively.

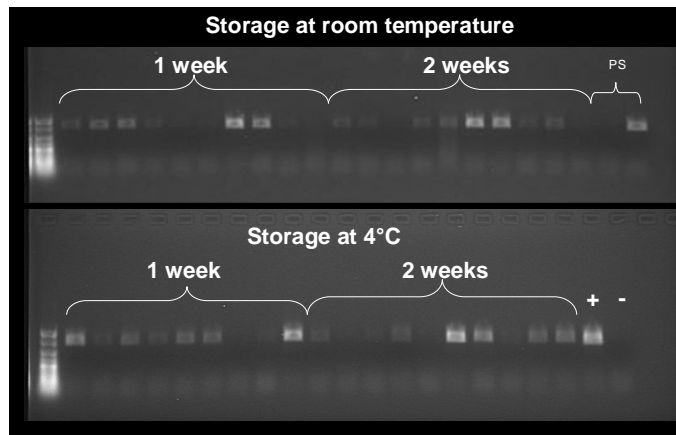


Figure 3.5: PCR amplification of slide mounted specimens at 1 week and 2 week time points. Plus and minus signs represent positive and negative PCR controls, respectively. PS = PCR products for unmounted nematodes amplified directly from DESS preservative, used as a comparison to mounted nematodes; failure of one 'PS' reaction was likely due to repeated freezing/thawing of genomic DNA.

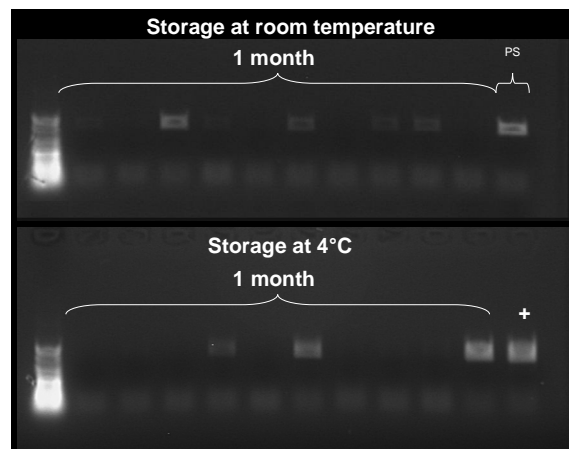


Figure 3.6: PCR amplification of slide mounted specimens at the 1 month time point. Plus and minus signs represent positive and negative PCR controls, respectively. PS = PCR products for unmounted nematodes amplified directly from DESS preservative, used as a comparison to mounted nematodes.

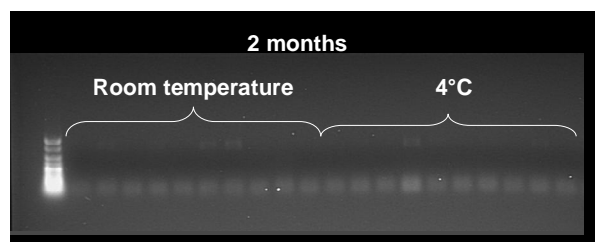


Figure 3.7: PCR amplification of slide mounted specimens at the 2 month time point

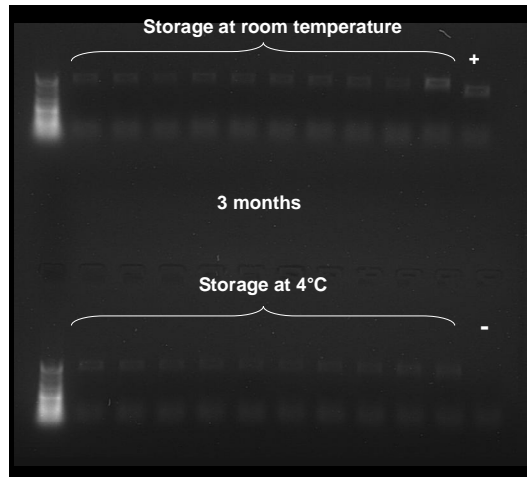


Figure 3.8: PCR amplification of slide mounted specimens at the 3 month time point. Plus and minus signs represent positive and negative PCR controls, respectively.

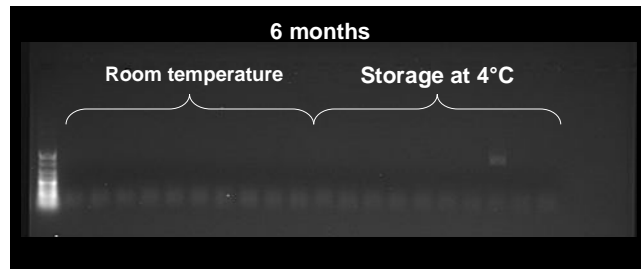


Figure 3.9: PCR amplification of slide mounted specimens at the 6 month time point

The overall success of PCR reactions is summarized in Figure 3.10. The amount of DNA in successful PCR reactions was subsequently quantified by comparing band intensities of nematode samples with the appropriately sized band of the quantitative ladder. The 400 bp band of Hyperladder V (representing 60 ng of DNA) was used as a marker for evaluating the strength of the nematode PCR products on all gels run. Gel bands that were equally intense or brighter than the ladder band were classed as containing equal or greater amounts of DNA (≥ 60 ng), whilst weaker bands were classed as containing less DNA (< 60 ng) than the ladder. All category assignments were completed by eye after visual inspection of each gel photo.

For slide-mounted specimens, both temperature treatments show similar success of overall PCR amplification for each time point (Figure 3.10). However, quantification of these PCR products reveals that the storage of slide mounted nematodes at 4°C resulted in more robust PCR amplifications. Room temperature specimens often contained a substantial proportion of weak bands (< 60 ng) with these low intensity bands becoming

the dominant category at later time points (Figure 3.11). The cold treatment group exhibited a greater proportion of strong band intensities (≥ 60 ng) at each time point (Figure 3.12) compared with specimens kept at room temperature. Furthermore, amplification of unmounted nematodes remains strong at time points where the PCR success of slide-mounted specimens is reduced or has virtually failed (Figure 3.10).

For unmounted nematodes that were amplified straight from DESS preservative, PCR amplification success is similar between weak and full-strength solutions (Figure 3.13). Quantification of PCR products reveals that strong bands (≥ 60 ng) dominate at most time points for both 5% and 20% DMSO concentrations. Preservation in 5% DMSO DESS does seem to result in a greater proportion of weak bands per time point (Figure 3.14), although overall PCR amplification is equal or greater to 20% DMSO DESS. Full-strength DESS shows overwhelmingly strong gel bands (≥ 60 ng) at all time points with very few weak bands (< 60 ng) amongst all PCR products obtained (Figure 3.14).

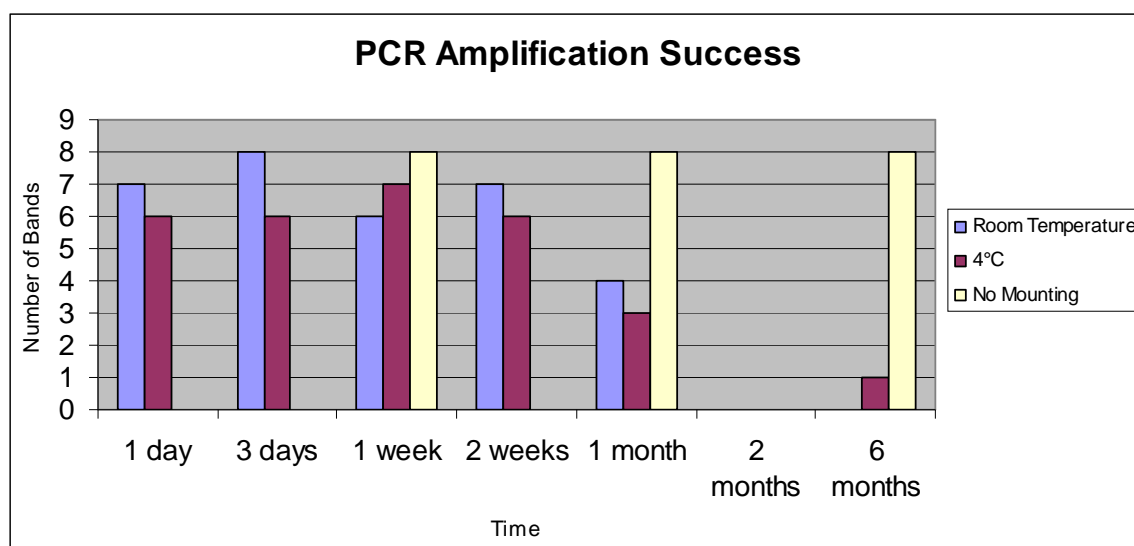


Figure 3.10: PCR Amplification success over time for slide mounted and unmounted nematodes. Bars represent the number of nematodes from which the 18S gene was successfully amplified; PCR was conducted on 10 specimens at each time point and treatment group. Bars for unmounted worms represent nematodes amplified directly from full strength DESS preservative (20% DMSO content). Note that unmounted worms were not amplified at the 1 day, 3 day, 2 week, or 2 month time points.

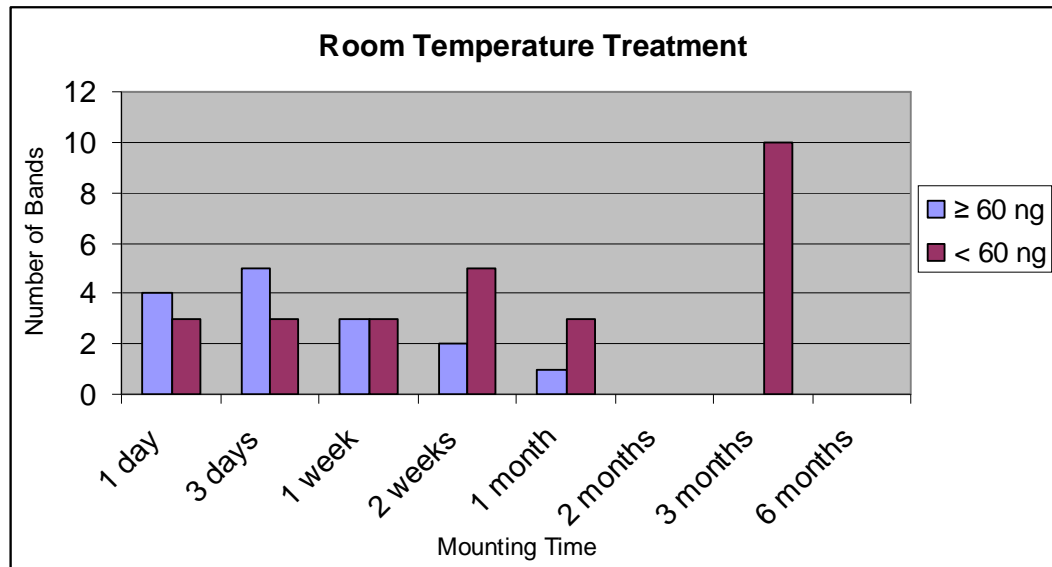


Figure 3.11: Quantification of DNA content in bands appearing on gel photographs for slide mounted worms stored at room temperature; PCR was conducted on 10 specimens at each time point. DNA content estimated per 5µl PCR product.

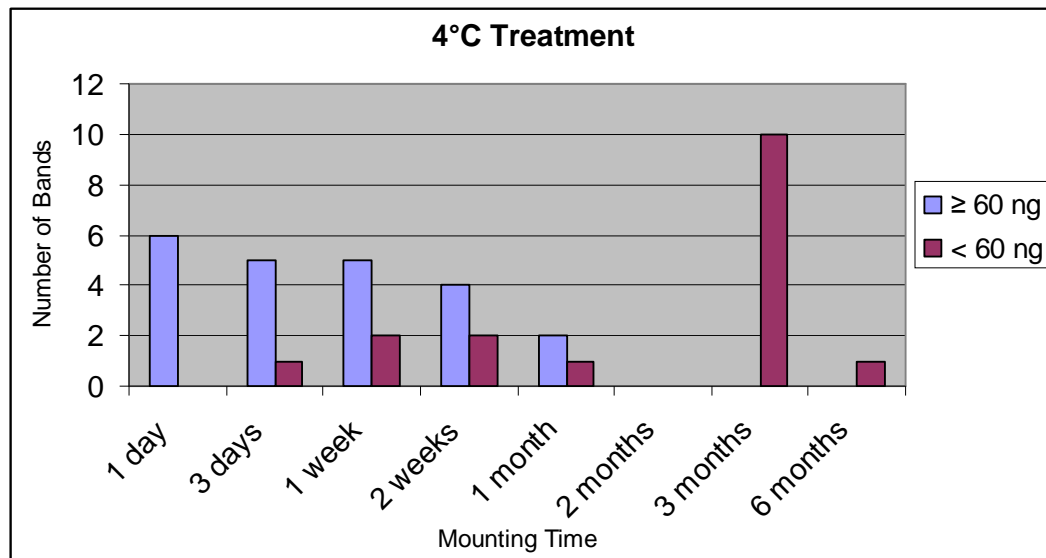


Figure 3.12: Quantification of DNA content in bands appearing on gel photographs for slide mounted worms stored at 4°C; PCR was conducted on 10 specimens at each time point. DNA content estimated per 5µl PCR product.

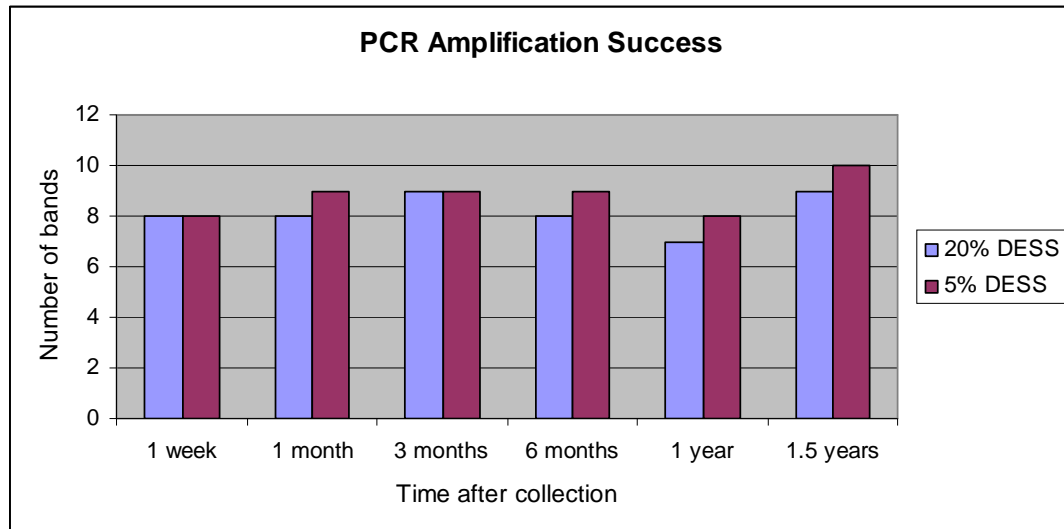


Figure 3.13: PCR Amplification success over time for unmounted nematodes amplified directly from DESS preservative; PCR was conducted on 10 specimens at each time point. Bars represent the number of nematodes from which the 18S gene was successfully amplified.

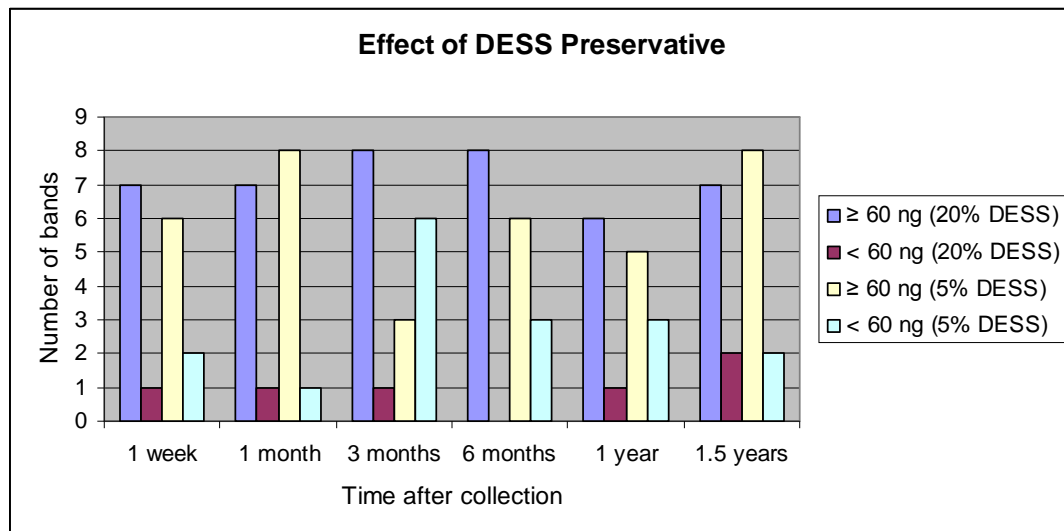


Figure 3.14: Quantification of DNA content in bands appearing on gel photographs for unmounted nematodes amplified directly from DESS preservative; PCR was conducted on 10 specimens at each time point and treatment group. DNA content estimated per 5µl PCR product.

3.4 Discussion

Slide mounting is likely to remain an important step for integrative studies, although the exact methodology currently varies amongst researchers. Techniques currently used include temporary mounts of live nematodes (De Ley *et al.* 2005), semi-permanent (Bhadury *et al.* 2006; Bhadury *et al.* 2008), or permanent (Eyualem & Blaxter 2003) mounts of specimens in glycerol. Although the nematodes picked straight out of DESS display high success rates of PCR at all time points, the morphology of these non-desiccated, preserved nematodes is less than ideal for identification and video capture. However, the clarity of morphology in DESS-preserved specimens can equal or exceed that of formalin-fixed specimens if nematodes are subject to desiccation and subsequently mounted in glycerol (Yoder *et al.* 2006).

Results from the DESS preservation time series seem to indicate that both weak and full-strength DESS (5% and 20%, respectively) are capable of long-term preservation of nematode DNA. Results from statistical tests did not indicate any significant correlations between preservative strength and PCR success. Despite the higher proportion of weak PCR products (<60 ng) observed for nematodes preserved in 5% DMSO DESS, there is no significant difference in overall amplification success between different DESS concentrations. Weak bands may simply represent smaller nematodes, where there may be less starting genomic template available for PCR reactions (resulting in comparatively weaker bands). Weak bands can be easily sequenced with simple changes to PCR protocols (such as increasing the number of cycles to obtain stronger bands), or amplification of genomic template before PCR. Thus, weak bands seen in 5% DMSO DESS do not necessarily offer any insight on the ability of weak DESS to preserve DNA. Yoder *et al.* (2006) have suggested that the integrity of DNA is maintained for at least 2 years after preservation in full-strength DESS (20% DMSO content). Furthermore, good-quality PCR products were obtained from Enoplid nematodes extracted from CROZET samples; this material has been preserved in 5% DMSO DESS since 2005, indicating that even weak-strength DESS can suitably preserve DNA for at least four years after collection. It appears the previous difficulties in amplifying CROZET material stemmed instead from slide mounting methodology.

Statistical tests were applied to data from the slide mounting time series, but no significant correlations were found; however, visual inspection of gel photos suggests a definite trend. In the slide mounting time series, the success rate of PCR amplification of

nematode DNA falls sharply after 2 weeks of storage in slide mounts, with eventual failure of PCR amplification. The low level amplification seen at the 3-month interval is unlikely to represent nematode DNA, given the reduced PCR success for most slide-mounted nematodes at 1 month and overall failure of amplification at 2 and 6 months. Considering that the negative control is blank, any contaminant would need to be present in the nematode genomic template and not present in the master mix of PCR reagents. While it cannot be determined for certain what these bands represent, environmental fungal contamination is suspected. The bands obtained from experimental samples at the 3-month time point are slightly larger in size than expected (compared to the nematode positive control); at previous time intervals for slide-mounted and unmounted samples, the positive control is equivalent in size to the experimental bands. Similar weak banding patterns have been seen during this study, typically for nematodes removed from slide mounts after long periods of storage. Further attempts at sequencing such bands usually resulted in failed sequencing reactions or intermittent short sequence reads. Sequence similarity searches on GenBank indicated that the resulting contaminant sequences matched (similarity often >90%) to marine fungi (Bhadury *et al.* In preparation). Certain regions of the 18S rRNA gene are highly conserved across eukaryotes and even nematode-specific primers have been known to co-amplify fungal 18S genes from environmental samples (Bhadury *et al.* 2006). Fungi are a well known source of food for terrestrial nematodes (Munn & Munn 2002) and the ubiquity of fungi in marine and estuarine ecosystems (Hyde *et al.* 1998) makes them a likely source of food for nematodes in those environments as well. Thus, genomic extraction protocols which involve the digestion of whole specimens may also inadvertently extract the DNA of any fungi that may be present within the digestive tract.

There is a clear need for specific taxonomic protocols that will facilitate the success of molecular work on mounted specimens, especially considering the continued expansion of molecular work on free-living nematodes. Previous studies have indicated that nematode degradation in glycerol is unpredictable and DNA can be affected at times ranging from days to months (Cook *et al.* 2005). This study has also found similar variation in success: DNA has degraded after only a few weeks on slides for some specimens, whilst for other nematodes PCR amplifications and sequencing have been successful even though specimens were kept stored in slide mounts for several months. Meldal (2004) kept specimens mounted in glycerol for a maximum of 2 weeks before

removing them for molecular work. Results from the present study further support this timeframe as an acceptable window for storing nematodes in slide mounts.

The desiccation and slide mounting process appears to reduce overall band intensity immediately: after only 1 day in slide mounts there were fewer strong bands (≥ 60 ng) in both temperature treatments compared to the first time point of the unmounted treatment. Specimens amplified directly from full-strength DESS consistently exhibit high success rates of PCR and a high overall DNA content per band at all time points (Figure 3.14), whereas slide-mounted nematodes show a decrease in the number of successful PCRs and weakening band intensity as time progresses (Figures 3.10 to 3.12). Storing slide mounts at 4°C seems to increase the strength of PCR amplifications in the short term. The cold treated slides showed a higher proportion of strong bands (≥ 60 ng) at each time point compared to the room temperature treatment, even though the total number of bands present per time point was almost always higher for the room temperature treatment. Strong bands are preferred if the PCR product is to be purified and sequenced; higher DNA content increases the chance of successfully sequencing the amplified gene region, although it is not uncommon for weaker bands to return good quality sequences. The likelihood of a failed sequencing reaction increases as the quantity of DNA within a PCR reaction (and thus band intensity) decreases.

We have not found a suitable explanation that conclusively accounts for DNA degradation in slide-mounted nematodes. Glycerol and DMSO (a component of DESS preservative) can be used as additives to aid PCR success, but neither substances have been shown to inhibit reactions at high concentrations (Bickley & Hopkins 1999). Sodium chloride, another component of DESS preservative, is known to inhibit PCR reactions at concentrations >25 mM (Bickley & Hopkins 1999), but if this compound was solely responsible we would expect failure of all PCR reactions from preserved nematodes. One plausible explanation relates to the decreased thermal stability of DNA in the presence of glycerol and sodium ions (Sorokin *et al.* 1997). Individual DNA strands are quite stable at high temperatures and it is standard procedure to keep DNA at 95°C for several minutes in PCR reactions. At this temperature, hydrogen bonds between complementary DNA strands are broken and double stranded DNA separates into single strands although the integrity of individual strands is not diminished (Turner *et al.* 2000). Sorokin *et al.* (1997) note that glycerol normally enhances the thermal stability of DNA molecules, but when glycerol and sodium ions are present concurrently this stabilising effect is greatly reduced. Reduced thermal stability could increase the likelihood of individual DNA strands to

denature when heated; this could prevent PCR amplification if the template DNA is structurally damaged. In DESS preservative, DMSO increases the porosity of cell membranes and allows NaCl to physically enter cells and inactivate nuclease enzymes (Yoder *et al.* 2006). This preserves DNA integrity by preventing shearing, but also results in high cellular concentrations of sodium chloride. After desiccation has been carried out, glycerol has also been introduced to nematode tissues. Slide mounting protocols require slides to be briefly placed on a hotplate at 65°C in order to melt the wax ring and secure the cover slip. This seemingly benign step may, in fact, have significant implications for the longevity of cellular DNA. The heating of desiccated specimens containing high cellular concentrations of glycerol and Na⁺ ions may lead to physical alterations of DNA structure and/or chemical interactions resulting in decreasing integrity of DNA over time for mounted nematodes. Future studies will need to investigate whether DNA storage can be improved by avoiding heat during slide mounting.

The slide mounting process remains an undeniably essential component for morphological identification of nematode specimens. This PhD investigation has utilised a timeframe of 3 days maximum from initial desiccation of nematodes until extraction of genomic DNA; hundreds of PCR amplicons and sequence fragments of the 18S rRNA gene have been successfully obtained, with only occasional failures. After the extraction of genomic DNA has been completed, samples can be safely stored at -20°C until required for molecular work, with no further need for concern regarding the integrity of nematode DNA.

For integrative studies, it is crucial to obtain correct taxonomic identifications and capture a record of digital voucher images if the specimen is going to be destroyed for molecular work. The desiccation and slide mounting process is especially necessary for inexperienced taxonomists who may not be able to decipher morphological features from specimens extracted straight out of preservative solution. Knowledge of nematode diversity remains sparse and reliable identifications derived from DNA sequences are unlikely to be accurate given the current depauperate state of nematode sequence databases. Collection of morphological data will continue to be utilised in nematode studies for years to come.

4. Resolving phylogenetic relationships within the basal clade Enoplida

4.1 Analysis of SSU data

Higher clade relationships within the Enoplida were investigated using both large-scale SSU phylogenies (including all nematode taxa plus metazoan outgroups), as well as smaller datasets comprising only Enoplid and Dorylaimid taxa (utilising 563 SSU sequences, including Chromadorid outgroup taxa). Exhaustive tests were carried out on both small datasets (Table 4.1) and large-scale nematode phylogenies (Table 4.2) in order to evaluate the robustness of tree topologies and test the effects of different phylogenetic parameters. For the small dataset, both Maximum Likelihood (ML) (Figures 4.1 to 4.3) and Bayesian phylogenies (Figure 4.4) were constructed utilising 18S gene sequences from a total of 548 Enoplid and Dorylaimid nematodes; 15 Chromadorid nematode sequences were utilised as outgroup taxa. Duplicate gene sequences were included in these trees in order to graphically illustrate the phylogenetic placement of nematode specimens obtained from different geographic locations. Large-scale Maximum Likelihood phylogenies were constructed using 1336 nematode taxa and four closely related metazoan phyla as outgroup taxa (Nematomorpha, Priapulida, Kinorhyncha, and Tardigrada). The internal phylogenetic structure of the Enoplid and Dorylaimid clades was identical in both large and small trees—as a result, the figures and discussion outlined in this chapter will focus primarily on the results from the small datasets. A full discussion of the large-scale phylogenies is detailed in Chapter 5.

The small nematode dataset was analysed under various phylogenetic parameters and conditions. The internal structure of most Enoplid clades was consistent across all analyses (Tables 4.1 and 4.2); the exception was the Oxystominidae/Oncholaimidae clade where sub-clades relationships were observed to vary. Some higher clade relationships were also unstable; the Ironidae and Alaimina generally appeared as sister taxa, but occasionally this relationship was not recovered. Finally, the sister taxon to the clade containing the Tripyloididae/Trefusiidae remains unresolved; this sister group consistently alternated between the Syringolaimus/Campydora clade and the Ironidae/Alaimia clade. Within the large-scale phylogenies (Table 4.2), the Dorylaimia and Enoplia were observed to alternate as the earliest splitting nematode lineage; however, these higher clade placements did not affect the internal structure of either group. To evaluate tree topologies, SSU alignments were first run under 'standard conditions' (Figure 4.1), using

estimation of invariable sites (P-invar parameter) and no structural alignment partitions. Phylogenies were constructed both with and without the P-invar parameter that estimates the proportion of invariable sites, to test whether this additional parameter interfered with phylogenetic inference (Stamatakis 2008). Some authors (including the authors of RAxML) advise against simultaneously estimating P-Invar and gamma distributions (the latter being automatically estimated by RAxML's algorithms), arguing that these two parameters cannot be independently estimated from one dataset (Gu *et al.* 1995; Yang 2006; Stamatakis 2008). Removal of the P-Invar parameter did not have any effect on tree topologies. SSU alignments were also separated into Stem/Loop regions based on secondary structure information and subjected to ML analysis using partitioned gene alignments (Figure 4.2); topologies using secondary structure partitions were compared to non-partitioned ML runs. The position of stems and loops in 18S sequences is included in all alignments downloaded from the SILVA rRNA database; partitioned gene alignments were constructed by separately exporting stem and loop alignment sites using the ARB program, and manually combining the data into a single alignment. Finally, gene alignments were analysed using the Gblocks program (Figure 4.3); this program trims sequence alignments to represent only conserved blocks, eliminating poorly aligned sites and potentially saturated or overly divergent regions (Castresana 2000). Gblocks analysis resulted in some rearrangement of higher clade relationships, but relationships amongst lower taxonomic levels were consistent with other analyses. Bayesian SSU phylogenies (Figure 4.4) agreed with phylogenetic topologies obtained from ML analyses. Figures 4.5 (ML phylogeny from Figure 4.1) and 4.6 (Bayesian phylogeny from Figure 4.4) have both been expanded and annotated to display lower taxonomic relationships recovered amongst Enoplid genera.

The subsequent discussion of results from molecular phylogenies (Chapters 4-6) will utilise higher taxon names outlined by De Ley and Blaxter (2002).

Table 4.1: Overview of Enoplid clade topologies using different phylogenetic parameters for the small nematode dataset (Enoplia/Dorylaimia only, 563 taxa) Syringo = Syringolaimus, O = Oncholaimoidea, T = Thalassoalaimus/Litinium, Ox = Oxystomina H = Halalaimus, A = Anoplostoma, An = Anticomidae, C = Chaetonema, L = Leptosomatidae, Th = Thoracostomopsidae, E= Enoplolaimus, Ph = Phanodermopsis. Hyphens represent hierarchal derivation of clades, while slashes (e.g. A/B) denote clades appearing as sister taxa.

Job Number	Outgroup	P-Invar Estimate	Likelihood	Clade Placement Ironidae/ Alaimina	Sister Clade to Tripyloididae/ Trefusiidae	Clade Placement Oncholaimoidea/ Oxystominidae	Clade Placement Leptosomatidae/ Anticomidae/ Anoplostomatidae	Clade Placement Thoracostomopsidae
<i>Main topology using all Enoplid taxa</i>								
65991	Chromadorida	Yes	-73636	Condensed	(None)	O-T-Ox/H	A-An-C/L	Th-E/Ph
<i>Gblocks Analysis</i>								
887889	Chromadorida	Yes	-37672	Split	Syringo	T-O-OxH	A-An/C-L	Th-E/Ph
<i>Nucleotide model without estimation of P-Invar parameter</i>								
405816	Chromadorida	No	-73750	Condensed	Syringo	O-T-Ox/H	C-A-L- An	Th-E/Ph
<i>Gene partitions according to stem/loop secondary structure</i>								
66027	Chromadorida	Yes	-72699	Condensed	Syringo	O-T-Ox/H	A-An-C/L	Th-E/Ph

Table 4.2: Overview of Enoplid clade topologies using different phylogenetic parameters for the large nematode dataset (all nematodes, 1100-1400 taxa) Syringo = Syringolaimus, Iron = Ironidae, Alaim = Alaimina, O = Oncholaimoidea, T = Thalassoalaimus/Litinium, Ox = Oxystomina H = Halalaimus, A = Anoplostoma, An = Anticomidae, C = Chaetonema, L = Leptosomatidae, Th = Thoracostomopsidae, E = Enoplolaimus, Ph = Phanodermopsis. Hyphens represent hierarchal derivation of clades, while slashes (e.g. A/B) denote clades appearing as sister taxa. All analyses using GTR+CAT+P-Invar unless otherwise noted.

Job Number	Outgroup	P-Invar Estimate	Likelihood	Earliest splitting clade	Clade Placement Ironidae/ Alaimina	Sister Clade to Tripyloididae/ Treflusiidae	Clade Placement Oncholaimoidea/ Oxystominidae	Clade Placement Leptosomatidae/ Anticomidae/ Anoplostomatidae	Clade Placement Thoracostomopsidae
<i>Removal of long branch nematode taxa</i>									
830442	All Outgroups	Yes	-217364	Enoplia	Condensed	Iron/Alaim	Ox-O-H/T	A-An-C/L	Th-E/Ph
830456	Tardigrada	Yes	-208653	Dorylaimia	Condensed	Syringo	O/T-H/O	A-An-C/L	Th-E/Ph
830461	Priapulida	Yes	-197978	Enoplia	Condensed	Syringo	O-T-Ox/H	A-An-C/L	Th-E/Ph
830465	Kinorhyncha	Yes	-199540	Enoplia	Condensed	Syringo	O-T-Ox/H	A-An-C/L	Th-E/Ph
830047	Nematomorpha	Yes	-200810	Dorylaimia	Condensed	Syringo	O-T-Ox/H	A-An-C/L	Th-E/Ph
<i>Removal of both outlier and long branch nematode taxa</i>									
830104	Nematomorpha	Yes	-196069	Dorylaimia	Condensed	Iron/Alaim	O/T-H/Ox	A-An-C/L	Th-E/Ph
830319	Tardigrada	Yes	-203926	Dorylaimia	Condensed	Syringo	O/T-H/Ox	A-An-C/L	Th-E/Ph
830320	Priapulida	Yes	-193251	Enoplia	Condensed	Iron/Alaim	O-T-Ox/H	A-An-C/L	Th-E/Ph
830328	Kinorhyncha	Yes	-194815	Enoplia	Condensed	Syringo	O-T-Ox/H	A-An-C/L	Th-E/Ph
830407	All Outgroups	Yes	-212643	Enoplia	Condensed	Iron/Alaim	O/T-H/Ox	A-An-C/L	Th-E/Ph
<i>Removal of outlier nematode taxa</i>									
77787	All Outgroups	Yes	-269230	Enoplia	Condensed	Iron/Alaim	Ox-T-O/H	A-An-C/L	Th-E/Ph
822337	Nematomorpha	Yes	-252690	Dorylaimia	Condensed	Iron/Alaim	Ox-T-O/H	A-An-C/L	Th-E/Ph

Job Number	Outgroup	P-Invar Estimate	Likelihood	Earliest splitting clade	Clade Placement Ironidae/ Alaimina	Sister Clade to Tripyloidea/ Trefusiidae	Clade Placement Oncholaimoidea/ Oxystominidae	Clade Placement Leptosomatidae/ Anticomidae/ Anoplostomatidae	Clade Placement Thoracostomopsidae
<i>GTR+CAT+P-Invar using all nematode taxa</i>									
830467	Nematomorpha	Yes	-257448	Dorylaimia	Condensed	Iron/Alaim	Ox-T-O/H	A-An-C/L	Th-E/Ph
830473	Priapulida	Yes	-254626	Enoplia	Condensed	Iron/Alaim	Ox-T-O/H	A-An-C/L	Th-E/Ph
830485	Tardigrada	Yes	-265252	Dorylaimia	Condensed	Syringo	O-T-Ox/H	A-An-C/L	Th-E/Ph
830519	Kinorhyncha	Yes	-256203	Enoplia	Condensed	Iron/Alaim	O-T-Ox/H	A-An-C/L	Th-E/Ph
830526	All Outgroups	Yes	-273996	Enoplia	Condensed	Syringo	O-T-Ox/H	A-An-C/L	Th-E/Ph

GTR+CAT (without estimation of P-Invar parameter) using all nematode taxa

995794	All Outgroups	No	-274127	Enoplia	Condensed	Iron/Alaim	O-T-Ox/H	A-An-C/L	Th-E/Ph
995867	Kinorhyncha	No	-256331	Enoplia	Condensed	Iron/Alaim	O-T-Ox/H	A-An-C/L	Th-E/Ph
995979	Priapulida	No	-254753	Enoplia	Condensed	Iron/Alaim	O-T-Ox/H	A-An-C/L	Th-E/Ph
879770	Nematomorpha	No	-257558	Dorylaimia	Condensed	Iron/Alaim	O-T-Ox/H	A-An-C/L	Th-E/Ph
884354	Tardigrada	No	-265380	Doryla/Enop	Condensed	Syringo	O-T-Ox/H	A-An-C/L	Th-E/Ph

Gene partitions according to stem/loop secondary structure

992781	All Outgroups	Yes	-271125	Enoplia	Condensed	Iron/Alaim	O/T-H/Ox	A-An-C/L	Th-E/Ph
992843	All Outgroups	No	-271250	Enoplia	Condensed	Iron/Alaim	O/T-H/Ox	A-An-C/L	Th-E/Ph
993046	Kinorhyncha	Yes	-253504	Dorylaimia	Condensed	Iron/Alaim	Ox-T-O/H	A-An-C/L	Th-E/Ph
993157	Nematomorpha	Yes	-254713	Dorylaimia	Condensed	Iron/Alaim	O/T-H/Ox	A-C-An/L	Th-E/Ph
993260	Priapulida	Yes	-251913	Dorylaimia	Condensed	Syringo	O/T-H/Ox	A-An-C/L	Th-E/Ph
993461	Tardigrada	Yes	-262437	Dorylaimia	Condensed	Iron/Alaim	Ox-T-O/H	A-An-C/L	Th-E/Ph

Job Number	Outgroup	P-Invar Estimate	Likelihood	Earliest splitting clade	Clade Placement Ironidae/ Alaimina	Sister Clade to Tripyloidea/ Trefusiidae	Clade Placement Oncholaimoidea/ Oxystominidae	Clade Placement Leptosomatidae/ Anticomidae/ Anoplostomatidae	Clade Placement Thoracostomopsidae
<i>Outgroup effects: topology tests using different combinations</i>									
898961	Nematomorpha, Tardigrada	Yes	-269584	Dorylaimia	Condensed	Iron/Alaim	O-T-Ox/H	A-An-C/L	Th-E/Ph
901362	Nematomorpha, Kinorhyncha	Yes	-260508	Dorylaimia	Condensed	Iron/Alaim	Ox-T-O/H	A-An-C/L	Th-E/Ph
901536	Nematomorpha, Priapulida	Yes	-258932	Enoplia	Condensed	Iron/Alaim	O-T-Ox/H	A-An-C/L	Th-E/Ph
901987	Tardigrada, Kinorhyncha	Yes	-268328	Dorylaimia	Condensed	Iron/Alaim	O/T-H/Ox	A-An-C/L	Th-E/Ph
903685	Tardigrada, Priapulida	Yes	-266747	Enoplia	Condensed	Syringo	O-T-Ox/H	A-An-C/L	Th-E/Ph
904672	Kinorhyncha, Priapulida	Yes	-257601	Enoplia	Condensed	Iron/Alaim	O-T-Ox/H	A-An-C/L	Th-E/Ph
905042	All minus Nematomorpha	Yes	-269695	Enoplia	Condensed	Iron/Alaim	Ox-T-O/H	A-An-C/L	Th-E/Ph
905265	All minus Tardigrada	Yes	-261893	Enoplia	Condensed	Iron/Alaim	Ox-T-O/H	A-An-C/L	Th-E/Ph
906184	All minus Kinorhyncha	Yes	-271043	Doryla/Enop	Condensed	Iron/Alaim	Ox-T-O/H	A-An-C/L	Th-E/Ph
906503	All minus Priapulida	Yes	-272620	Dorylaimia	Condensed	Iron/Alaim	Ox-T-O/H	A-An-C/L	Th-E/Ph

Removal of the Trichinellida

77880	All Outgroups	Yes	-270785	Doryla/Enop	Condensed	Syringo	O-T-Ox/H	A-An-C/L	Th-E/Ph
77929	Kinorhyncha	Yes	-252998	Enoplia	Condensed	Syringo	O-T-Ox/H	A-An-C/L	Th-E/Ph
77963	Nematomorpha	Yes	-254241	Dorylaimia	Condensed	Iron/Alaim	Ox-T-O/H	A-An-C/L	Th-E/Ph
78054	Priapulida	Yes	-251451	Enoplia	Condensed	Syringo	O-T-Ox/H	A-An-C/L	Th-E/Ph
78067	Tardigrada	Yes	-262062	Doryla/Enop	Condensed	Syringo	Ox-T-O/H	A-An-C/L	Th-E/Ph

Gblocks Analysis

885458	All Outgroups	Yes	-58345	Dorylaimia	Split	(None)	O-Ox-T/H	L-An/C	E-Th/Ph
--------	---------------	-----	--------	------------	-------	--------	----------	--------	---------

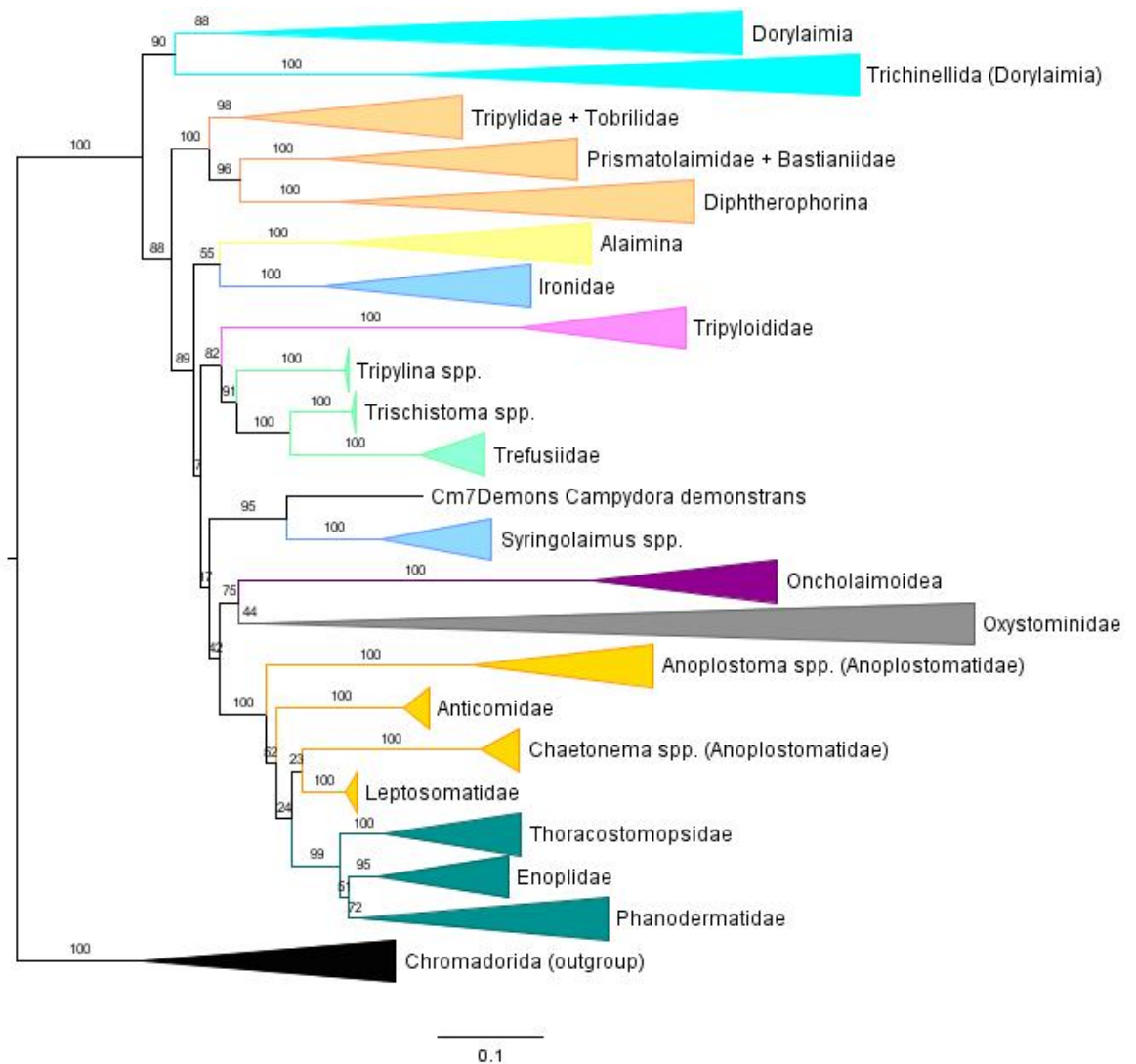


Figure 4.1: Maximum Likelihood SSU phylogeny displaying the major clades within the Enoplia. Tree built using 563 taxa with estimation of the P-Invar parameter, and no secondary structure gene partitions. (RAXML Job #65991). Scale bar represents nucleotide substitutions per site.

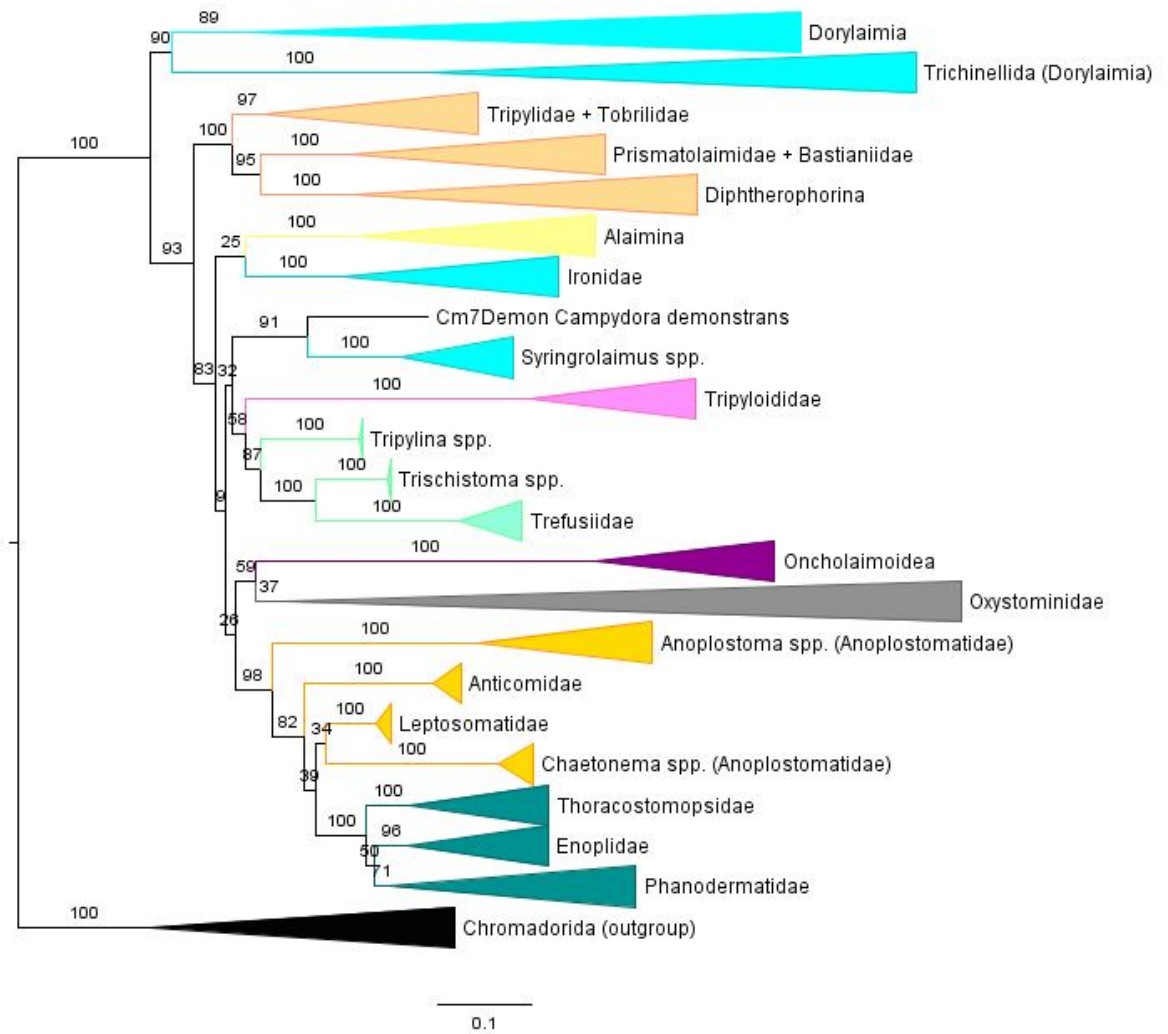


Figure 4.2: Maximum Likelihood SSU phylogeny displaying the major clades within the Enoplia. Tree built using 563 taxa with estimation of the P-Invar parameter, and using gene partitions according to rRNA stem and loop structures. (RAxML Job #66027). Scale bar represents nucleotide substitutions per site.

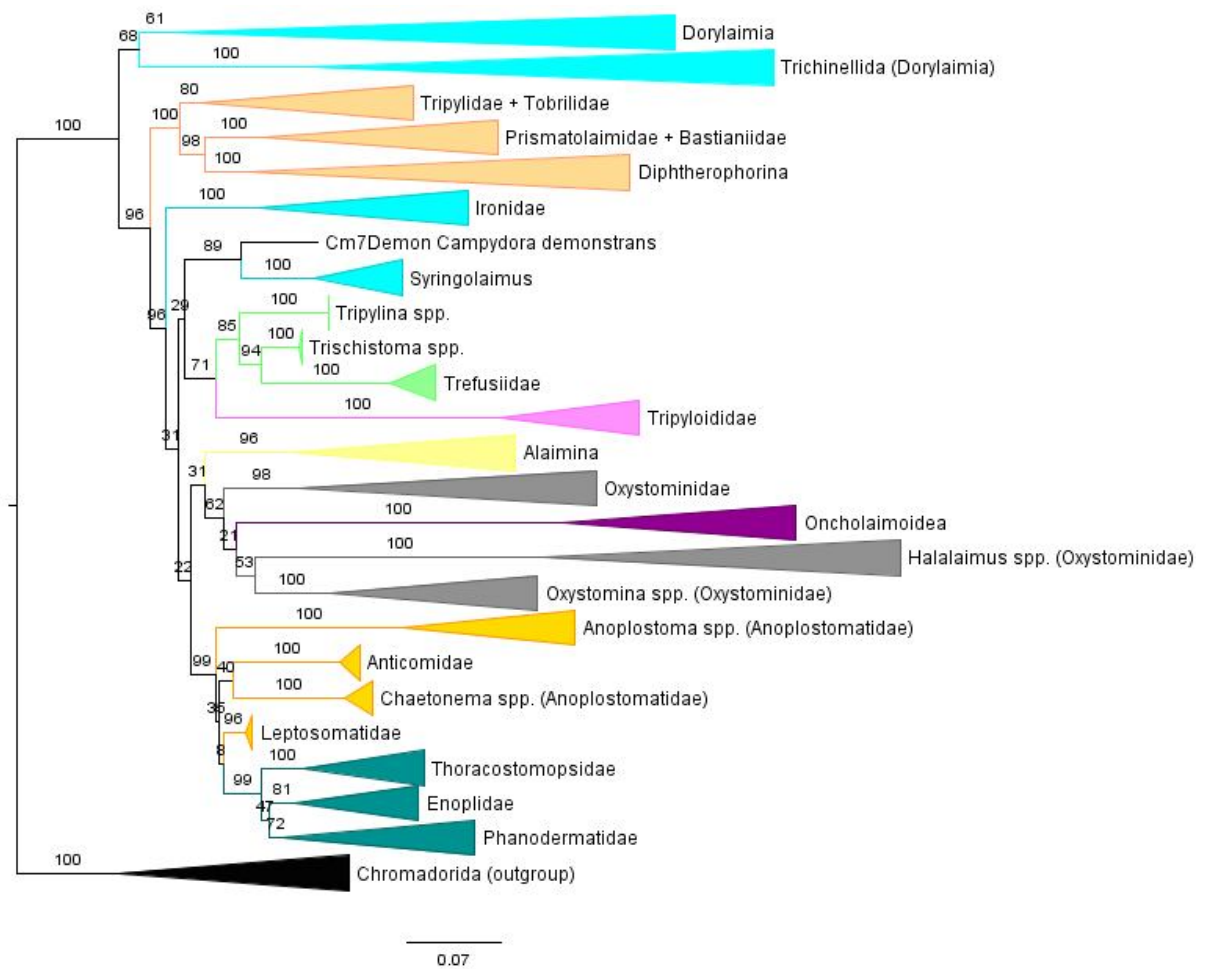


Figure 4.3: Maximum Likelihood SSU phylogeny displaying the major clades within the Enoplia. Variable alignment sites were trimmed using the Gblocks program prior to phylogenetic analysis. Tree built using 563 taxa with estimation of the P-Invar parameter, and no secondary structure gene partitions. (RAxML Job #547483). Scale bar represents nucleotide substitutions per site.

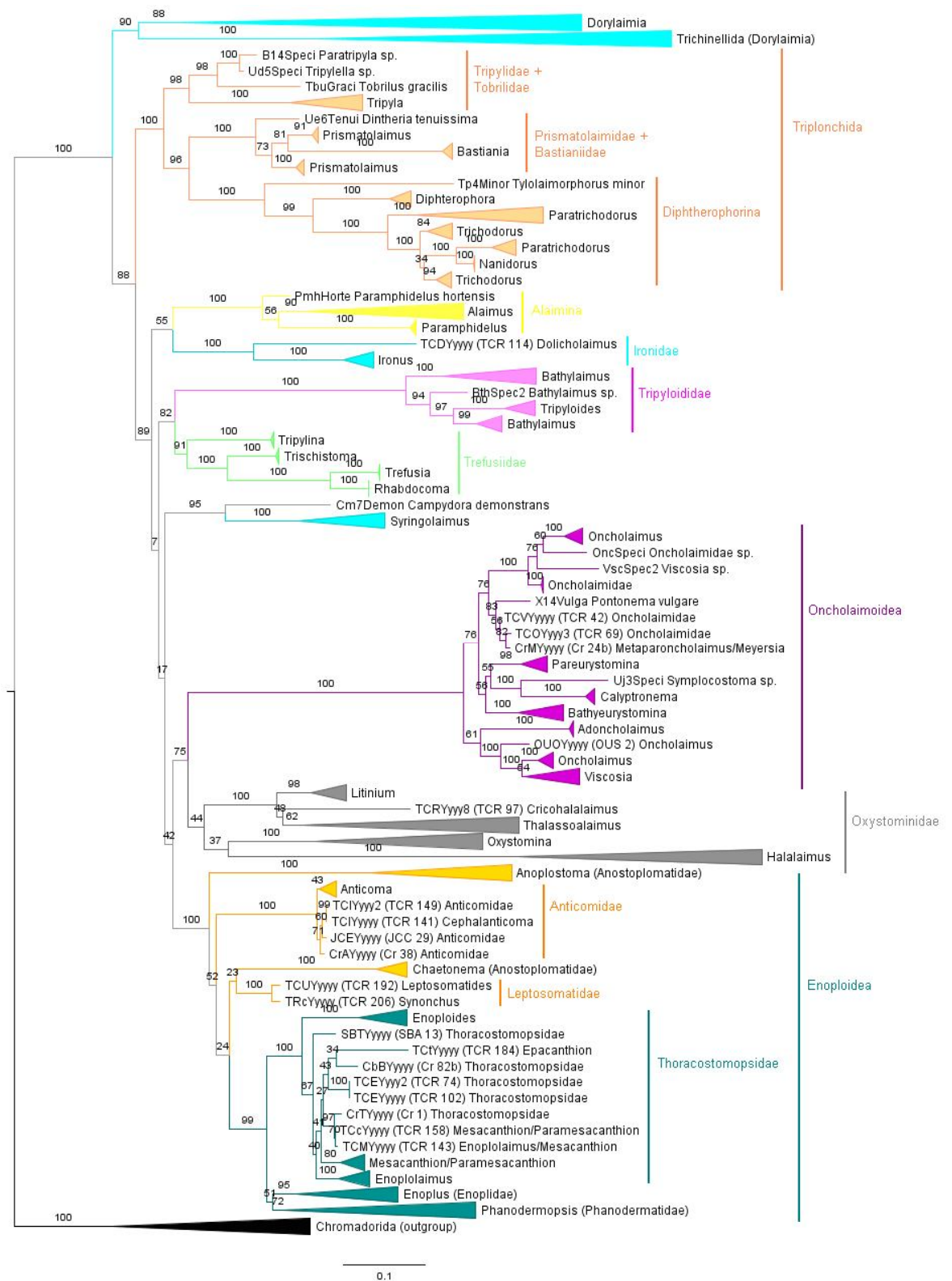


Figure 4.5: Maximum Likelihood SSU phylogeny displaying the major clades within the Enoplia, expanded to show relationships between genera. Tree built using 563 taxa with estimation of the P-Invar parameter, and no secondary structure gene partitions. (RAXML Job #65991). Scale bar represents nucleotide substitutions per site.

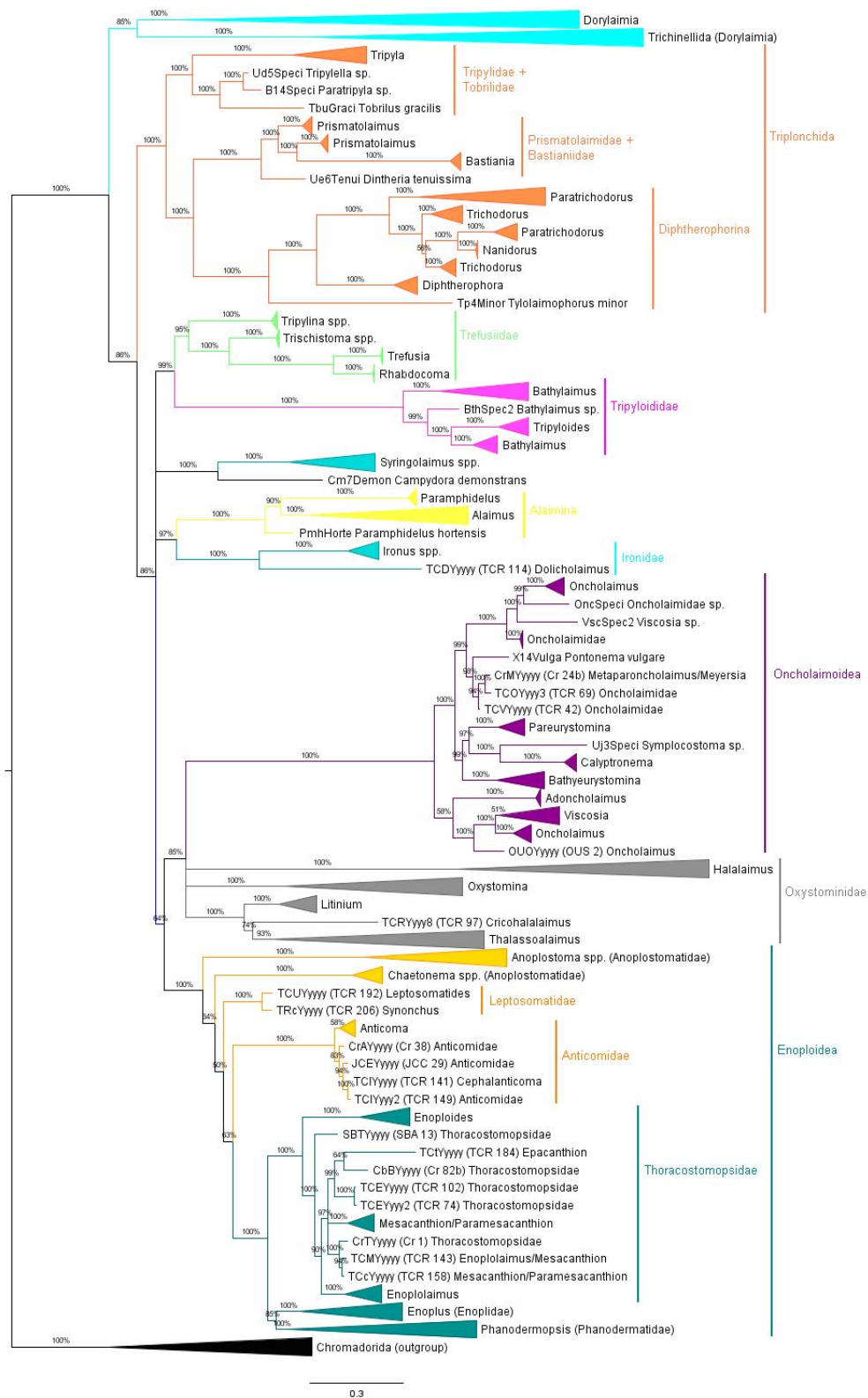


Figure 4.6: Bayesian SSU phylogeny displaying the major clades within the Enoplia, expanded to show relationship between genera. Tree built using 563 taxa using the GTR+G+I model of nucleotide substitution, and no secondary structure gene partitions. Scale bar represents nucleotide substitutions per site.

4.2 Consistency of SSU phylogenies with previous frameworks

SSU phylogenies have provided substantial insight on relationships within the previously neglected Enoplid clade. This investigation has obtained the first gene sequences from Enoplid genera (e.g. *Chaetonema*) and even families (Leptosomatidae) that are notably absent from public sequence databases. This increased taxon sampling (over 250 gene sequences) has allowed the first comprehensive assessment of lower taxonomic relationships within the Enoplida. It appears that the inclusion of as many taxa as possible is key to recovering highly-supported and accurate phylogenies. The recovery of the Enoplida in this study exhibited similarity to another recent large-scale phylogeny by Van Megan *et al.* (2009) that used less than 50 Enoplid sequences. However, there appear to be some obvious inaccuracies in this published tree, such as the splitting of the Oxystominidae (always recovered in a monophyletic clade along with the Oncholaimoidea in this study), a sister relationship between the Alaimina and Anoplostomatidae/Enoplidae (never recovered in this study), and a sister relationship between the genus *Oxystomina* and the *Syringolaimus/Campydora* clade (never recovered in this study). When tree topologies were in accordance (such as the clade containing the Tripyloididae, Trefusiidae, and Tripylidae), Van Megan *et al.*'s (2009) phylogeny reported much lower support values.

The Enoplia is divided into two orders, the Triplonchida and the Enoplida. This separation is highly supported by all ML analyses (>88 support), and agrees with previous molecular frameworks (De Ley & Blaxter 2002; Holterman *et al.* 2006; Van Megan *et al.* 2009). The Triplonchida was consistently recovered as monophyletic, in line with previous phylogenies (De Ley & Blaxter 2002; Holterman *et al.* 2006; Meldal *et al.* 2007). De Ley and Blaxter (2004) outlined three suborders within the Triplonchida, based on molecular data: Diptherophorina, Tobrilina and Tripylina. This study further confirms the presence of three major clades within this group, although the membership of some groups differs slightly from De Ley and Blaxter's classification. The topologies of all three Triplonchidid clades were firmly supported, with each clade consistently demonstrating support values above 97. The suborder Diptherophorina was recovered in accordance with De Ley and Blaxter, containing the Trichodoridae and Diptherophoridae. Although *Tylolaimophorus* is currently classified within the Diptherophoridae (Abebe *et al.* 2006), this genus appears quite divergent in ML tree topologies and should probably be placed within its own family. Past morphological classification previously grouped the Trichodoridae and Diptherophoridae within the Dorylaimia (Filipjev 1934; Chitwood & Chitwood 1950; Clark

1961; De Coninck 1965; Andr ssy 1976; Lorenzen 1981). Siddiqi (1983) was the only author to propose a close relationship with the Enoplida, placing these two families in their own order (the Triplonchida); he argued that the buccal cavity morphology, amphid shape, structure of excretory ducts, arrangement of reproductive organs, and spicular protractor muscles in the Triplonchida were not typical of the morphology seen in most Dorylaimid species.

The Tripylina is highly supported by both ML (>98) and Bayesian (100) analyses, with the genera *Tobrilus*, *Tripyla*, *Paratripyla* and *Tripylella* consistently recovered within this clade. This investigation did not recover a close relationship between the Prismatolaimidae and the Tobrilidae, as suggested by De Ley and Blaxter (2002). It appears that a close relationship between *Tobrilus* and the Prismatolaimidae is only reported when few taxa are utilized in phylogenetic analyses; Meldal *et al.* (2007) also reported *Tobrilus* and the Prismatolaimidae as sister taxa in one analysis, but this placement was not consistent and only based on two gene sequences. The Tripylidae has typically been classified within the Enoplida (e.g. Lorenzen 1981), and many authors put this group into a separate suborder (Andr ssy 1976) or superfamily (Chitwood & Chitwood 1950; Clark 1961; De Coninck 1965) along with the Ironidae. *Tobrilus* has previously been grouped with the Tripylidae in morphological classifications (Clark 1961; De Coninck 1965; Andr ssy 1976). Only De Coninck included the Prismatolaimidae within the same subfamily as *Tobrilus*, whereas other authors separated these taxa into different families. The highly supported placement of *Tobrilus* within the Tripylidae appears to confirm the historical classification of this genus, and this placement is further corroborated by Van Megen *et al.*'s (2009) recent large-scale phylogeny.

The vestiges of De Ley and Blaxter's Tobrilina was recovered as the third clade within the Triplonchida, containing the Prismatolaimidae in accordance with past classifications (De Ley & Blaxter 2002; De Ley & Blaxter 2004), and additionally containing species representing the Bastianiidae. This topology is supported by recent molecular phylogenies; Holterman *et al.* (2006) recovered the Prismatolaimidae and Bastianiidae as sister taxa, although the authors did not include the genus *Tobrilus* in their analysis. Van Megen *et al.* (2009) recovered the Bastianiidae within the Prismatolaimidae but labelled this family as *incertae sedis*. Previous authors have noted morphological congruence between the Bastianiidae and the Prismatolaimidae (Lorenzen 1981; Coomans & Raski 1988); Lorenzen (1981) noted that these two groups both possess dorsally spiral amphids,

exhibit a similar cuticle structure, and display similar positioning and structure in cephalic setae and pre-anal papillae.

The Diphtherophorina and the Prismatolaimid/Bastianiid clade were always recovered as sister taxa, with the *Tripylina* appearing as the earliest branching lineage within the Triplonchida. Tree topologies indicate that the relationships between some Triplonchid genera require further analysis. The genera *Trichodorus*, *Paratrachodorus*, and *Prismatolaimus* appeared to be paraphyletic based on SSU data. However, this may be a function of gene sequences being too conserved to clearly elucidate relationships at lower taxonomic levels within these groups. LSU sequences were able to separate similar 'paraphyletic' genera within the Tripyloididae (refer to Section 4.4.1 for a full discussion). Unfortunately, LSU sequences were not available for most representatives of the Triplonchida, preventing a detailed analysis of relationships between genera.

ML and Bayesian analyses recovered five main clades within the order Enoplida (Figures 4.5 and 4.6). Clade 1 contained the Alaimina and Ironidae (excluding *Syringolaimus*) as sister taxa. Clade 2 contained another set of sister taxa, the Tripyloididae and the Trefusiidae (including the genera *Tripylina* and *Trischistoma*). Clade 3 contained only the genus *Syringolaimus* and *Campydora demonstrans* as its sister taxon. Clade 4 contained both the superfamily Oncholaimoidea and the Oxystominidae. Clade 5 formed a major grouping consisting of the superfamily Enoploidea *sensu* Lorenzen (1981) but additionally including the Leptosomatidae. Increased taxon sampling has significantly refined the proposed classification outlined by De Ley and Blaxter (2002). The previous placement of the Leptosomatidae and Oxystominidae within the suborder Ironina is clearly incorrect. The Leptosomatidae are well supported as members of the Enoploidea, while the Oxystominidae should be incorporated into the suborder Oncholaimina. This study suggests that the Ironidae and Alaimina should be grouped within a single suborder, and that the Trefusiida should be integrated within the suborder Tripyloidina. Furthermore, the clade containing *Syringolaimus*/*Campydora* should be designated as its own separate suborder. In addition to deep phylogenetic splits within the Enoplida, SSU data was able to elucidate many relationships at lower taxonomic levels.

The Oxystominidae and superfamily Oncholaimoidea were always recovered as a monophyletic grouping, although relationships within internal clades are not fully resolved. The Oncholaimoidea is always recovered as monophyletic; however, the placement of genera within the Oxystominidae is not very stable, and this group is often recovered as paraphyletic. The four clades containing the Oncholaimoidea,

Thalassolaimus/Cricohalalaimus/Litinium, *Oxystomina*, and *Halalaimus* are all noted to be quite divergent from other Enoplid taxa and display very long branches on all tree topologies. Thus, the occasional splitting of the Oxystominidae is probably related to long-branch attraction. The Oncholaimoidea is firmly supported as monophyletic in all tree topologies and includes both the Oncholaimidae and the Enchelidiidae, in line with previous phylogenies (De Ley & Blaxter 2002; Meldal *et al.* 2007; Van Megen *et al.* 2009). The Enchelidiidae appears to be a derived clade within the Oncholaimoidea; this family is consistently recovered as monophyletic, although support values vary (55-75). Support values for the Oncholaimoidea-Oxystominidae clade were not always high (ranging from 50-75), but this group was consistently recovered in all tree topologies. There are some morphological similarities which support the close relationship between the Oncholaimoidea and Oxystominidae. Lorenzen (1981) noted that all species examined from both groups possess 'orthometaneme' type metanemes with associated caudal filaments; most other Enoplid taxa that possess this specific type of metaneme do not have associated caudal filaments, with the exception of a few isolated species.

This study recovered the superfamilies Tripyloidoidea and Trefusioidea within a single, highly supported clade; this clade also contains two genera formerly grouped within the Tripylidae, *Tripylina* and *Trischistoma*. Support values for this grouping were generally >70 for Maximum Likelihood topologies, and over 99 in Bayesian phylogenies. Within this clade, the Tripyloidae appeared as the most basal monophyletic taxon. *Tripylina*, *Trischistoma*, and the Trefusiidae form a highly supported (usually >90) monophyletic clade that appears as a sister group to the Tripyloidae. The Trefusiidae and the genus *Trischistoma* appear as sister taxa, with *Tripylina* appearing to be the more basal taxon within this group. This clade topology was also recovered by Van Megen *et al.* (2009), although their study reported lower nodal support values.

The Trefusiidae was historically grouped within the Enoplida; the placement of Trefusiid genera varied between systems, although later classifications placed *Trefusia* within the Oxystominidae (Filipjev 1934; De Coninck 1965; Andr ssy 1976). Lorenzen (1981) placed the Trefusiidae within a completely separate suborder, arguing that the lack of metanemes precluded inclusion of this group within the Enoplida. Molecular data supported the association between the Trefusiida and Enoplia, and recent evidence suggested that *Trefusia zostericola* should be placed within the Enoplida (Rusin *et al.* 2001). De Ley and Blaxter (2002) originally placed the Trefusiida as a third order within the Enoplia, but later recommended that its rank be reduced to a suborder within the Enoplida

(De Ley & Blaxter 2004). The position of the Tripyloididae has presented some confusion for past taxonomists; some placed this group within the Enoplia because of similarities in head shape (Filipjev 1918; Filipjev 1934), while others argued that the spiral shaped amphids warranted classification within the Araeolaimida (Andrássy 1976) or Chromadorida (Chitwood & Chitwood 1950; De Coninck 1965). Most recently, Lorenzen (1981) grouped the Tripyloidea within the Enoplida based on the presence of metanemes. Molecular data have firmly placed the Tripyloididae within the Enoplida, although early frameworks never grouped the Tripyloididae and Trefusiida together (De Ley & Blaxter 2002; De Ley & Blaxter 2004). However, Siddiqi (1983) suggested a relationship between the Tripylidae and the Tripyloididae, placing them together in the order Tripylida.

Trischistoma and *Tripylina* were historically placed within the Dorylaimia based on morphology (Andrássy 1976; Lorenzen 1981) or within the Triplonchida according to molecular evidence (De Ley & Blaxter 2002; De Ley & Blaxter 2004; Abebe *et al.* 2006). Meldal (2004) confirmed that both these genera were excluded from the Triplonchida, but was unable to resolve their exact placement. Placement of *Trischistoma* within the Enoplida was also suggested by Meldal *et al.* (2007). Holterman *et al.* (2006) and Van Megen *et al.* (2009) further recovered *Trischistoma* and The Trefusiid genus *Trefusia* as sister taxa, supporting the relationships recovered in this study.

The proposed monophyly of the superfamily Enoploidea (De Ley & Blaxter 2002; Meldal *et al.* 2007) was also supported under the current analysis, but this study additionally recovered the Leptosomatidae within this grouping. This large clade is comprised of the Enoplidae, Thoracostomopsidae, Anoplostomatidae, Phanodermatidae, and Anticomidae, and Leptosomatidae. Within this clade, the Thoracostomopsidae, Enoplidae, and Phanodermatidae are all recovered as monophyletic clades with high support values. The Anoplostomatidae are recovered as paraphyletic; the genus *Anoplostoma* appears to split off first from other taxa in the Enoploidea, while the genus *Chaetonema* occupies a more derived position. The Leptosomatidae also appears to be monophyletic, although this group was not extensively sampled—only two gene sequences were obtained during this study. Nonetheless, the genera *Leptosomatides* and *Synonchus* are always recovered within a single clade; this clade was often recovered as a sister taxon to the genus *Chaetonema* under ML analyses. The Anticomidae was also recovered as monophyletic, and was usually placed as the second most basal clade within Enoplidae after *Anoplostoma*. The Thoracostomopsidae, Enoplidae and Phanodermatidae are always recovered as a monophyletic clade (with support values of >97%) that appears to

occupy the most derived position within the Enoploidea. The Phanodermatidae and Enoplidae are usually recovered as sister taxa, although support values are low under ML analysis (40-50%) and not especially high in Bayesian topologies (79%).

Lorenzen created the Anoplostomatidae as a new taxon to include *Anoplostoma* and *Chaetonema*, placing these two groups together on the basis of buccal cavity and cephalic capsule structure. *Chaetonema* was previously placed within the Enchelidiidae (Filipjev 1934) or within the Enoploidea as a member of the Rhabdodemaniidae (De Coninck 1965; Andr ssy 1976). *Anoplostoma* was first placed within the Phanodermatidae (Filipjev 1934), but later excluded completely from the Enoploidea and considered part of the Oncholaimoidea (Filipjev 1934; Clark 1961; De Coninck 1965; Andr ssy 1976). Most morphological classifications did not support a close relationship between *Chaetonema* and *Anoplostoma*, and phylogenetic analysis confirms that these two genera belong to independent lineages.

The Leptosomatidae was traditionally classed within the superfamily Enoploidea (Chitwood & Chitwood 1950; Clark 1961; De Coninck 1965; Maggenti 1982), although some authors removed it from this grouping. Andr ssy (1976) placed the Leptosomatidae within the superfamily Leptosomatoidea, and Lorenzen (1981) grouped this family within the Ironoidea along with the Ironidae and Oxystominidae. The Anticomidae was largely considered a subfamily within the Leptosomatidae (Filipjev 1934; Clark 1961; De Coninck 1965; Andr ssy 1976) and only a few authors separated this group and raised it to family rank (Hope & Murphy 1972; Lorenzen 1981). Lorenzen's (1981) separation of the Anticomidae was based on the left-hand position of gonads and the existence of pre-anal tubules in males of these species (the latter feature not being present in any members of the Leptosomatidae). Tree topologies clearly place the Leptosomatidae within the Enoploidea, supporting older morphological classifications that included this taxon as part of the superfamily. Although the Leptosomatidae and Anticomidae are both placed within the Enoploidea, these two groups are never recovered as a monophyletic clade, apparently supporting Lorenzen's separation of these two families.

The Thoracostomopsidae and Enoplidae have seen significant rearrangements. Most genera were usually grouped into the Enoplidae along with *Enoplus*, while *Thoracostomopsis* represented the sole genus within the Thoracostomopsidae (Filipjev 1934; Clark 1961; De Coninck 1965; Andr ssy 1976; Maggenti 1982). Lorenzen instead considered *Enoplus* as the only genus within the Enoplidae; all other genera previously placed within this group were moved into the Thoracostomopsidae (comprising

subfamilies Thoracostomopsinae, Trileptiinae, and Enoplolaiminae). This separation of *Enoplus* was based on the differences in metaneme structure, gland arrangements, and the absence of onchia. Lorenzen noted that the Thoracostomopsidae are morphologically very similar to the Phanodermatidae with respect to these morphological features. Tree topologies suggest a sister relationship between the Phanodermatidae and *Enoplus* (with these taxa forming a larger monophyletic clade along with the Thoracostomopsidae), suggesting that the morphological differences in *Enoplus* represent derived adaptations. Membership of the Phanodermatidae has been largely consistent amongst classification schemes, and this family was always placed within the Enoploidea (Clark 1961; De Coninck 1965; Andr  ssy 1976; Lorenzen 1981; Maggenti 1982). Molecular data confirms the monophyly of the Phanodermatidae and also seems to support the Lorenzen's classification of the Enopliidae and Thoracostomopsidae. *Enoplus* is always recovered as separate clade and never placed within the Thoracostomopsidae. However, this study only included Thoracostomopsidae species within the subfamily Enoplolaiminae; further analysis is needed to determine if other genera such as *Thoracostomopsis* and *Trileptium* (subfamilies Thoracostomopsinae and Trileptiinae, respectively) also belong within the Thoracostomopsidae *sensu* Lorenzen.

The genus *Syringolaimus* was always recovered as a sister taxa to *Campydora demonstrans* (ML support values >90%, and 100% support in Bayesian topologies), and these two genera were always recovered as a separate clade within the Enopliida. The genus *Campydora* has typically been classified within the Dorylaimia based on morphology (Thorne 1939; De Coninck 1965; Jairajpuri & Ahmad 1992). Only Siddiqi (1983) suggested a relationship within the Enoplia based on structure of the pharynx and amphids, and this proposed classification was later supported by molecular data (Mullin *et al.* 2003). Meldal *et al.* (2007) later confirmed *Campydora*'s position within the Enopliida and further elucidated a sister relationship with *Syringolaimus*. The placement of *Syringolaimus* clearly denotes the paraphyly of the Ironidae. Morphological classifications either grouped *Syringolaimus* within the Ironidae (Filipjev 1934; Clark 1961; De Coninck 1965), or within the Rhabdolaimidae in the Araeolaimida (Gerlach & Riemann 1973; Andr  ssy 1976). Lorenzen returned *Syringolaimus* to the Ironidae, and supported the monophyly of this family based on buccal cavity morphology (Lorenzen 1981). Noting the consistent separation of the *Ironus* and *Syringolaimus*, Meldal *et al.* suggested that the movable teeth seen in all Ironidae species are in fact homoplastic, and that functional requirements have resulted in convergent evolution within this group. Van Megen *et al.* (2009) recovered the

Rhabdolaimidae as a highly supported (100%) sister taxon to the *Syringolaimus/Campydora* clade, but labelled this family as a group of *incertae sedis*. Unfortunately, this investigation did not include any gene sequences from the Rhabdolaimidae, and thus the placement of this group remains uncertain.

Relationships amongst other Ironidae species remain unresolved, although it appears that at least several genera form a monophyletic grouping. *Dolicholaimus* and *Ironus* were consistently recovered as single clade with high support (100% under both ML and Bayesian analyses). This analysis only utilised gene sequences from two Ironidae genera; additional data will be required to resolve placement of other member taxa. The Ironidae clade was further recovered as a sister group to the Alaimina. This topology was not overwhelmingly supported in ML phylogenies; support values ranged from 25-60%, and these taxa were observed to split under certain phylogenetic parameters (e.g. Gblocks analysis). However, Bayesian analysis showed very high support (95%) for this proposed sister taxa relationship, and the Alaimina/Ironidae relationship was largely consistent across most ML topologies. Recent molecular frameworks have placed both the Alaimina and Ironidae within the Enoplida but were unable to resolve the exact placement within this clade; morphological classifications have also struggled to firmly place these two groups.

The Ironidae has been placed in either the Dorylaimia (Filipjev 1934) or within the Enoplida. Clark (1961) and De Coninck (1965) suggested a close relationship with the Tripylidae, placing the Ironidae in the superfamily Tripyloidea. Chitwood and Chitwood (1950) supported this grouping but additionally placed the Alaimina within the Tripyloidea. Andrassy (1976) raised the Ironidae to the rank of superfamily and placed this group alongside the Tripyloidea, Oxystominidae and Alaimidae in the suborder Tripylina. Siddiqi (1983) designated the Ironidae as its own suborder. Lorenzen (1981) eventually grouped the Ironidae within the Enoplida, alongside the Enoploidea. Despite previous morphological and molecular evidence that proposed the Ironidae as a potentially basal group within the Dorylaimia (Filipjev 1918; Maggenti 1963; Meldal 2004), this study placed the Ironidae firmly within the Enoplida.

The placement of the Alaimina has oscillated between the Dorylaimia (Filipjev 1934; Thorne 1939; De Coninck 1965; Lorenzen 1981; Maggenti 1982) and the Enoplida (Chitwood & Chitwood 1950; Andrassy 1976). Clark (1961) placed the Alaimina within their own suborder, separate from either the Enoplina or Dorylaimina. Lorenzen (1981) argued that the Alaimina belonged in the Dorylaimina because this taxon lacked

metanemes and exhibits posterior-facing oesophageal gland outlets; however, Meldal *et al.* (2007) has questioned the validity of using the direction of such gland outlets as a phylogenetic character. Both Filipjev (1934) and Chitwood and Chitwood (1950) have insinuated a close relationship between the Ironidae and Alaimina; Filipjev placed both as subfamilies within the Dorylaimidae, while Chitwood and Chitwood included these groups within the superfamily Tripyloidea in the Enoplida. There does not appear to be any obvious morphological features which would immediately suggest a relationship between the Ironidae and Alaimidae; Lorenzen's metanemes are notably absent in the Alaimida, although Ironidae species do exhibit this character.

4.3 Phylogenetic structuring in the Enoplia according to habitat

Internal relationships within the Enoplia demonstrate that nematode lineages are primarily separated according to habitat (Figures 4.7 and 4.8). Both Bayesian and Maximum Likelihood tree topologies resolved two primary Enoplid clades: one comprised entirely of terrestrial/freshwater species (the Triplonchida), and a second clade containing mostly marine taxa and a few freshwater species (the Enoploidea, Alaimina, Tripyloididae, etc.). The vast majority of marine Enoplid species are grouped within the Enoplina (De Ley & Blaxter 2002), a solely marine suborder containing the Enoploidea plus the Leptosomatidae. Insight from the marine clade indicates that some marine taxa may have evolved from terrestrial forms. The Family Trefusiidae appears as a sister taxon the terrestrial/freshwater genus *Trischistoma*, and these two groups appear to be themselves derived from the terrestrial genus *Tripylina*; this suggests that the Trefusiidae may represent a reversal back to a marine lifestyle, or alternatively, that the terrestrial genera *Tripylina* and *Trischistoma* arose from a marine ancestor. Clade topologies also suggest that marine species of the Ironidae (e.g. *Dolicholaimus sp.*) may be descendents of terrestrial ancestors. However, taxon sampling within the Ironidae was not extensive, and further investigation may reveal a different pattern. Morphological classification did not typically separate Enoplid genera according to habitat—Maggenti (1983) was the sole taxonomist to propose that this order evolved along separate terrestrial and marine lineages, and suggested separating the Enoplia into the superorders Marenoplica and Terraenoplica. Other authors vociferously dismissed the possibility that Enoplids could have developed this way (Siddiqi 1983). The separation of marine and terrestrial lineages

presents intriguing possibilities in the search for the 'ancestral nematode'; refer to Section 5.5.2 for a detailed discussion of this topic.

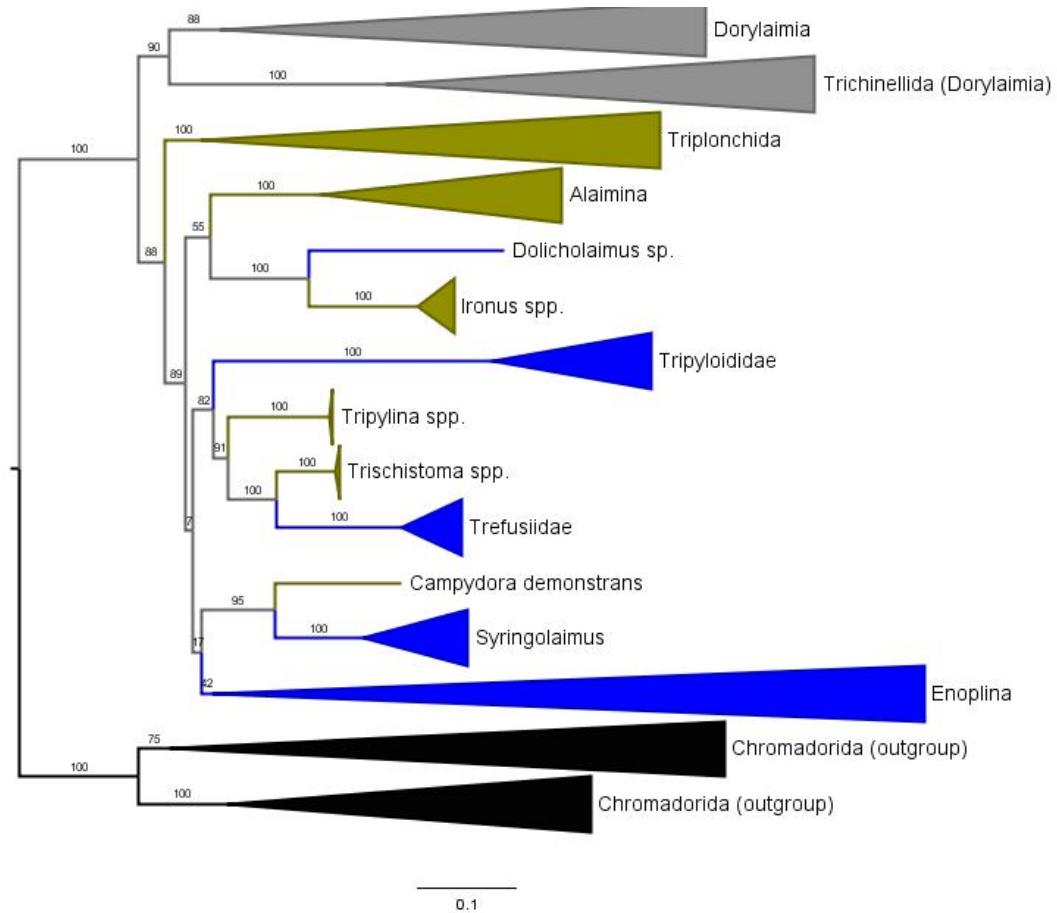


Figure 4.7: Maximum Likelihood SSU phylogeny displaying separation of marine (blue) and terrestrial (brown) taxa within the Enoplida; gray and black clades represent Dorylaimid and outgroup taxa, respectively. Tree Built using 563 taxa with estimation of the P-Invar parameter, and no secondary structure gene partitions (RAxML Job #65991). Scale bar represents nucleotide substitutions per site.

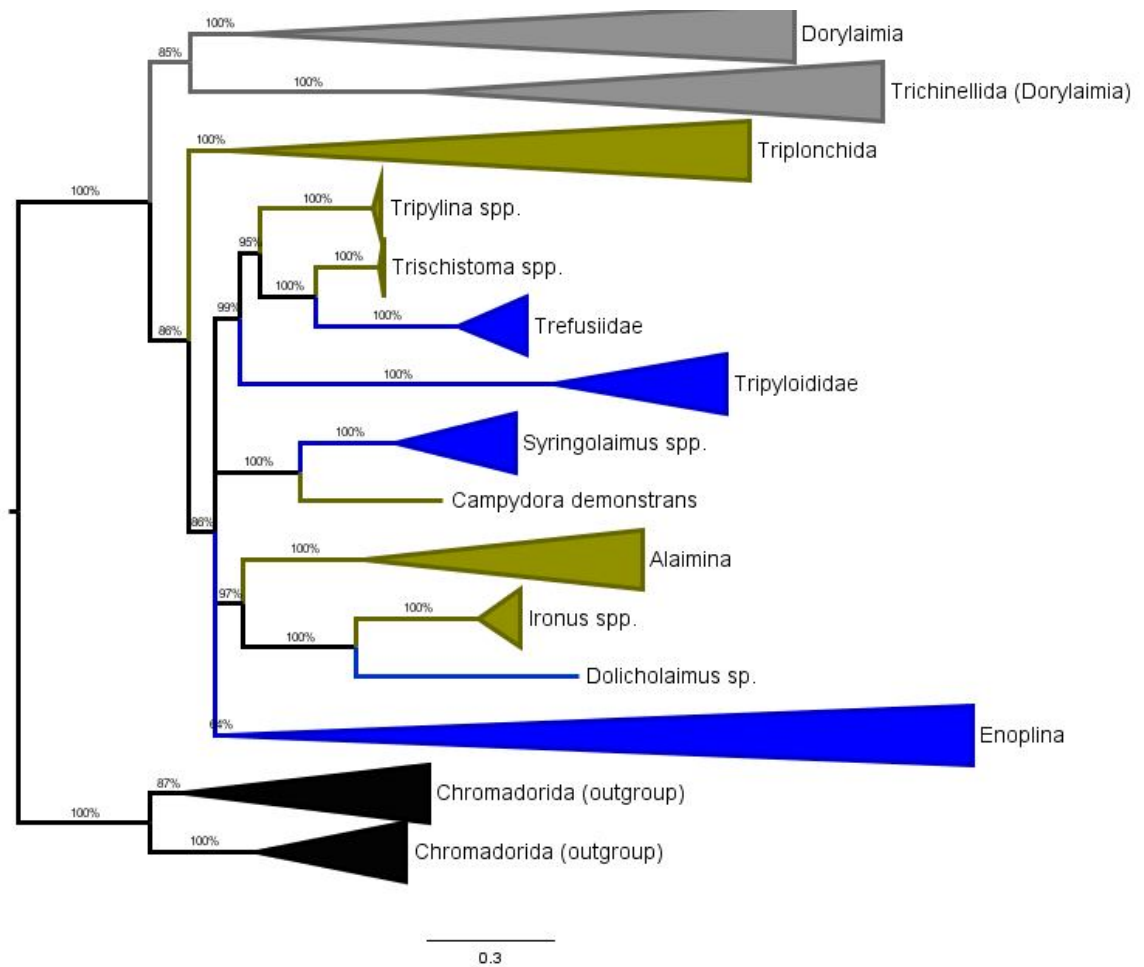


Figure 4.8: Bayesian SSU phylogeny displaying separation of marine (blue) and terrestrial (brown) taxa within the Enoplida; gray and black clades represent Dorylaimid and outgroup taxa, respectively. Tree Built using 563 taxa using the GTR+G+I model of nucleotide substitution, and no secondary structure gene partitions. Scale bar represents nucleotide substitutions per site.

4.4 Lower taxonomic relationships within the Enoplia

4.4.1 Inferences from LSU data

Out of the 256 Enopliid nematodes studied during this investigation, both SSU and LSU gene sequences were obtained from each specimen, and Cox1 was further isolated from a subset of individuals (85 specimens). LSU and Cox1 are too variable for inferring deep phylogeny, but they are useful at elucidating lower taxonomic relationships. Despite downloading pre-aligned LSU structural alignments from the SILVA database, the LSU dataset was not very well aligned and it was difficult to infer homology amongst variable regions. This investigation focused on the D2/D3 expansion segment of the LSU gene, which contains three conserved regions in between variable segments. Because of the higher variability seen in the 28S gene, the higher clade relationships observed in LSU tree topologies did not correspond with the results from SSU data (Figures 4.9 and 4.10). Maximum Likelihood trees were constructed using a large dataset (Figure 4.9) comprising all available nematode taxa (1062 taxa), as well as a smaller dataset (Figure 4.10) representing only Enopliid and Dorylaimid nematodes (433 taxa). Both datasets used the Nematomorpha, Priapulida, Kinorhyncha, and Tardigrada as outgroups. An attempt was made to construct a Bayesian phylogeny using LSU sequences, but the variability of the gene sequences (and the large number of taxa included) did not result in convergence, even after several million generations. This Bayesian topology was not coherent, and a decision was made to abandon use of this method for LSU sequences. LSU gene sequences are much less conserved than SSU sequences; it was difficult to produce accurate alignments in variable LSU regions, especially in a dataset containing very distantly related taxa. Thus, the gene alignment for the large Maximum Likelihood phylogeny was trimmed to represent only the three conserved gene regions (corresponding to primer binding regions) in the D2/D3 expansion segment. This was carried out in order to reduce site saturation in variable regions and hopefully produce a more accurate tree topology. Full gene alignments were used to construct the smaller Enopliid/Dorylaimid trees; although alignments were probably not completely accurate in variable regions, it was much easier to align sites between these two closely related groups.

Data from additional genetic loci (LSU and Cox1) were used to infer lower taxonomic relationships between genera, as recommended by previous studies (De Ley *et*

al. 2005). The results from this study support these recommendations; phylogenies based on LSU and Cox1 data were not able accurately reconstruct deep phylogenetic relationships, but Data from these genes provided useful insight on relationships between genera. Furthermore, clade membership largely corresponded between LSU and SSU phylogenies. A primary focus of this investigation was to collect multiple gene sequences from individual Enoplid nematodes; this allowed for independent assessments of phylogenetic placement and evolutionary relationships for single specimens. Unfortunately, sequences collected as part of this investigation were only obtained from marine taxa; online sequence databases did not contain many sequences representing terrestrial Enoplid nematodes, so it was not feasible to fully clarify lower taxonomic relationships within these groups. It is highly unlikely that public gene sequences (SSU and LSU) representing the same genus would have been amplified from the same specimens, so no attempt was made to compare public LSU and SSU sequences from terrestrial genera.

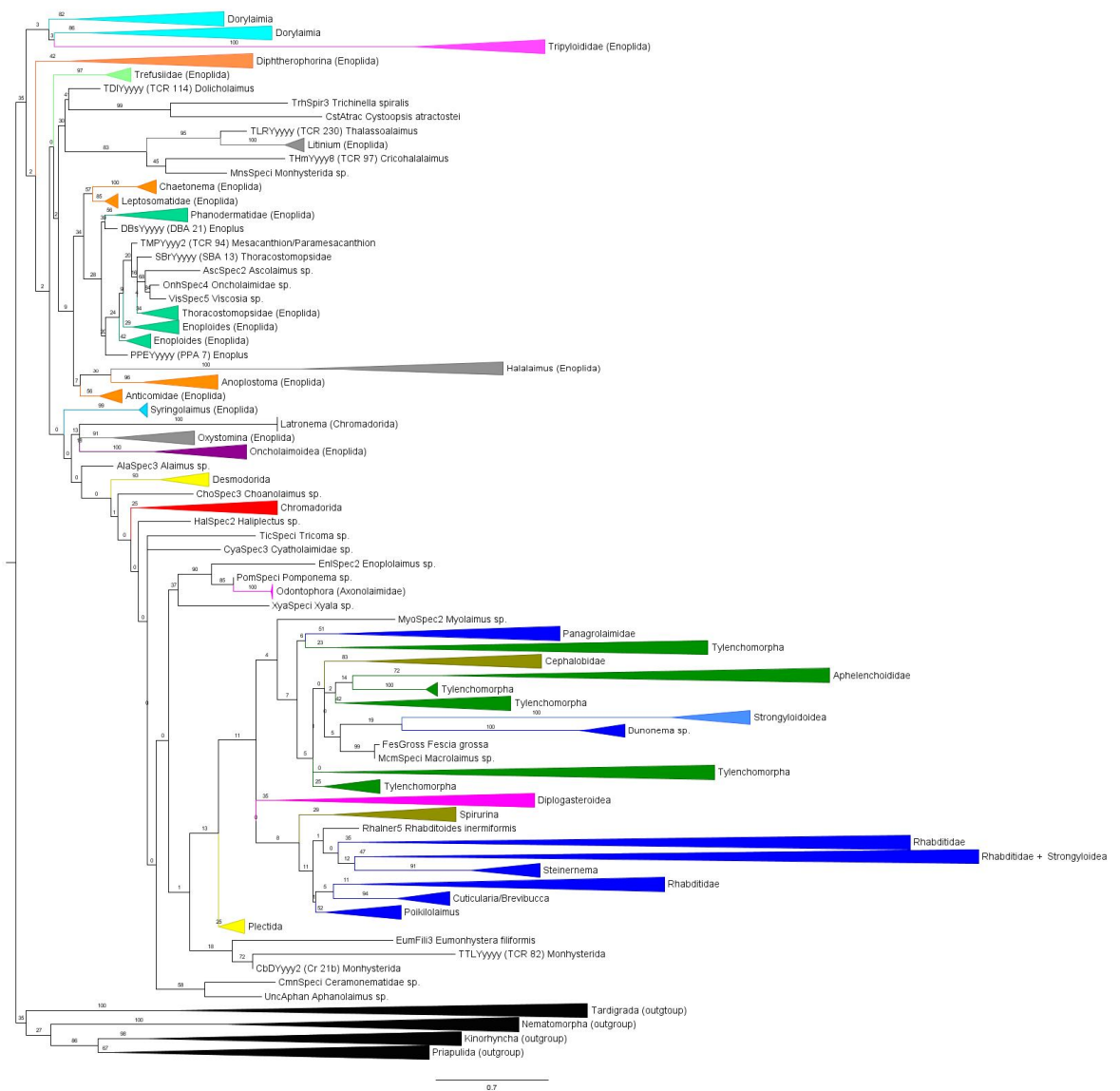


Figure 4.9: Maximum Likelihood LSU phylogeny built using sequences from the D2/D3 expansion segment. Variable alignment regions were excluded from the analysis. Tree built using 1062 taxa, with estimation of P-Invar parameter. (RAxML Job #400). Scale bar represents nucleotide substitutions per site.



Figure 4.10: Maximum Likelihood LSU phylogeny built using sequences from the D2/D3 expansion segment. No alignment regions were excluded from the analysis. Tree built using 433 taxa, with estimation of P-Invar parameter. (RAxML Job #643538). Scale bar represents nucleotide substitutions per site.

The full nematode tree (Figure 4.9) showed a vague resemblance to SSU tree topologies; Enoplid and Dorylaimid nematodes appeared closer to the base of the tree, compared to Rhabditid and Tylenchid nematodes which occupied more derived positions. However the overall placement of clades was clearly incorrect. The Enoplia was not recovered as a monophyletic group, although nematodes were accurately clustered according to genus. A similar result was seen ML trees built using the smaller dataset. Higher clade relationships could not be trusted, and LSU data was unable to correctly group some nematode genera according to family. This effect seemed to be more pronounced for families where genera were especially divergent (e.g. the Oxystominidae) or families that represent a large number of lower taxa (e.g. the Enoploidea).

LSU was useful for elucidating relationships within some families with less divergent taxa. SSU data does not fully resolve relationships within the Tripyloididae; the genera *Bathylaimus* and *Tripyloides* do not form distinct, separate lineages (Figure 4.11). However, LSU data was able to add further resolution regarding relationships within this clade. Maximum Likelihood phylogenies built using LSU data (Figure 4.12) clearly differentiate one genus from the other and denote a sister relationship for these two taxa. Morphological evidence seems to support the observed separation between *Bathylaimus* and *Tripyloides*; there are distinct anatomical differences between the two genera, relating to buccal cavity morphology, amphid shape, shape and position of cervical setae, tail shape, and spicule shape in male specimens. The extent of this morphological differentiation seems to suggest an older split between the two genera (e.g. according to LSU data) rather than a more recent divergence (e.g. according to SSU data). Cox1 data seems to support the more recent, derived placement of *Tripyloides* (refer to Section 4.4.2); however, mitochondrial trees were built using a much smaller subset of taxa and the increased taxon sampling may produce a tree topology similar to LSU phylogenies. Additional sequence data will be required to clearly elucidate the evolutionary relationship between *Tripyloides* and *Bathylaimus*.

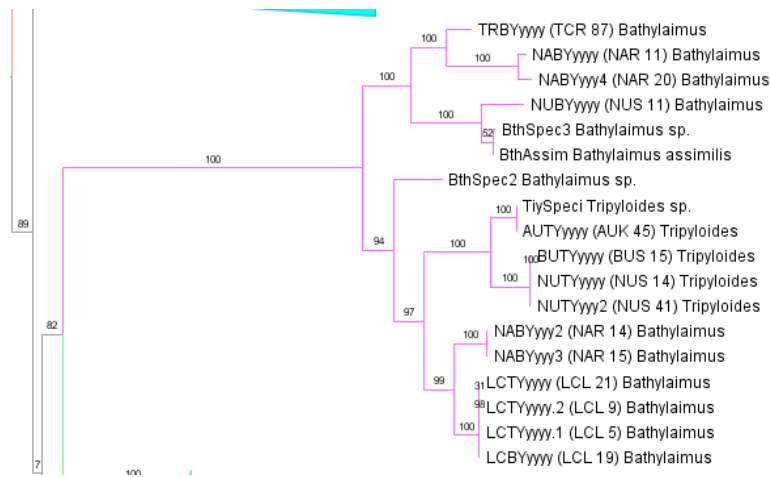


Figure 4.11: Maximum Likelihood phylogeny built using SSU sequences, showing the separation of genera within the Tripyloididae. Tree Built using 563 taxa with estimation of the P-Invar parameter, and no secondary structure gene partitions (RAxML Job #65991).

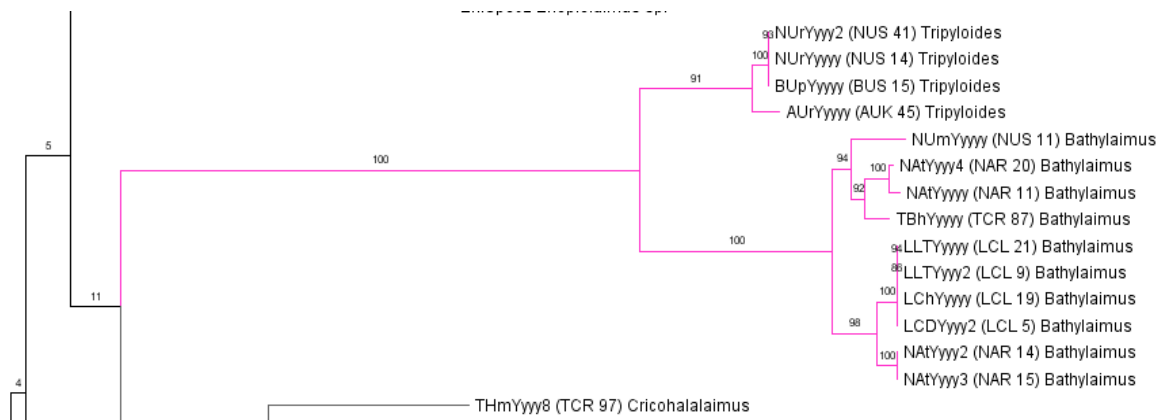


Figure 4.12: Maximum Likelihood phylogeny built using LSU sequences, showing the separation of genera within the Tripyloididae (RAxML Job #643538).

SSU data recovered several genera within the Diptherophorina as paraphyletic. *Trichodorus* and *Paratrachodorus* were both split into multiple lineages, although the Trichodoridae was always recovered as monophyletic (see Figures 4.5 and 4.6). LSU data was not able to fully resolve relationships within this clade (Figure 4.13), given that fewer sequences were available in public databases and Trichodorid specimens were not amplified as part of this study. There is some indication that *Paratrachodorus* may also be recovered as paraphyletic in LSU phylogenies; *Paratrachodorus renifer* was placed outside the main group of *Paratrachodorus* species, within an independent lineage. Additional LSU

sequences from a wide variety of Trichodorid species will be needed to determine the placement of species within the Trichodoridae.

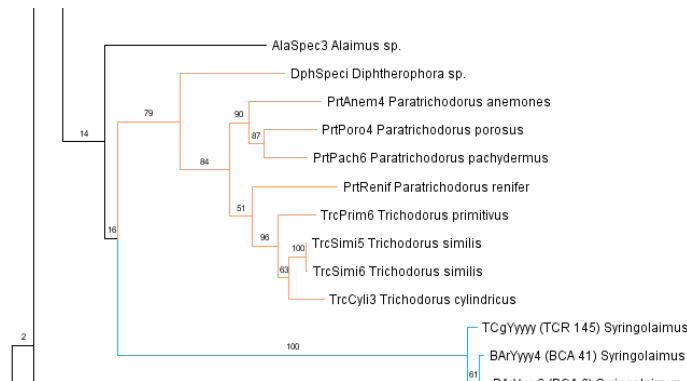


Figure 4.13: Maximum Likelihood phylogeny built using LSU sequences, showing the separation of genera within the Diphtherophorina (RAxML Job #643538).

The Oncholaimoidea was recovered as a highly supported monophyletic clade (support values usually 100%) using both LSU (Figure 4.14) and SSU data (Figure 4.15). Within the Oncholaimidae, specimens identified as belonging to the genera *Oncholaimus* and *Viscosia* do not exhibit neat phylogenetic groupings; these nematodes appear to be quite diverse at the molecular level, probably representing a taxonomic lumping of divergent species complexes. These two taxa are quite morphologically similar. During this study, it was often quite difficult to definitively identify a specimen as belonging to either genus. The position of the largest subventral tooth was often the only character that could be used to identify the genus of female specimens; this feature was often obscured if the buccal cavity was filled with detritus, or if a specimen was damaged or awkwardly mounted. Despite the difficult morphology in these two groups, a large number of species have been described in both genera. According to molecular data, most shallow water *Oncholaimus* specimens sequenced during this study were placed in a clade next to *Viscosia* (as indicated in Figures 4.14 and 4.15); however, there appeared to be another divergent group of *Oncholaimus* nematodes that included all the deep-sea specimens (labelled TCR) as well as some shallow water taxa (labelled AUK). Publically available sequences (taxa that lack alphanumeric codes in brackets in Figures 4.14 and 4.15) also failed to cluster with the majority of specimens sequenced during this study; two *Oncholaimus spp.* and one *Viscosia sp.* that were isolated from shallow water habitats appeared more closely related to the divergent *Oncholaimus* group containing deep-sea specimens, and not to the main clades which contained most intertidal nematodes. These

molecular data suggest that *Oncholaimus* and *Viscosia* represent artificial, paraphyletic taxonomic groupings. Given the difficult morphology in these two genera, it is not surprising that current classifications have lumped divergent species together.

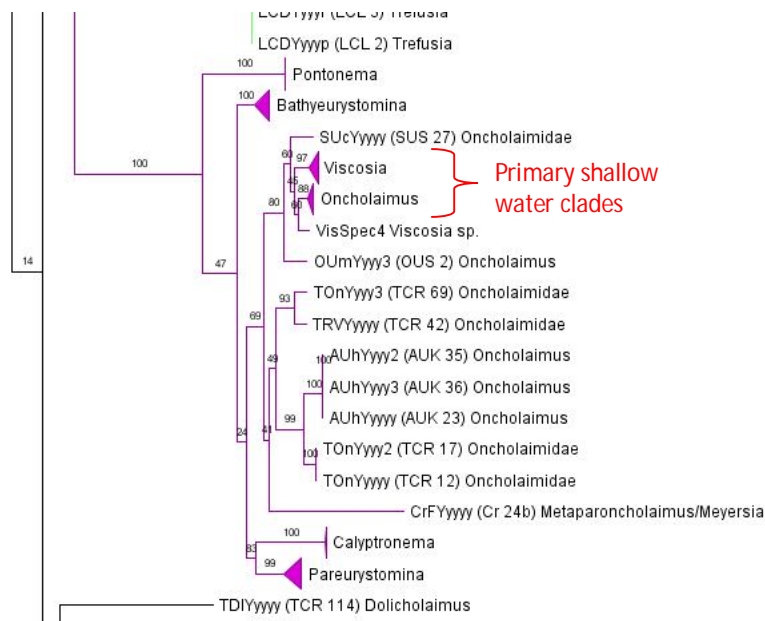


Figure 4.14: Maximum Likelihood phylogeny built using LSU sequences, showing the separation of genera within the Oncholaimoidea (RAxML Job #643538).

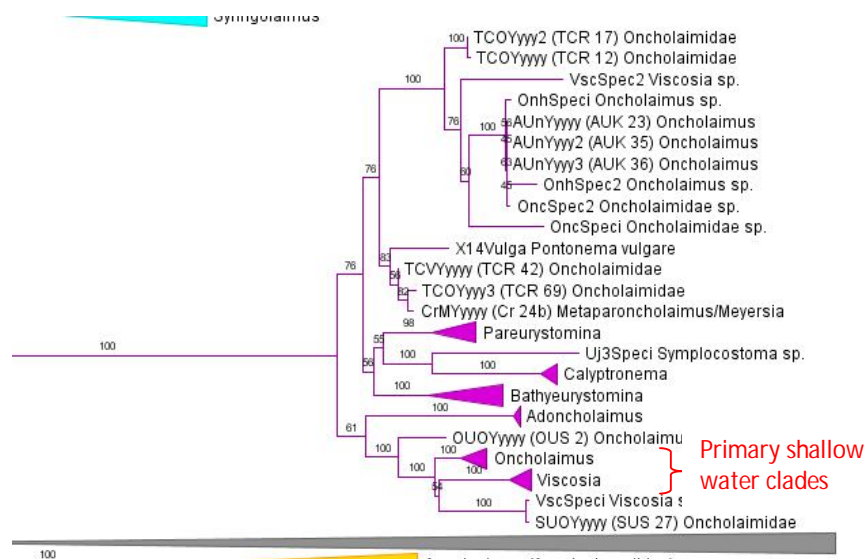


Figure 4.15: Maximum Likelihood phylogeny built using SSU sequences, showing the separation of genera within the Oncholaimoidea. Tree Built using 563 taxa with estimation of the P-Invar parameter, and no secondary structure gene partitions (RAxML Job #65991).

The phylogenetic placement of *Bathyeurystomina* and *Pontonema* differs between LSU and SSU tree topologies. SSU phylogenies (Figure 4.15) support the placement of *Bathyeurystomina* within the Enchelidiidae *sensu* Lorenzen (1981); previous authors (Filipjev 1934; Andr ssy 1976) had separated this group into at least two subfamilies, the Eurystomininae and Enchelidiinae, but Lorenzen did not see a valid reason for separating genera into two subfamilies. Although genera traditionally placed in the subfamily Enchelidiinae form a monophyletic grouping in SSU trees (e.g. *Calyptronema* and *Symplocostoma*), the two members of the Eurystomininae appear to be paraphyletic. *Bathyeurystomina* represents a divergent lineage within the Enchelidiidae which splits early from other taxa, while *Pareurystomina* occupies a more derived position amongst other genera from the Enchelidiinae. Thus, SSU sequences also support Lorenzen's (1981) classification of genera within one large family. In LSU trees (Figure 4.14), *Bathyeurystomina* occupies a position near *Pontonema* and appears as an early-splitting lineage in the Oncholaimoid topologies.

Similarly, in SSU trees the only two specimens that exhibit equal-sized subventral teeth (*Pontonema* and *Meyersia*/*Metaparoncholaimus*) appear to cluster together into a single clade along with two other deep-sea Oncholaimids (Figure 4.15). Unfortunately, the rotation and orientation of both deep-sea specimens did not allow for a clear view of buccal cavity morphology, and visual inspection of video capture files was unable to confirm whether the subventral teeth are equal in size. LSU data suggests that *Pontonema* is actually a divergent lineage that split early from other Oncholaimid taxa. The positions of *Bathyeurystomina* and *Pontonema* in the LSU tree may simply be a reflection of divergent LSU sequences; conserved SSU sequences appear more likely to reveal true evolutionary relationships of divergent genera, whereas LSU sequences seem to incorrectly place such taxa (e.g. separation of the Oxystominidae in the LSU tree). However, the placement of these two genera warrants further investigation.

The recovery of clades within the Thoracostomopsidae is mostly similar between SSU (Figure 4.16) and LSU phylogenies (Figure 4.17). *Enoploides* was always recovered as the earliest splitting clade within this family, and the two clades representing *Enoplolaimus* and *Mesacanthion*/*Paramesacanthion* were observed as monophyletic in both analyses. Identifying specimens within the Thoracostomopsidae was also challenging, although not for lack of morphological features. The rotation of the specimen or the presence of food in the mouth sometimes prevented accurate interpretation of the complex buccal cavity morphology. Nematodes within the clade labelled '*Mesacanthion*/*Paramesacanthion*'

were not accurately assigned to either genus; male spicule shape was needed to make an accurate genus assignment, but all identified specimens within this group were female. In addition, several specimens from relatively unstudied areas (e.g. deep sea sites and South African beaches) did not appear to fit well into existing genera and were generally identified as 'Thoracostomopsidae'. More detailed analysis of morphological features is needed to determine whether these nematodes represent new species in existing genera or novel lineages. LSU phylogenies of the Thoracostomopsidae exhibited some notable discrepancies in the placement of several sequences obtained from GenBank (Figure 4.17). Two *Enoploides* spp. (EnopSpec7 and EnopSpec8) were not recovered within the main *Enoploides* clade, although they were placed nearby in the tree topology; these may represent divergent species within this genus, or alternatively misidentified nematodes. Another *Enoploides* specimen (EnopSpec6) was placed as a sister taxa to the genus *Enoplolaimus*. Closer inspection revealed that this sequence is quite short in length (only ~500bps) compared to other D2/D3 sequences in the tree (>800bps), and this incorrect phylogenetic placement may have resulted from this length difference—similar incorrect placements of short sequences in ML phylogenies were observed during SSU tree construction. Finally, two sequences appear completely out of place and potentially represent misidentified specimens. *Oncholaimus* sp. (OnhSpec4) and *Viscosia* sp. (VisSpec5) (both sequences obtained from GenBank) were placed within the Thoracostomopsidae in LSU tree topologies; inspection of gene alignments revealed that these sequences did not appear closely related to Oncholaimidae specimens, and thus the taxonomic assignments in GenBank may be incorrect.

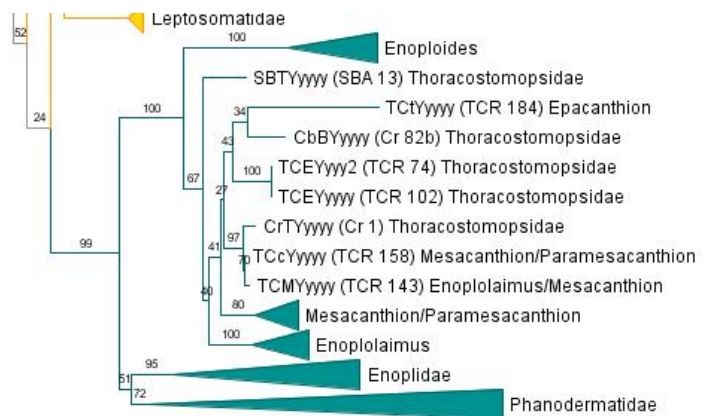


Figure 4.16: Maximum Likelihood phylogeny built using SSU sequences, showing the separation of genera within the Phanodermatidae, Thoracostomopsidae, and Enoplidae. Tree Built using 563 taxa with estimation of the P-Invar parameter, and no secondary structure gene partitions (RAxML Job #65991).

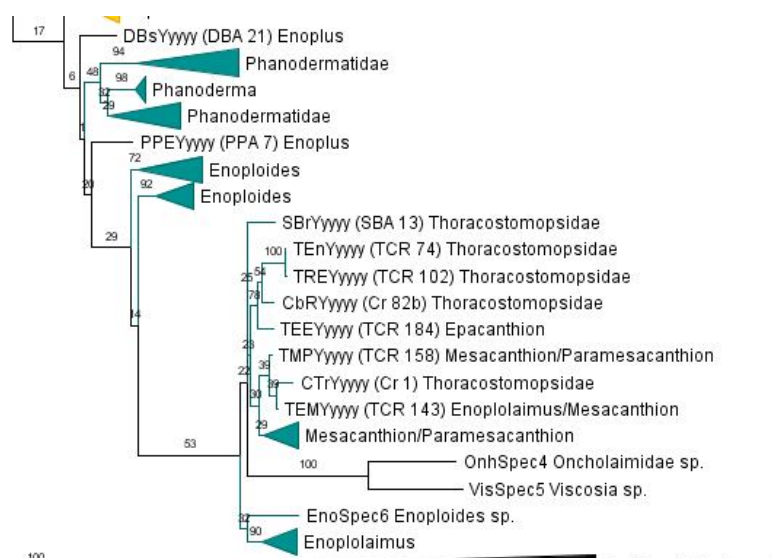


Figure 4.17: Maximum Likelihood phylogeny built using LSU sequences, showing the separation of genera within the Phanodermatidae, Thoracostomopsidae, and Enopliidae (RAxML Job #643538).

The Phanodermatidae is another example of a morphologically similar family that is quite diverse at the molecular level. Most specimens identified within the Phanodermatidae had few distinguishing morphological features; these nematodes exhibited smooth cuticles, pocket-shaped amphids and no unique buccal cavity morphology. Most specimens identified in this study were morphologically identified as *Phanodermopsis*, although smaller or badly preserved specimens were more generally grouped as 'Phanodermatidae'. SSU (Figure 4.18) and LSU (Figure 4.19) phylogenies confirm the monophyly of the Phanodermatidae, but tree topologies divide the family into three main groups of taxa (labelled as Clades 1, 2 and 3 in Figures 4.18 and 4.19). Limited data from Cox1 trees also supports this division into multiple clades (refer to Section 4.4.2). In LSU trees (Figure 4.19), the clade containing *Phanoderma* (represented by publically available sequences) shows similar divergence compared to Clades 1, 2 and 3. This observed phylogenetic divergence suggests that the three primary clades recovered within the Phanodermatidae may represent several species or even several genera.

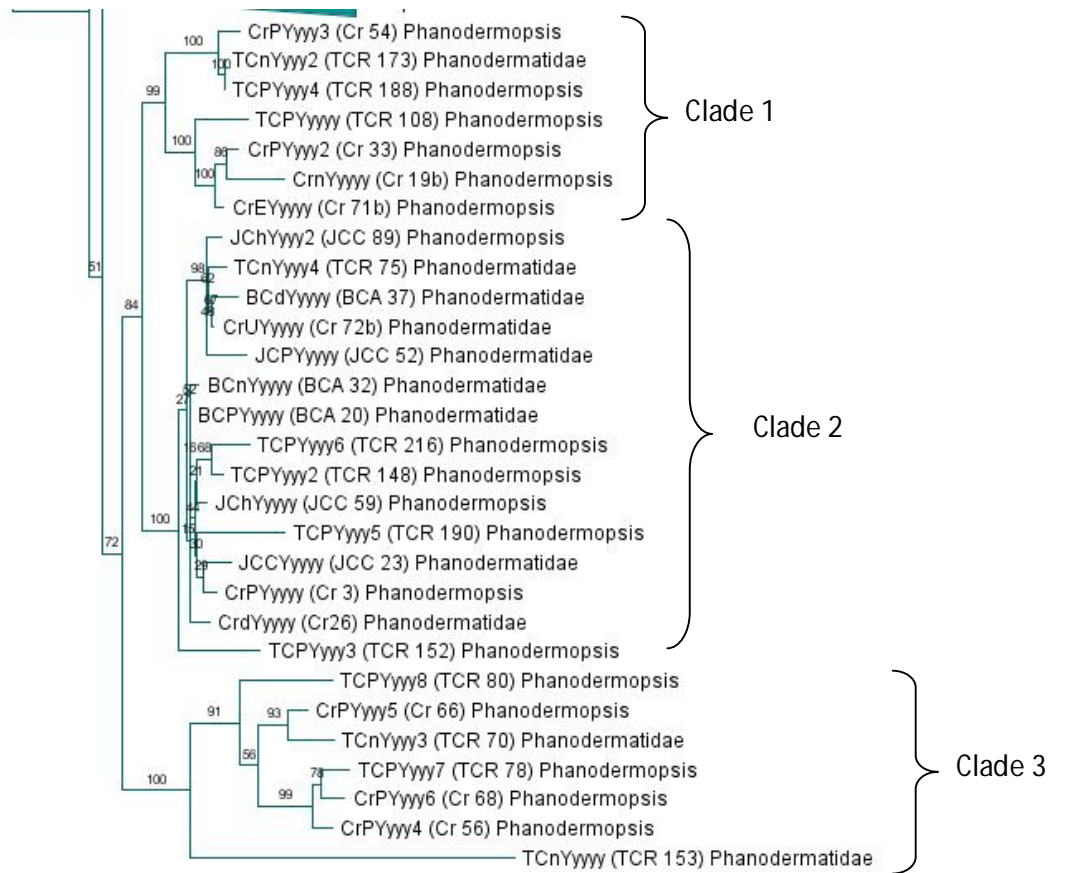


Figure 4.18: Maximum Likelihood phylogeny built using SSU sequences, showing the separation of genera within the Phanodermatidae. Tree Built using 563 taxa with estimation of the P-Invar parameter, and no secondary structure gene partitions (RAxML Job #65991).

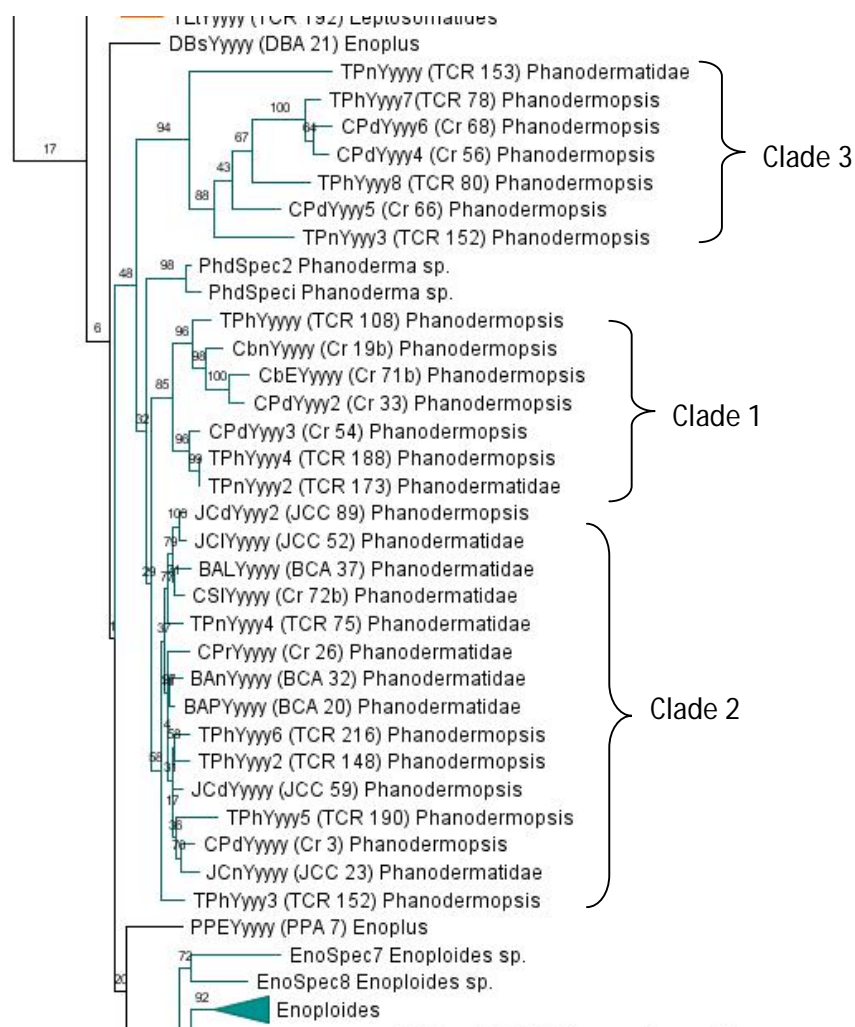


Figure 4.19: Maximum Likelihood phylogeny built using LSU sequences, showing the separation of genera within the Phanodermatidae (RAxML Job #643538).

4.4.2 Inferences from cytochrome *c* oxidase subunit 1

Cox1 is not widely utilised in nematode studies, and thus it was only possible to construct phylogenies using the sequences generated during this investigation. Cox1 sequences were only obtained from a small subset of nematode specimens (90 Enoplids), and thus the resulting phylogenies were not ideal for elucidating lower taxonomic relationships. However, mitochondrial data provided some useful insight regarding geographic relationships (refer to Chapter 6 for full discussion). Cox1 gene alignments contained 105 taxa and represented 396 nucleotide sites; Fifteen sequences from *Pellioiditis marina* (a Rhabditid nematode) were used for outgroup comparisons. Duplicate Cox1 sequences from Enoplid nematodes were included in phylogenetic analyses in order to visually illustrate relationships between specimens collected at disparate geographic locations. Cox1 sequences were aligned using translated protein sequences and subsequently untranslated back to nucleotide sequences before phylogenetic analysis. Bayesian (Figure 4.20) and Maximum Likelihood (Figure 4.21) trees were built using partitioned gene alignments that accounted for three separate codon positions. Tree topologies obtained from Cox1 were not coherent at higher taxonomic levels (similar to LSU trees), and clade placements did not agree with frameworks based on SSU data. However, both genes were useful for clarifying some lower taxonomic relationships (e.g. within the Tripyloididae), as well as inferring species distributions amongst different geographic locations (refer to Chapter 6 for a full discussion).

The sequence labelled 'TCR 89 Litinium' exhibited a very long branch length within both ML and Bayesian topologies. Additional trees were constructed without this particular sequence, but excluding this long-branch taxon did not have any impact on tree topology. Cox1 sequences labelled 'TCR 189 Litinium' and 'TCR 190 Phanodermatidae' were both placed within the Thoracostomopsidae, despite their apparent taxonomic identities. Upon further investigation, it was discovered that these two gene sequences were identical to nematodes labelled SBA 8, SBA 9 and SBA 13. Furthermore, both SSU and LSU data confirms that TCR 190 belongs within the Phanodermatidae. These two sequences most likely represent contamination or mislabelling of molecular reactions, and thus the taxonomic labels are probably inaccurate—these two sequences should be considered as Thoracostomopsidae.

Cox1 trees were generally able to recover families as monophyletic clades with high support values. The Oxystominidae was not recovered as monophyletic within the Cox1

tree topology; this is probably related to the high sequence divergence observed between *Oxystomina* and *Halalaimus*. Within the Tripyloididae, there was no clear distinction between genera, as seen in LSU data; *Tripyloides* specimens appeared nested among *Bathylaimus* specimens, similar to the topology recovered in SSU trees. The Phanodermatidae was recovered as two separate clades (support values of 20 and 99 in Bayesian topologies) that correspond to the clustering of taxa observed in SSU and LSU tree topologies (Figures 4.18 and 4.19). This further suggests an unexpected molecular diversity within this group, despite apparent morphological similarities between nematodes identified as Phanodermatidae specimens. Finally, mitochondrial data highly supports the phylogenetic placement of the Enchelidiidae (*sensu* Lorenzen) within the Oncholaimoidea.

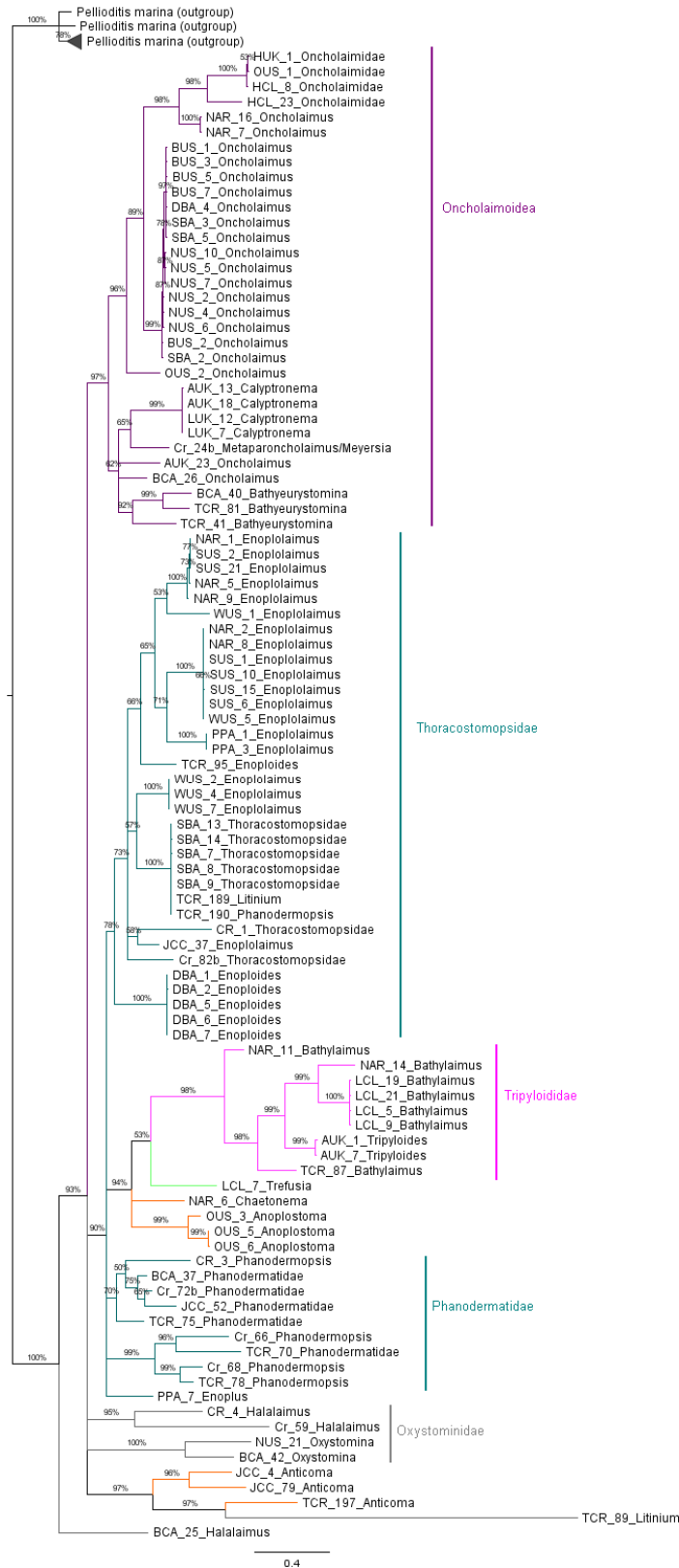


Figure 4.20: Bayesian phylogeny built using Cox1 gene sequences. Tree constructed using a 3 alignment partitions according to codon positions, using 2 million generations, and chain heating temperature of 0.1. Final average standard deviation = 0.014216. Scale bar represents nucleotide substitutions per site.

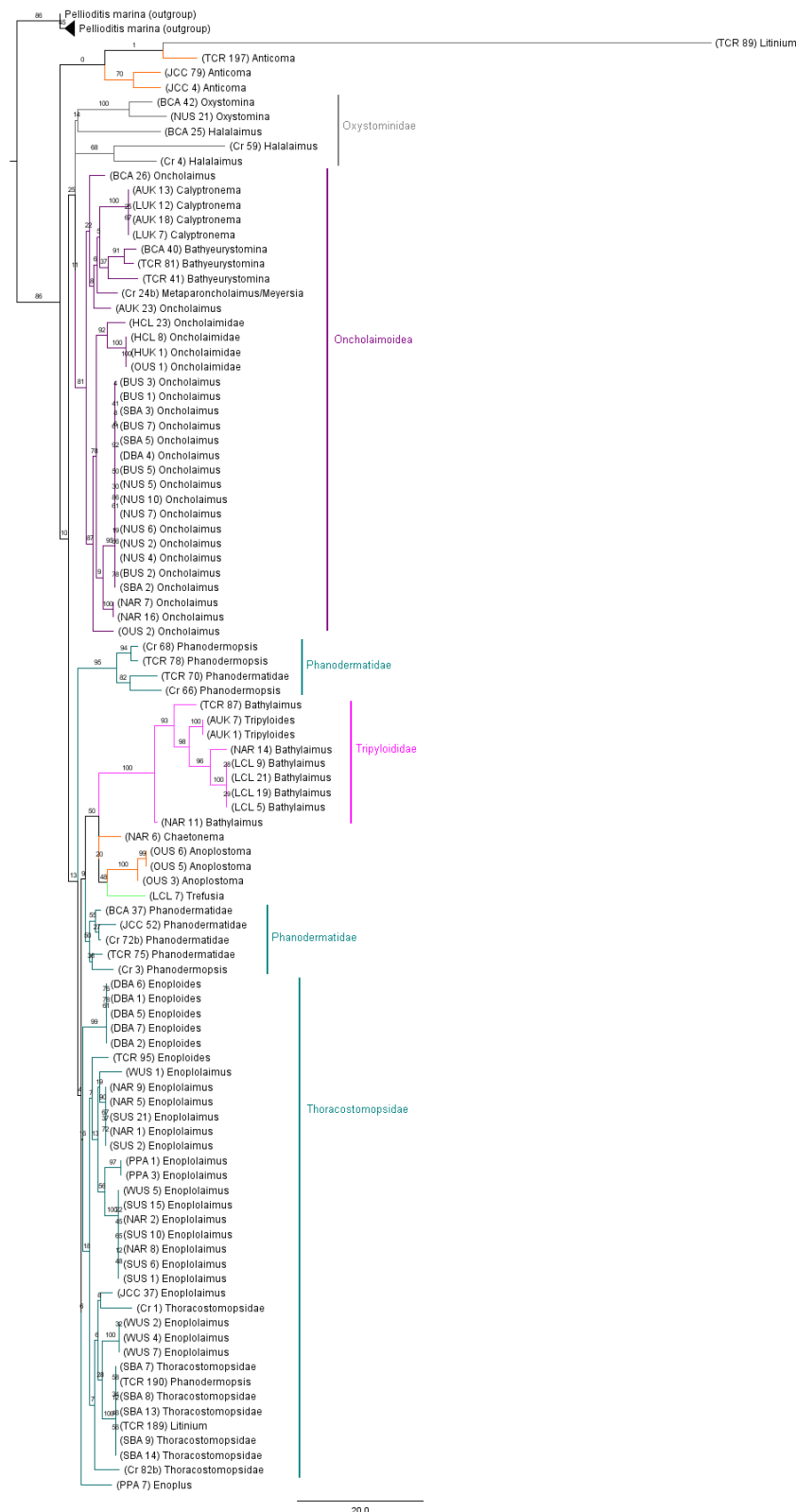


Figure 4.21: Maximum Likelihood phylogeny built using Cox1 gene sequences. Tree constructed using a 3 alignment partitions according to codon positions, and using estimation of the P-Invar parameter. Scale bar represents nucleotide substitutions per site.

4.5 Conclusions

Increased taxon sampling within the Enoplid clade was able to clarify evolutionary relationships amongst families and genera. Over 250 sequences were added to those available from public databases, including many families and genera that previously lacked gene sequences. The resulting molecular phylogenies exhibited clear differences between past morphological classifications, and refined the molecular framework proposed by De Ley and Blaxter (2002). The phylogenetic relationships between Enoplid specimens were consistent and continually replicated using different analysis methods and genetic loci. Higher clade relationships were not always in agreement between SSU and LSU tree topologies, but this variation was due to the less conserved nature of the LSU gene; LSU often separated divergent taxa even when relationships were highly supported in SSU phylogenies. The results from this study support recommendations from previous authors (De Ley *et al.* 2005), who discourage the use of LSU for higher clade relationships. Despite the variability of LSU, gene sequences appear to be conserved enough to elucidate relationships amongst closely related species within a genus (e.g. the Tripyloididae). Ribosomal data suggests that some morphologically homogenous groups (e.g. Oncholaimidae, Phanodermatidae) exhibit extensive molecular diversity. Additional gene sequences representing the Oncholaimidae suggest that current taxonomic classifications lump morphologically similar (but genetically divergent) species. Similarly, the Phanodermatidae species analysed during this study appeared to be morphologically homogenous, but trees suggested a complex phylogenetic structure within this group. Relationships within such taxa warrant further investigation to elucidate potentially cryptic species.

5. Resolving the Basal Clade of the Phylum Nematoda

5.1 Increased taxon sampling and large-scale phylogenies

This investigation has greatly expanded the scale of past phylogenetic efforts, constructing a large-scale phylogeny using 18S rRNA sequence data and using increased taxon sampling within the Enoplid clade. A total of 256 SSU gene sequences were collected from marine Enoplid species, and these were analysed in addition to published sequences obtained from online databases. The final dataset contained a total of 1335 nematode sequences, including 548 sequences from the Enoplid clade—significantly improving representation of this basal group compared to past phylogenies. Enoplid specimens sequenced during this investigation represented several families and genera which previously had not been subjected to molecular analysis; the addition of more sequences within previously analysed groups (e.g. the Oncholaimidae) allowed for fine-scale resolution of evolutionary relationships within some nematode groups. Out of the Enoplid sequences obtained during this investigation, duplicate identical sequences were eliminated from this large-scale dataset. Multiple sequence alignments were used to construct phylogenies using both Maximum Likelihood (ML) and Bayesian Inference methods. Four closely related metazoan phyla were chosen as outgroups (Nematomorpha, Priapulida, Kinorhyncha, and Tardigrada), representing the closest relatives of nematodes according to Dunn *et al.* (2008).

A wide variety of parameters were used to evaluate the robustness of tree topologies using ML analysis. Long-branch clades and taxa of *incertae sedis* were removed and included in analyses to test whether either group was potentially destabilising the tree. All possible outgroup combinations were tested in order to evaluate how outgroup choice affected major topological changes in the placement of nematode clades. SSU alignments were separated into Stem/Loop regions based on secondary structure information and subjected to ML analysis using partitioned gene alignments; topologies using secondary structure partitions were compared to non-partitioned ML runs. The position of stems and loops in 18S sequences is included in all alignments downloaded from the SILVA rRNA database; partitioned gene alignments were constructed by separately exporting stem and loop alignment sites using the ARB program, and manually combining the data into a single alignment. Furthermore, trees were constructed both

with and without the P-invar parameter that estimates the proportion of invariable sites, simultaneously estimating rate variation and invariant sites may detrimentally affect phylogenetic inference (Stamatakis 2008).

5.2 Consistency of ML topologies with previous classifications

Maximum Likelihood topologies were largely consistent with the most recent nematode frameworks (Holterman *et al.* 2006; Meldal *et al.* 2007; Van Megen *et al.* 2009), recovering all major clades and providing increased resolution at certain nodes (Figures 5.1 to 5.4; a list of all taxa recovered in all major nematode clades is included in appendix Table A2.2) The inclusion of over 1300 nematode taxa was effective at resolving the placement of certain problematic taxa. For example, the genus *Choanolaimus* was consistently placed with Chromadorida, a taxon noted as having an unsure clade placement when only a small dataset was analysed (Holterman *et al.* 2008). The following discussion will outline the results of this study in relation to the most recently published molecular frameworks (Holterman *et al.* 2006; Meldal *et al.* 2007; Holterman *et al.* 2008; Van Megen *et al.* 2009); discussion of relationships within the Enoplida can be found in Chapter 4.

The Dorylaimia was recovered in accordance with previous topologies, consisting of three major clades: the Dorylaimida, Mononchida (including the Mermithida), and Trichinellida (in certain topologies). The Microlaimoidea, Chromadorida, and Desmodorida were all recovered as monophyletic, with the three clades splitting consecutively in that order. Molecular analysis suggests that the Desmoscolecidae (represented by *Desmoscolex sp.*) belongs in its own order above the Monhysterida. The Monhysterida was confirmed as paraphyletic and split into two clades, as first suggested by Meldal *et al.* (2007). The primary Monhysterid clade contained the majority of families, including the Aegialoalaimidae, Xyalidae, Monhysteridae, Diplopeltidae, Linhomoeidae (*Tershellia* spp. only), Sphaerolaimidae and Comesomatidae (formerly placed within the Araeolaimida). The second, smaller Monhysterid clade contained the Siphonolaimidae and other members of the Linhomoeidae (*Desmolaimus spp.*). The Linhomoeidae is clearly paraphyletic, but only two genera were included in this study; further analysis will be needed to determine the placement of remaining genera within this family.

The Araeolaimida was also recovered as paraphyletic, and nematodes within this group were split into three separate clades. The first clade contained the Axonolaimidae and Cylindrolaimidae, and was usually recovered as a sister taxon to the Monhysterid clade containing the Linhomoeidae/Siphonolaimidae. Two other Araeolaimida clades were placed within a larger grouping that also contained the Plectidae and Teterocephaloidea. The Leptolaimidae appeared to be paraphyletic; the most basal Araeolaimida clade contained the genera *Aphanonchus*, *Leptolaimus* and *Paraplectonema*, while the more derived clade contained the genera *Camacolaimus*, *Onchium*, and *Procamacolaimus*. This derived clade also contained several other Araeolaimid families, namely the Chronogasteridae, Ohridiidae, and Halaphanolaimidae. The arrangement of the Araeolaimida, Plectidae and Teterocephaloidea clades equates to 'Clade 6' of Holterman *et al.*'s tree topology; the inclusion of more sequences representing species within this group has further elucidated four robust sub-clades within this clade. The arrangement of these four clades was consistently supported by topological tests, despite low support values for several internal nodes. The topology of this clade also agrees with Van Megen *et al.*'s (2009) large-scale phylogeny, who used a similar set of taxa for this group.

Recovery of the most derived nematode clades was largely in accordance with the topology of clades 9-12 recovered by Holterman *et al.* (2006) and Van Megen *et al.* (2009); the authors indicated that these crown clades exhibit accelerated substitution rates compared to other nematode groups. This faster evolution most likely allowed for highly accurate topologies in previous, smaller phylogenies. The placement of *Brevibucca* was not consistent in past phylogenies, and increased taxon sampling appears to have further elucidated its correct placement within the nematode tree. *Brevibucca* and *Cuticularia* were most often grouped with *Steinernema* spp. (Figure 5.5), but occasionally split from this clade and instead clustered with *Myolaimus* sp. and *Odontopharynx longicaudata* (Figure 5.6). The scenario may reflect an erroneous placement resulting from specific phylogenetic parameters (refer to Section 5.4 for further discussion). Van Megen *et al.* (2009) recovered the Brevibuccidae as a family of *incertae sedis*, although this group was associated with *Myolaimus* sp. and *Odontopharynx longicaudata* in their large-scale phylogeny.

The placement of *Isolaimum* sp. agreed with Meldal *et al.*'s (2007) results; this genus was always recovered alongside *Aulolaimus* sp., with these two species forming a separate clade splitting off before the Araeolaimida/Plectidae/Teterocephaloidea. In contrast, Van Megen *et al.* (2009) reported this clade splitting after the Monhysterida. It

appears these two species represent a divergent lineage, but the clade's uncertain placement is probably related to low taxon sampling within this group. *Myolaimus sp.* and *Odontopharynx longicaudata* were recovered as taxa of *incertae sedis*, although both species were always placed together and were never included in any major clade grouping. The placement of these two taxa varied frequently; sometimes they were placed near the Spirurina, as recovered by Meldal *et al.* (2007), but other times they were recovered within the Rhabditida, as indicated by Holterman *et al.* (2006) and Van Megan *et al.* (2009).

5.3 Unresolved Bayesian topologies

Because of computational limitations, Bayesian trees were only constructed using the full 18S dataset (including all four outgroup phyla). The Bayesian topology was able to recover the same clade groupings as ML analysis (Figure 5.4), and confirm the position of Dorylaimia and the Enoplia at the base of the nematode tree. However, the final topology did not elucidate which clade split first from all other nematodes, the Trichinellida and Dorylaima were not recovered as monophyletic. Bayesian analysis also failed to resolve the hierarchy of more derived nematode clades, although the splitting order of the Microlaimoidea, Chromadorida, and Desmodorida was identical for both ML and Bayesian topologies. Large-scale Bayesian analyses consistently failed to reach convergence in this analysis, resulting in the low resolution seen in full nematode frameworks. Bayesian Inference requires computationally expensive algorithms—all analyses required nearly a week to complete 2,000,000 generations, despite being run on large supercomputer clusters (the CIPRES project, hosted at the University of California, San Diego). There is a strict 7-day limit for all jobs run on CIPRES, and thus it was not possible to extend the analysis of full-nematode frameworks with additional generations. All jobs were run using MrBayes3.2; this newest version was recommended by CIPRES administrators for resulting in faster convergence. Several Bayesian runs were also completed with consecutively lower chain heating temperatures (ranging from 0.1 to 0.06), as this is another useful method for increasing the likelihood of convergence without adding additional generations (Hall 2008). Despite many runs and parameter variations, the best Bayesian topology (Figure 5.4) had only obtained an average standard deviation of 0.074387—clearly indicating a lack of convergence. Generally convergence has only occurred when the average standard deviation becomes significant (<0.05 , but ideally <0.01) (Hall 2008).

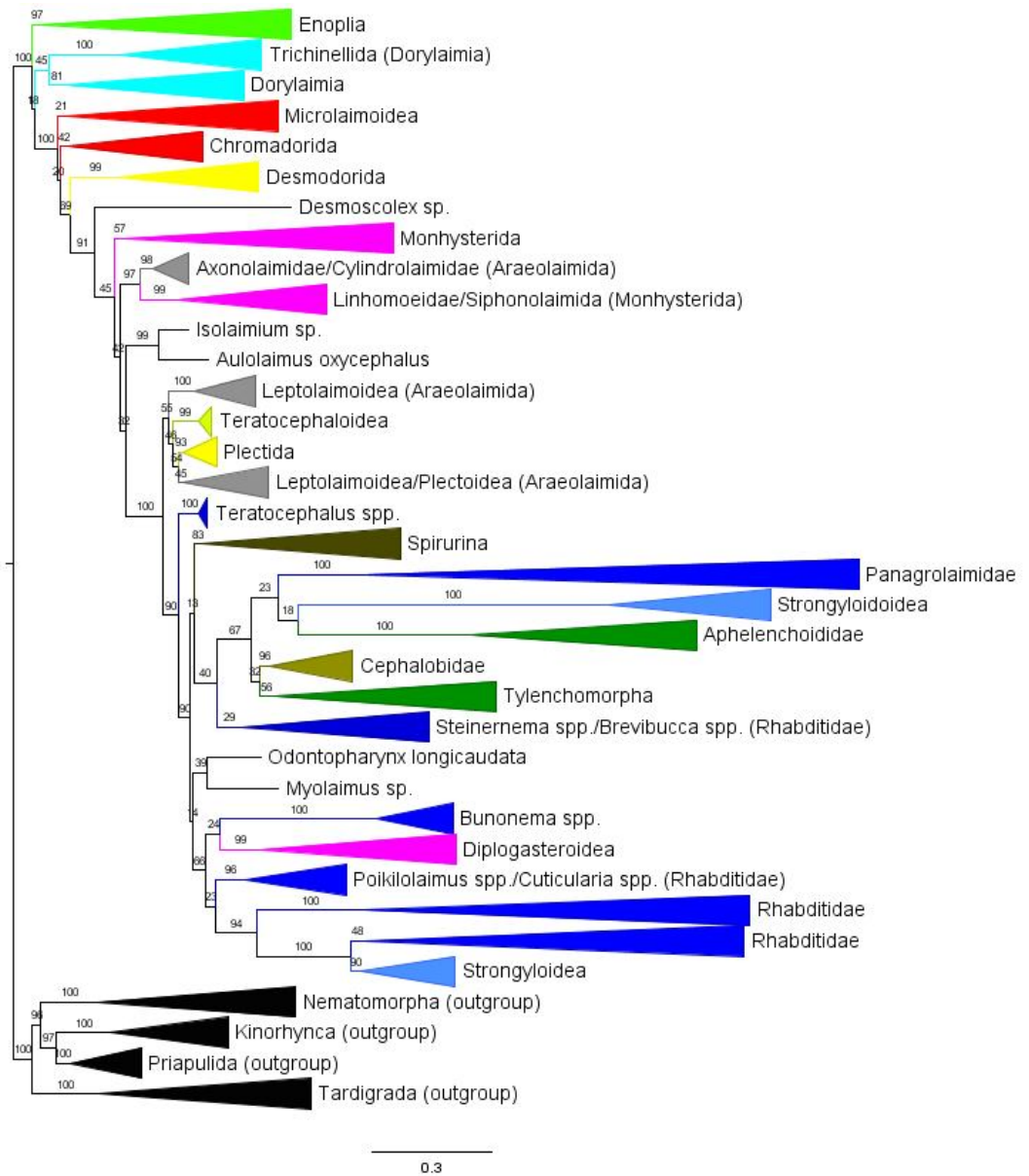


Figure 5.1: An example of a Maximum Likelihood topology which recovered the Enoplia as the earliest splitting lineage (RAxML Job #830526). Tree built using 1336 nematode taxa, all four outgroup phyla, estimation of the P-Invar parameter, and no secondary structure gene partitions

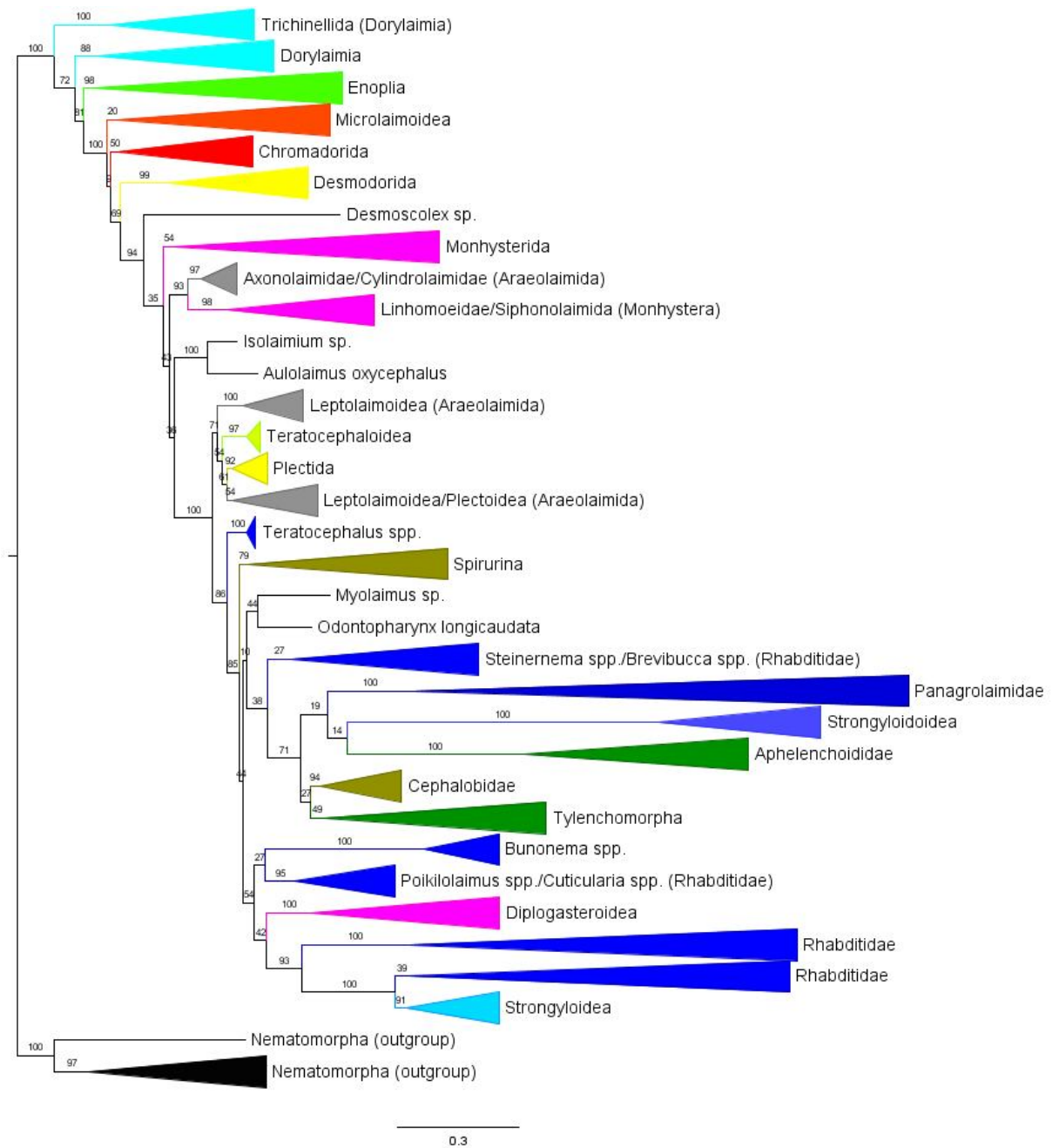


Figure 5.2: An example of a Maximum Likelihood topology which recovered the Dorylaimia as the earliest splitting lineage (RAxML Job #830467). Tree built using 1336 nematode taxa, the Nematomorpha as a single outgroup phylum, estimation of the P-Invar parameter, and no secondary structure gene partitions.

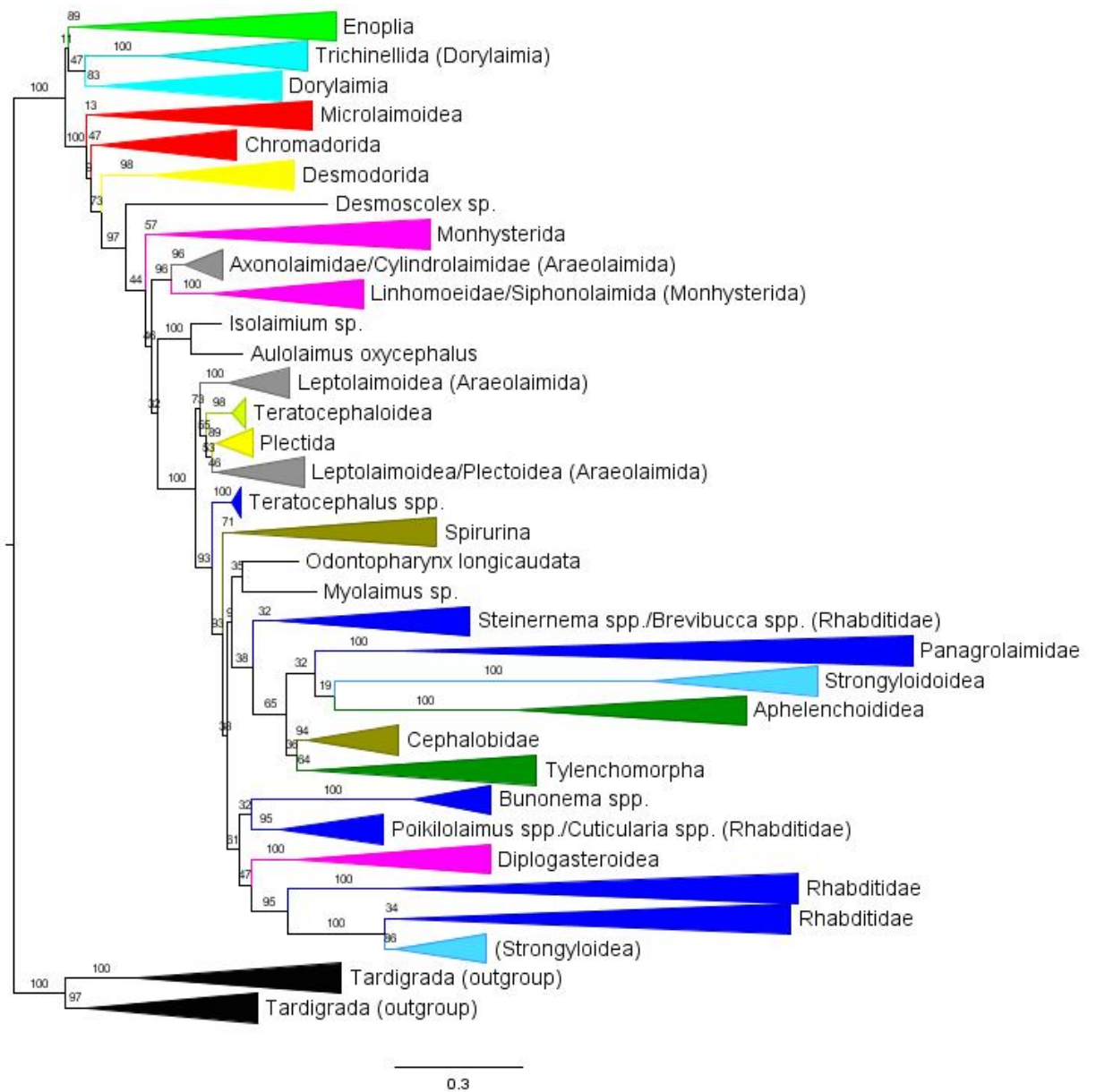


Figure 5.3: An example of a Maximum Likelihood topology which recovered the Dorylaimia/Enoplia as sister taxa which split early from all other nematodes (RAxML Job #884354). Tree built using 1336 nematode taxa, the Tardigrada as a single outgroup phylum, no estimation of the P-Invar parameter, and no secondary structure gene partitions.

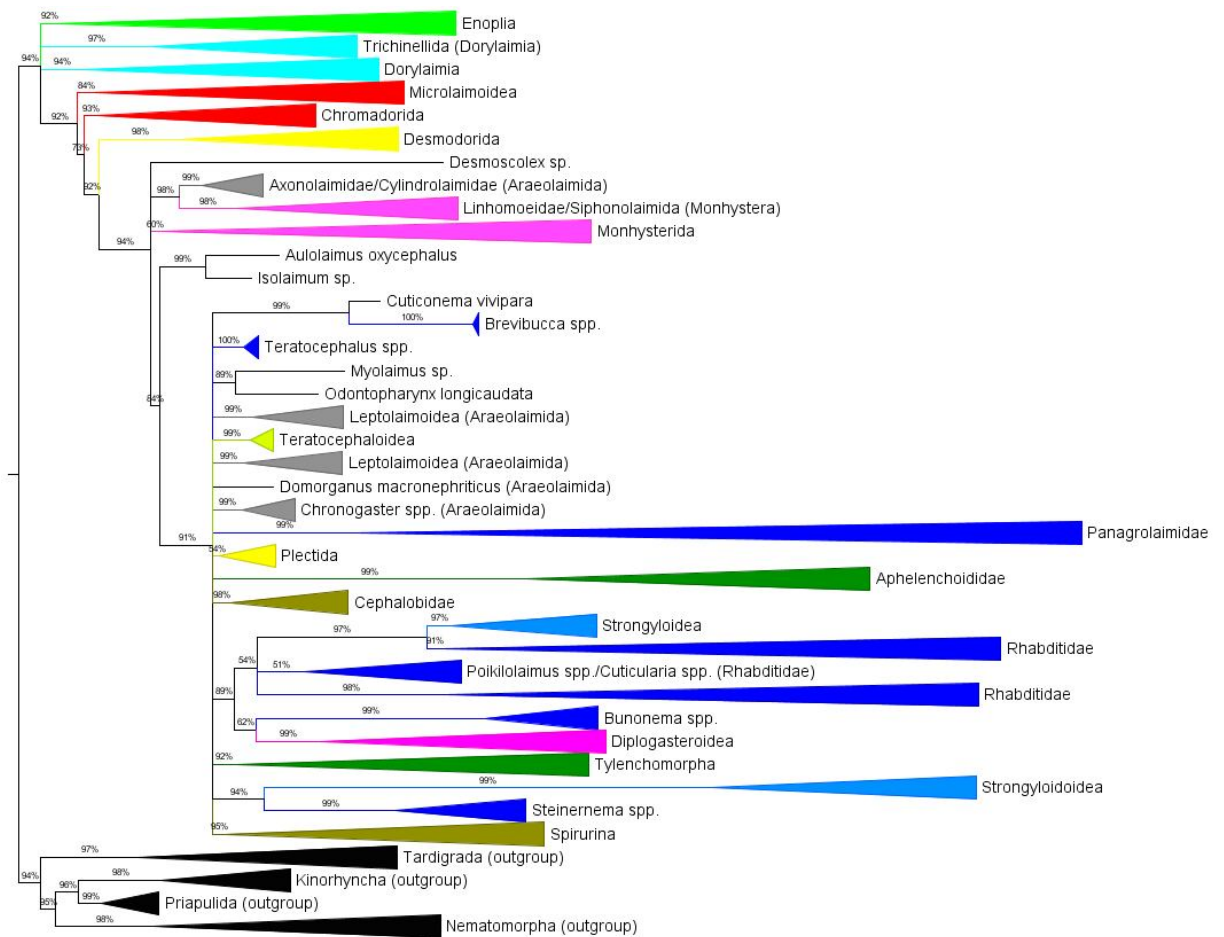


Figure 5.4: A Bayesian tree built using 1336 nematode taxa and all four outgroup phyla. Analysis was run for 2,000,000 generations using the GTR+I+G model of nucleotide substitution, 4 MCMC chains, and a heating temperature of 0.06.

Table 5.1 (following page): Earliest splitting lineage recovered during various tree topology tests. Enoplia = the Enoplia represent the basal clade and all other nematode clades are derived; Dorylaimia = the Dorylaimia represent the basal clade and all other nematode clades are derived; Doryla/Enop = the Dorylaimia and Enoplia appear as sister taxa in a single basal clade, with all other nematodes forming a separate, non-derived clade

Nematode Taxa	Outgroup	P-Invar Estimate	Earliest Splitting Clade
All Nematode Taxa	All	Yes	Enoplia
All Nematode Taxa	Nematomorpha	Yes	Dorylaimia
All Nematode Taxa	Priapulida	Yes	Enoplia
All Nematode Taxa	Tardigrada	Yes	Dorylaimia
All Nematode Taxa	Kinorhyncha	Yes	Enoplia
All Nematode Taxa	All	No	Enoplia
All Nematode Taxa	Kinorhyncha	No	Enoplia
All Nematode Taxa	Priapulida	No	Enoplia
All Nematode Taxa	Nematomorpha	No	Dorylaimia
All Nematode Taxa	Tardigrada	No	Doryla/Enop
All Nematode Taxa	Nematomorpha, Tardigrada	Yes	Dorylaimia
All Nematode Taxa	Nematomorpha, Kinorhyncha	Yes	Dorylaimia
All Nematode Taxa	Nematomorpha, Priapulida	Yes	Enoplia
All Nematode Taxa	Tardigrada, Kinorhyncha	Yes	Dorylaimia
All Nematode Taxa	Tardigrada, Priapulida	Yes	Enoplia
All Nematode Taxa	Kinorhyncha, Priapulida	Yes	Enoplia
All Nematode Taxa	All minus Nematomorpha	Yes	Enoplia
All Nematode Taxa	All minus Tardigrada	Yes	Enoplia
All Nematode Taxa	All minus Kinorhyncha	Yes	Dorylaimia
All Nematode Taxa	All minus Priapulida	Yes	Dorylaimia
All Nematode Taxa, Gblocks alignment	All	Yes	Dorylaimia
Trichinellida Removed	All	Yes	Doryla/Enop
Trichinellida Removed	Kinorhyncha	Yes	Enoplia
Trichinellida Removed	Nematomorpha	Yes	Dorylaimia
Trichinellida Removed	Priapulida	Yes	Enoplia
Trichinellida Removed	Tardigrada	Yes	Doryla/Enop
Long Branch taxa removed	All	Yes	Enoplia
Long Branch taxa removed	Tardigrada	Yes	Dorylaimia
Long Branch taxa removed	Priapulida	Yes	Enoplia
Long Branch taxa removed	Kinorhyncha	Yes	Enoplia
Long Branch taxa removed	Nematomorpha	Yes	Dorylaimia
Outlier taxa removed	All	Yes	Enoplia
Outlier taxa removed	Nematomorpha	Yes	Dorylaimia
Long Branch and outlier taxa removed	All	Yes	Enoplia
Long Branch and outlier taxa removed	Nematomorpha	Yes	Dorylaimia
Long Branch and outlier taxa removed	Tardigrada	Yes	Dorylaimia
Long Branch and outlier taxa removed	Priapulida	Yes	Enoplia
Long Branch and outlier taxa removed	Kinorhyncha	Yes	Enoplia
All taxa, with Stem/Loop partitions	All	Yes	Enoplia
All taxa, with Stem/Loop partitions	Kinorhyncha	Yes	Dorylaimia
All taxa, with Stem/Loop partitions	Nematomorpha	Yes	Dorylaimia
All taxa, with Stem/Loop partitions	Priapulida	Yes	Dorylaimia
All taxa, with Stem/Loop partitions	Tardigrada	Yes	Dorylaimia

Table 5.2: Overview of clade topologies using different nematode taxa, outgroup combinations, and phylogenetic parameters. M = Microlaimoidea, C = Chromadorida, D = Desmodorida, Mo = Monhystera, ALS = Axonolaimidae/Linhomoeidae/Siphonolaimida. Hyphens represent hierarchal derivation of clades, while slashes (e.g. A/B) denote clades appearing as sister taxa. All analyses using GTR+CAT+P-Invar unless otherwise noted.

Job Number	Outgroup Taxa	P-Invar Estimate	Likelihood	Earliest splitting clade	Microlaimoidea	Group 2 Clade Order	Group 3 Clade Order	Spirurina and Rhabditina (More Basal Clade)	Steinernema and Brevibucca	Diplogasteroidea and Bunonema
<i>Removal of long branch nematode taxa</i>										
830442	All Outgroups	Yes	-217364	Enoplia	Condensed	M-C-D	Mo-ALS	Rhabditina	Condensed	Condensed
830456	Tardigrada	Yes	-208653	Dorylaimia	Condensed	M-C-D	Mo-ALS	Rhabditina	Condensed	Condensed
830461	Priapulida	Yes	-197978	Enoplia	Split	M-C-D	Mo-ALS	Rhabditina	Condensed	Condensed
830465	Kinorhyncha	Yes	-199540	Enoplia	Condensed	M-C-D	Mo-ALS	Rhabditina	Condensed	Condensed
830047	Nematomorpha	Yes	-200810	Dorylaimia	Condensed	M-C-D	Mo-ALS	Rhabditina	Split	Condensed
<i>Removal of both outlier and long branch nematode taxa</i>										
830104	Nematomorpha	Yes	-196069	Dorylaimia	Condensed	M-C-D	Mo-ALS	Rhabditina	Condensed	Condensed
830319	Tardigrada	Yes	-203926	Dorylaimia	Split	M-C-D	Mo-ALS	Rhabditina	Condensed	Condensed
830320	Priapulida	Yes	-193251	Enoplia	Split	M-C-D	Mo-ALS	Rhabditina	Condensed	Condensed
830328	Kinorhyncha	Yes	-194815	Enoplia	Split	M-C-D	Mo-ALS	Rhabditina	Condensed	Condensed
830407	All Outgroups	Yes	-212643	Enoplia	Condensed	M-C-D	Mo-ALS	Rhabditina	Condensed	Condensed
<i>Removal of outlier nematode taxa</i>										
77787	All Outgroups	Yes	-269230	Enoplia	Condensed	M-C-D	Mo-ALS	Spirurina	Condensed	Split
822337	Nematomorpha	Yes	-252690	Dorylaimia	Condensed	M-C-D	Mo-ALS	Spirurina	Condensed	Split

Job Number	Outgroup Taxa	P-Invar Estimate	Likelihood	Earliest splitting clade	Microloaimoidea	Group 2 Clade Order	Group 3 Clade Order	Spirurina and Rhabditina (More Basal Clade)	Steinernema and Brevibucca	Diplogasteroidea and Bunonema
<i>Main topology using all nematode taxa</i>										
830467	Nematomorpha	Yes	-257448	Dorylaimia	Condensed	M-C-D	Mo-ALS	Spirurina	Condensed	Split
830473	Priapulida	Yes	-254626	Enoplia	Split	M-C-D	Mo-ALS	Rhabditina	Condensed	Split
830485	Tardigrada	Yes	-265252	Dorylaimia	Condensed	M-C-D	Mo-ALS	Spirurina	Condensed	Split
830519	Kinorhyncha	Yes	-256203	Enoplia	Split	M-C-D	Mo-ALS	Spirurina	Condensed	Split
830526	All Outgroups	Yes	-273996	Enoplia	Condensed	M-C-D	Mo-ALS	Rhabditina	Condensed	Condensed

All nematode taxa, without estimation of P-Invar parameter

995794	All Outgroups	Yes	-274127	Enoplia	Condensed	M-C-D	Mo-ALS	Spirurina	Condensed	Split
995867	Kinorhyncha	Yes	-256331	Enoplia	Condensed	M-C-D	Mo-ALS	Spirurina	Condensed	Split
995979	Priapulida	Yes	-254753	Enoplia	Condensed	M-C-D	Mo-ALS	Spirurina	Condensed	Split
879770	Nematomorpha	Yes	-257558	Dorylaimia	Condensed	M-C-D	Mo-ALS	Spirurina	Split	Split
884354	Tardigrada	Yes	-265380	Doryla/Enop	Condensed	M-C-D	Mo-ALS	Spirurina	Condensed	Split

Gene partitions according to stem/loop secondary structure

992781	All Outgroups	Yes	-271125	Enoplia	Condensed	M-C-D	ALS-Mo/outliers	Rhabditina	Split	Split
992843	All Outgroups	No	-271250	Enoplia	Condensed	M-C-D	Mo-outliers-ALS	Spirurina	Split	Split
993046	Kinorhyncha	Yes	-253504	Dorylaimia	Condensed	M-C-D	Mo-outliers-ALS	Spirurina	Split	Split
993157	Nematomorpha	Yes	-254713	Dorylaimia	Split	M/C-D	Mo-ALS	Spirurina	Condensed	Split
993260	Priapulida	Yes	-251913	Dorylaimia	Condensed	M-D-C	Mo-outliers-ALS	Spirurina	Split	Split
993461	Tardigrada	Yes	-262437	Dorylaimia	Split	M/C-D	Mo-outliers-ALS	Spirurina	Split	Condensed

Job Number	Outgroup Taxa	P-Invar Estimate	Likelihood	Earliest splitting clade	Microloaimoidea	Group 2 Clade Order	Group 3 Clade Order	Spirurina and Rhabditina (More Basal Clade)	Steinernema and Brevibucca	Diplogasteroidea and Bunonema
<i>Outgroup effects: topology tests using different combinations</i>										
898961	Nematomorpha, Tardigrada	Yes	-269584	Dorylaimia	Condensed	M-C-D	Mo-ALS	Rhabditina	Condensed	Split
901362	Nematomorpha, Kinorhyncha	Yes	-260508	Dorylaimia	Condensed	M-C-D	Mo-ALS	Spirurina	Condensed	Split
901536	Nematomorpha, Priapulida	Yes	-258932	Enoplia	Condensed	M-C-D	Mo-ALS	Rhabditina	Condensed	Split
901987	Tardigrada, Kinorhyncha	Yes	-268328	Dorylaimia	Split	M-C-D	Mo-ALS	Spirurina	Split	Split
903685	Tardigrada, Priapulida	Yes	-266747	Enoplia	Condensed	M-C-D	Mo-ALS	Spirurina	Split	Split
904672	Kinorhyncha, Priapulida	Yes	-257601	Enoplia	Condensed	M-C-D	Mo-ALS	Spirurina	Split	Split
905042	All minus Nematomorpha	Yes	-269695	Enoplia	Condensed	M-C-D	Mo-ALS	Spirurina	Split	Split
905265	All minus Tardigrada	Yes	-261893	Enoplia	Condensed	M-C-D	Mo-ALS	Spirurina	Condensed	Split
906184	All minus Kinorhyncha	Yes	-271043	Doryla/Enop	Condensed	M-C-D	Mo-ALS	Rhabditina	Condensed	Split
906503	All minus Priapulida	Yes	-272620	Dorylaimia	Condensed	M-C-D	Mo-ALS	Spirurina	Condensed	Split

Removal of the Trichinellida

77880	All Outgroups	Yes	-270785	Doryla/Enop	Condensed	M-C-D	Mo-ALS	Rhabditina	Condensed	Condensed
77929	Kinorhyncha	Yes	-252998	Enoplia	Condensed	M-C-D	Mo-ALS	Rhabditina	Condensed	Split
77963	Nematomorpha	Yes	-254241	Dorylaimia	Condensed	M-C-D	Mo-ALS	Spirurina	Condensed	Split
78054	Priapulida	Yes	-251451	Enoplia	Condensed	M-C-D	Mo-ALS	Spirurina	Condensed	Split
78067	Tardigrada	Yes	-262062	Doryla/Enop	Condensed	M-C-D	Mo-ALS	Spirurina	Split	Split

Gblocks Analysis

885458	All Outgroups	Yes	-58345	Dorylaimia	Condensed	D/C-M	Mo-ALS	Rhabditina	Split	Split
--------	---------------	-----	--------	------------	-----------	-------	--------	------------	-------	-------

5.4 Assessing support for tree topologies

A wide variety of parameters were used to evaluate the robustness of tree topologies using ML analysis (Table 5.2). Nematode taxa were analysed alongside both single and multiple outgroups, using all possible outgroup combinations to assess topological changes. Tree topologies were mostly consistent using different outgroup arrangements, although the placement of the Dorylaimia and Enoplia showed noticeable shifts in response to outgroup choice. Secondary structure information was used to separate gene alignments according to stem and loop structures present in folded ribosomal subunits; tree topologies from these partitioned gene alignments were compared to non-partitioned ML runs. The designation of stem/loop partitions did not result in vastly improved tree topologies, and seemed to disrupt some otherwise stable groupings. For example, the Axonolaimidae/Cylindrolaimida (Araeolaimida) clade and the Linhomoeidae/Siphonolaimida (Monhysterida) clades were consistently placed as sister taxa derived from the Monysterida, but designation of stem/loop partitions disrupted this topology. In addition, stem/loop partitions seemed to promote attraction between taxa of *incertae sedis*, resulting in some clades with long branches and minimal support.

To assess the impact of seemingly rogue taxa, long-branch clades and taxa of *incertae sedis* were both removed and included in analyses to test for any potentially destabilising effects. All major clades were still recovered when these taxa were excluded from analyses, and clade hierarchy also remained unchanged. Trees were constructed both with and without the P-invar parameter in RAxML which estimates the proportion of invariable sites. Some authors (including the authors of RAxML) advise against simultaneously estimating P-Invar and gamma distributions, arguing that these two parameters cannot be independently estimated from one dataset (Gu *et al.* 1995; Yang 2006; Stamatakis 2008). Removal of the P-Invar parameter did not appear to have any effect on tree topologies. As a final test, trees were built using only conserved alignment sites. The Gblocks program (Castresana 2000) was used to select conserved blocks from 18S alignments, with the aim of eliminating poorly aligned sites and potentially saturated or overly divergent regions. Trees were also built using only the alignment sites that represented conserved stems in the ribosomal secondary structure. ML trees built using both methods showed reduced clade support for many groups (compared to trees built using all alignment positions), and tree topologies were sometimes not consistent with previously published phylogenies. Trimming 18S alignments to reflect only conserved

positions appeared to severely limit the information content available for phylogenetic inference, and did not result in robust tree topologies.

Three particular areas of the nematode tree varied consistently across different topological tests. The Microlaimoidea was generally observed to be monophyletic, but occasionally this clade was recovered as paraphyletic. The tendency of this clade to split was probably related to insufficient taxon sampling within this group—only 9 public sequences were available for inclusion in this analysis. Previous published phylogenies have recovered this group as monophyletic (Meldal *et al.* 2007), and most ML trees from this investigation also supported this grouping. The genera *Brevibucca* and *Cuticonema* were usually placed into a clade containing the genus *Steinernema* (Figure 5.5), but occasionally these taxa were instead placed with the outlier taxa *Myolaimus sp.* and *Odontopharynx longicaudata* (Figure 5.6). The placement of these two outlier taxa was not consistent in different ML trees, suggesting they were unstable within the overall tree topology. Furthermore, *Brevibucca* and *Cuticonema* were observed to have very long branches when placed alongside outlier taxa, suggesting this placement was a result of long branch attraction rather than being reflective of a true evolutionary relationship.

The genus *Bunonema* was recovered either as a sister taxon of the Diplogasteroidea (Figures 5.1 and 5.4), or alternatively, as a sister taxon to the clade containing the genera *Poikilolaimus/Cuticularia* (Figures 5.2 and 5.3). Published phylogenies have grouped *Bunonema* with the Diplogasteroidea (Holterman *et al.* 2006; Meldal *et al.* 2007; Van Megen *et al.* 2009), although this clade relationship was only recovered when long branch taxa were excluded from this analysis. *Bunonema* was more likely to be recovered alongside *Poikilolaimus/Cuticularia* when all nematode taxa were included in the tree, although Bayesian analysis appeared to support a sister relationship with the Diplogasteroidea. However, both placements of *Bunonema* demonstrate low support values under ML (<40) and Bayesian Analysis (62%), and the position of this genus remains unresolved. Van Megen *et al.* 's (2009) large-scale phylogeny also reported low support values for the grouping of *Bunonema* and the Diplogasteroidea

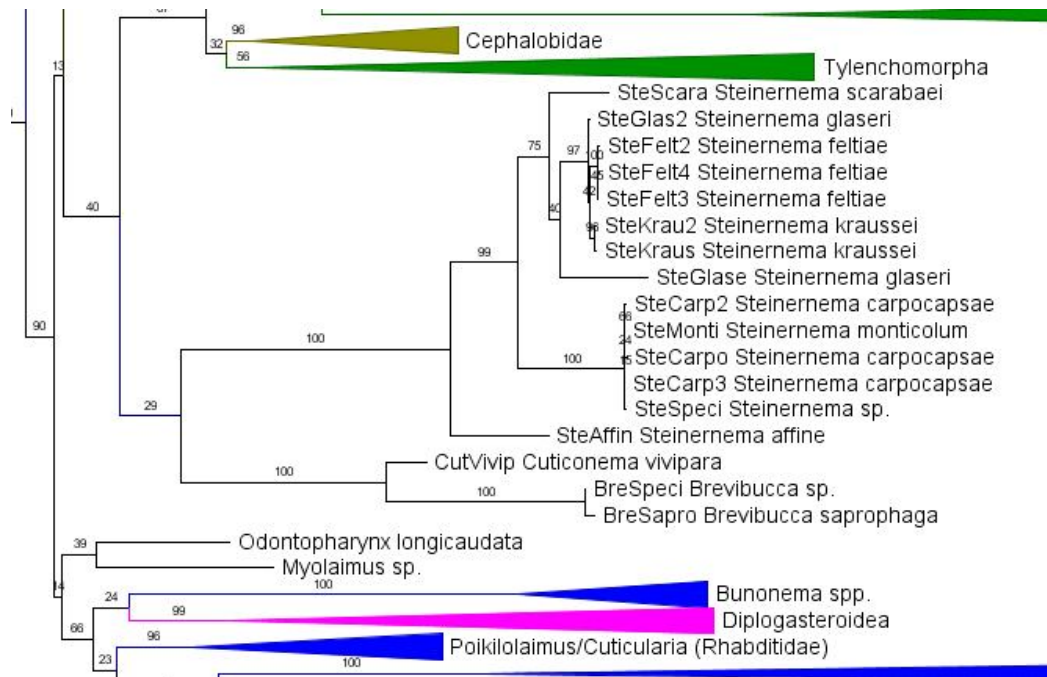


Figure 5.5: Maximum Likelihood topology showing the typical clustering of *Brevibucca*, *Cuticularia*, and *Steinernema* species. (RAXML Job #830526)

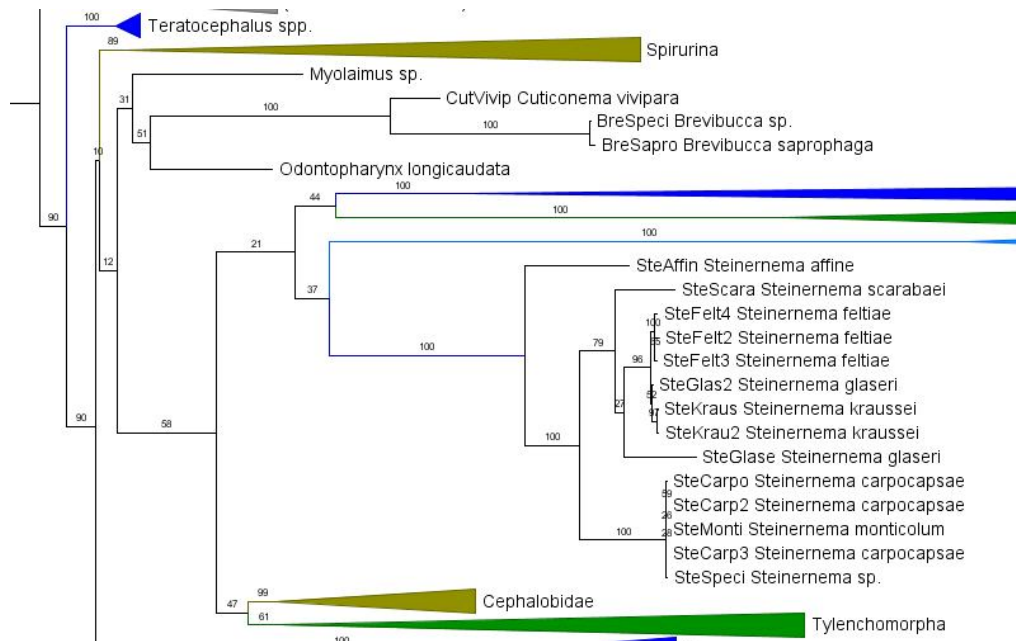


Figure 5.6: Maximum Likelihood topology showing clade topologies when *Brevibucca* and *Cuticularia* split from the main clade containing and *Steinernema* species. (RAXML Job #992781)

5.5 Resolving earliest split in the nematode tree

The positions of the oldest nematode lineages, the Dorylaimia and the Enoplia, were observed to vary widely across tree topologies. The base of the nematode tree was represented by one of three scenarios: the Enoplia splitting first, representing a sister taxon to all other nematodes (Figure 5.1), the Dorylaimia splitting first representing a sister taxon to all other nematodes (Figure 5.2), or Dorylaimia and Enoplia appearing as sister taxa in a clade that basally splits from all other nematodes (Figure 5.3). The splitting order of the Dorylaimia and the Enoplia under different analysis conditions is summarized in (Table 5.1).

When nematode taxa were analysed alongside single outgroups, the choice of outgroup phylum had a significant impact on the order of the earliest splitting clades. The Enoplia was repeatedly observed to split off first when using either the Priapulida or Kinorhyncha as outgroups, with the exception of partitioned structural alignments where the Enoplia split second after the Dorylaimia. The Dorylaimia always represented the earliest splitting lineage when the Nematomorpha was chosen as an outgroup. The Tardigrade outgroup usually resulted in the Dorylaimia splitting off first, although occasionally the Enoplia and Dorylaimia were recovered as a sister taxa. Adding a second or third outgroup to the dataset did not improve resolution at the base of the tree, and there seemed to be an equal probability of recovering the Dorylaimia or Enoplia as the earliest splitting lineage. When all four outgroups were used to construct nematode phylogenies, the Enoplia was usually observed to split off first.

In tree topologies where the Dorylaimia was observed as the earliest splitting group, the Trichinellida (a group of animal parasites) were often observed as a divergent lineage that split early from other taxa; other Dorylaimid clades containing free-living taxa appear to have split off and diversified more recently. The Trichinellid clade contained comparatively long branch lengths compared to other Dorylaimid taxa, and further topological tests were carried out to assess whether this clade reduces resolution at the base of the nematode tree. Removal of the Trichinellida did not result in an unequivocal tree topology—outgroup choice continued to dictate the order of early splits.

5.5 Discussion

5.5.1 Problems faced in resolving the base of the nematode tree

Despite exhaustive topological tests and greatly improved taxon sampling, our large-scale phylogeny was still unable to resolve which group split off the earliest within the Phylum Nematoda. Maximum likelihood methods using a large SSU dataset have alternatively identified both the terrestrial Dorylaimid clade and the primarily marine Enopliid clade as the earliest splitting lineage (Figures 5.1 and 5.2). The large-scale Bayesian analysis provided even less resolution regarding the position of these two groups (Figure 5.4). Although the clade recovery seen in the Bayesian topology agrees with previously published phylogenies, this large-scale analysis failed to provide hierarchical resolution for more recently splitting groups (e.g. Tylenchomorpha and Rhabditida). Despite using the newest version of MrBayes and running data on a large supercomputer cluster, Bayesian analysis was computationally intensive, slow running, and provided inferior outputs compared to RAxML analyses. Thus, the sole use of Bayesian Inference is not currently recommended for large-scale ribosomal phylogenies.

The uncertain placement of the Dorylaimia and Enoplia is likely related to the choice of a single, conserved gene for phylogeny reconstruction. Holterman *et al.* (2006) note that nematodes in the more recently derived Rhabditid and Tylenchid clades exhibit high substitution rates within the SSU gene, allowing for species-level distinctions in most cases. Differential rates of gene evolution may explain the difficulties in resolving deep relationships at the base of the nematode tree, as sequences from older nematode lineages seem to possess less phylogenetic signal compared to highly derived clades. Currently, the 18S gene is the only locus known to resolve deep phylogenetic relationships amongst nematodes. Other genes such as LSU and Cox1 are only informative at lower taxonomic levels (De Ley *et al.* 2005); neither of these genes produce coherent tree topologies for inferring higher clade relationships (e.g. Figure 4.9). Resolving the order of early splits amongst nematodes will require intensive efforts to locate other informative genes—ideally protein-coding—which can supplement evolutionary inferences from SSU data. Phylogeny reconstruction in other taxa has already embraced multi-gene phylogenies (e.g. Hines *et al.* 2007; Shalchian-Tabrizi *et al.* 2008), and efforts are now moving towards phylogenomic methods (Hackett *et al.* 2008; Burki *et al.* 2009). The SSU

gene has previously transformed our understanding of taxonomic relationships amongst nematodes, but it cannot autonomously resolve the early history of the phylum.

Outgroup choice appears to have a significant impact on the order of early splitting clades. The most reliable phylogenies are normally obtained when using the closest sister taxa as an outgroup, or alternatively, including a mixture of close relatives and more distantly related species (Maddison *et al.* 1984; Sanderson & Shaffer 2002). Although the relationships amongst Metazoan phyla are still hotly debated, mounting molecular evidence supports the Nematomorpha as the sister phylum to the Nematoda (Glenner *et al.* 2004; Halanych 2004; Giribet *et al.* 2007; Dunn *et al.* 2008). Amongst the various topological tests completed during this study, it would be reasonable to argue that the most robust clade placements should occur when using either the Nematomorpha alone as an outgroup or all four outgroups in combination. However, these two scenarios give conflicting results: the Dorylaimia is always observed to split off first when the Nematomorpha is used as a single outgroup (Figure 5.1), while the Enoplia tends to be the earliest splitting lineage when using all four outgroups (Figure 5.2). When variable ribosomal regions are removed from alignments using the Gblocks program, the Dorylaimia split first despite the inclusion of all four outgroups. ML and Bayesian analysis of the Enoplia and Dorylaimia using a nematode outgroup (Figure 4.1 and 4.4) recovers both clades as sister taxa and does not indicate a splitting order. These smaller tree topologies also suggest ample support for the monophyly of the Trichinellida and Dorylaimia. The cohesiveness of the Dorylaimid clade has been supported by previous molecular phylogenies (De Ley & Blaxter 2002; Holterman *et al.* 2006; Meldal *et al.* 2007; Van Megen *et al.* 2009); thus, the observed split between the Dorylaimia and Trichinellida observed in full tree topologies is highly suspect.

5.5.2 Elucidating the habitat of the ancestral nematode

These conflicting results highlight the shortcomings of the SSU gene for reconstructing early splits amongst extant nematode lineages, and consequently, inferring the habitat of the ancestral nematode. Although phylogenies cannot confirm either a terrestrial origin or marine origin for nematodes, there are plausible arguments in favour of either scenario. If the Enoplia split off first from all other nematodes, this may indicate a marine origin of the phylum. Many authors assume that Enoplids are oldest nematode group (Abebe *et al.* 2006; Holterman *et al.* 2006), despite the continued lack of resolution in molecular phylogenies. Those who favour the Enoplia as the earliest splitting lineage cite the evidence of ‘ancestral’ traits that resemble typical characteristics of other animal phyla. Some Enoplid nematodes exhibit unique developmental pathways that deviate substantially from the standard patterns observed in most other nematodes. Blastomeres in *Enoplos brevis* and *Pontonema vulgare* exhibit a distinct lack of organisation in cell-lineage pattern; this is a stark contrast to patterns in other nematode groups, where blastomeres can be distinguished even after the first division (Voronov *et al.* 1998). *Tobrilus diversipapillatus* and several marine Enoplid species undergo symmetric embryonic cleavage, whereas other nematodes show clearly asymmetric patterns (Malakhov 1994; Schierenberg 2005). Morphological evidence further suggests that Enoplids retain the ancestral trait of a nuclear envelope present in mature spermatozoa, compared to all other nematode groups which lack this anatomical feature (Baccetti *et al.* 1983; Justine 2002; Yushin 2003).

Visual inspection of tree topologies reveals large genetic divergences between some Enoplid groups (e.g. *Halalaimus*, *Oxystomina*). Assuming that the rate of SSU evolution is slower in basal clades (Holterman *et al.* 2006), this observed phylogenetic distance could potentially suggest an old age for Enoplid lineages. In contrast, highly diverse Dorylaimid species exhibit surprisingly little genetic divergence—potentially signifying a quite recent evolutionary origin for terrestrial species (De Ley & Blaxter 2002). Nematodes are thought to have arisen during the Pre-Cambrian or Cambrian, although there is no fossil evidence to document the emergence of the phylum during these epochs; however, tardigrade fossils have been isolated from sediments representing marine environments in the mid-Cambrian (Labandeira 2005). Some molecular studies have suggested that the tardigrades and nematodes are close relatives within the Metazoa

(Dunn *et al.* 2008), and thus evidence from tardigrade fossils lends indirect support for a marine origin of nematodes.

Arguments that favour a terrestrial origin for nematodes (potentially indicated by the Dorylaimia splitting first from all other nematodes) are more speculative. Dorylaimid species exhibit vastly different lifestyles and span a broad ecological ranges—this diversity has prompted speculation of an early terrestrial evolution and radiation within this group (De Ley & Blaxter 2002). De Ley and Blaxter (2004) present an intriguing discussion that suggests a resemblance (and potentially common ancestry) between Dorylaimid mouth structures and protrusible ‘introvert’ structures seen in Kinorhyncha, Priapulida, and juvenile Nematomorpha. Although there is currently little morphological and developmental evidence to insinuate that the Dorylaimia branched off first from other nematodes, this does not rule out the possibility of this group as the earliest splitting lineage. Our large-scale phylogenies persistently observed the Dorylaimia to split off first under a range of parameters—the Dorylaimia was consistently recovered as earliest splitting lineage under ‘robust conditions’, e.g. when excluding variable alignment positions, or when using the closest outgroup relative (Nematomorpha). Low genetic divergence of Dorylaimid nematodes does not preclude an ancient origin, and could instead imply an especially slow rate of evolution for the SSU gene within this group (De Ley & Blaxter 2002). Furthermore, there is no direct fossil evidence that places nematodes in marine habitats during the Cambrian; the oldest nematode fossil in existence represents a terrestrial nematode from the early Devonian (Poinar Jr. *et al.* 2008).

A terrestrial origin of nematodes could even be possible if the Enoplida is firmly resolved as the earliest splitting lineage. Although there is a clear phylogenetic split between marine and terrestrial species (Figures 4.7 and 4.8), these major clades were recovered as sister taxa. Insight from the marine clade indicates that some marine taxa may have evolved from terrestrial forms (e.g. the Trefusiidae and *Dolicholaimus sp.*). There is evidence to suggest that terrestrial Enoplids represent an ancient lineage. Patterns of embryogenesis seen in one terrestrial Enoplid, *Tobrilus diversipapillatus* (a member of the Triplonchida), resembles ‘classical’ patterns seen in myriad animal taxa but not generally observed in nematodes (Schierenberg 2005). In addition, several marine taxa appear to have terrestrial nematode taxa as sister groups, and ML analyses show that the largest marine group (the Enoploidea) appears to be a more recently derived Enoplid clade. Although no firm conclusions can be made, it is feasible to suggest that colonization of marine habitats may have occurred secondarily within the Enoplida.

5.6 Conclusions

A large-scale phylogeny of the Phylum Nematoda was unable to resolve the splitting order of the Enoplia and Dorylamia using 18S data, despite increased taxon sampling in these groups and comprehensive topological tests. The question of the oldest nematode lineage remains even more puzzling. Both a marine or terrestrial origin of nematodes seems equally plausible—the first group which split off from other nematodes consistently alternated between the terrestrial Dorylaimia and the primarily marine Enoplia. The Enopliid clade is further divided into terrestrial and marine lineages, so a basal position of this clade would also allow for a terrestrial nematode ancestor. The SSU gene has previously revolutionised our understanding of nematode systematics, leading to increasingly comprehensive molecular frameworks for the phylum. This investigation has highlighted the limits of 18S data. No other genes have been identified in nematodes that provide comparable deep phylogenetic resolution; other ribosomal and mitochondrial genes (e.g. 28S, ITS, Cox1) are only informative at lower taxonomic levels. Reconstructing the earliest splits amongst nematodes will be no easy task—it will require a concentrated effort to isolate other informative, protein-coding genes from diverse nematode taxa.

6. Geographic inferences from Enoplid Nematodes

6.1 Evolution of deep-sea genera

SSU tree topologies provide substantial insight regarding the evolution of deep-sea species. The placement of deep-sea and shallow water nematode taxa within the Enoplida is summarized in Figure 6.1, and this phylogeny is expanded (detailing collection depths and sample sites) in Figure 6.2. In both Maximum Likelihood and Bayesian phylogenies, the structure of taxa within the Enoplida suggests that any given deep-sea genus is most closely related to the same genus isolated from shallow water habitats. Many deep-sea specimens appear as sister taxa to their shallow water relatives, as clearly seen for *Syringolaimus*, *Bathylaimus*, *Oxystomina*, *Halalaimus*, and *Chaetonema* species. Molecular data confirms that within the same genus, nematode taxa from deep-sea and shallow water habitats are always recovered as sister taxa—despite past suggestions (J. Lamshead, unpublished data), deep-sea taxa do not cluster into their own independent lineage within the Nematoda.

Additionally, tree topologies suggest that some shallow-water taxa may be secondarily derived from deep-sea species. *Oxystomina* and *Halalaimus* are prominent genera in deep-sea habitats, but nematodes from these groups were also isolated from intertidal sediments. In both groups, shallow water nematodes do not appear within early splitting lineages, but instead occupy more derived positions within both clades. There appear to be five independent, recently derived shallow-water lineages within the genus *Halalaimus*, and two derived shallow water clades amongst *Oxystomina* species. The opposite pattern seems to apply to other Enoplid clades. Shallow-water clades represent the earliest splitting lineages within the Oncholaimoidea and Triplylroididae, and most deep-sea clades within these groups appear as sister taxa to intertidal species. However, within the Enchelidiidae, the purely deep-sea genus *Bathyeurystomina* appears as an early splitting, divergent group. Despite these phylogenetic topologies, an early splitting deep-sea (or shallow water) clade does not necessarily mean that nematodes first evolved in that habitat. The deep-sea has undergone historical cycles of mass extinction and recolonization as a result of historical anoxic events (Rogers 2000), and a shallow water origin is likely for at least some deep-sea nematode species. However, the scale of such anoxic events is largely unknown, and it is possible that oxygen minimum zones were

patchy and localised rather than globally encompassing the entire deep-sea. The survival of fauna in localised pockets would potentially facilitate later radiations back into shallow water. The deep-sea could also have acted as a major source habitat under certain snowball earth scenarios, where continental ice sheets and frozen ocean margins may have restricted fauna to pelagic or deep-sea environments (Runnegar 2000). Under this scenario, one would expect to find secondarily derived shallow water taxa. The picture is far from clear, but perhaps the true answer lies somewhere in the middle—e.g. a shallow-water origin for some species, and a deep-sea origin for other taxa.

Deep-sea nematodes within the Enoplida represent a wide phylogenetic breadth. Deep-sea species were recovered in most marine families—the absence of representatives within some genera is probably due to limited sampling effort, as opposed to the complete exclusion of these taxa from deep-sea habitats. For some genera, such as *Pareurystomina* and *Chaetonema*, the low divergence between deep-sea and shallow water species suggests a relatively recent origin for these taxa—although such relationships do not provide any information regarding the habitat in which such genera first evolved. However, the presence of highly divergent basal clades within genera such as *Oxystomina* and *Halalaimus* suggests that the deep-sea fauna in these groups represents more ancient lineages.

Fossil evidence from other phyla suggests that deep-sea species simply represent radiations from nearby shallow-water habitats (Jablonski & Bottjer 1988; Sepkoski 1991); following initial colonization into the deep sea, certain taxa retreated from shallow water habitats altogether and became strictly deep-sea groups. Isopods are widespread in the deep sea, and the origin and evolution of this group has been heavily studied. There is evidence to suggest that deep-sea isopods within the superfamily Janiroidea originated in shallow water and subsequently radiated into the depths through isothermal water columns (e.g. at high latitudes) (Hessler & Thistle 1975). Several shallow water species within the family also lack eyes, and this distinct morphology points to a reinvasion of shallow habitats by deep-sea taxa (Hessler & Thistle 1975; Hessler *et al.* 1979). Molecular evidence from isopods further supports multiple deep-sea colonization events, suggesting four independent invasions within the Janiroidea (Brandt *et al.* 2007). It appears there have been continuous, multiple speciation events within the Janiroidea, as well as vertical migration up and down shelf habitats—thus, deep-sea taxa within this group probably represent ancient evolutionary lineages (Wilson 1998). Reinvasion of shallow habitats has also been observed in other groups, such as stylasterid corals (Lindner *et al.* 2008). Other

groups of deep-sea isopods appear to represent more recently derived taxa. The Flabellifera are suspected to have invaded deep-sea habitats subsequent to anoxic oceanic conditions that prompted mass deep-water extinctions in the Palaeocene (Wilson 1998). The Flabellifera contains no endemic deep-sea families (in contrast to the Janiroidea which contains seven), and exhibits low diversity in deep habitats. Evidence from isopods suggests that the current deep-sea fauna evolved via multiple routes—this supports patterns seen in nematodes, where some deep-sea taxa appear to be recently derived from shallow water lineages, while other clades appear much older. Within the genus *Halalaimus*, there appear to be several divergent deep-sea clades that branch off early from other taxa, while other deep-sea clades appear more recently derived and seem more closely related to shallow water forms. It is possible that this genus contains both ancient deep-sea lineages as well as more recent invasions. Clade divergence and phylogenetic structure within this one genus also suggests a high species diversity in the deep-sea.

Morphological evidence from the nematode genus *Acantholaimus* suggests that species within this typical deep-sea group have migrated up to shallower shelf habitats in the Weddell Sea (De Mesel *et al.* 2006). *Acantholaimus* species are rarely found in shelf sites and only one species has been described from shallow water (Platt & Zhang 1982). The overall absence of this genus from shallow water could represent a secondary reduction of species in these habitats, following radiation events and speciation into the deep-sea; alternatively, *Acantholaimus* could be an endemic deep-sea lineage. The presence of *Acantholaimus* on the Antarctic shelf may represent a recent migration; molecular evidence will be needed to confirm whether this shelf fauna is more closely related to deep-sea genera or shallow water forms. Nevertheless, the wide depth range found in *Acantholaimus* morphospecies suggests that eurybathy is common amongst deep-sea nematodes, at least in the Antarctic; many Enoplid clades in this study were found to inhabit abyssal, bathyal and Antarctic shelf habitats (refer to Section 6.3 for a full discussion).

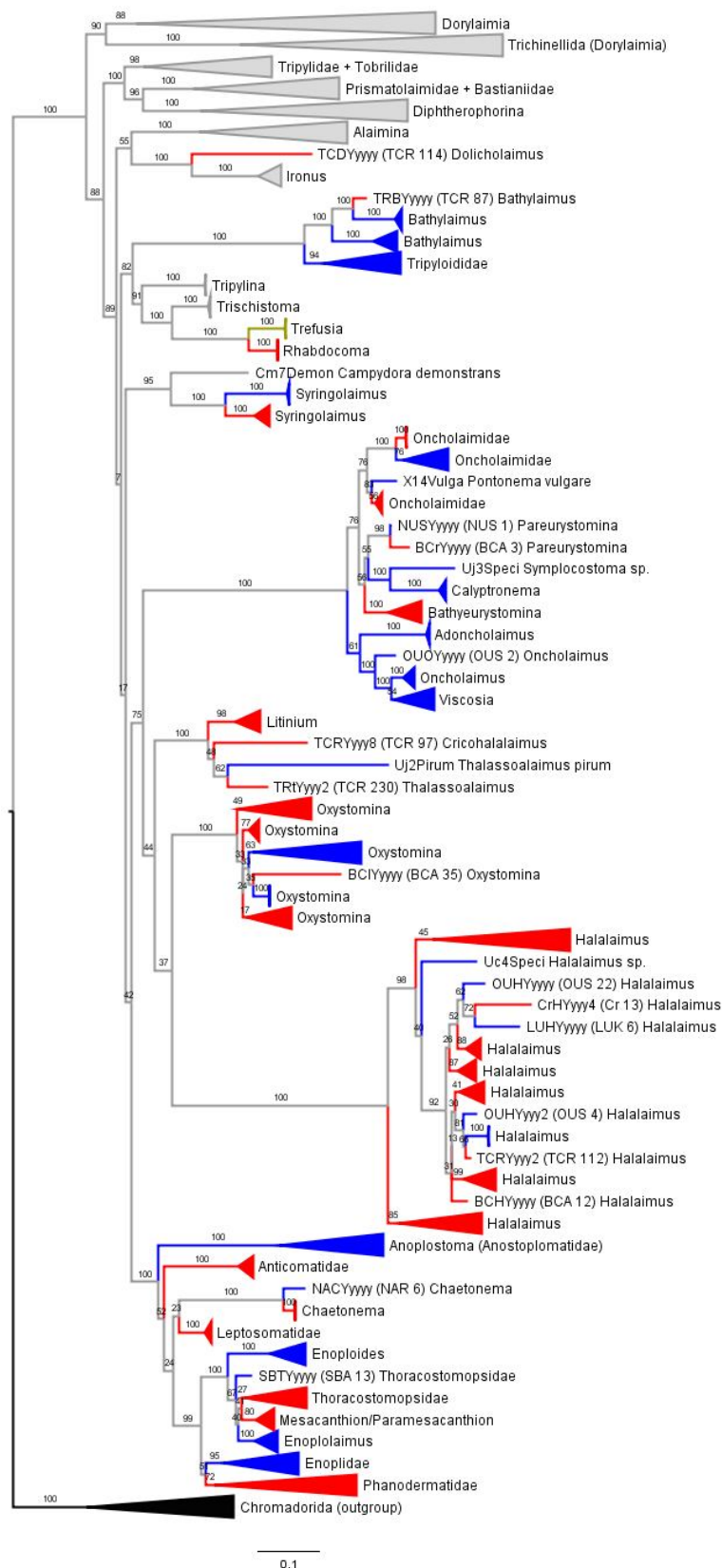
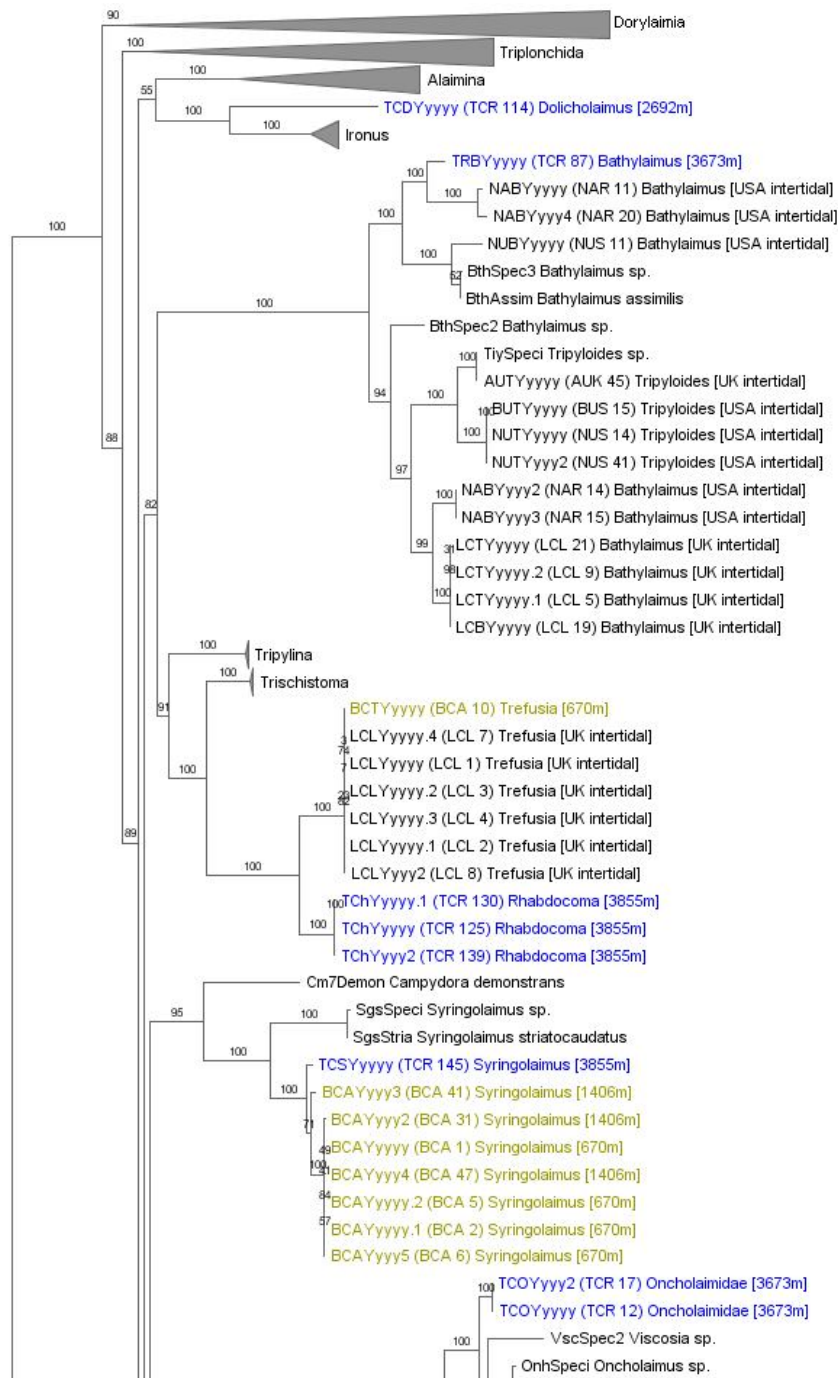
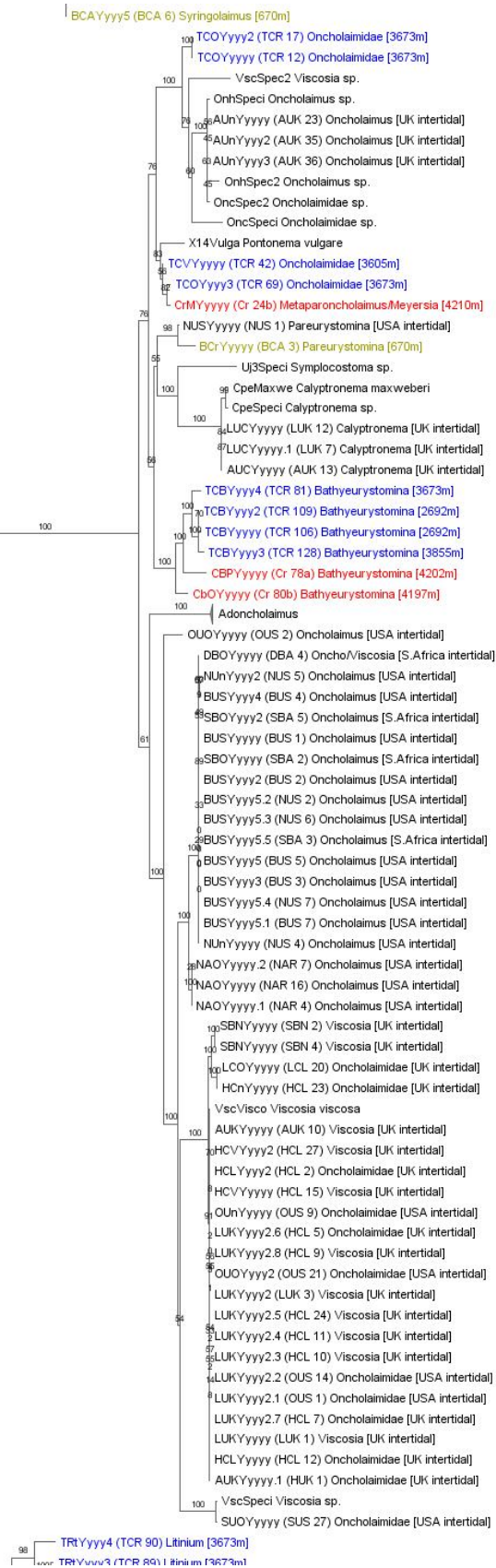
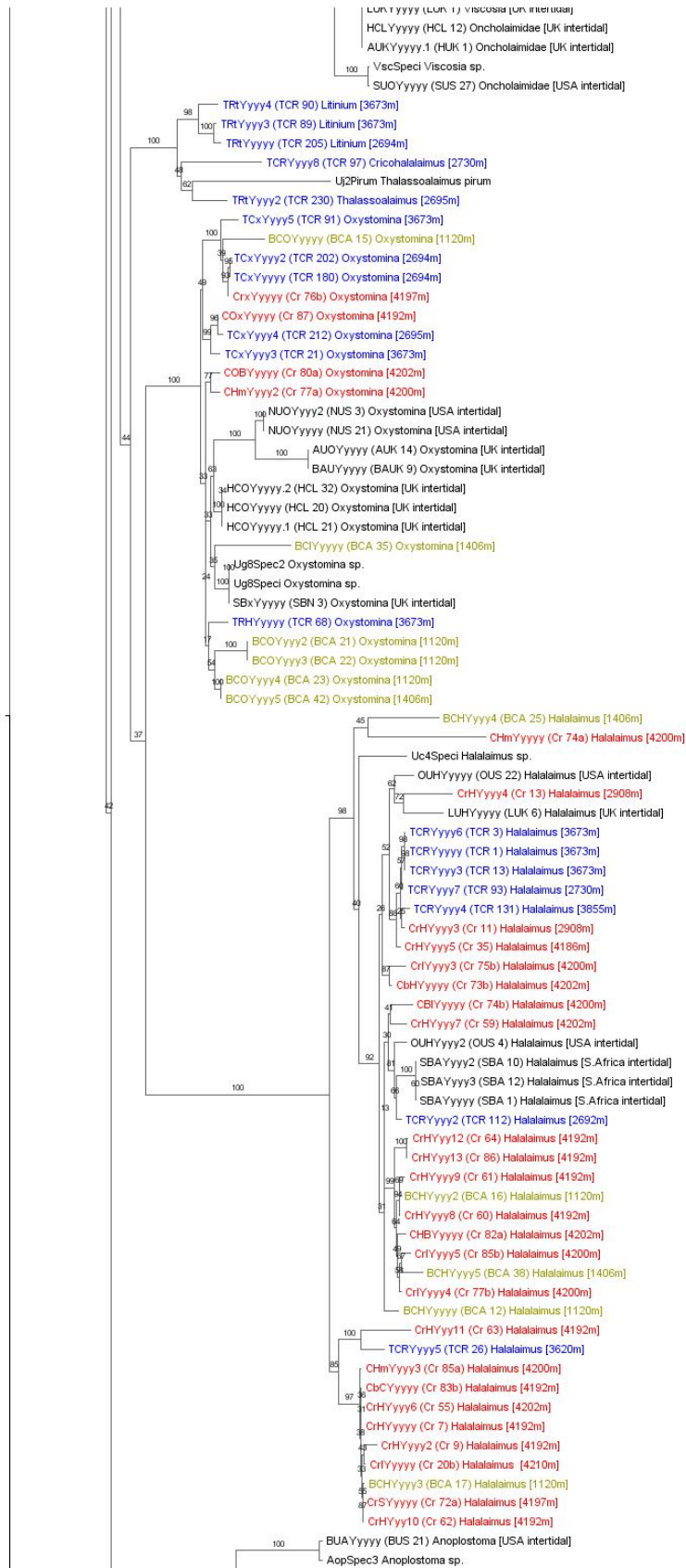


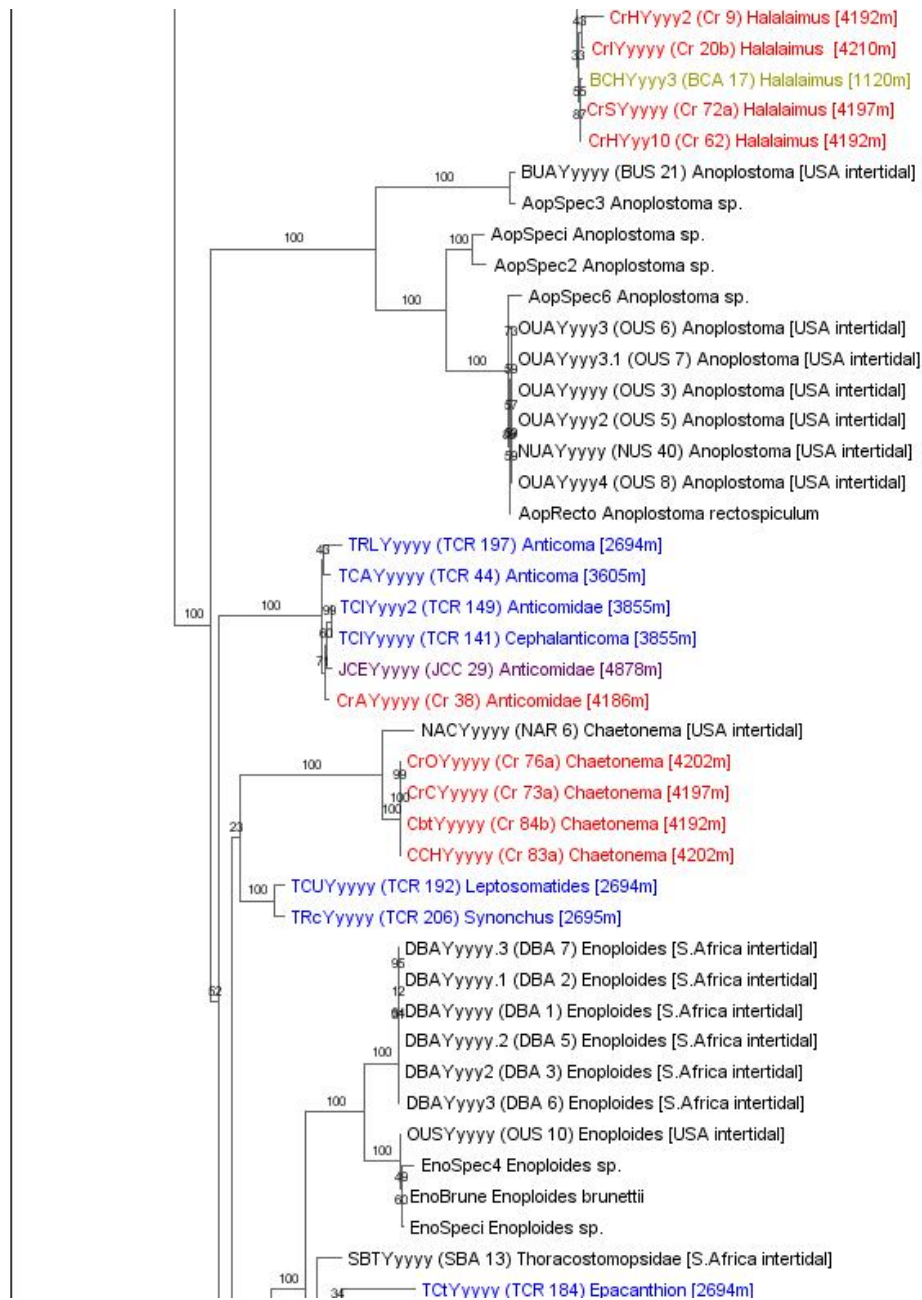
Figure 6.1: Maximum Likelihood phylogeny based on SSU data displaying the habitats of marine nematodes within the Enoplida. Red clades indicate deep-sea species, blue clades represent shallow water species, and yellow clades contain species from both environments. (RAXML Job #65991)

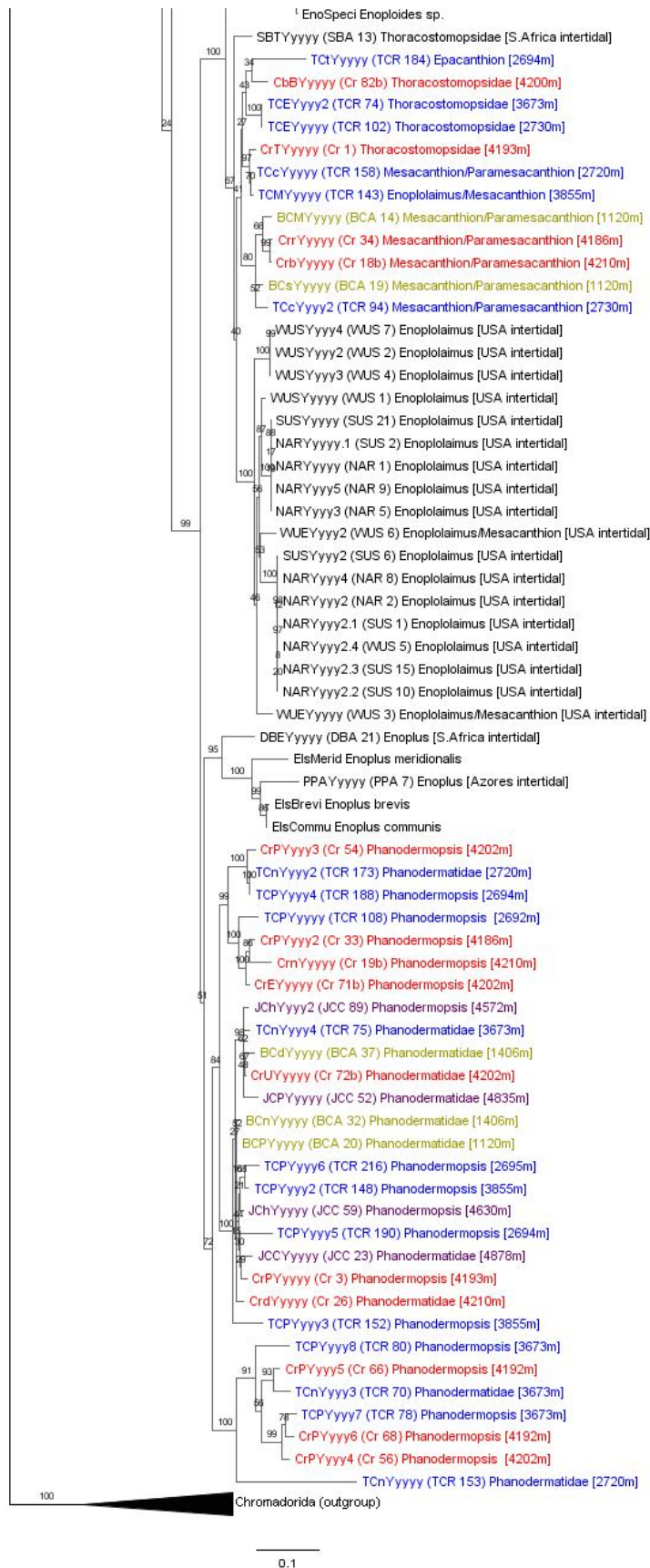
Figure 6.2: Maximum Likelihood phylogeny based on SSU data displaying the habitats of marine nematodes within the Enoplida, expanded to show all taxa (next 5 pages). Black taxa = shallow-water, red taxa = deep-sea sub-Antarctic (CROZET), blue taxa = deep-sea Pacific, and yellow taxa = deep-sea Antarctic shelf. Collection depths listed after all deep-sea specimens. (RAxML Job #65991)











6.2 Recovery of identical gene sequences

Sequence data from multiple genes provides some evidence for widespread (and potentially cosmopolitan) distributions in some nematode species. Pairwise sequence identity comparisons were performed on datasets of SSU, LSU, and Cox1 sequences, and taxa were grouped together if they were observed to possess identical gene sequences. The result of this analysis is outlined in Tables 6.1 through 6.3. Identical gene sequences were, unsurprisingly, most often observed amongst specimens collected at the same sample site. However, the same gene sequences were also recovered in taxa from disparate geographic locations. Barcoding studies typically allow 2-3 base pair differences amongst SSU sequences isolated from the same species (Floyd *et al.* 2002; Blaxter *et al.* 2005), and integrative studies suggest that these cutoff values are an accurate indicator of biological species (Eyualem & Blaxter 2003). Observed nucleotide differences in LSU sequences do not always reliably correspond to species boundaries (De Ley *et al.* 2005), due to the faster rate of evolution at this locus. Cox1 has been widely used to identify species in barcoding methods (Hebert *et al.* 2003; Hajibabaei *et al.* 2006; Gómez *et al.* 2007), and this locus is useful for differentiating closely related nematode species (Derycke *et al.* 2005). Data from this study suggests some degree of intraspecific variability in LSU sequences. Certain groups of taxa that possessed identical SSU and Cox1 sequences did not share exact copies of LSU; usually the difference in LSU sequences was limited to a single nucleotide position, but one group of *Calyptronema* specimens exhibited variation in 11 nucleotide positions. Additionally, some groups of taxa that possessed identical SSU sequences (and only 1 difference amongst LSU sequences) exhibited several Cox1 haplotypes. These Cox1 variants differed at 1-3 nucleotide positions, equating to a genetic divergence <1%; this low divergence is comparable to intraspecific variation observed in other nematode species (Derycke *et al.* 2005). Thus, low-level variation in the Cox1 gene does not necessarily represent cryptic speciation. Given the above evidence, it is reasonable to assume that identical SSU copies recovered in this study (representing ~1600 bp) effectively equate to the same biological species.

Analysis of shallow-water nematodes revealed that identical copies of both SSU and LSU genes were particularly common in Oncholaimid nematodes collected from disparate geographic locations (denoted as Groups 1 and 2 in Table 6.1). One species of *Viscosia* (Group 1) was found around the UK coastline (representing sites in Devon, Wales, the Thames Estuary, and the Clyde Estuary) and on a beach in New Hampshire, USA. A species

of *Oncholaimus* (Group 2) was additionally found at two sites in Massachusetts as well as on two South African beaches. Nematodes with identical sequences were isolated over much smaller distances in the deep-sea (Table 6.3), but data seems to indicate that the same species can persist across relatively large expanses. One species of *Syringolaimus* apparently inhabits shelf habitats in Pine Island Bay, Antarctica, as well as a site in the Bellinghausen Sea nearly 700 miles away. Most interestingly, identical SSU sequences were observed amongst *Trefusia* specimens was found in both the Clyde estuary and a bathyal site on the Antarctic shelf (although only one deep-sea specimen was isolated).

Based solely on identical gene sequences recovered in this study, one could hypothesize that dispersal ability is impacted by depth. Some shallow water nematode species appear to be cosmopolitan and distributed over large distances (Table 6.1). Deep-sea species appeared much more geographically restricted (Table 6.3) and identical sequences were only recovered from specimens collected up to 15 miles apart. Nematodes from the Antarctic shelf perhaps display an intermediate distribution, exhibiting species ranges that extend for hundreds of miles. Such suggestions are, of course, completely speculative. The sampling regime in this study was essentially a random process and focused on nematodes representing a single taxonomic order. More intensive sampling efforts (that encompass a wide taxonomic range of nematodes) may reveal identical deep-sea sequences collected thousands of miles apart. In addition, Oncholaimid nematodes were the only group to exhibit a wide geographic distribution in shallow water—perhaps cosmopolitanism is only characteristic of certain species.

Table 6.1: Groups of shallow-water nematodes exhibiting identical ribosomal sequences. Solid boxes represent specimens that possess identical SSU and LSU gene sequences, with thick horizontal lines separating different clusters of taxa. Dotted vertical lines within boxes designate different LSU haplotypes; in these cases, all taxa possess identical SSU sequences but dotted lines separate groups of specimens according to LSU variant. In these cases, italicized text indicates the pairwise sequence identity between LSU variants; the number of differences observed between sequences is listed below in brackets. If no dotted line is present, all taxa within a box share identical copies of both LSU and SSU.

LUK 1 Viscosia (UK)	AUK 10 Viscosia (UK) <i>LSU identity 99%</i> HCL 5 Oncholaimidae (UK) <i>(1 gap)</i> HCL 7 Oncholaimidae (UK) HCL 9 Viscosia (UK) HCL 2 Oncholaimidae (UK) HCL 10 Viscosia (UK) HCL 11 Viscosia (UK) HCL 12 Oncholaimidae (UK) HCL 15 Viscosia (UK) HCL 24 Viscosia (UK) HCL 27 Viscosia (UK) HUK 1 Oncholaimidae (UK) LUK 3 Viscosia (UK) OUS 1 Oncholaimidae (USA) OUS 14 Oncholaimidae (USA) OUS 21 Oncholaimidae (USA) OUS 9 Oncholaimidae (USA)	Group 1
AUK 23 Oncholaimus (UK)	AUK 35 Oncholaimus (UK) <i>LSU identity 99%</i> AUK 36 Oncholaimus (UK) <i>(1 gap)</i>	
BUS 1 Oncholaimus (USA) BUS 2 Oncholaimus (USA) BUS 3 Oncholaimus (USA) BUS 4 Oncholaimus (USA) BUS 7 Oncholaimus (USA) NUS 2 Oncholaimus (USA) NUS 5 Oncholaimus (USA) NUS 6 Oncholaimus (USA) NUS 7 Oncholaimus (USA)	BUS 5 Oncholaimus (USA) <i>LSU identity 99%</i> NUS 4 Oncholaimus (USA) <i>(1 gap)</i> DBA 4 Oncholaimus (S.Africa) SBA 2 Oncholaimus (S.Africa) SBA 3 Oncholaimus (S.Africa) SBA 5 Oncholaimus (S.Africa)	Group 2
AUK 13 Calyptonema (UK) LUK 7 Calyptonema (UK) **1 gap between LSU in this box	LUK 12 Calyptonema (UK) <i>LSU identity 98%</i> <i>(11 gaps)</i>	
AUK 14 Oxystomina (UK)	BAUK 9 Oxystomina (UK) <i>LSU identity 99%</i> <i>(1 gap)</i>	
BUS 15 Tripyloides (USA) NUS 14 Tripyloides (USA) NUS 41 Tripyloides (USA)		
NAR 1 Enoplolaimus (USA) NAR 5 Enoplolaimus (USA) NAR 9 Enoplolaimus (USA) SUS 2 Enoplolaimus (USA) SUS 21 Enoplolaimus (USA)		
NAR 14 Bathylaimus (USA) NAR 15 Bathylaimus (USA)		
NAR 16 Oncholaimus (USA) NAR 4 Oncholaimus (USA) NAR 7 Oncholaimus (USA)		

NAR 2 Enoplolaimus (USA) NAR 8 Enoplolaimus (USA) SUS 1 Enoplolaimus (USA) SUS 10 Enoplolaimus (USA) SUS 15 Enoplolaimus (USA) SUS 6 Enoplolaimus (USA) WUS 5 Enoplolaimus (USA)
NUS 40 Anoplostoma (USA) OUS 3 Anoplostoma (USA) OUS 5 Anoplostoma (USA) OUS 6 Anoplostoma (USA) OUS 7 Anoplostoma (USA) OUS 8 Anoplostoma (USA)
WUS 2 Enoplolaimus (USA) WUS 4 Enoplolaimus (USA) WUS 7 Enoplolaimus (USA)
DBA 1 Enoploides (S.Africa) DBA 2 Enoploides (S.Africa) DBA 3 Enoploides (S.Africa) DBA 5 Enoploides (S.Africa) DBA 6 Enoploides (S.Africa) DBA 7 Enoploides (S.Africa)
HCL 20 Oxystomina (UK) HCL 21 Oxystomina (UK) HCL 32 Oxystomina (UK)
HCL 23 Oncholaimidae (UK) LCL 20 Oncholaimidae (UK)
BCA 10 Trefusia (670m deep-sea Antarctic, sample site BC 470) LCL 1 Trefusia (UK) LCL 2 Trefusia (UK) LCL 3 Trefusia (UK) LCL 4 Trefusia (UK) LCL 7 Trefusia (UK) LCL 8 Trefusia (UK)
LCL 19 Bathylaimus (UK) LCL 21 Bathylaimus (UK) LCL 5 Bathylaimus (UK) LCL 9 Bathylaimus (UK)
SBA 1 Halalaimus (S.Africa) SBA 10 Halalaimus (S.Africa) SBA 12 Halalaimus (S.Africa)
SBN 2 Viscosia (UK) SBN 4 Viscosia (UK)
NUS 21 Oxystomina (USA) NUS 3 Oxystomina (USA)

Table 6.2: Groups of nematodes exhibiting identical mitochondrial sequences. Solid boxes represent specimens that possess identical Cox1 gene sequences, with thick horizontal lines separating different clusters of taxa. All taxa within a box share identical copies of Cox1. Groups in bold additionally share identical SSU and LSU copies, while taxa in italics share only SSU copies

HUK 1 Oncholaimidae (UK)	DBA 1 Enoploides (S.Africa)
OUS 1 Oncholaimidae (USA)	DBA 5 Enoploides (S.Africa)
NAR 1 Enoplolaimus (USA)	DBA 6 Enoploides (S.Africa)
SUS 2 Enoplolaimus (USA)	DBA 7 Enoploides (S.Africa)
SUS 21 Enoplolaimus (USA)	LCL 19 Bathylaimus (UK)
NAR 16 Oncholaimus (USA)	LCL 21 Bathylaimus (UK)
NAR 7 Oncholaimus (USA)	LCL 5 Bathylaimus (UK)
NAR 8 Enoplolaimus (USA)	LCL 9 Bathylaimus (UK)
SUS 1 Enoplolaimus (USA)	PPA 1 Enoplolaimus (Azores)
SUS 6 Enoplolaimus (USA)	PPA 3 Enoplolaimus (Azores)
WUS 2 Enoplolaimus (USA)	PPA 5 Enoplolaimus (Azores)
WUS 4 Enoplolaimus (USA)	SBA 13 Thoracostomopsidae (S.Africa)
WUS 7 Enoplolaimus (USA)	SBA 8 Thoracostomopsidae (S.Africa)
<i>AUK 18 Calyptonema (UK)</i>	SBA 9 Thoracostomopsidae (S.Africa)
<i>LUK 12 Calyptonema (UK)</i>	TCR 189 Litinium (deep-sea Pacific)
<i>LUK 7 Calyptonema (UK)</i>	TCR 190 Phanodermopsis (deep-sea Pacific)
<i>NUS 6 Oncholaimus (USA)</i>	NUS 10 Oncholaimus (USA)
<i>NUS 2 Oncholaimus (USA)</i>	NUS 5 Oncholaimus (USA)
<i>NUS 4 Oncholaimus (USA)</i>	NUS 7 Oncholaimus (USA)
<i>BUS 2 Oncholaimus (USA)</i>	
<i>SBA 2 Oncholaimus (S.Africa)</i>	
<i>BUS 1 Oncholaimus (USA)</i>	
<i>BUS 3 Oncholaimus (USA)</i>	
<i>DBA 4 Oncholaimus (S.Africa)</i>	
<i>SBA 3 Oncholaimus (S.Africa)</i>	
<i>SBA 5 Oncholaimus (S.Africa)</i>	
<i>BUS 7 Oncholaimus (USA)</i>	

Table 6.3: Groups of deep-sea nematodes exhibiting identical ribosomal sequences. Solid boxes represent specimens that possess identical copies of both SSU and LSU gene sequences, with thick horizontal lines separating different clusters of taxa. Taxa within the last three boxes (denoted by italicized text) share identical SSU sequences only—these specimens all possess different LSU variants.

Nematode Taxa	Distance
Cr 55 Halalaimus (4202m deep-sea sub-Antarctic, sample site 15775#3) Cr 83b Halalaimus (4192m deep-sea sub-Antarctic, sample site 15775#33)	8 miles
BCA 1 Syringolaimus (670m deep-sea Antarctic, sample site BC 470) BCA 2 Syringolaimus (670m deep-sea Antarctic, sample site BC 470) BCA 31 Syringolaimus (1406m deep-sea Antarctic, sample site BC 477) BCA 47 Syringolaimus (1406m deep-sea Antarctic, sample site BC 477) BCA 5 Syringolaimus (670m deep-sea Antarctic, sample site BC 470) BCA 6 Syringolaimus (670m deep-sea Antarctic, sample site BC 470)	687 miles
BCA 21 Oxystomina (1120m deep-sea Antarctic, sample site BC 476) BCA 22 Oxystomina (1120m deep-sea Antarctic, sample site BC 476)	(same site)
BCA 23 Oxystomina (1120m deep-sea Antarctic, sample site BC 476) BCA 42 Oxystomina (1406m deep-sea Antarctic, sample site BC 477)	27 miles
Cr 73a Chaetonema (4197m deep-sea sub-Antarctic, sample site 15775#32) Cr 76a Chaetonema (4202m deep-sea sub-Antarctic, sample site 15775#25) Cr 83a Chaetonema (4202m deep-sea sub-Antarctic, sample site 15775#25) Cr 84b Chaetonema (4192m deep-sea sub-Antarctic, sample site 15775#33)	2-15 miles
TCR 1 Halalaimus (3673m deep-sea Pacific, sample site 518 nem) TCR 13 Halalaimus (3673m deep-sea Pacific, sample site 518 nem) TCR 3 Halalaimus (3673m deep-sea Pacific, sample site 518 nem)	(same site)
TCR 12 Oncholaimidae (3673m deep-sea Pacific, sample site 518 nem) TCR 17 Oncholaimidae (3673m deep-sea Pacific, sample site 518 nem)	(same site)
TCR 125 Rhabdocoma (3855m deep-sea Pacific, sample site 712 nem) TCR 130 Rhabdocoma (3855m deep-sea Pacific, sample site 712 nem) TCR 139 Rhabdocoma (3855m deep-sea Pacific, sample site 712 nem)	(same site)
TCR 173 Phanodermatidae (2720m, deep-sea Pacific, sample site 817 nem) TCR 188 Phanodermopsis (2694m deep-sea Pacific, sample site 856 nem)	0.5 miles
TCR 180 Oxystomina (2694m deep-sea Pacific, sample site 856 nem) TCR 202 Oxystomina (2694m deep-sea Pacific, sample site 856 nem)	(same site)
TCR 143 Enoplolaimus/Mesacanthion (3855m deep-sea Pacific, sample site 712 nem) TCR 158 Mesacanthion/Paramesacanthion (2720m deep-sea Pacific, sample site 817 nem)	16 miles
<i>Cr 64 Halalaimus (4192m deep-sea sub-Antarctic, sample site 15775#37)</i> <i>Cr 86 Halalaimus (4192m deep-sea sub-Antarctic, sample site 15775#33)</i> <i>LSU identity 99% (5 mismatches)</i>	4 miles
<i>TCR 102 Thoracostomopsidae (2730m deep-sea Pacific, sample site 418 nem)</i> <i>TCR 74 Thoracostomopsidae (3673m deep-sea Pacific, sample site 312 nem)</i> <i>LSU identity 99% (3 mismatches)</i>	23.5 miles
<i>TCR 106 Bathyeurystomina (2692m deep-sea Pacific, sample site 617 nem)</i> <i>TCR 109 Bathyeurystomina (2692m deep-sea Pacific, sample site 617 nem)</i> <i>LSU identity 97% (12 mismatches, 2 gaps)</i>	(same site)

The search for cosmopolitan species amongst small, diverse phyla is an active area of research. Theories of worldwide species distributions stem from Baas-Becking (1934), who proposed what is commonly referred to as the 'Everything is Everywhere' hypothesis. Fenchel and Finlay (2004) propose that everything is indeed everywhere for organisms under 2mm in length, suggesting that high dispersal rates and infrequent local extinctions contribute to cosmopolitan species distributions in microscopic species. The authors reason that the sheer abundance of microscopic organisms plays an important role in dispersal—some individuals from dense populations are likely to be transported through inadvertent events. Thus, even if species do not possess any particular mechanisms for long-distance dispersal, sporadic transfer (e.g. via larger, motile animals or anthropogenic factors) could help maintain wide species ranges. High abundance may also result in low rates of local extinction; community compositions may change over time and previously dominant species may become rare, but it is perhaps unlikely that a species would completely disappear from a given habitat. This may be especially true if patch dynamics are in effect; a species may become extinct over small spatial scales, but populations are likely to persist (and perhaps even dominate) in other nearby patches.

Most of the evidence defending the 'everything is everywhere' hypothesis comes from studies of microbes and protozoa (Finlay 2002; Fenchel & Finlay 2004; Fenchel 2005), but evidence from metazoan species is slowly emerging. Molecular evidence has unveiled pan-European and global species ranges in bdelloid rotifers (Fontaneto *et al.* 2008), although patchy species distributions are often found over smaller scales (Fontaneto *et al.* 2006). Homogenous genetic populations of the ascidian *Phallusia nigra* have recently been recorded along 8000 km of the West Atlantic coastline (Nóbrega *et al.* 2004). Identical gene sequences have also been isolated from several foraminiferan species inhabiting both Arctic and Antarctic habitats (Darling *et al.* 2000). Based on DNA evidence, some polychaete taxa seem to be geographically restricted, while other species exhibit truly global distributions (Westheide & Schmidt 2003). However, cosmopolitan species seem to be the exception rather than the rule; although taxonomists had previously proposed a plethora of cosmopolitan morphospecies, molecular evidence is revealing that many of these taxa are composed of genetically structured, cryptic lineages (Knowlton 2000). Some small organisms which fit the criteria for cosmopolitan distribution are also much more limited in their dispersal—for example, tardigrade species seem to be tied to particular habitats, and this dependence greatly restricts the distribution of taxa (Guil *et al.* 2009). Among meiofaunal organisms, it appears that phyla

can be grouped according to life history. Tardigrades appear to follow patterns seen in larger animals: generally low local species richness and abundance, coupled with specific habitat requirements. Rotifers, on the other hand, appear to exhibit high abundances, high local species richness, and high dispersal rates—much more similar to patterns seen in microbes.

If small size, local abundance and species richness are good indicators of species' ranges, then nematodes exhibit a strong resemblance to microbial populations. Nematode densities range from 10^5 to 10^8 individuals per square metre, and marine studies typically recover between 30-45 species per hundred specimens (Lambhead & Boucher 2003). The immense taxonomic deficit within the phylum means that we have no accurate estimate of overall diversity, although previous estimates have suggested anywhere between 10^6 to 10^8 nematode species worldwide. This is, of course, assuming limited dispersal capabilities and a resulting high endemism across geographic regions—the true global species richness for nematodes may be much lower if cosmopolitan is rife. Indeed, there is already some evidence of cosmopolitan nematode species; Bhadury *et al.* (2008) recorded broad geographical and ecological ranges for *Terschellingia longicaudata* based on 18S rRNA data, and Derycke *et al.* (2008) found evidence for transatlantic dispersal in *Pellioditis marina* based on ITS and COI haplotypes. This study also presents additional evidence for wide distributions of Oncholaimid species.

Assuming that some nematode species are cosmopolitan, what mechanisms allow long-distance dispersal? For small phyla with supposedly limited dispersal abilities, Giere (2009) describes cosmopolitan distributions as a 'meiofaunal paradox'. Little research has been conducted on this topic, but there is some evidence to suggest potential mechanisms for long-range dispersal. Microbes and bdelloid rotifers are able to avoid hostile environmental conditions (e.g. where desiccation or freezing is likely) by reverting to dormant life stage. Some microbe species can form desiccation-resistant endospores (Fenchel & Finlay 2004). Adult rotifers exhibit anhydrobiosis and can morph into a dormant 'tun', while rotifer eggs are quite resistant to desiccation (Cáceres 1997); either life stage can act as a propulstage for dispersal. Dormancy has also been demonstrated for some terrestrial and freshwater nematodes. Eggs, juvenile forms, and adult worms are all able to enter quiescent stages in order to survive desiccation and temperature extremes—such resistant forms have been able to survive in dormant form for between 2-25 years (Poinar Jr. 1991; Cáceres 1997). Juvenile and adult nematodes can exhibit anhydrobiosis, adopting a tightly coiled form to prevent water loss. Although resistant

stages have been mainly studied in parasites, dormancy also appears prevalent in free living nematodes (Cáceres 1997; Shannon *et al.* 2005). Two Dorylaimid species were reported as surviving for 10 years in a suspended state (Lee 1961). Such dormant life stages have been suggested as key strategies adopted by cosmopolitan species (Rundle *et al.* 2000). Little is known about quiescent stages in marine nematodes, although adaptations to avoid desiccation are presumably not required in oceanic habitats. Perhaps marine taxa instead exhibit specialised reproductive strategies that facilitate dispersal—for example, resilient eggs that require specific environmental factors to stimulate development.

Frequent transoceanic dispersal could also occur by chance, via water-column processes, natural rafts (vegetation masses, sea ice, marine snow) or anthropogenic transport. Marine nematodes are generally thought to be poor swimmers, and intertidal species usually reside within the sediment (Palmer 1988), although some species such as *Trichotheristus* can apparently move actively throughout the water column (Ullberg & Ólafsson 2003). Hydrodynamic forces have been shown to play an important role in the transport of shallow-water meiofauna. Heavy storms are known to erode sediments up to 25m depth and carry sediments up to 50km away (Giere 2008), while more typical tidal actions can transport meiofauna at a rate of 10km per day as a result of erosion and passive drift (Hagerman & Rieger 1981). Longer distances (e.g. transoceanic) could potentially be traversed by attachment to rafts comprised of organic matter. Nematodes are known to be abundant in certain floating rafts, including mangrove detritus (Faust & Gullledge 1996), drifting algae (Arroyo *et al.* 2006), and *Phaeocystis* 'seafoam' (Armonies 1989). Meiofauna have also been observed to aggregate in clumps of 'marine snow' (Shanks & Edmondson 1990), and transport via these small organic parcels would presumably provide nutritional sustenance during pelagic journeys. *Pellioiditis marina* apparently exhibits transatlantic dispersal (although the frequency of such dispersal events is unknown), and this species has been found floating to macroalgae rafts in the North Sea (Derycke *et al.* 2008). Raft attachment may thus play an important role in the long-distance dispersal of nematodes. Some authors have also suggested that meiofauna can be transported via sea ice (Giere 2008). Anthropogenic transport is likely to be more frequent and occur over shorter time scales. Ballast water (and its associated sediment) and fouling on vessels are both known to carry meiofaunal populations across oceans during shipping operations (Giere 2008). The wide distribution of the ascidian *Phallusia nigra* is suspected to be at least partially due to such human factors, as this species is

typically found in busy harbours (Nóbrega *et al.* 2004). Floating pieces of rubbish are also thought to act as artificial rafts that can transport sessile organisms (Barnes & Milner 2005).

The recovery of identical gene sequences from Oncholaimids in disparate geographic locations suggests one of three scenarios: 1) These species possess as-yet unknown mechanisms for long distance dispersal, 2) Recovery of identical species represents a recent transfer event (e.g. by human activity), or 3) Rates of nuclear and mitochondrial gene evolution are exceedingly slow in these species. The last scenario seems highly implausible, given that SSU has been proven to distinguish nematode species (Floyd *et al.* 2002; De Ley *et al.* 2005; Bhadury *et al.* 2006); other Oncholaimid clades within this study exhibited normal evolutionary patterns. Furthermore, Cox1 variations are adept at separating populations even within the same species (Derycke *et al.* 2005), so identical mitochondrial sequences support the identical Oncholaimid specimens as belonging to a single species. Given the emerging evidence for broad species ranges in nematodes (Bhadury *et al.* 2008), it appears that some Oncholaimid species may be able to sustain globally distributed populations. There is evidence that species within the Oncholaimidae may be particularly capable of long-distance dispersal. *Viscosia viscosa* often inhabits the surface layers of sediment and is apparently capable of floating (Moens *et al.* 1999; Da Fonsêca-Genevois *et al.* 2006), increasing the probability that this species will be resuspended in the water column and passively transported. In addition, there is evidence to suggest that Oncholaimids can actively and rapidly transport themselves to suitable new habitats (Lorenzen *et al.* 1987; Prien 1988; Da Fonsêca-Genevois *et al.* 2006), supplementary to passive mechanisms.

The observation of identical *Trefusia* specimens in the Clyde Estuary and an Antarctic shelf site raises some intriguing questions. Unfortunately, only one specimen was recovered from the Antarctic site—although it is possible that this specimen represents contamination from another sample, the lab procedures followed during this investigation make this an unlikely scenario. Molecular protocols at the start of this study were plagued with difficulty (refer to Chapter 3 for full discussion), and strict standards of cleanliness and organisation were followed after the adoption of new protocols. In addition, Clyde and Antarctic samples were processed separately and over a month apart; contamination would be much more likely if samples were processed on the same day or a few days apart. *Trefusia* is known to inhabit Antarctic sediments, as morphological studies have previously isolated this genus from the Weddell Sea (Vanhove *et al.* 1999).

Molecular data from additional Trefusid nematodes will be required to validate the suggestion of identical genotypes in Antarctic shelf habitats. Nevertheless, the suggestion of identical species in these two disparate habitats does not seem so far-fetched based on apparent long-distance dispersal in other nematodes. In addition, the existence of identical fauna at opposite high latitudes (bipolarity) has long been suspected (Lindbergh 1991; Crame 1993), and recently confirmed in foraminifera using molecular data (Darling *et al.* 2000). The *Trefusia* specimen from the Antarctic was collected from a depth of 670m, whereas Clyde specimens were sampled from intertidal sediments. Antarctic invertebrates have been shown to possess wide bathymetric ranges (Brey *et al.* 1996; Brandt *et al.* 2007), so the recovery of a shallow water species at 670m is not entirely surprising. Eurybathy could also explain the wide distribution of *Syringolaimus* specimens, collected from 1406m and 670m depth. Some bathyal species are known to occupy large depth ranges (Rex *et al.* 2005), and evidence from nematodes suggests that very few genera are vertically limited in Antarctic habitats (Vanhove *et al.* 1999).

6.3 Species distributions in the deep sea

The deep-sea nematodes analysed during this study represent a range of oceanic depths and geographic locations. A wide variety of deep-sea specimens were recovered within the Phanodermatidae and Oxystominidae, and these two families provide substantial insight on species distributions within the deep sea. Previous morphological assessment of deep-sea sites suggested that historical forces may have dictated the current distribution of nematode assemblages. Lamshead et al. (2003) found distinct community assemblages typical of different ocean basins; biogeographic data further demonstrated that the deep-sea taxa form a distinct grouping, with abyssal and bathyal locations from the same ocean basins clustering together (J. Lamshead, unpublished data). Molecular analyses do not support a geographic clustering pattern—the phylogenetic structure of the Enoplida shows no apparent grouping of nematodes according to either depth or sample site in SSU or LSU tree topologies. If historical events continued to dictate species distributions, molecular evidence would unequivocally suggest biogeographic patterns within tree topologies—taxa from the same geographic locations would form distinct, independent clusters. Furthermore, local deep-sea clades would exhibit sister-taxa relationships with the nearest shallow-water fauna (from which they would presumably be derived). However, no such patterns have been observed in this study. A similar phylogenetic structure was observed in both SSU and LSU tree topologies; analysis of both genes (using both ML and Bayesian methods) resulted in similar phylogenetic placements of most deep-sea taxa (refer to section 4.4.1 for comparison of LSU and SSU topologies).

Within the Phanodermatidae (Figure 6.3), Clade 2a contains members from almost all deep-sea sample areas, with specimens collected from a wide range of depths. The specimen TCR 75 belongs to a taxonomic assemblage that also includes Atlantic (JCC 89, 52), Antarctic (BCA 37), and sub-Antarctic (Cr 72b) nematodes; TCR 75 is more closely related to specimens from these disparate locations than to other Phanodermatidae specimens isolated from the same Pacific site (e.g. TCR 70, 78). Similar patterns are seen in clade 3, where Pacific and sub-Antarctic specimens exhibit sister relationships (e.g. Cr 66 and TCR 70). This phylogenetic structure seems to indicate widely distributed, closely related species assemblages in the deep-sea. Species within Clade 2a of the Phanodermatidae show pairwise sequence identities above >98%. Clade 2b also exhibits high sequence identities amongst specimens; visual inspection suggests that some outlier

species may represent divergent lineages, and pairwise comparisons confirm a lower sequence identity. For example, the nematode TCR 152 exhibits only 96% identity with TCR 75 in the main clade grouping, and this outlier specimen probably represents a separate species.

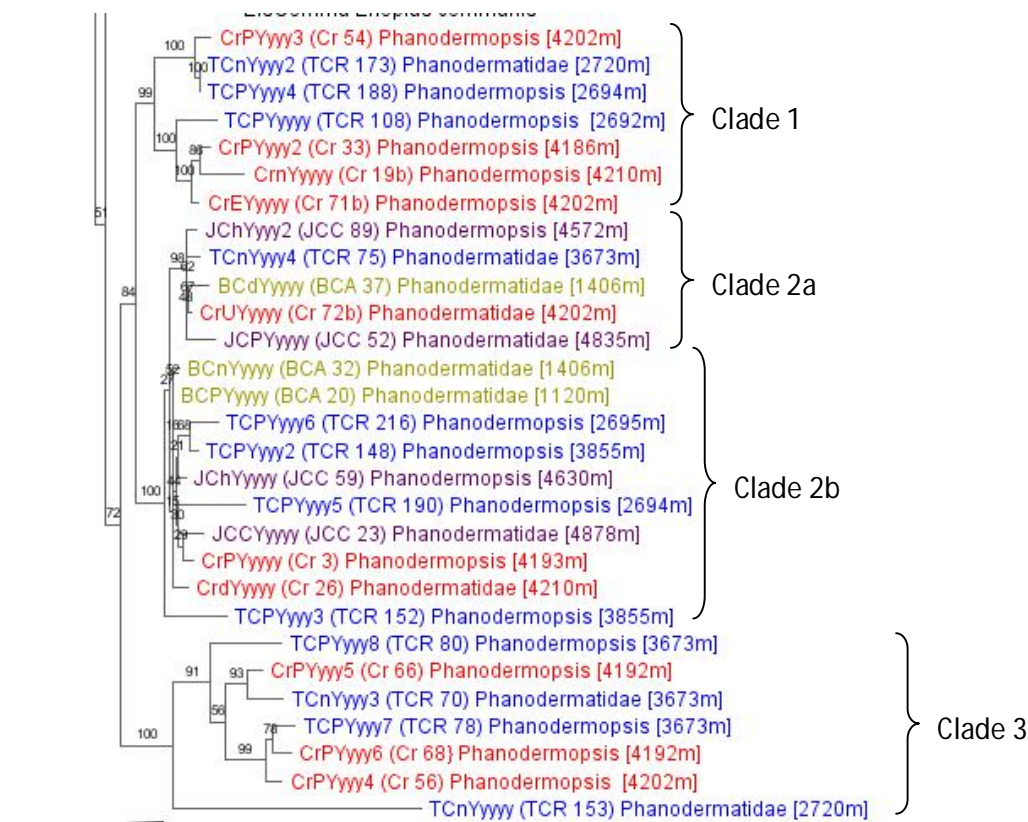


Figure 6.3: Maximum Likelihood phylogeny built using SSU sequences, showing the collection depths of deep-sea specimens within the Phanodermatidae (RAxML Job #65991). Colours equate to collection location of samples: Blue = deep-sea Pacific, Red = deep-sea sub-Antarctic (CROZET project), Yellow = Antarctic shelf, Purple = deep-sea Atlantic.

Phylogenetic clusters in SSU tree topologies most likely represent species or species complexes in the deep-sea—the observed pairwise identities correspond with cutoffs for species delimitation in barcoding studies and molecular taxonomy. Microbial communities are generally separated into ‘phylotypes’ using a sequence identity cutoff of 97% (Venter *et al.* 2004; Shaw *et al.* 2008), while past studies of nematodes have indicated that morphospecies can be separated using 98% cutoff values (Blaxter *et al.* 1998). The most recent metagenomic studies of nematode communities indicate that an identity cutoff value somewhere between 95-99% should define Operationally Clustered Taxonomic Units (OCTUs) that broadly correlate with biological species, although one

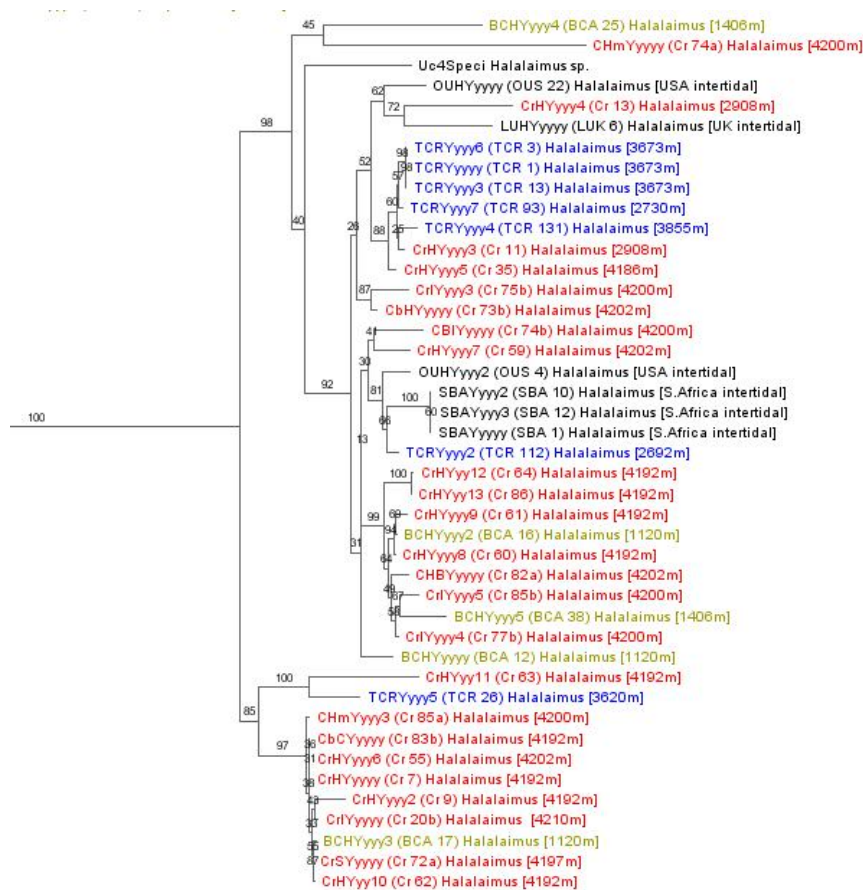


Figure 6.5: Maximum Likelihood phylogeny built using SSU sequences, showing the collection depths of deep-sea specimens within the genus *Halalaimus* (RAXML Job #65991). Colours equate to collection location of samples: Blue = deep-sea Pacific, Red = deep-sea sub-Antarctic (CROZET project), Yellow = Antarctic shelf.

This high sequence identity in deep-sea nematodes potentially indicates the same species occupying wide geographic ranges. However, delimiting biological species according to molecular cutoff values is still contentious and not thoroughly tested across all taxa. Investigations within *Panagrolaimus* have shown that using a cutoff value of 3 base pair difference per 500bps of the SSU gene (~99% sequence identity) can accurately infer reproductive isolation and define biological species (Eyualem & Blaxter 2003). Further testing is needed to determine whether such a cutoff value is applicable for other nematode genera in other habitats—molecular divergence in the deep-sea may be governed by different factors and evolutionary processes. Sequences that share 99% identity are not identical gene sequences, indicating at least some (albeit minimal) molecular divergence. Nematodes gathered from disparate habitats may represent reproductively isolated populations that are currently diverging, and rRNA sequences still

represent the genotype of a recent ancestor. The recovery of identical sequences in this study (Section 6.2) suggests that nematodes can maintain populations over large distances, but this phenomenon may be restricted to shallow water species that are more easily dispersed. Data from foraminifera (Pawlowski *et al.* 2007) and the bivalve *Deminucula atacellana* (Zardus *et al.* 2006) suggest that some benthic species exist as metapopulations that span huge geographic ranges in the deep-sea. However, both of these groups possess reproductive strategies which probably help maintain gene flow over large distances: benthic forams produce dispersive propagule stages (Alve & Goldstein 2003), while *Deminucula atacellana* produces pelagic, lecithotrophic larvae (Scheltema & Williams 2009). Further work is needed to determine whether deep-sea nematode species can maintain gene flow over large distances.

If phylogenetic clusters with high sequence identities represent biological species in the deep sea, the situation evokes many pressing questions: How do nematodes disperse over such large geographic distances? Are there cosmopolitan species in the deep-sea? Do shallow water and deep-sea habitats share any nematode species? Evidence from molluscs suggests that deep-sea species show much greater genetic divergence across depth gradients (e.g. bathyal to abyssal) than geographic distances. Geographically disparate populations of the bivalve *Deminucula atacellana* living bellow 3000m showed very low divergence in mtDNA, despite being separated by thousands of kilometres (Zardus *et al.* 2006); in contrast, proximate populations separated by a depth gradient exhibited much higher molecular diversity. Some abyssal species of benthic foraminifera also show very little genetic differentiation between sites in the Atlantic Ocean, with apparently bipolar gene flow (Pawlowski *et al.* 2007). However, shallow water and deep-sea forams are recovered as independent evolutionary lineages (Brandt *et al.* 2007), similar to the sister taxa relationship observed between deep-sea and shallow water nematode clades. This suggests that both deep-sea and shallow-water fauna can exhibit wide species ranges in their respective habitats, but the physiological differences (e.g. pressure, temperature) between the two habitats prevent the same species from inhabiting both deep and shallow waters. Little research has been conducted on dispersal mechanisms for deep-sea phyla that lack obvious propagative phases. There is some evidence to suggest long-distance dispersal mechanisms in shallow-water nematodes (see Section 6.2), but this seems to be aided by high-energy hydrodynamic events and the ease of inadvertent transfer. Some meiofaunal taxa are also known to actively emerge from the sediment and into the water column (Palmer

1988), and this behaviour is thought to play an important role in the recruitment and colonization of shallow water habitats. Recently, emergence has also been demonstrated in some deep-sea harpacticoid copepods (Thistle *et al.* 2007), suggesting that infaunal taxa can use near-bottom currents to disperse in these habitats. Although nematodes are generally thought to be poor swimmers only passively dispersed, evidence from Oncholaimids (see Section 6.2) suggests that at least some species can actively change location. If emergence behaviours are adopted by deep-sea nematode species, it may help to explain the wide species ranges proposed for these taxa.

Past morphological studies have indicated that many nematode species are endemic to certain deep-sea sites, and this phenomenon is particularly noted in Antarctic waters. Although no endemic genera have been identified in the Southern Ocean (Sebastian *et al.* 2007), a number of morphological studies have reported endemic Antarctic species (Vermeeren *et al.* 2004; De Mesel *et al.* 2006). Some species inhabiting the Antarctic are clearly not restricted to the Southern Ocean, as indicated by the low molecular divergence observed between species inhabiting geographically disparate areas (e.g. Antarctic and Pacific deep-sea). However, this study does not completely rule out the possibility of Antarctic endemism—several clades within the genera *Oxystomina* and *Halalaimus* are comprised entirely of specimens isolated from Antarctic waters (sample codes Cr and BCA, coloured red and yellow, respectively in Figures 6.4 and 6.5). Such ‘endemism’ could alternatively reflect insufficient sampling efforts. Restricted sampling protocols in morphological studies (e.g. analysis of <100 nematodes per sample site) may have previously prompted such conclusions, or alternatively, morphometric data used to separate species may represent intraspecific morphological variation or juvenile stages within certain taxa. Morphological studies of the deep-sea generally focus on all nematode taxa present at a sample site, encompassing a huge taxonomic breadth. Species accumulation curves rarely reach asymptote in these studies (Lambshhead 2004), so it is likely that many nematode taxa remain unknown even for frequently studied sites. This study aimed to intensively sample Enoplids from each sample area, but the sampling regime only examined a limited number of sediment cores representing a very small area of the seabed. Each sediment core represents only ~78 cm² of the seafloor, and only 10 cores were analysed from the Pacific deep-sea—a total area 785 cm². Thus, the Enoplid species that were collected from the Southern Ocean may also appear in other oceanic basins, but have not been represented in any sediment cores collected during this study. More intensive sampling regimes (including molecular analysis) will be required to

determine whether some nematode species are endemic to Antarctic habitats. Data from other phyla suggests that Antarctic endemism is a widespread and well-recorded phenomenon, potentially resulting from the long isolation of Antarctica. For macrobenthic species, between 35% (scleractinian corals) to 90% (pycnogonids) of taxa recorded in Antarctic habitats are endemic to that region (Arntz *et al.* 1997). There is also evidence to suggest regional endemism; De Broyer & Jazdzewski (1996) reported that 38% of gammaridean amphipods were endemic to eastern Antarctica, and 54% endemic to western regions. This trend has also been observed in meiofauna, although the evidence is more limited and suggests that endemism is less widespread—only 16% of harpacticoid copepod species were restricted to the Southern Ocean (Razouls *et al.* 2000).

Deep-sea nematode species do not appear to be restricted to narrow depth ranges, and there is some evidence that some taxa inhabit both deep abyssal and shelf habitats. For example, Clade 2b in the Phanodermatidae (Figure 6.3) contains nematodes that represent depths from 1120m down to ~5000m. Invertebrate species inhabiting the Antarctic shelf have been shown to display an extended level of eurybathy (Brey *et al.* 1996), and the extended depth range of nematode species may be specific to Antarctic shelf habitats. Eurybathy in the Southern Ocean is thought to stem from historical cycles of shelf ice formation and retreat—periodic extinction of shelf fauna was followed by upwards migration of deep-sea taxa. Apart from an isolated genotype observed in *Trefusia* specimens from the Clyde estuary and the Antarctic shelf (see Section 6.2), there was no overlap between deep-sea clades and shallow water habitats outside the Antarctic. Future investigations will need to include sample sites from shelf habitats outside the Antarctic to determine whether or not deep-sea taxa can typically inhabit shallower depths.

Finally, this study provides the first molecular evidence for endemic deep-sea lineages. Previous morphological studies have reported novel deep-sea genera (Bussau 1993; Muthumbi *et al.* 1997; Fonseca *et al.* 2006), but in the absence of molecular evidence it is impossible to determine whether these species represent truly divergent lineages, or simply extreme morphological variation. The genus *Cricohalalaimus* was first identified in the deep-sea by Bussau (1993), who placed this taxon within the Oxystominidae (subfamily Halalaiminae) and suggested a close evolutionary relationship with *Halalaimus* species. Both *Cricohalalaimus* and *Halalaimus* possess amphids that appear as long, longitudinal slits; in other respects, *Cricohalalaimus* is quite morphologically distinct within this family, displaying a thick, annulated cuticle and long,

setiform cervical setae. This investigation suggests that *Cricohalalaimus* represents a divergent lineage that is more closely related to *Thalassoalaimus* and *Litinium*, despite its morphological resemblance to *Halalaimus*. Both SSU (Figure 6.2) and LSU (Figure 4.10) data demonstrate high support (>98%) for this relationship. *Cricohalalaimus* is consistently placed in a clade between *Litinium* and *Thalassoalaimus*, although the distinct morphology of *Cricohalalaimus* does not intuitively suggest a relationship to either genus. Morphological and molecular divergence suggests that *Cricohalalaimus* should be formally denoted as a new genus, with species currently only known from deep-sea habitats.

6.4 Conclusions

Deep-sea nematode genera exhibit a close phylogenetic relationship to shallow water species, and species within a genus are often recovered as sister taxa. Evidence from other phyla suggests that the deep-sea was colonized via multiple evolutionary routes, and tree topologies recovered in this study support a similar scenario for deep-sea nematodes. Some clades appear to contain ancient deep-sea lineages with recent invasions of shallow water, while other groups contain primarily shallow water species with a few recently derived deep-sea clades. There does not appear to be any structuring of nematode taxa between depth or ocean basin, and evidence from Antarctic shelf nematodes suggests an extended degree of eurybathy for deep-sea species in the Southern Ocean. Identical sequences recovered from disparate shallow water habitats suggest that some taxa maintain wide geographic ranges, although the extent and frequency of long-distance dispersal events is not yet known. Despite the intensive sampling effort of this investigation, deep-sea nematodes were only isolated from a small number of sites representing a tiny area of the seafloor. Future molecular investigations should be expanded to include the entire deep-sea nematode fauna, with samples representing a wider range of shelf, bathyal, and abyssal locations. This study has provided the first insight into the evolution of deep-sea nematode fauna, but many knowledge gaps remain.

7. Summary and Future Prospects

7.1 Summary of Conclusions

This investigation has provided substantial insight regarding evolutionary relationships within the previously understudied subclass Enoplia. Prior investigations have resolved relationships in most major nematode groups (with especially extensive work in certain terrestrial clades), but up until recently marine species had been largely excluded from most analyses. This study has produced a number of important results. Firstly, the first comprehensive (and robust) phylogenetic framework has been produced for the nematode order Enoplida. The integration of marine Enoplid sequences with terrestrial taxa from the Triplonchida has produced a robust, well-sampled molecular framework for the nematode subclass Enoplia. Secondly, this investigation has shown that increased taxon sampling and rigorous phylogenetic analysis is still insufficient for clearly elucidating the earliest-splitting lineage within the nematode tree. SSU sequences indicate that both the Enoplia and Dorylaimia are ancient lineages that split off early from all other taxa; however, we still do not understand the historical order of this split, and the base of the nematode tree remains unresolved.

Perhaps most importantly, this investigation has obtained the first sequences from deep-sea nematodes and integrated these taxa into phylogenetic framework. Our previous knowledge of deep-sea nematode species was based solely on morphology; gene sequences have provided the first insight regarding the evolution of nematodes in extreme, isolated environments such as the deep-sea. In molecular frameworks, deep-sea genera appear as sister taxa to their shallow water counterparts. Phylogenetic topologies appear to suggest that several evolutionary patterns may exist for nematode taxa in different clades; some deep-sea lineages appear to be early-splitting and ancient, while other deep-sea taxa seem to be more recently derived from shallow water species. Molecular data has also provided further evidence to support the existence of cosmopolitan nematode species. Identical gene sequences (representing several loci) isolated from Oncholaimid nematodes appear to indicate that at least some nematode species can maintain gene flow over huge geographic ranges—however, this pattern appears to be the exception rather than the rule.

Finally, this study has provided long overdue guidance regarding the integration of taxonomic and molecular protocols. These two disciplines have very disparate goals,

meaning that nematode studies requiring morphology and gene sequences can be notoriously difficult to undertake. The adoption of DESS preservative by the nematode community constituted a major step for integrative studies; this study has continued such progress with the development of a slide mounting protocol that can be reliably adopted for studies requiring both morphological identifications and molecular work.

7.2 Our current understanding of evolutionary relationships amongst nematodes

A suite of molecular studies have substantially restructured and refined our understanding of nematode phylogenetics over the past ten years. Although many nematologists still rely on outdated morphological classifications and morphometric techniques, taxonomists are slowly embracing molecular techniques and realising their vast potential for nematode research—sequence data is routinely helping to elucidate relationships for taxa with persistently difficult morphology (Eyualem & Blaxter 2003; Stock & Nadler 2006). The ubiquity of molecular protocols for nematodes (De Ley & Bert 2002; De Ley *et al.* 2005; Floyd *et al.* 2005; Bhadury *et al.* 2007) has encouraged the application of genetic techniques, and methodological insights from this study (Chapter 3) will further facilitate the use of integrated methods. Nematode barcoding methods have been tested and refined for single-worm PCR (Floyd *et al.* 2002; Blaxter *et al.* 2005; Bhadury *et al.* 2006), and the development of high throughput, next-generation sequencing platforms looks set to further revolutionise these meiofaunal barcoding techniques. Given the ever-present taxonomic deficit for nematodes, these new techniques offer a rare opportunity for greatly expanding our knowledge of nematode biodiversity.

With Van Megen *et al.*'s (2009) recent publication of the first large-scale nematode phylogeny (and further contributions from this investigation), we are finally reaching the stage where we have a comprehensive, molecular framework that firmly elucidates evolutionary relationships amongst all major nematode groups. Molecular knowledge in nematodes lags far behind the intensive research seen in other invertebrate (e.g. insects) and vertebrate taxa. Despite this seemingly grim assessment, many metazoan taxa remain far more elusive and unknown (e.g. Gastrotricha, Priapulida, Kinorhyncha)—continued research in nematodes may provide a future template for research in these small, diverse metazoan phyla.

7.3 Future prospects for research

Despite recent large-scale molecular frameworks, there are still many nematode groups where internal relationships remain unresolved; this is predominantly related to the lack of publically available gene sequences for these groups. For example, the entire public database of nematode sequences contains approximately 10 full-length SSU sequences representing the (predominantly marine) Microlaimoidea; the Chromadorida (which also includes many marine taxa) is only slightly better represented with around 35 SSU sequences. The genus *Desmoscolex* appears to represent a divergent clade within the nematode framework, yet only one sequence represented this entire group in this investigation. Future molecular investigations will need to fill in these obvious gaps in the nematode tree—we may have outlined the skeleton of the nematode tree, but there is still much work to be done before we have fully explored all layers of this species-rich phylogeny. Additionally, there needs to be a much stronger focus on marine species. Free-living nematodes are ubiquitous, abundant, and diverse in marine environments; however, the majority of nematode studies focus on terrestrial species. Of the studies that encompass marine taxa, most published work tends to focus on intertidal species from northwest Europe. Future molecular investigations of marine species will need to expand the geographic breadth of their sampling efforts, including samples from a range of depths (from intertidal sediments down to abyssal plains), latitudes, and sediment types. This study isolated deep-sea specimens from a single nematode order; subsequent investigations will need to supplement this data with gene sequences from deep-sea nematodes in from other families (e.g. the Monhysterida, Chromadorida, etc.). In this respect, intensive sampling efforts may reveal previously unknown branches of the nematode tree. Additionally, a continued focus on dense taxon sampling will only continue to improve the resolution (and support values) observed amongst major nematode clades. Future investigations will require a concentrated effort in order to resolve the earliest splitting branch of the nematode tree. SSU data alone appears to be too conserved to resolve the basal node; multi-gene phylogenies or phylogenomic methods (including a sufficient number of free-living and marine representatives) will likely be the only methods which can firmly answer this longstanding question.

High-throughput protocols for nematodes have recently been developed using so-called 'next-generation' sequencing platforms (Porazinska *et al.* 2009; Creer *et al.* In press). Past work has utilised chain-termination sequencing methods to amplify the SSU gene, but the newest sequencing technologies (e.g. the GS FLX by Roche) offer faster,

cheaper (per base), and more informative methods for biodiversity research. Metagenomic studies likely to represent the high-throughput incarnation of nematode barcoding—in the future, such analyses may greatly facilitate biodiversity research, as well as be invaluable for environmental surveys and monitoring. Current environmental surveys of meiofauna are labour-intensive and require a team of skilled taxonomists; future metagenomic surveys of biodiversity may only require minimal expertise and a few hours of sequencing. Metagenomic investigations offer powerful tools, but there is a pressing need to test and refine current methodology—the ultimate goal is to derive valid biological conclusions from the massive amounts of generated data (up to 1 million sequence reads from a typical 454 run). Future research will focus on empirically validating 454 sequencing protocols, as well as testing and refining computational pipelines that process and interpret data. In studies of microbes, metagenomic investigations have expanded known diversity by several orders of magnitude (Edwards *et al.* 2006; Sogin *et al.* 2006), and preliminary results from metazoan phyla have indicated similarly huge numbers of uncharacterised taxa (Fonseca *et al.* Submitted). Next-generation sequencing looks set to revolutionise our understanding of nematode diversity and biogeography.

Appendix I: Electronic Appendices on CD

The supplementary CD contains the following files:

FASTA file containing all SSU sequences amplified during this study:

<Enoplid_SSU_sequences.FASTA>

FASTA file containing all LSU sequences amplified during this study:

<Enoplid_SSU_sequences.FASTA>

FASTA file containing all Cox1 sequences amplified during this study:

<Enoplid_Cox1_sequences.FASTA>

ARB Database used to build large nematode tree (1438 taxa), containing SSU gene alignment: <ARB_LargeDB.arb>

ARB Database used to build small Enoplid/Dorylaimid tree (563 taxa), containing SSU gene alignment: <ARB_SmallDB.arb>

ARB Database used to build LSU phylogeny (433 taxa), containing LSU gene alignment:

<ARB_LSU_DB.arb>

Cox1 gene alignment:

<Cox1_alignment.FASTA>

Taxa list and ARB codes used to build smaller Enoplid/Dorylaimid phylogenies:

<EnopTree_TaxaList.xls>

Best scoring maximum likelihood trees obtained during topological tests: unannotated tree files (text files) and annotated tree graphics (.PNG files) included in folders named according to RAxML job number.

Appendix II: Supplementary Tables

Table A2.1: List of Enoplid specimens isolated during this investigation, including alphanumeric molecular ID, taxonomic identification, sample site, and slide ID (used to label video capture files). Parentheses indicate uncertain genus assignments. Gene sequences obtained from each specimen are listed after taxonomic information; Shaded boxes indicate sequences that were eliminated from trees, based on short length or redundancy (e.g. duplicates).

Sequence ID	Taxonomic ID	Slide ID	Sample Core	Sex	Comments	SSU	LSU	Cox1
AUK 1	<i>Tripyloides</i>	1(1)	3					Cox1 (393bps)
AUK 7	<i>Tripyloides</i>	19(2)	3				D2D3 (642 bps)	
AUK 10	<i>Viscosia</i>	22(1)	3			SSU (1611 bps)	D2D3 (613 bps)	
AUK 13	<i>Calyptronema</i>	29(2)	3			SSU (1625 bps)	D2D3 (611 bps)	Cox1 (393bps)
AUK 14	<i>Oxystomina</i>	30(1)	3			SSU (1638 bps)	D2D3 (671 bps)	
AUK 23	<i>Oncholaimus</i>	9(4)	2			SSU (1629 bps)	D2D3 (646 bps)	Cox1 (392bps)
AUK 35	<i>Oncholaimus</i>	1(3)	2	Male		SSU (1618 bps)	D2D3 (591 bps)	
AUK 36	<i>Oncholaimus</i>	1(4)	2			SSU (1638 bps)	D2D3 (599 bps)	
AUK 45	<i>Tripyloides</i>	7(5)	2	Male		SSU (1665 bps)	D2D3 (677 bps)	
BAUK 9	<i>Oxystomina</i>	6(9)	2			SSU (1631 bps)	D2D3 (660 bps)	
BCA 1	<i>Syringolaimus</i>	1(1)	BC 470			SSU (1635 bps)	D2D3 (659 bps)	
BCA 2	<i>Syringolaimus</i>	4(2)	BC 470	Male		SSU (1635 bps)	D2D3 (662 bps)	
BCA 3	<i>Pareurystomina</i>	5(1)	BC 470			SSU (1632 bps)	D2D3 (599 bps)	
BCA 5	<i>Syringolaimus</i>	6(5)	BC 470			SSU (1635 bps)	D2D3 (659 bps)	
BCA 6	<i>Syringolaimus</i>	7(2)	BC 470			SSU (1635 bps)	D2D3 (658 bps)	
BCA 10	<i>Trefusia</i>	12(2)	BC 470			SSU (1654 bps)	D2D3 (678 bps)	
BCA 12	<i>Halalaimus</i>	1(3)	BC 476			SSU (1624 bps)	D2D3 (615 bps)	
BCA 14	<i>Mesacanthion/ Paramesacanthion</i>	3(2)	BC 476		Small setae near head anterior	SSU (1636 bps)	D2D3 (621 bps)	
BCA 15	<i>Oxystomina</i>	4(5)	BC 476			SSU (1610 bps)	D2D3 (657 bps)	
BCA 16	<i>Halalaimus</i>	5(3)	BC 476			SSU (1623 bps)	D2D3 (587 bps)	

BCA 17	<i>Halalaimus</i>	6(2)	BC 476	Male		SSU (1618 bps)	D2D3 (617 bps)	
BCA 19	<i>Mesacanthion/ Paramesacanthion</i>	8(2)	BC 476		Small setae near head anterior	SSU (1640 bps)	D2D3 (630 bps)	
BCA 20	Phanodermatidae	8(5)	BC 476			SSU (1642 bps)	D2D3 (642 bps)	
BCA 21	<i>Oxystomina</i>	12(1)	BC 476			SSU (1594 bps)	D2D3 (674 bps)	
BCA 22	<i>Oxystomina</i>	14(1)	BC 476			SSU (1640 bps)	D2D3 (648 bps)	
BCA 23	<i>Oxystomina</i>	23(1)	BC 476			SSU (1621 bps)	D2D3 (646 bps)	
BCA 25	<i>Halalaimus</i>	1(4)	BC 477			SSU (1620 bps)	D2D3 (580 bps)	
BCA 26	<i>Oncholaimus</i>	2(1)	BC 477					Cox1 (385bps)
BCA 31	<i>Syringolaimus</i>	4(3)	BC 477	Male		SSU (1635 bps)	D2D3 (662 bps)	
BCA 32	Phanodermatidae	4(4)	BC 477			SSU (1641 bps)	D2D3 (637 bps)	
BCA 35	<i>Oxystomina</i>	6(5)	BC 477	Male	Big amphid, mix of circle/slit	SSU (1596 bps)	D2D3 (662 bps)	
BCA 37	Phanodermatidae	8(1)	BC 477			SSU (1640 bps)	D2D3 (646 bps)	
BCA 38	<i>Halalaimus</i>	8(4)	BC 477			SSU (1584 bps)	D2D3 (617 bps)	
BCA 40	<i>Bathyeurystomina</i>	11(1)	BC 477	Male	Winged supplements			Cox1 (393bps)
BCA 41	<i>Syringolaimus</i>	12(3)	BC 477			SSU (1635 bps)	D2D3 (659 bps)	
BCA 42	<i>Oxystomina</i>	13(2)	BC 477	Male		SSU (1642 bps)	D2D3 (646 bps)	
BCA 47	<i>Syringolaimus</i>	19(1)	BC 477			SSU (1635 bps)	D2D3 (662 bps)	
BUS 1	<i>Oncholaimus</i>	1(3)	1	Male		SSU (1617 bps)	D2D3 (635 bps)	Cox1 (393bps)
BUS 2	<i>Oncholaimus</i>	3(5)	1	Male		SSU (1613 bps)	D2D3 (636 bps)	Cox1 (393bps)
BUS 3	<i>Oncholaimus</i>	7(1) a	1	Male		SSU (1597 bps)	D2D3 (595 bps)	Cox1 (393bps)
BUS 4	<i>Oncholaimus</i>	7(2) b	1	Male		SSU (1610 bps)	D2D3 (633 bps)	Cox1 (368bps)
BUS 5	<i>Oncholaimus</i>	12(3)	1			SSU (1617 bps)	D2D3 (616 bps)	Cox1 (393bps)
BUS 7	<i>Oncholaimus</i>	19(4)	1	Male		SSU (1617 bps)	D2D3 (610 bps)	Cox1 (393bps)
BUS 15	<i>Tripyloides</i>	26(1) a	1		Different tail shape	SSU (1691 bps)	D2D3 (691 bps)	
BUS 21	<i>Anoplostoma</i>	11(5)	2			SSU (1623 bps)	D2D3 (640 bps)	
Cr 1	Thoracostomopsidae	1(1)	15773#21			SSU (1599 bps)	D2D3 (634 bps)	Cox1 (393bps)

Cr 3	<i>Phanodermopsis</i>	5(1)	15773#21			SSU (1630 bps)	D2D3 (638 bps)	Cox1 (369bps)
Cr 4	<i>Halalaimus</i>	7(2)	15773#21					Cox1 (362bps)
Cr 7	<i>Halalaimus</i>	2(2)	15775#37			SSU (1602 bps)	D2D3 (610 bps)	
Cr 9	<i>Halalaimus</i>	6(4)	15775#37			SSU (1618 bps)	D2D3 (607 bps)	
Cr 11	<i>Halalaimus</i>	6(1)	15772#2			SSU (1623 bps)	D2D3 (594 bps)	
Cr 13	<i>Halalaimus</i>	8(2)	15772#2			SSU (1624 bps)	D2D3 (598 bps)	
Cr 18 b	<i>Mesacanthion/ Paramesacanthion</i>	1(2)	15773#27			SSU (1604 bps)	D2D3 (636 bps)	
Cr 19 b	<i>Phanodermopsis</i>	2(3)	15773#27			SSU (1620 bps)	D2D3 (641 bps)	
Cr 20 b	<i>Halalaimus</i>	2(5)	15773#27			SSU (1585 bps)	D2D3 (597 bps)	
Cr 21 b	Comesomatidae	3(1)	15773#27		(not an Enoplid)	SSU (1590 bps)	D2D3 (646 bps)	
Cr 24 b	<i>Metaparoncholaimus/Meyersia</i>	5(3)	15773#27		Subventral teeth equal	SSU (1525 bps)	D2D3 (587 bps)	Cox1 (393bps)
Cr 26	Phanodermatidae	5(5)	15773#27			SSU (1598 bps)	D2D3 (644 bps)	
Cr 33	<i>Phanodermopsis</i>	3(3)	15773#18			SSU (1601 bps)	D2D3 (639 bps)	
Cr 34	<i>Mesacanthion/ Paramesacanthion</i>	3(4)	15773#18			SSU (1627 bps)	D2D3 (620 bps)	
Cr 35	<i>Halalaimus</i>	4(3)	15773#18	Male		SSU (1618 bps)	D2D3 (555 bps)	
Cr 38	Anticomidae	6(4)	15773#18			SSU (1607 bps)	D2D3 (648 bps)	
Cr 54	<i>Phanodermopsis</i>	1(5)	15775#3			SSU (1613 bps)	D2D3 (637 bps)	
Cr 55	<i>Halalaimus</i>	2(3)	15775#3	Male		SSU (1615 bps)	D2D3 (587 bps)	
Cr 56	<i>Phanodermopsis</i>	2(5)	15775#3			SSU (1624 bps)	D2D3 (652 bps)	
Cr 59	<i>Halalaimus</i>	7(1)	15775#3			SSU (1557 bps)	D2D3 (580 bps)	Cox1 (360bps)
Cr 60	<i>Halalaimus</i>	1(5)	15775#37			SSU (1618 bps)	D2D3 (597 bps)	
Cr 61	<i>Halalaimus</i>	2(4)	15775#37			SSU (1594 bps)	D2D3 (596 bps)	
Cr 62	<i>Halalaimus</i>	2(5)	15775#37	Male		SSU (1610 bps)	D2D3 (602 bps)	
Cr 63	<i>Halalaimus</i>	3(1)	15775#37	Male		SSU (1620 bps)	D2D3 (622 bps)	
Cr 64	<i>Halalaimus</i>	3(5)	15775#37	Male		SSU (1618 bps)	D2D3 (578 bps)	

Cr 66	<i>Phanodermopsis</i>	4(4)	15775#37			SSU (1620 bps)	D2D3 (700 bps)	Cox1 (393bps)
Cr 68	<i>Phanodermopsis</i>	5(1)	15775#37	Male		SSU (1624 bps)	D2D3 (701 bps)	Cox1 (393bps)
Cr 72a	<i>Halalaimus</i>	1(3)	15775#32	Male		SSU (1610 bps)	D2D3 (610 bps)	
Cr 73a	<i>Chaetonema</i>	2(4)	15775#32	Male		SSU (1647 bps)	D2D3 (626 bps)	
Cr 74a	<i>Halalaimus</i>	2 (1/5)	15775#25/ 15775#32	(Male)	(Sample site uncertain--tubes mixed up)	SSU (1617 bps)	D2D3 (619 bps)	
Cr 76a	<i>Chaetonema</i>	3(2)	15775#25	Male		SSU (1634 bps)	D2D3 (676 bps)	
Cr 77a	<i>Oxystomina</i>	4(3)	15775#32	Male	Long oval amphids	SSU (1635 bps)	D2D3 (716 bps)	
Cr 78a	<i>Bathyeurystomina</i>	4(3)	15775#25			SSU (1615 bps)	D2D3 (674 bps)	
Cr 80a	<i>Oxystomina</i>	4(5)	15775#25		Side view of amphids	SSU (1537 bps)	D2D3 (712 bps)	
Cr 82a	<i>Halalaimus</i>	5(4)	15775#25			SSU (1610 bps)	D2D3 (624 bps)	
Cr 83a	<i>Chaetonema</i>	5(5)	15775#25			SSU (1621 bps)	D2D3 (682 bps)	
Cr 85a	<i>Halalaimus</i>	7(7)/1(4)	15775#25/ 15775#33		(Sample site uncertain--tubes mixed up)	SSU (1612 bps)	D2D3 (611 bps)	
Cr 71b	<i>Phanodermopsis</i>	1(1)	15775#25			SSU (1612 bps)	D2D3 (688 bps)	
Cr 72b	Phanodermatidae	1(3)	15775#25	Male		SSU (1611 bps)	D2D3 (681 bps)	Cox1 (393bps)
Cr 73b	<i>Halalaimus</i>	1(5)	15775#25			SSU (1609 bps)	D2D3 (629 bps)	
Cr 74b	<i>Halalaimus</i>	2 (1/5)	15775#25/ 15775#32	(Male)	(Sample site uncertain--tubes mixed up)	SSU (1608 bps)	D2D3 (633 bps)	
Cr 75b	<i>Halalaimus</i>	2(4)/3(5)	15775#25/ 15775#32	(Male)	(Sample site uncertain--tubes mixed up)	SSU (1609 bps)	D2D3 (630 bps)	
Cr 76b	<i>Oxystomina</i>	3(6)	15775#32			SSU (1614 bps)	D2D3 (703 bps)	
Cr 77b	<i>Halalaimus</i>	3(4)	15775#25			SSU (1611 bps)	D2D3 (621 bps)	
Cr 80b	<i>Bathyeurystomina</i>	7(4)	15775#32			SSU (1608 bps)	D2D3 (640 bps)	
Cr 82b	Thoracostomopsidae	1(1)	15775#33			SSU (1634 bps)	D2D3 (583 bps)	Cox1 (393bps)
Cr 83b	<i>Halalaimus</i>	1(2)	15775#33			SSU (1577 bps)	D2D3 (598 bps)	
Cr 84b	<i>Chaetonema</i>	1(3)	15775#33		Female	SSU (1642 bps)	D2D3 (713 bps)	

Cr 85b	<i>Halalaimus</i>	7(7)/1(4)	15775#25/ 15775#33		(Sample site uncertain--tubes mixed up)	SSU (1623 bps)	D2D3 (624 bps)	
Cr 86	<i>Halalaimus</i>	2(4)	15775#33			SSU (1588 bps)	D2D3 (578 bps)	
Cr 87	<i>Oxystomina</i>	2(6)	15775#33	Male		SSU (1602 bps)	D2D3 (720 bps)	
DBA 1	<i>Enoploides</i>	1(2)	1			SSU (1631 bps)	D2D3 (667 bps)	Cox1 (393bps)
DBA 2	<i>Enoploides</i>	1(3)	1			SSU (1631 bps)	D2D3 (638 bps)	Cox1 (393bps)
DBA 3	<i>Enoploides</i>	1(5)	1			SSU (1620 bps)	D2D3 (619 bps)	
DBA 4	<i>Oncholaimus</i>	2(2)	1		No tail video captured (V.C.)	SSU (1640 bps)	D2D3 (653 bps)	Cox1 (393bps)
DBA 5	<i>Enoploides</i>	2(5)	1			SSU (1631 bps)	D2D3 (667 bps)	Cox1 (393bps)
DBA 6	<i>Enoploides</i>	3(1)	1			SSU (1620 bps)	D2D3 (580 bps)	Cox1 (393bps)
DBA 7	<i>Enoploides</i>	3(5)	1			SSU (1631 bps)	D2D3 (667 bps)	Cox1 (362bps)
DBA 21	<i>Enoplus</i>	7(1)	2			SSU (1644 bps)	D2D3 (643 bps)	
HCL 2	Oncholaimidae	2(3)	1	Male		SSU (1642 bps)	D2D3 (638 bps)	
HCL 5	Oncholaimidae	5(1)	1		No tail V.C.	SSU (1630 bps)	D2D3 (638 bps)	
HCL 7	Oncholaimidae	6(4)	1			SSU (1630 bps)	D2D3 (600 bps)	
HCL 9	<i>Viscosia</i>	7(3)	1	Male		SSU (1630 bps)	D2D3 (638 bps)	
HCL 10	<i>Viscosia</i>	8(4)	1			SSU (1630 bps)	D2D3 (638 bps)	
HCL 11	<i>Viscosia</i>	8(5)	1			SSU (1630 bps)	D2D3 (638 bps)	
HCL 12	Oncholaimidae	9(1)	1	Male		SSU (1637 bps)	D2D3 (600 bps)	
HCL 15	<i>Viscosia</i>	10(4)	1	Male		SSU (1637 bps)	D2D3 (638 bps)	
HCL 20	<i>Oxystomina</i>	18(1)	1	Male		SSU (1641 bps)	D2D3 (667 bps)	
HCL 21	<i>Oxystomina</i>	3(5)	2			SSU (1641 bps)	D2D3 (667 bps)	
HCL 23	Oncholaimidae	5(1)	2		No tail V.C.	SSU (1630 bps)	D2D3 (638 bps)	Cox1 (393bps)
HCL 24	<i>Viscosia</i>	6(3)	2	Male	Small subventral tooth, double tipped (V. viscosia?)	SSU (1630 bps)	D2D3 (638 bps)	
HCL 27	<i>Viscosia</i>	7(3)	2			SSU (1641 bps)	D2D3 (638 bps)	

HCL 32	<i>Oxystomina</i>	12(1)	2	Male		SSU (1641 bps)	D2D3 (667 bps)	
HUK 1	Oncholaimidae	2(4)	1		Food in mouth; hard to see teeth	SSU (1611 bps)	D2D3 (610 bps)	Cox1 (381bps)
JCC 4	<i>Anticoma</i>	1(4)	JC27-22#1					Cox1 (393bps)
JCC 23	Phanodermatidae	4(4)	JC27-29			SSU (1643 bps)	D2D3 (639 bps)	
JCC 29	Anticomidae	9(1)	JC27-29		Can't see mouth (too small) Long tail	SSU (1650 bps)	D2D3 (638 bps)	
JCC 37	<i>Enoplolaimus</i>	4(5)	JC27-45		No tail v.c.			Cox1 (393bps)
JCC 52	Phanodermatidae	11(5)	JC27-45		More setae than usual--Two under amphid, and somatic	SSU (1639 bps)	D2D3 (608 bps)	Cox1 (393bps)
JCC 59	<i>Phanodermopsis</i>	2(5)	JC27-25#2			SSU (1643 bps)	D2D3 (636 bps)	Cox1 (355bps)
JCC 79	<i>Anticoma</i>	4(5)	JC27-43					Cox1 (358bps)
JCC 89	<i>Phanodermopsis</i>	9(2)	JC27-43			SSU (1641 bps)	D2D3 (638 bps)	
LCL 1	<i>Trefusia</i>	1(2)	2			SSU (1656 bps)	D2D3 (676 bps)	
LCL 2	<i>Trefusia</i>	1(5)	2			SSU (1656 bps)	D2D3 (676 bps)	
LCL 3	<i>Trefusia</i>	2(1)	2			SSU (1656 bps)	D2D3 (676 bps)	Cox1 (351bps)
LCL 4	<i>Trefusia</i>	3(1)	2		No tail V.C.'d	SSU (1656 bps)	D2D3 (676 bps)	
LCL 5	<i>Trefusia</i>	3(5)	2			SSU (1697 bps)	D2D3 (638 bps)	Cox1 (393bps)
LCL 7	<i>Trefusia</i>	1(3)	2	Male		SSU (1656 bps)	D2D3 (676 bps)	Cox1 (393bps)
LCL 8	<i>Trefusia</i>	2(1)	2			SSU (1655 bps)	D2D3 (676 bps)	
LCL 9	<i>Tripyloides</i>	2(2)	2	Male		SSU (1697 bps)	D2D3 (633 bps)	Cox1 (393bps)
LCL 19	<i>Bathylaimus</i>	6(1)	2	Male		SSU (1692 bps)	D2D3 (636 bps)	Cox1 (393bps)
LCL 20	Oncholaimidae (Viscosia)	9(1)	2			SSU (1637 bps)	D2D3 (638 bps)	
LCL 21	<i>Tripyloides</i>	10(4)	2			SSU (1697 bps)	D2D3 (628 bps)	Cox1 (393bps)
LUK 1	<i>Viscosia</i>	8(1)	2			SSU (1634 bps)	D2D3 (616 bps)	
LUK 3	<i>Viscosia</i>	19(1)	2		<i>V. viscosia</i> or <i>V. elegans</i>	SSU (1630 bps)	D2D3 (613 bps)	
LUK 6	<i>Halalaimus</i>	9(1)	3	Male		SSU (1588 bps)	D2D3 (590 bps)	

LUK 7	<i>Calyptronema</i>	17(1)	3			SSU (1626 bps)	D2D3 (611 bps)	Cox1 (393bps)
LUK 12	<i>Calyptronema</i>	25(3)	3			SSU (1626 bps)	D2D3 (620 bps)	Cox1 (393bps)
NAR 1	<i>Enoplolaimus</i>	1(1)	1			SSU (1625 bps)	D2D3 (637 bps)	Cox1 (393bps)
NAR 2	<i>Enoplolaimus</i>	3(1)	1			SSU (1627 bps)	D2D3 (629 bps)	Cox1 (393bps)
NAR 4	<i>Oncholaimus</i>	9(1)	1	Male		SSU (1610 bps)	D2D3 (628 bps)	
NAR 5	<i>Enoplolaimus</i>	11(1)	1	Male		SSU (1621 bps)	D2D3 (665 bps)	Cox1 (393bps)
NAR 6	<i>Chaetonema</i>	11(2)	1			SSU (1630 bps)	D2D3 (662 bps)	Cox1 (393bps)
NAR 7	<i>Oncholaimus</i>	12(2)	1	Male		SSU (1610 bps)	D2D3 (631 bps)	Cox1 (359bps)
NAR 8	<i>Enoplolaimus</i>	13(1) a	1			SSU (1620 bps)	D2D3 (638 bps)	Cox1 (393bps)
NAR 9	<i>Enoplolaimus</i>	13(2) b	1	Male		SSU (1627 bps)	D2D3 (634 bps)	Cox1 (393bps)
NAR 11	<i>Bathylaimus</i>	14(4)	1	Male		SSU (1674 bps)	D2D3 (634 bps)	Cox1 (393bps)
NAR 14	<i>Bathylaimus</i>	16(1)	1	Male		SSU (1684 bps)	D2D3 (680 bps)	Cox1 (393bps)
NAR 15	<i>Bathylaimus</i>	18(1)	1			SSU (1674 bps)	D2D3 (678 bps)	
NAR 16	<i>Oncholaimus</i>	1(4)	2			SSU (1610 bps)	D2D3 (607 bps)	Cox1 (393bps)
NAR 20	<i>Bathylaimus</i>	7(1)	2			SSU (1690 bps)	D2D3 (671 bps)	
NUS 1	<i>Pareurystomina</i>	1(1)	1			SSU (1540 bps)	D2D3 (611 bps)	
NUS 2	<i>Oncholaimus</i>	2(1) a	1			SSU (1617 bps)	D2D3 (643 bps)	Cox1 (393bps)
NUS 3	<i>Oxystomina</i>	2(2) b	1			SSU (1603 bps)	D2D3 (678 bps)	
NUS 4	<i>Oncholaimus</i>	2(3) c	1	Male		SSU (1547 bps)	D2D3 (647 bps)	Cox1 (393bps)
NUS 5	<i>Oncholaimus</i>	2(6) d	1	Male		SSU (1617 bps)	D2D3 (633 bps)	Cox1 (393bps)
NUS 6	<i>Oncholaimus</i>	3(4) a	1	Male		SSU (1617 bps)	D2D3 (638 bps)	Cox1 (392bps)
NUS 7	<i>Oncholaimus</i>	3(5) b	1			SSU (1617 bps)	D2D3 (635 bps)	Cox1 (393bps)
NUS 10	<i>Oncholaimus</i>	5(3)	1					Cox1 (393bps)
NUS 11	<i>Bathylaimus</i>	7(2) a	1			SSU (1691 bps)	D2D3 (695 bps)	
NUS 14	<i>Tripylodes</i>	11(2) b	1			SSU (1689 bps)	D2D3 (709 bps)	
NUS 21	<i>Oxystomina</i>	13(7) c	1	Male		SSU (1640 bps)	D2D3 (705 bps)	Cox1 (393bps)
NUS 40	<i>Anoplostoma</i>	9(4)	2			SSU (1346 bps)	D2D3 (644 bps)	

NUS 41	<i>Tripyloides</i>	11(1)	2			SSU (1655 bps)	D2D3 (701 bps)	
OUS 1	Oncholaimidae	1(1) a	1			SSU (1630 bps)	D2D3 (628 bps)	Cox1 (393bps)
OUS 2	<i>Oncholaimus</i>	1(2) b	1			SSU (1628 bps)	D2D3 (622 bps)	Cox1 (393bps)
OUS 3	<i>Anoplostoma</i>	3(1)	1	Male		SSU (1630 bps)	D2D3 (640 bps)	Cox1 (393bps)
OUS 4	<i>Halalaimus</i>	4(1)	1	Male		SSU (1595 bps)	D2D3 (579 bps)	
OUS 5	<i>Anoplostoma</i>	5(1)	1			SSU (1623 bps)	D2D3 (634 bps)	Cox1 (393bps)
OUS 6	<i>Anoplostoma</i>	6(3) a	1		Live nems visible in vivo	SSU (1633 bps)	D2D3 (634 bps)	Cox1 (393bps)
OUS 7	<i>Anoplostoma</i>	6(4) b	1	Male		SSU (1633 bps)	D2D3 (634 bps)	
OUS 8	<i>Anoplostoma</i>	8(3)	1		Live nems visible in vivo	SSU (1617 bps)	D2D3 (634 bps)	
OUS 9	Oncholaimidae	1(5)	1a			SSU (1632 bps)	D2D3 (624 bps)	
OUS 10	<i>Enoploides</i>	3(1)	1a			SSU (1610 bps)	D2D3 (642 bps)	
OUS 14	Oncholaimidae	4(2)	1a	Male		SSU (1630 bps)	D2D3 (619 bps)	Cox1 (319bps)
OUS 21	Oncholaimidae	10(4)	1a			SSU (1629 bps)	D2D3 (620 bps)	
OUS 22	<i>Halalaimus</i>	11(2)	1a			SSU (1605 bps)	D2D3 (632 bps)	
PPA 1	<i>Enoplolaimus</i>	1(1)	1	Male				Cox1 (393bps)
PPA 3	<i>Enoplolaimus</i>	1(4)	1	Male				Cox1 (393bps)
PPA 7	<i>Enoplus</i>	2(3)	1			SSU (1646 bps)	D2D3 (639 bps)	Cox1 (393bps)
SBA 1	<i>Halalaimus</i>	1(1)	1	Male		SSU (1587 bps)	D2D3 (575 bps)	
SBA 2	<i>Oncholaimus</i>	2(3)	1	Male		SSU (1640 bps)	D2D3 (636 bps)	Cox1 (393bps)
SBA 3	<i>Oncholaimus</i>	3(4)	1	Male		SSU (1617 bps)	D2D3 (636 bps)	Cox1 (393bps)
SBA 5	<i>Oncholaimus</i>	4(4)	1	Male		SSU (1636 bps)	D2D3 (636 bps)	Cox1 (393bps)
SBA 7	Thoracostomopsidae	7(1)	1		New genus?			Cox1 (393bps)
SBA 8	Thoracostomopsidae	7(2)	1		New genus?			Cox1 (393bps)
SBA 9	Thoracostomopsidae	7(4)	1	Male	New genus?			Cox1 (393bps)
SBA 10	<i>Halalaimus</i>	1(1)	2	Male		SSU (1624 bps)	D2D3 (575 bps)	
SBA 12	<i>Halalaimus</i>	2(1)	2			SSU (1619 bps)	D2D3 (575 bps)	

SBA 14	Thoracostomopsidae	3(1)	2	Male	New genus?			Cox1 (393bps)
SBA 13	Thoracostomopsidae	2(2)	2	Male	New genus? Long spicule and large supplement	SSU (1640 bps)	D2D3 (631 bps)	Cox1 (393bps)
SBN 2	<i>Viscosia</i>	2(2)	1			SSU (1638 bps)	D2D3 (633 bps)	
SBN 3	<i>Oxystomina</i>	2(3)	1			SSU (1640 bps)	D2D3 (665 bps)	
SBN 4	<i>Viscosia</i>	2(4)	1			SSU (1631 bps)	D2D3 (637 bps)	
SUS 1	Enoplolaimus	1(1) a	1			SSU (1627 bps)	D2D3 (643 bps)	Cox1 (393bps)
SUS 2	Enoplolaimus	1(2) b	1			SSU (1625 bps)	D2D3 (653 bps)	Cox1 (393bps)
SUS 6	Enoplolaimus	3(1) a	1			SSU (1598 bps)	D2D3 (651 bps)	Cox1 (393bps)
SUS 10	Enoplolaimus	4(2) b	1	Male		SSU (1627 bps)	D2D3 (660 bps)	Cox1 (393bps)
SUS 15	Enoplolaimus	7(3)	1			SSU (1627 bps)	D2D3 (660 bps)	Cox1 (393bps)
SUS 21	Enoplolaimus	10(4) b	1	Male		SSU (1625 bps)	D2D3 (638 bps)	Cox1 (393bps)
SUS 27	Oncholaimidae	1(3)	2			SSU (1489 bps)	D2D3 (655 bps)	
TCR 1	<i>Halalaimus</i>	1(2)	518 nem			SSU (1573 bps)	D2D3 (584 bps)	
TCR 3	<i>Halalaimus</i>	2(5)	518 nem			SSU (1578 bps)	D2D3 (588 bps)	
TCR 12	Oncholaimidae	11(1)	518 nem		New genus?	SSU (1506 bps)	D2D3 (611 bps)	
TCR 17	Oncholaimidae	13(1)	518 nem		New genus?	SSU (1621 bps)	D2D3 (603 bps)	
TCR 21	<i>Oxystomina</i>	20(3)	518 nem			SSU (1634 bps)	D2D3 (666 bps)	
TCR 26	<i>Halalaimus</i>	3(5)	112 nem			SSU (1588 bps)	D2D3 (617 bps)	
TCR 41	<i>(Bathyeurystomina)</i>	1(6)	221 nem					Cox1 (393bps)
TCR 42	<i>Oncholaimidae</i>	2(3)	221 nem			SSU (1559 bps)	D2D3 (516 bps)	
TCR 44	<i>Anticoma</i>	4(3)	221 nem			SSU (1612 bps)	D2D3 (637 bps)	
TCR 68	<i>Oxystomina</i>	5(1)	312 nem			SSU (1602 bps)	D2D3 (665 bps)	
TCR 69	Oncholaimidae	5(3)	312 nem			SSU (1598 bps)	D2D3 (632 bps)	Cox1 (297bps)
TCR 70	Phanodermatidae	6(1)	312 nem			SSU (1617 bps)	D2D3 (640 bps)	Cox1 (393bps)
TCR 74	Thoracostomopsidae	9(3)	312 nem			SSU (1614 bps)	D2D3 (660 bps)	
TCR 75	Phanodermatidae	9(4)	312 nem			SSU (1609 bps)	D2D3 (671 bps)	Cox1 (393bps)
TCR 78	<i>Phanodermopsis</i>	10(5)	312 nem			SSU (1402 bps)	D2D3 (669 bps)	Cox1 (393bps)

TCR 80	<i>Phanodermopsis</i>	11(4)	312 nem			SSU (1623 bps)	D2D3 (680 bps)	
TCR 81	<i>Bathyeurystomina</i>	12(1)	312 nem			SSU (1566 bps)	D2D3 (580 bps)	Cox1 (393bps)
TCR 82	Comesomatidae	12(3)	312 nem		(not an Enoplid)	SSU (1598 bps)	D2D3 (640 bps)	
TCR 87	<i>Bathylaimus</i>	17(2)	312 nem			SSU (1685 bps)	D2D3 (689 bps)	Cox1 (393bps)
TCR 89	<i>Litinium</i>	21(1)	312 nem	Male		SSU (1623 bps)	D2D3 (663 bps)	Cox1 (390bps)
TCR 90	<i>Litinium</i>	21(3)	312 nem	Male		SSU (1628 bps)	D2D3 (664 bps)	
TCR 91	<i>Oxystomina</i>	22(1)	312 nem			SSU (1613 bps)	D2D3 (660 bps)	
TCR 93	<i>Halalaimus</i>	3(2)	418 nem			SSU (1618 bps)	D2D3 (632 bps)	
TCR 94	<i>Mesacanthion/ Paramesacanthion</i>	3(3)	418 nem			SSU (1615 bps)	D2D3 (628 bps)	
TCR 97	<i>Cricohalalaimus</i>	6(3)	418 nem	Male	10-12 Cephalic setae + 2 somatic setae, slit like amphid, punctuated cuticle	SSU (1540 bps)	D2D3 (622 bps)	
TCR 102	Thoracostomopsidae	15(2)	418 nem			SSU (1622 bps)	D2D3 (646 bps)	
TCR 106	<i>Bathyeurystomina</i>	1(5)	617 nem			SSU (1594 bps)	D2D3 (622 bps)	
TCR 108	<i>Phanodermopsis</i>	3(1)	617 nem			SSU (1626 bps)	D2D3 (639 bps)	
TCR 109	<i>Bathyeurystomina</i>	5(1)	617 nem			SSU (1625 bps)	D2D3 (602 bps)	
TCR 112	<i>Halalaimus</i>	7(1)	617 nem	Male		SSU (1577 bps)	D2D3 (603 bps)	
TCR 114	<i>Dolicholaimus</i>	8(4)	617 nem		All teeth seem single; tail clavate	SSU (1637 bps)	D2D3 (631 bps)	
TCR 125	<i>Rhabdocoma</i>	2(3)	712 nem			SSU (1615 bps)	D2D3 (664 bps)	
TCR 128	<i>Bathyeurystomina</i>	4(1)	712 nem			SSU (1424 bps)	D2D3 (633 bps)	
TCR 130	<i>Rhabdocoma</i>	4(5)	712 nem			SSU (1615 bps)	D2D3 (660 bps)	
TCR 131	<i>Halalaimus</i>	5(1)	712 nem	Male		SSU (1577 bps)	D2D3 (619 bps)	
TCR 139	<i>Rhabdocoma</i>	7(5)	712 nem			SSU (1358 bps)	D2D3 (656 bps)	
TCR 141	<i>(Cephalanticoma)</i>	9(3)	712 nem		Teeth in mouth, long tail	SSU (1641 bps)	D2D3 (638 bps)	

TCR 143	<i>Enoplolaimus/</i> <i>Mesacanthion</i>	11(4)	712 nem			SSU (1640 bps)	D2D3 (616 bps)	
TCR 145	<i>Syringolaimus</i>	13(5)	712 nem		Oesophageal bulb present	SSU (1597 bps)	D2D3 (652 bps)	
TCR 148	<i>Phanodermopsis</i>	15(2)	712 nem			SSU (1605 bps)	D2D3 (652 bps)	
TCR 149	Anticomidae	16(1)	712 nem		Teeth in mouth? Small specimen, tail broken	SSU (1617 bps)	D2D3 (638 bps)	
TCR 152	<i>Phanodermopsis</i>	18(1)	712 nem			SSU (1611 bps)	D2D3 (638 bps)	
TCR 153	Phanodermatidae	1(2)	817 nem			SSU (1622 bps)	D2D3 (655 bps)	
TCR 158	<i>Mesacanthion/</i> <i>Paramesacanthion</i>	3(1)	817 nem			SSU (1598 bps)	D2D3 (658 bps)	
TCR 173	Phanodermatidae	11(1)	817 nem			SSU (1603 bps)	D2D3 (659 bps)	
TCR 180	<i>Oxystomina</i>	4(3)	856 nem			SSU (1622 bps)	D2D3 (667 bps)	
TCR 184	(<i>Epicanthion</i>)	5(4)	856 nem		Striated lips. Seems to be cuticle btwn mandible bars	SSU (1563 bps)	D2D3 (667 bps)	
TCR 188	(<i>Phanodermopsis</i>)	9(4)	856 nem			SSU (1604 bps)	D2D3 (655 bps)	
TCR 189	<i>Litinium</i>	9(5)	856 nem	Male				Cox1 (393bps)
TCR 190	<i>Phanodermopsis</i>	10(2)	856 nem			SSU (1644 bps)	D2D3 (638 bps)	Cox1 (393bps)
TCR 192	<i>Leptosomatides</i>	10(5)	856 nem			SSU (1639 bps)	D2D3 (638 bps)	
TCR 197	<i>Anticoma</i>	12(2)	856 nem			SSU (1650 bps)	D2D3 (650 bps)	Cox1 (393bps)
TCR 202	<i>Oxystomina</i>	15(1)	856 nem	Male		SSU (1605 bps)	D2D3 (667 bps)	
TCR 205	<i>Litinium</i>	19(1)	856 nem			SSU (1628 bps)	D2D3 (663 bps)	
TCR 206	<i>Synonchus</i>	1(1)	861 nem			SSU (1646 bps)	D2D3 (629 bps)	
TCR 212	(<i>Oxystomina</i>)	3(2)	861 nem		Can't see amphid. 6 (single) + 4 setae	SSU (1624 bps)	D2D3 (666 bps)	
TCR 216	(<i>Phanodermopsis</i>)	5(1)	861 nem	Male		SSU (1393 bps)	D2D3 (637 bps)	

TCR 230	<i>Thalassoalaimus</i>	10(5)	861 nem		Side view of amphids, end of tail cuticularised	SSU (1607 bps)	D2D3 (659 bps)	
WUS 1	<i>Enoplolaimus</i>	3(4)	1			SSU (1620 bps)	D2D3 (636 bps)	Cox1 (393bps)
WUS 2	<i>Enoplolaimus</i>	10(1)	1	Male		SSU (1624 bps)	D2D3 (631 bps)	Cox1 (393bps)
WUS 3	<i>Enoplolaimus/ Mesacanthion</i>	12(1)	1			SSU (1625 bps)	D2D3 (636 bps)	Cox1 (367bps)
WUS 4	<i>Enoplolaimus</i>	13(5)	1		Punctuated Cuticle, no tail	SSU (1588 bps)	D2D3 (636 bps)	Cox1 (393bps)
WUS 5	<i>Enoplolaimus</i>	14(3) a	1		No tail	SSU (1627 bps)	D2D3 (635 bps)	Cox1 (393bps)
WUS 6	<i>Enoplolaimus/ Mesacanthion</i>	14(4) b	1			SSU (1624 bps)	D2D3 (634 bps)	
WUS 7	<i>Enoplolaimus</i>	17(1)	1		Striated cuticle	SSU (1625 bps)	D2D3 (635 bps)	Cox1 (393bps)

Table A2.2: List of all SSU nematode sequences utilised in this study, including accession numbers, taxonomic information from EMBL, and ARB alphanumeric code used in phylogenetic trees. Colours correspond to clades in full nematode phylogenies (Chapter 5).

Major Clade	Sub-Clades	ARB Code	Taxonomic ID (from EMBL)	Accession No.
Enoplia		AdoFusc4	Adoncholaimus fuscus	AY854195
		AdoSpec5	Adoncholaimus sp.	AF036642
		AlaParv2	Alaimus parvus	AY284738
		AlaSpec2	Alaimus sp. PDL-2005	AJ966514
		AlaSpeci	Alaimus sp. 1247	FJ040489
		AnoRecto	Anoplostoma rectospiculum	AY590149
		AnoSpec3	Anoplostoma sp. PB-2005	AM235215
		AnoSpec4	Anoplostoma sp. BHMM-2005	AY854194
		AnoSpec5	Anoplostoma sp. 1093	FJ040492
		AnoSpec6	Anoplostoma sp. 1058	FJ040491
		AUCYyyy	AUK_13_Calyptronema_SSU	(Present Study)
		AUKYyyy	AUK_10_Viscosia_SSU	(Present Study)
		AUncYyy2	AUK_36_Oncholaimus_SSU	(Present Study)
		AUncYyyy	AUK_35_Oncholaimus_SSU	(Present Study)
		AUnYyyy	AUK_23_Oncholaimus_SSU	(Present Study)
		AUOYyyy	AUK_14_Oxystomina_SSU	(Present Study)
		AUTYyyy	AUK_45_Tripyloides_SSU	(Present Study)
		BatAssim	Bathylaimus assimilis	AJ966476
		BatSpec2	Bathylaimus sp. BHMM-2005	AY854201
		BatSpec3	Bathylaimus sp. 1263	FJ040504
		BatSpeci	Bathylaimus sp. PB-2005	AM234619
		BAUYyyy	BAUK_9_Oxystomina_SSU	(Present Study)
		BCASYyy2	BCA_41_Syringolaimus_SSU	(Present Study)
		BCASYyy3	BCA_47_Syringolaimus_SSU	(Present Study)

BCASYyy4	BCA_6_Syngolaimus_SSU	(Present Study)
BCASYyyy	BCA_31_Syngolaimus_SSU	(Present Study)
BCAYyyyy	BCA_1_Syngolaimus_SSU	(Present Study)
BCdYyyyy	BCA_37_Phanodermatidae_SSU	(Present Study)
BCgYyyyy	BCA_2_Syngolaimus_SSUr	(Present Study)
BCHIYyy2	BCA_17_Halalaimus_SSU	(Present Study)
BCHIYyy3	BCA_25_Halalaimus_SSU	(Present Study)
BCHIYyy4	BCA_38_Halalaimus_SSU_	(Present Study)
BCHIYyyy	BCA_16_Halalaimus_SSU	(Present Study)
BCHYyyyy	BCA_12_Halalaimus_SSU	(Present Study)
BCIYyyyy	BCA_35_Oxystomina_SSU	(Present Study)
BCMYYYY	BCA_14_Mesacanthion_Paramacanthion_SSU	(Present Study)
BCnYyyyy	BCA_32_Phanodermatidae_SSU	(Present Study)
BCOxYyy2	BCA_22_Oxystomina_SSU	(Present Study)
BCOxYyy3	BCA_23_Oxystomina_SSU	(Present Study)
BCOxYyy4	BCA_42_Oxystomina_SSU	(Present Study)
BCOxYyyy	BCA_21_Oxystomina_SSU	(Present Study)
BCOYyyyy	BCA_15_Oxystomina_SSU	(Present Study)
BCPYyyyy	BCA_20_Phanodermatidae_SSU	(Present Study)
BCrYyyyy	BCA_3_Pareurystomina_SSU	(Present Study)
BCsYyyyy	BCA_19_Mesacanthion_Paramacanthion_SSU	(Present Study)
BCTYyyyy	BCA_10_Trefusia_SSU_	(Present Study)
BCUYyyyy	BCA_5_Syngolaimus_SSUs	(Present Study)
BstGrac2	Bastiania gracilis	AY284726
BstGraci	Bastiania gracilis	AY284725
BUAYyyyy	BUS_21_Anoplostoma_SSU	(Present Study)
BUOYyyyy	BUS_7_Oncholaimus_SSUa	(Present Study)
BUSOYyy2	BUS_3_Oncholaimus_SSU	(Present Study)

BUSOYyy3	BUS_4_Oncholaimus_SSU	(Present Study)
BUSOYyy4	BUS_5_Oncholaimus_SSU	(Present Study)
BUSOYyyy	BUS_2_Oncholaimus_SSU	(Present Study)
BUSYyyyy	BUS_1_Oncholaimus_SSU	(Present Study)
BUTYyyyy	BUS_15_Tripyloides_SSU	(Present Study)
CamDemo3	Campydora demonstrans	AY552965
CbBYyyyy	Cr_82b_Thoracostomopsidae_SSU	(Present Study)
CbCYyyyy	Cr_83b_Halalaimus_SSU	(Present Study)
CbHYyyyy	Cr_73b_Halalaimus_SSU	(Present Study)
CbIYyyyy	Cr_74b_Halalaimus_SSU	(Present Study)
CbOYyyyy	Cr_80b_Bathyeurystomina_SSU	(Present Study)
CBPYyyyy	Cr_78a_Bathyeurystomina_SSU	(Present Study)
CbSYyyyy	Cr_72b_Phanodermatidae_SSU	(Present Study)
CbtYyyyy	Cr_84b_O_Chaeto_SSU	(Present Study)
CCHYyyyy	Cr_83a_C_Halal_SSU	(Present Study)
CHBYyyyy	Cr_82a_Halalaimus_SSU	(Present Study)
CHIIYyy2	Cr_85a_Halalaimus_SSU	(Present Study)
CHIIYyyy	Cr_77a_Oxystomina_SSU	(Present Study)
CHIYyyyy	Cr_74a_Halalaimus_SSU	(Present Study)
ClpMaxwe	Calyptonema maxweberi	AY854199
ClpSpeci	Calyptonema sp. 1068	FJ040503
COBYyyyy	Cr_80a_Oxystomina_SSU	(Present Study)
COxYyyyy	Cr_87_Oxystomina_SSU	(Present Study)
CrAYyyyy	Cr_38_Anticomidae_SSU	(Present Study)
CrbYyyyy	Cr_18b_Mesacanthion_Paramacanthion_SSU	(Present Study)
CrCYyyyy	Cr_73a_H_Chaeto_SSU	(Present Study)
CrdYyyyy	Cr_26_Phanodermatidae_SSU	(Present Study)
CrEYyyyy	Cr_71b_Phanodermopsis_SSU	(Present Study)

CrHalYy2	Cr_63_Halalaimus_SSU	(Present Study)
CrHalYy3	Cr_64_Halalaimus_SSU	(Present Study)
CrHalYy4	Cr_86_Halalaimus_SSU	(Present Study)
CrHalYyy	Cr_62_Halalaimus_SSU	(Present Study)
CrHaYyy2	Cr_11_Halalaimus_SSU	(Present Study)
CrHaYyy3	Cr_13_Halalaimus_SSU	(Present Study)
CrHaYyy4	Cr_35_Halalaimus_SSU	(Present Study)
CrHaYyy5	Cr_55_Halalaimus_SSU	(Present Study)
CrHaYyy6	Cr_59_Halalaimus_SSU	(Present Study)
CrHaYyy7	Cr_60_Halalaimus_SSU	(Present Study)
CrHaYyy8	Cr_61_Halalaimus_SSU	(Present Study)
CrHaYyyy	Cr_9_Halalaimus_SSU	(Present Study)
CrHYyyy	Cr_7_Halalaimus_SSU	(Present Study)
CrIIYyy2	Cr_75b_Halalaimus_SSU	(Present Study)
CrIIYyy3	Cr_77b_Halalaimus_SSU	(Present Study)
CrIIYyy4	Cr_85b_Halalaimus_SSU	(Present Study)
CrIYyyy	Cr_20b_Halalaimus_SSU	(Present Study)
CrMYyyy	Cr_24b_Metaparoncholaimus_Meyersia_SSU	(Present Study)
CrnYyyy	Cr_19b_Phanodermopsis_SSU	(Present Study)
CrOYyyy	Cr_76a_Chaetonema_SSU	(Present Study)
CrPhYyy2	Cr_54_Phanodermopsis_SSU	(Present Study)
CrPhYyy3	Cr_56_Phanodermopsis_SSU	(Present Study)
CrPhYyy4	Cr_66_Phanodermopsis_SSU	(Present Study)
CrPhYyy5	Cr_68_Phanodermopsis_SSU	(Present Study)
CrPhYyyy	Cr_33_Phanodermopsis_SSU	(Present Study)
CrPYyyy	Cr_3_Phanodermopsis_SSU	(Present Study)
CrrYyyy	Cr_34_Mesacanthion_Paramacanthion_SSU	(Present Study)
CrSYyyy	Cr_72a_Halalaimus_SSU	(Present Study)

CrTYyyy	Cr_1_Thoracostomopsidae_SSU	(Present Study)
CrxYyyy	Cr_76b_Oxystomina_SSU	(Present Study)
DBAEYyy2	DBA_6_Enoploides_SSU	(Present Study)
DBAEYyyy	DBA_3_Enoploides_SSU	(Present Study)
DBAYyyy	DBA_1_Enoploides_SSU	(Present Study)
DBEYyyy	DBA_21_Enoplus_SSU	(Present Study)
DBIYyyy	DBA_7_Enoploides_SSUv	(Present Study)
DBnYyyy	DBA_2_Enoploides_SSUt	(Present Study)
DBOYyyy	DBA_4_Oncho_Viscosia_SSU	(Present Study)
DBpYyyy	DBA_5_Enoploides_SSUu	(Present Study)
DinTenui	Dintheria tenuissima	FJ040487
DphObes3	Diphterophora obesus	AY552968
DprCommu	Diphterophora communis	AY593955
DprObes2	Diphterophora obesa	AY284839
DprObesa	Diphterophora obesa	AY284838
EnoBrun2	Enoploides brunettii	AY854193
EnoSpec3	Enoploides sp. PB-2005	AM234621
EnoSpec4	Enoploides sp. 1252	FJ040490
EnpBrevi	Enoplus brevis	U88336
EnpCommu	Enoplus communis	AY854192
EnpMerid	Enoplus meridionalis	Y16914
HCCYyyy	HCL_11_Viscosia_SSUx	(Present Study)
HCGYyyy	HCL_9_Viscosia_SSU_gate	(Present Study)
HCHYyyy	HCL_5_Oncholaimus_SSU_cat	(Present Study)
HCL0Yyyy	HCL_2_Oncholaimus_SSU	(Present Study)
HCLYyyy	HCL_12_Oncholaimus_SSU	(Present Study)
HCMYyyy	HCL_7_Oncholaimus_SSU_date	(Present Study)
HCnYyyy	HCL_23_Oncho_Viscosia_SSU	(Present Study)

HCOYyyyy	HCL_20_Oxystomina_SSU	(Present Study)
HCsYyyyy	HCL_10_Viscosia_SSUw	(Present Study)
HCTYyyyy	HCL_32_Oxystomina_SSU_bat	(Present Study)
HCUYyyyy	HCL_24_Viscosia_SSUz	(Present Study)
HCVsYyyy	HCL_27_Viscosia_SSU	(Present Study)
HCVYyyyy	HCL_15_Viscosia_SSU	(Present Study)
HCxYyyyy	HCL_21_Oxystomina_SSUyz	(Present Study)
HIISpeci	Halalaimus sp. 1034	FJ040501
HUKYyyyy	HUK_1_Oncholaimus_SSUb	(Present Study)
IroDenti	Ironus dentifurcatus	AJ966487
IroLongi	Ironus longicaudatus	FJ040495
IroSpec3	Ironus sp. 2-PM-2004	AY552970
IroSpec4	Ironus sp. 1992	FJ040496
JCCYyyyy	JCC_23_Phanodermatidae_SSU	(Present Study)
JCEYyyyy	JCC_29_Anticomidae_SSU	(Present Study)
JChnYyyy	JCC_89_Phanodermopsis_SSU	(Present Study)
JChYyyyy	JCC_59_Phanodermopsis_SSU	(Present Study)
JCPYyyyy	JCC_52_Phanodermatidae_SSU	(Present Study)
LCBYyyyy	LCL_19_Bathylaimus_SSU	(Present Study)
LCfYyyyy	LCL_3_Trefusia_SSU_state	(Present Study)
LCLTYyyy	LCL_8_Trefusia_SSU	(Present Study)
LCLYyyyy	LCL_1_Trefusia_SSU	(Present Study)
LCmYyyyy	LCL_7_Trefusia_SSU_mop	(Present Study)
LCOYyyyy	LCL_20_Oncholaimidae_SSU	(Present Study)
LCpYyyyy	LCL_9_Tripy_Bathy_SSU_kip	(Present Study)
LCrYyyyy	LCL_2_Trefusia_SSU_fate	(Present Study)
LCsYyyyy	LCL_4_Trefusia_SSU_rate	(Present Study)
LCTYyyyy	LCL_21_Bathylaimus_SSU	(Present Study)

LCUYyyyy	LCL_5_Trefusia_SSU_put	(Present Study)
LUCYyyyy	LUK_12_Calyptronema_SSU	(Present Study)
LUHYyyyy	LUK_6_Halalaimus_SSU	(Present Study)
LUKVYyyy	LUK_3_Viscosia_SSU	(Present Study)
LUKYyyyy	LUK_1_Viscosia_SSU	(Present Study)
LUIYyyyy	LUK_7_Calyptronema_SSUc	(Present Study)
NABtYyy2	NAR_15_Bathylaimus_SSU	(Present Study)
NABtYyy3	NAR_20_Bathylaimus_SSU	(Present Study)
NABtYyyy	NAR_14_Bathylaimus_SSU	(Present Study)
NABYyyyy	NAR_11_Bathylaimus_SSU	(Present Study)
NAhYyyyy	NAR_6_Chaetonema_SSU	(Present Study)
NAIYyyyy	NAR_4_Oncholaimus_SSUd	(Present Study)
NAmYyyyy	NAR_7_Oncholaimus_SSUe	(Present Study)
NanNanu2	Nanidorus nanus	FJ040485
NanNanus	Nanidorus nanus	FJ040486
NAOYyyyy	NAR_16_Oncholaimus_SSU	(Present Study)
NAREYyy2	NAR_5_Enoplolaimus_SSU	(Present Study)
NAREYyy3	NAR_8_Enoplolaimus_SSU	(Present Study)
NAREYyy4	NAR_9_Enoplolaimus_SSU	(Present Study)
NAREYyyy	NAR_2_Enoplolaimus_SSU	(Present Study)
NARYyyyy	NAR_1_Enoplolaimus_SSU	(Present Study)
NUAYyyyy	NUS_40_Anoplostoma_SSU	(Present Study)
NUBYyyyy	NUS_11_Bathylaimus_SSU	(Present Study)
NUcYyyyy	NUS_2_Oncholaimus_SSUf	(Present Study)
NUhYyyyy	NUS_6_Oncholaimus_SSUg	(Present Study)
NUIYyyyy	NUS_7_Oncholaimus_SSUh	(Present Study)
NUncYyyy	NUS_5_Oncholaimus_SSU	(Present Study)
NUnYyyyy	NUS_4_Oncholaimus_SSU	(Present Study)

NUOxYyyy	NUS_3_Oxystomina_SSU	(Present Study)
NUOYyyyy	NUS_21_Oxystomina_SSU	(Present Study)
NUSYyyyy	NUS_1_Pareurystomina_SSU	(Present Study)
NUTrYyyy	NUS_41_Tripyloides_SSU	(Present Study)
NUTYyyyy	NUS_14_Tripyloides_SSU	(Present Study)
OncSpec2	Oncholaimus sp. BHMM-2005	AY854196
OnhSpec2	Oncholaimidae sp. MHMH-2008	FJ040493
OnhSpeci	Oncholaimidae sp. XS-2005	AY866479
OUAAnYyy2	OUS_6_Anoplostoma_SSU	(Present Study)
OUAAnYyy3	OUS_8_Anoplostoma_SSU	(Present Study)
OUAAnYyyy	OUS_5_Anoplostoma_SSU	(Present Study)
OUAAYyyyy	OUS_3_Anoplostoma_SSU	(Present Study)
OUCYyyyy	OUS_1_Oncholaimus_SSUi	(Present Study)
OUIHYyyy	OUS_4_Halalaimus_SSU	(Present Study)
OUIHYyyyy	OUS_22_Halalaimus_SSU	(Present Study)
OUIYyyyy	OUS_14_Oncholaimus_SSUj	(Present Study)
OUnYyyyy	OUS_9_Oncho_Viscosia_SSU	(Present Study)
OUnOnYyyy	OUS_21_Oncholaimus_SSU	(Present Study)
OUnOYyyyy	OUS_2_Oncholaimus_SSU	(Present Study)
OUpYyyyy	OUS_7_Anoplostoma_SSUk	(Present Study)
OUSYyyyy	OUS_10_Enoploides_SSU	(Present Study)
OxsSpec2	Oxystomina sp. 1262	FJ040498
OxsSpeci	Oxystomina sp. 1282	FJ040499
PonVulga	Pontonema vulgare	AF047890
PPAYyyyy	PPA_7_Enoplus_SSU	(Present Study)
PrmHorte	Paramphidelus hortensis	AY284739
PrmSpec2	Paramphidelus sp. JH-2004	AY284742
PrmSpec3	Paramphidelus sp. JH-2004	AY284741

PrmSpeci	Paramphidelus sp. JH-2004	AY284740
PrtAlli2	Paratrichodorus allius	AJ439572
PrtAlli3	Paratrichodorus allius	AM087124
PrtAnem3	Paratrichodorus anemones	AF036600
PrtDiver	Paratrichodorus divergens	DQ345528
PrtHisp2	Paratrichodorus hispanus	AJ439577
PrtHispa	Paratrichodorus hispanus	DQ345527
PrtMacr2	Paratrichodorus macrostylus	AJ439507
PrtMacro	Paratrichodorus macrostylus	AJ439622
PrtMin10	Paratrichodorus minor	AM269897
PrtPach2	Paratrichodorus pachydermus	AJ439574
PrtPoro3	Paratrichodorus porosus	DQ345524
PrtTere3	Paratrichodorus teres	AM087125
PsmDoli3	Prismatolaimus dolichurus	AY593957
PsmInte2	Prismatolaimus intermedius	AY284729
PsmInte3	Prismatolaimus intermedius	AF036603
PsmtlCf2	Prismatolaimus cf. dolichurus JH-2004	AY284728
PsmtlCf3	Prismatolaimus cf. dolichurus JH-2004	AY284727
PtrSpeci	Paratripyla sp. JH-2004	AY284737
SBAHYyy2	SBA_12_Halalaimus_SSU	(Present Study)
SBAHYyyy	SBA_10_Halalaimus_SSU	(Present Study)
SBAYYYY	SBA_1_Halalaimus_SSU	(Present Study)
SBcYyyy	SBA_3_Oncholaimus_SSU_sat	(Present Study)
SBNVYyyy	SBN_4_Viscosia_SSU	(Present Study)
SBNYYYY	SBN_2_Viscosia_SSU	(Present Study)
SBOYyyy	SBA_5_Oncholaimus_SSU	(Present Study)
SBOYYYY	SBA_2_Oncholaimus_SSU	(Present Study)
SBTYyyy	SBA_13_Thoracostomopsidae_SSU	(Present Study)

SBxYyyyy	SBN_3_Oxystomina_SSU	(Present Study)
SUEYyyyy	SUS_1_Enoplolaimus_SSUI	(Present Study)
SUmYyyyy	SUS_2_Enoplolaimus_SSUo	(Present Study)
SUnYyyyy	SUS_10_Enoplolaimus_SSUm	(Present Study)
SUOYyyyy	SUS_27_Oncholaimidae_SSU	(Present Study)
SUpYyyyy	SUS_15_Enoplolaimus_SSUn	(Present Study)
SUSEYyyy	SUS_6_Enoplolaimus_SSU	(Present Study)
SUSYyyyy	SUS_21_Enoplolaimus_SSU	(Present Study)
SymSpeci	Symplocostoma sp. 1279	FJ040502
SyrSpeci	Syringolaimus sp. 1060	FJ040497
SyrStria	Syringolaimus striatocaudatus	AY854200
TCAyyyyy	TCR_44_Anticoma_SSU	(Present Study)
TCBtYyy2	TCR_128_Bathyeurystomina_SSU	(Present Study)
TCBtYyy3	TCR_81_Bathyeurystomina_SSU	(Present Study)
TCBtYyyy	TCR_109_Bathyeurystomina_SSU	(Present Study)
TCBYyyyy	TCR_106_Bathyeurystomina_SSU	(Present Study)
TCcnYyyy	TCR_94_Mesacanthion_Paramacanthion_SSU	(Present Study)
TCcYyyyy	TCR_158_M_Paramacanthion_SSU	(Present Study)
TCDYyyyy	TCR_114_Dolicholaimus_SSU	(Present Study)
TCEnYyyy	TCR_74_Thoracostomopsidae_SSU	(Present Study)
TCEYyyyy	TCR_102_Thoracostomopsidae_SSU	(Present Study)
TChbYyyy	TCR_139_Rhabdocoma_SSU	(Present Study)
TChYyyyy	TCR_125_Rhabdocoma_SSU	(Present Study)
TCItYyyy	TCR_149_Anticomidae_SSU	(Present Study)
TCIYyyyy	TCR_141_Cephalanticoma_SSU	(Present Study)
TCMYyyyy	TCR_143_Enoplolaimus_Mesacanthion_SSU	(Present Study)
TCndYyy2	TCR_70_Phanodermatidae_SSU	(Present Study)
TCndYyy3	TCR_75_Phanodermatidae_SSU	(Present Study)

TCndYyyy	TCR_173_Phanodermatidae_SSU	(Present Study)
TCnYyyy	TCR_153_Phanodermatidae_SSU	(Present Study)
TCOnYyy2	TCR_69_Oncholaimidae_SSU	(Present Study)
TCOnYyyy	TCR_17_Oncholaimidae_SSU	(Present Study)
TCOYyyy	TCR_12_Oncholaimidae_SSU	(Present Study)
TCPhYyy2	TCR_152_Phanodermopsis_SSU	(Present Study)
TCPhYyy3	TCR_188_Phanodermopsis_SSU	(Present Study)
TCPhYyy4	TCR_190_Phanodermopsis_SSU	(Present Study)
TCPhYyy5	TCR_216_Phanodermopsis_SSU	(Present Study)
TCPhYyy6	TCR_78_Phanodermopsis_SSU	(Present Study)
TCPhYyy7	TCR_80_Phanodermopsis_SSU	(Present Study)
TCPhYyyy	TCR_148_Phanodermopsis_SSU	(Present Study)
TCPYyyy	TCR_108_Phanodermopsis_SSU	(Present Study)
TCRHYyy2	TCR_13_Halalaimus_SSU	(Present Study)
TCRHYyy3	TCR_131_Halalaimus_SSU	(Present Study)
TCRHYyy4	TCR_26_Halalaimus_SSU	(Present Study)
TCRHYyy5	TCR_3_Halalaimus_SSU	(Present Study)
TCRHYyy6	TCR_93_Halalaimus_SSU	(Present Study)
TCRHYyy7	TCR_97_Cricohalalaimus_SSU	(Present Study)
TCRHYyyy	TCR_112_Halalaimus_SSU	(Present Study)
TCRYyyy	TCR_1_Halalaimus_SSU	(Present Study)
TCSYyyy	TCR_145_Syringolaimus_SSU	(Present Study)
TCtYyyy	TCR_184_Epicanthion_SSU	(Present Study)
TCUYyyy	TCR_192_Leptosomatides_SSU	(Present Study)
TCVYyyy	TCR_42_Oncholaimidae_SSU	(Present Study)
TCxsYyy2	TCR_21_Oxystomina_SSU	(Present Study)
TCxsYyy3	TCR_212_Oxystomina_SSU	(Present Study)
TCxsYyy4	TCR_91_Oxystomina_SSU	(Present Study)

TCxsYyyy	TCR_202_Oxystomina_SSU	(Present Study)
TCxYyyyy	TCR_180_Oxystomina_SSU	(Present Study)
ThbYyyyy	TCR_130_Rhabdocoma_SSU_tap	(Present Study)
ThlPirum	Thalassoalaimus pirum	FJ040500
TlmMinor	Tylolaimophorus minor	AJ966512
TobGraci	Tobrilus gracilis	AJ966506
TplSpeci	Tripylella sp. 1031	FJ040488
TRBYyyyy	TCR_87_Bathylaimus_SSU	(Present Study)
TrcNanj2	Trichodorus nanjingensis	AJ439579
TrcNanji	Trichodorus nanjingensis	AJ439580
TrcPaki2	Trichodorus pakistanensis	AJ439581
TrcPrim2	Trichodorus primitivus	AF036609
TrcPrim5	Trichodorus primitivus	AJ439517
TrcSimi2	Trichodorus similis	AJ439585
TrcSimi3	Trichodorus similis	AJ439584
TrcSpar2	Trichodorus sparsus	AJ439589
TrcVario	Trichodorus variopapillatus	AY284841
TriMonoh	Trischistoma monohystera	AJ966509
TriSpec3	Tripylodes sp. BHMM-2005	AY854202
TriSpec4	Trischistoma sp. 1 JH-2004	AY284735
TriSpec5	Trischistoma sp. 2 JH-2004	AY284736
TrlCf003	Tripyla cf. filicaudata JH-2004	AY284731
TrlCf004	Tripyla cf. filicaudata JH-2004	AY284730
TrlSpec3	Tripyla sp. SAN-2007b	EF197730
TrlSpec4	Tripyla sp. SAN-2007d	EF197735
TrlSpec5	Tripyla sp. SAN-2007b	EF197731
TrlSpec6	Tripyla sp. JH-2004	AY284732
TrlSpec7	Tripyla sp. JH-2004	AY284733

Dorylaimia	Trichinellida	TrISpec8	Tripyla sp. SAN-2007d	EF197734
		TrISpec9	Tripyla sp. JH-2004	AY284734
		TRLyyyy	TCR_197_Anticoma_SSU	(Present Study)
		TRnmYyy2	TCR_89_Litinium_SSU	(Present Study)
		TRnmYyy3	TCR_90_Litinium_SSU	(Present Study)
		TRnmYyyy	TCR_230_Thalassoalaimus_SSU	(Present Study)
		TRnYyyyy	TCR_205_Litinium_SSU	(Present Study)
		TROYyyyy	TCR_68_Oxystomina_SSU	(Present Study)
		TrpSpec2	Tripylina sp. SAN-2007a	EF197727
		TrpSpec3	Tripylina sp. SAN-2007a	EF197729
		TrpSpec4	Tripylina sp. SAN-2007a	EF197728
		TRSYyyyy	TCR_206_Synonchus_SSU	(Present Study)
		VisSpec2	Viscosia sp. 1267	FJ040494
		VisSpeci	Viscosia sp. BHMM-2005	AY854197
		VisVisco	Viscosia viscosa	AY854198
		WUEMYyyy	WUS_6_Enoplolaimus_Mesacanthion_SSU	(Present Study)
		WUEYyyyy	WUS_3_Enoplolaimus_Mesacanthion_SSU	(Present Study)
		WUnYyyyy	WUS_5_Enoplolaimus_SSUq	(Present Study)
		WUSEYyy2	WUS_4_Enoplolaimus_SSU	(Present Study)
		WUSEYyy3	WUS_7_Enoplolaimus_SSU	(Present Study)
		WUSEYyyy	WUS_2_Enoplolaimus_SSU	(Present Study)
		WUSYyyyy	WUS_1_Enoplolaimus_SSU	(Present Study)
		TrhBrito	Trichinella britovi	AY851257
		TrhNati2	Trichinella nativa	AY487254
		TrhNativ	Trichinella nativa	AY851256
		TrhNelso	Trichinella nelsoni	AY851261
		TrhPapua	Trichinella papuae	AY851263
		TrhPseud	Trichinella pseudospiralis	AY851258

		TrhSpec3	Trichinella sp. T8	AY851262
		TrhSpira	Trichinella spiralis	U60231
		TrhSpir2	Trichinella spiralis	AY497012
		TrrMuris	Trichuris muris	AF036637
		TrrsSui2	Trichuris suis	AY856093
		TrrsSui3	Trichuris suis	AY851265
		TrrsSuis	Trichuris suis	EU790668
		TrrTrich	Trichuris trichiura	DQ118536
Dorylaimia	Bathyodontus	BatCyli2	Bathyodontus cylindricus	AY552964
		BatMirus	Bathyodontus mirus	AY284744
Dorylaimia	Mononchida	GraSpeci	Granonchulus sp. JH-2004	AY593953
Dorylaimia	Mermithidae	MrmNigr2	Mermis nigrescens	AF036641
		MrhSpeci	Mermithid sp. JH-2004	AY284743
		MrtSpec4	Mermithidae sp. MHMH-2008	FJ040480
Dorylaimia	Mononchida	AnaTrid2	Anatonchus tridentatus	AJ966474
		ClaPapi3	Clarkus papillatus	AY552966
		ClaPapi4	Clarkus papillatus	AY284750
		ClaPapi5	Clarkus papillatus	AY284749
		ClaPapi6	Clarkus papillatus	AY284748
		ClaSpec3	Clarkus sp. PDL-2005	AJ966479
		CooParv2	Coomansus parvus	AY284766
		CooParvu	Coomansus parvus	AY284767
		McnchCf6	Miconchus cf. fasciatus	AY552973
		MonAqua2	Mononchus aquaticus	AY284765
		MonAqua3	Mononchus aquaticus	AY297821
		MonAquat	Mononchus aquaticus	AY284764
		MonTrun2	Mononchus truncatus	AJ966493
		MonTrunc	Mononchus truncatus	AY284762

		MonTunb2	Mononchus tunbridgensis	AY593954
		MylAreni	Mylonchulus arenicolus	AF036596
		MylBrac3	Mylonchulus brachyuris	AY284754
		MylBrach	Mylonchulus brachyuris	AY284753
		MylRotun	Mylonchulus rotundicaudatus	AY284751
		MylSigm2	Mylonchulus sigmaturus	AY284756
		MylSigm3	Mylonchulus sigmaturus	AY284757
		MylSigma	Mylonchulus sigmaturus	AY284755
		MylSpec3	Mylonchulus sp. JH-2004	AY284761
		MylSpec4	Mylonchulus sp. JH-2004	AY284760
		MylSpec5	Mylonchulus sp. F6	AJ875156
		PrhMusc2	Prionchulus muscorum	AJ966500
		PrhMusco	Prionchulus muscorum	AY284745
		PrhPunc2	Prionchulus punctatus	AY284746
		PrhPunct	Prionchulus punctatus	AY284747
Dorylaimia	Cryptonchus	CrySpeci	Cryptonchus sp. 1453	FJ040479
		CryTrist	Cryptonchus tristis	EF207244
Dorylaimia	Dorylaimida	AldAndra	Allodorylaimus andrassyi	AY284801
		AldSpeci	Allodorylaimus sp. PDL-2005	AJ966472
		ApoObtu2	Aporcelaimellus obtusicaudatus	AY284811
		ApoObtus	Aporcelaimellus obtusicaudatus	DQ141212
		AporcCf9	Aporcelaimellus cf. paraobtusicaudatus JH-2004	AY284812
		ApoSpec3	Aporcelaimellus sp. G2	AJ875154
		ApoSpec4	Aporcelaimellus sp. F2	AJ875153
		AxnPropi	Axonchium propinquum	AY284820
		CalSpec4	Californidorus sp. Arkansas-WY-2003	AY283155
		CarBanat	Carcharodiscus banaticus	AY284827
		CfTylen2	cf. Tylencholaimus sp. JH-2004	AY284833

CfTylenc	cf. Tylencholaimus sp. JH-2004	AY284832
ChsAtte2	Chrysonema attenuatum	AY284779
ChsAtte3	Chrysonema attenuatum	EF207245
ChsAtten	Chrysonema attenuatum	AY593945
DiscoCf0	Discolaimus cf. major HHBM-2007a	EF207252
DisMajor	Discolaimus major	AY284828
DrIMonte	Dorylaimellus montenegricus	AY284821
DrIVirg6	Dorylaimellus virginianus	AY552969
DrmLimn2	Dorylaimoides limnophilus	AY593950
DrmMicol	Dorylaimoides micoletzkyi	AY284830
DrmSpeci	Dorylaimoides sp. JH-2004	AY593951
DrsStag2	Dorylaimus stagnalis	AY284776
DrsStagn	Dorylaimus stagnalis	AY284777
EcuMono3	Ecumenicus monohystera	AY284783
EcuMono4	Ecumenicus monohystera	AY284784
EcuSpec2	Ecumenicus sp. JH-2004	AY284781
EcuSpeci	Ecumenicus sp. JH-2004	AY284782
EncMacro	Enchodelus macrodorus	AY284791
EncSpec2	Enchodelus sp. JH-2004	AY284792
EncSpec3	Enchodelus sp. JH-2004	AY284793
EncSpeci	Enchodelus sp. HHBM-2007a	EF207247
EpiLugd4	Epidorylaimus lugdunensis	AY284803
EpiLugd5	Epidorylaimus lugdunensis	AY284802
EpiSpeci	Epidorylaimus sp. 1457	FJ040478
EudCarte	Eudorylaimus carteri	AJ966484
EudSpec5	Eudorylaimus sp. JH-2004	AY284800
LbrFero3	Labronema ferox	AY552972
LbrVulva	Labronema vulvapapillatum	AY284807

LepGran4	Leptonchus granulosus	AY284831
LonAtten	Longidorus attenuatus	AY687994
LonBifor	Longidorus biformis	AY283171
LonCrass	Longidorus crassus	AY283158
LonDiade	Longidorus diadecturus	AY283166
LonDunen	Longidorus dunensis	AY284819
LonElon2	Longidorus elongatus	AY687992
LonEuon2	Longidorus euonymus	AY687995
LonGrand	Longidorus grandis	AY283165
LonHelve	Longidorus helveticus	EF538759
LonLepto	Longidorus leptcephalus	EU503142
LonLitch	Longidorus litchii	AY687996
LonMacro	Longidorus macrosoma	EF538758
LonPara3	Longidorus paravineicola	AY283157
LonPoes2	Longidorus poessneckensis	EF538757
LonSpec3	Longidorella sp. 2 JH-2004	AY284790
LonSpec6	Longidorella sp. 1 JH-2004	AY284789
LonSpec7	Longidorus sp. Georgia-WY-2003	AY283168
LonUrosh	Longidorus uroshis	EF538760
LonVinea	Longidorus vineicola	AY283169
MicMise4	Microdorylaimus miser	AY284804
MicMode2	Microdorylaimus modestus	AY284806
MicModes	Microdorylaimus modestus	AY284805
MicSpeci	Microdorylaimus sp. PDL-2005	AJ966492
MsdAberr	Mesodorylaimus aberrans	AY593947
MsdBasti	Mesodorylaimus bastiani	AJ966488
MsdCent2	Mesodorylaimus centrocerus	EF207248
MsdCentr	Mesodorylaimus centrocerus	AY284799

MsdJapon	Mesodorylaimus japonicus	AJ966489
MsdrlCf3	Mesodorylaimus cf. nigrutilus AV-2005	AJ966490
MsdSpec2	Mesodorylaimus sp. JH-2004	AY284780
MtpSimpl	Metaporcelaimus simplex	AY593948
OpiSylp2	Opisthodorylaimus sylphoides	AY284785
OxdNeth3	Oxydirus nethus	EF207251
OxdOxyc2	Oxydirus oxycephalus	AY284825
OxdOxyc3	Oxydirus oxycephalus	AY284824
OxdOxyce	Oxydirus oxycephaloides	AY284823
PctMacr2	Paractinolaimus macrolaimus	AY993978
PctMacro	Paractinolaimus macrolaimus	AY284826
PctSpec2	Paractinolaimus sp. PM-2002	AY552975
PdrImMas	Prodorylaimus mas	AY593946
PdrSpeci	Prodorylaimus sp. HHBM-2007a	EF207246
PdrUligi	Prodorylaimus uliginosus	AY284778
PrxLaet2	Paraxonchium laetificans	AY284808
PrxLaet3	Paraxonchium laetificans	AY284809
PrxLaeti	Paraxonchium laetificans	AY284810
PunSilve	Pungentus silvestris	AY284788
PunSpec4	Pungentus sp. PDL-2005	AJ966501
SecBarba	Sectonema barbatoides	AY284814
SecSpeci	Sectonema sp. JH-2004	AY284815
ThoCircu	Thonus circulifer	AY284795
ThoMinut	Thonus minutus	AY284794
ThoSpec2	Thonus sp. JH-2004	AY284797
ThoSpec3	Thonus sp. JH-2004	AY284798
ThoSpeci	Thonus sp. JH-2004	AY284796
TlchICf2	Tylencholaimus cf. teres HHBM-2007a	EF207254

TlcMira3	Tylencholaimus mirabilis	AY284835
TlcMirab	Tylencholaimus mirabilis	EF207253
TlcSpec2	Tylencholaimus sp. PDL-2005	AJ966510
TlcSpeci	Tylencholaimus sp. JH-2004	AY284834
TIIAffi3	Tylencholaimellus affinis	AY552978
TIIStri3	Tylencholaimellus striatus	AY284837
XipAmer2	Xiphinema americanum	AY283170
XipAmer4	Xiphinema americanum	AY580056
XipBrasi	Xiphinema brasiliense	AY297836
XipDiff4	Xiphinema diffusum	AM086677
XipDiver	Xiphinema diversicaudatum	EF538761
XipElong	Xiphinema elongatum	AY297824
XipGeorg	Xiphinema georgianum	AM086688
XiphiCf3	Xiphinema cf. americanum RN-2005	AM086671
XiphiCf4	Xiphinema cf. americanum RN-2005	AM086679
XiphiCf6	Xiphinema cf. americanum RN-2005	AM086683
XipInco2	Xiphinema incognitum	AM086678
XipIncog	Xiphinema incognitum	AM086670
XipIndex	Xiphinema index	EF207249
XipLongi	Xiphinema longicaudatum	AY297829
XipParit	Xiphinema paritaliae	AY297831
XipRive2	Xiphinema rivesi	AF036610
XipSurin	Xiphinema surinamense	AY297833
XphBalca	Xiphidurus balcarceanus	AY297839
XphMino2	Xiphidurus minor	AY297830
XphMinor	Xiphidurus minor	AY604181
XphParth	Xiphidurus parthenus	AY604182
XphSpec2	Xiphidurus sp. 1 CMGO-2004	AY604183

Dorylaimia	Nygolaimidae	XphSpeci	Xiphidorus sp. RN-2003	AY297841
		XphYepe2	Xiphidorus yepesara yepesara	AY297838
		XphYepes	Xiphidorus yepesara parthenus	AY297837
		AquChri4	Aquatides christei	AY552963
		ClaSpec2	Clavicaudoides sp. PGM-2004	AY552967
		ClaTrop2	Clavicaudoides trophurus	AY593943
		ClaTrop3	Clavicaudoides trophurus	AY284772
		ClaTroph	Clavicaudoides trophurus	AY284773
		NygoCf2	Nygolaimus cf. parvus	AY552974
		NygoCf3	Nygolaimus cf. brachyuris JH-2004	AY284771
		NygoCf4	Nygolaimus cf. brachyuris JH-2004	AY284770
		ParHart4	Paravulvulus hartingii	AY552976
		ParHart5	Paravulvulus hartingii	AY284774
Microlaimoidea	Prodesmodora/ Microlaimidae	ParHart6	Paravulvulus hartingii	AY284775
		SolVulg3	Solididens vulgaris	AY552977
		HalSpeci	Haliplectus sp. JH-2004	AY593935
		PdsCirc3	Prodesmodora circulata	AY284722
Microlaimoidea	Microlaimidae	PdsSpec2	Prodesmodora sp. 1338	FJ040477
		PdsSpeci	Prodesmodora sp. 1287	FJ040476
		CImParah	Calomicrolaimus parahonestus	AY854218
Microlaimoidea	Monoposthiida	MolDema2	Molgolaimus demani	AY854220
		MnpCosta	Monoposthia costata	AY854221
		MnpSpeci	Monoposthia sp. 1266	FJ040505
Chromadorida	Chromadoridae	NudBipap	Nudora bipapillata	AY854222
		ChdSpeci	Chromadoridae sp. MHMH-2008	FJ040474
		ChmGerma	Chromadorina germanica	AY854207
		ChmSpec2	Chromadorina sp. 1257	FJ040470

		ChmSpeci	Chromadorina sp. 1971	FJ040471
		ChrNudic	Chromadora nudicapitata	AY854205
		ChromCf0	Chromadorita cf. leuckarti MHMH-2008	FJ040473
		ChrSpeci	Chromadora sp. BHMM-2005	AY854206
		ChrTenta	Chromadorita tentabundum	AY854208
		DicSpec7	Dichromadora sp. BHMM-2005	AY854209
		DicSpec8	Dichromadora sp. 1260	FJ040506
		NchBHMM2	Neochromadora BHMM-2005	AY854210
		PchSpeci	Prochromadora sp. ProcSp1	EF591341
		PtySpeci	Ptycholaimellus sp. 1092	FJ040472
		SpIParad	Spilophorella paradoxa	AY854211
Chromadorida	Chromadoridae	EthPrat2	Ethmolaimus pratensis	AY593942
		EthPrate	Ethmolaimus pratensis	FJ040475
Chromadorida	Cyatholaimidae	AchroCf0	Achromadora cf. terricola JH-2004	AY593940
		AchRuric	Achromadora ruricola	AY593941
		AchSpec2	Achromadora sp. JH-2004	AY284718
		AchSpeci	Achromadora sp. JH-2004	AY284717
		CthSpec2	Cyatholaimus sp. BHMM-2005	AY854213
		CthSpec3	Cyatholaimus sp. PB-2005	AM234618
		CyaSpec2	Cyatholaimidae sp. BHMM-2005	AY854212
		ParInter	Paracyatholaimus intermedius	AJ966495
		PdsCirc2	Prodesmodora circulata	AY284719
		PdsCirc4	Prodesmodora circulata	AY284721
		PdsCircu	Prodesmodora circulata	AY284720
		PraPunct	Praeacanthonchus punctatus	AY854214
		PraSpec4	Praeacanthonchus sp. 178510	AM234046
		PraSpec5	Praeacanthonchus sp.	AF036612
		PrcCaecu	Paracanthonchus caecus	AF047888

Chromadorida	Cyathlolaimidae/ Chromadorida	ChoPsam2	Choanolaimus psammophilus	FJ040467
		ChoPsam3	Choanolaimus psammophilus	AY284716
		HIhSpeci	Halichoanolaimus sp. HaChSp1	EF591338
		SynSpeci	Synonchiella sp. 1038	FJ040468
Desmodorida		AcnMican	Acanthopharynx micans	Y16911
		CatSpeci	Catanema sp.	Y16912
		ChpVivip	Chromadoropsis vivipara	AF047891
		CrnSpeci	Chromadorid sp. JH-2004	AY284713
		DesCommu	Desmodora communis	AY854215
		DesOvige	Desmodora ovigera	Y16913
		EpsSpeci	Epsilonematidae sp. Epsifamil1	EF591340
		EubDiana	Eubostriechus diana	Y16915
		EubParas	Eubostriechus parasitiferus	Y16916
		EubTopia	Eubostriechus topiarius	Y16917
		LaxCosmo	Laxus cosmopolitus	Y16918
		LaxOneis	Laxus oneistus	Y16919
		LepSpeci	Leptonemella sp.	Y16920
		MetRema2	Metachromadora remanei	AM234620
		MetReman	Metachromadora remanei	AY854216
		MetSpec2	Metachromadora sp. 1089	FJ040469
		MetSpec3	Metachromadora sp.	AF036595
		MetSpeci	Metachromadora sp. MAChSp1	EF591339
		RobHyper	Robbea hypermnestra (nomen nudum)	Y16921
		RobSpec2	Robbea sp. 3 SB-2008	EU784735
		RobSpec3	Robbea sp. 1 SB-2008	EU768870
		RobSpeci	Robbea sp. 2 SB-2008	EU768871

	SpiElon2	Spirinia elongata	EF527426
	SpiElong	Spirinia elongata	FJ429257
	SpiPara2	Spirinia parasitifera	AY854217
	StiMajum	Stilbonema majum	Y16922
	XyzSpeci	Xyzzors sp.	Y16923
Monhysterida	CrIIYyyy	Cr_21b_Comesomatidae	(Present Study)
	CrtElega	Cyartonema elegans	AY854203
	DapHirs4	Daptonema hirsutum	AY854223
	DapNorm2	Daptonema normandicum	AY854224
	DapOxyc2	Daptonema oxycerca	AY854225
	DapProce	Daptonema procerus	AF047889
	DapSeto4	Daptonema setosum	AM234045
	DapSpec3	Daptonema sp. 1255	FJ040463
	DapSpec4	Daptonema sp. PFN-2007	EF436228
	DipMeyl2	Diplolaimelloides meyli	AF036611
	DipMeyli	Diplolaimelloides meyli	AF036644
	DipSpe16	Diplolaimelloides sp. BCG-2008	EU551671
	DorPunct	Dorylaimopsis punctata	AM234047
	DplDiev2	Diplolaimella dievengatensis	AJ966482
	DppSpeci	Diplopeltula sp. DiPeSp1	EF591329
	EumFili2	Eumonhystera filiformis	AY593937
	EumonCf0	Eumonhystera cf. similis JH-2004	AY284691
	EumonCf2	Eumonhystera cf. simplex JH-2004	AY284692
	GeoSpeci	Geomonhystera sp. 1998	FJ040465
	GeoVillo	Geomonhystera villosa	EF591334
	HlmDisju	Halomonhystera disjuncta	AJ966485
	MetSpec4	Metadesmolaimus sp. PDL-2005	AJ966491
	MnhRiema	Monhystera riemanni	AY593938

	SabCelt4	Sabatieria celtica	AY854234
	SabPulc4	Sabatieria pulchra	EF591335
	SabPulc5	Sabatieria pulchra	FJ040466
	SabPunc2	Sabatieria punctata	AY854236
	SabPunc3	Sabatieria punctata	AY854237
	SabPunct	Sabatieria punctata	AY854235
	SabSpec7	Sabatieria sp. 210-BHMM-2005	AY854238
	SetHila3	Setosabatieria hilarula	AY854240
	SphHirs7	Sphaerolaimus hirsutus	AM234622
	SphHirs8	Sphaerolaimus hirsutus	AY854228
	TerLon93	Terschellingia longicaudata	AM234716
	TerLon94	Terschellingia longicaudata	AY854230
	TheAgil2	Theristus agilis	AY284694
	TheAgil3	Theristus agilis	AY284695
	TheAgili	Theristus agilis	AY284693
	TherAce4	Theristus acer	AJ966505
	TheSpec2	Theristus sp. 1268	FJ040464
	TrdSpeci	Tridentulus sp. PDL-2005	AJ966507
	TrRmYyyyy	TCR_82_Comesomatidae	(Present Study)
	UncDip38	uncultured Diplolaimelloides	EF659927
	UncDip39	uncultured Diplolaimelloides	EF659919
	UncDip40	uncultured Diplolaimelloides	EF659918
	UncDip41	uncultured Diplolaimelloides	EF659925
	UncDip42	uncultured Diplolaimelloides	EF659926
	UncDip43	uncultured Diplolaimelloides	EF659917
	UncDip44	uncultured Diplolaimelloides	EF659924
Desmoscolecidae	DssSpeci	Desmoscolex sp. DeCoSp2	EF591342

Monhysterida	Linhomoeidae/ Siphonolaimidae	AstSpec2	Astomonema sp. NCM-2006	DQ408760
		AstSpec3	Astomonema sp. NCM-2006	DQ408759
		AstSpeci	Astomonema sp. NCM-2006	DQ408761
		DsmSpec2	Desmolaimus sp. DeLaSp1	EF591332
		DsmSpeci	Desmolaimus sp. DeLaSp2	EF591333
		DsmZeela	Desmolaimus zeelandicus	AY854229
		LinSpec2	Linhomoeidae sp. DeLaSp3Z	EF591336
		LinSpeci	Linhomoeidae sp. DeLaSp4Z	EF591337
Araeolaimida	Axonolaimidae/ Cylindrolaimidae	AscElon2	Ascolaimus elongatus	AY854231
		AscElon3	Ascolaimus elongatus	AM234617
		AscolCf0	Ascolaimus cf. elongatus MHMH-2008	FJ040460
		AscolCf2	Ascolaimus cf. elongatus AscoElo2Z	EF591330
		AxoHelg4	Axonolaimus helgolandicus	AY854232
		AxoSpec2	Axonolaimus sp. 1277	FJ040462
		AxoSpec3	Axonolaimus sp. AxLaSp2	EF591331
		AxoSpeci	Axonolaimus sp. 1088	FJ040461
		CylCommu	Cylindrolaimus communis	AY593939
		CylSpec2	Cylindrolaimus sp. 202149	AF202149
		OdnRecta	Odontophora rectangula	AY854233
		OdnSpeci	Odontophora sp. 1273	FJ040459
Aulolaimidae/ Isolaimidae		AulOxyce	Aulolaimus oxycephalus	AY284724
		IsoSpec3	Isolaimium sp. 2-PM-2004	AY552971
Araeolaimida	Leptolaimoidea	ApchsCf0	Aphanonchus cf. europaeus AphNEurZ1	EF591319
		ApnAqua2	Aphanolaimus aquaticus	AY593932

		ApnAquat	Aphanolaimus aquaticus	AY593933
		LptSpec2	Leptolaimus sp. LeLaSp1	EF591323
		LptSpec3	Leptolaimus sp. LeLaSp2	EF591324
		LptSpeci	Leptolaimus sp. 1283	FJ040458
		PplPedun	Paraplectonema pedunculatum	EF591320
Araeolaimida	Leptolaimoidea/ Plectoidea	ChnBoett	Chronogaster boettgeri	AY593931
		ChnSpec2	Chronogaster sp. JH-2004	AY284709
		ChnSpec3	Chronogaster sp. 1189	FJ040455
		ChnSpeci	Chronogaster sp. JH-2004	AY284708
		ChnTypic	Chronogaster typica	FJ040456
		CmcSpec2	Camacolaimus sp. CamaSp1	EF591325
		CmcSpeci	Camacolaimus sp. CamaSp2	EF591327
		DeoPapi2	Deontolaimus papillatus	EF591322
		DeoPapil	Deontolaimus papillatus	FJ040457
		DomMacro	Domorganus macronephriticus	FJ040454
		OnmSpeci	Onchium sp. OChiSp1	EF591328
		PcmSpeci	Procamacolaimus sp. PrCoSp1	EF591326
		StsSpart	Setostephanolaimus spartinae	EF591321
		Teratocephaloidea		EutPalus
		EutSpeci	Euteratocephalus sp. JH-2004	AY284685
		MttCras2	Metateratocephalus crassidens	AY284687
		MttCras3	Metateratocephalus crassidens	AY284686
		MttCrass	Metateratocephalus crassidens	AY593934
		Plectida		AnaGran2
		AnaGrand	Anaplectus grandepapillatus	AY284698
		AnaPoro2	Anaplectus porosus	FJ040453
		AnaPoros	Anaplectus porosus	AY284696

	AnaSpec2	Anaplectus sp. PDL-2005	AJ966473
	CrpArmat	Ceratoplectus armatus	AY284706
	PlcSpec3	Plectidae sp. PDL-2005	AJ966478
	PlcSpec4	Plectidae sp. PDL-2005	AJ966508
	PlectCf6	Plectus cf. cirratus JH-2004	AY284701
	PleAcumi	Plectus acuminatus	AF037628
	PleAqua2	Plectus aquatilis	AF036602
	PleAquat	Plectus aquatilis	AY284700
	PlectCf7	Plectus cf. parvus JH-2004	AY284699
	PlectCf8	Plectus cf. parietinus JH-2004	AY284703
	PlectCf9	Plectus cf. parietinus JH-2004	AY284702
	PleRhiz2	Plectus rhizophilus	AY593929
	PleRhizo	Plectus rhizophilus	AY593928
	PleSpec4	Plectus sp.	U61761
	TylAuri2	Tylocephalus auriculatus	AF202155
	TylAuric	Tylocephalus auriculatus	AY284707
	WilOtop2	Wilsonema otophorum	AY593927
	WilSchuu	Wilsonema schuurmansstekhoveni	AJ966513
Teratocephalidae	TrtLirel	Teratocephalus lirellus	AF036607
	TrtTerr2	Teratocephalus terrestris	AY284683
Strongyloidea	PngNemat	panagrolaimoid nematode KR3021	U81580
	PrgTrich	Parastrongyloides trichosuri	AJ417024
	RhpSpeci	Rhabditophanes sp. KR3021	AF202151
	RhtSpeci	Rhabditoid sp. YQ-2006	DQ531722
	StrCall2	Strongyloides callosciureus	AB272229
	StrCall4	Strongyloides callosciureus	AB272230
	StrCallo	Strongyloides callosciureus	AB453326
	StrCebu2	Strongyloides cebus	AB272236

Aphelenchoididae	StrFuel3	Strongyloides fuelleborni	AB453317
	StrFuel9	Strongyloides fuelleborni fuelleborni	AB272235
	StrMirza	Strongyloides mirzai	AB453311
	StrMyopo	Strongyloides myopotami	AB453313
	StrProc2	Strongyloides procyonis	AB205054
	StrProcy	Strongyloides procyonis	AB272234
	StrRanso	Strongyloides ransomi	AB453327
	StrRatt4	Strongyloides ratti	AF036605
	StrRatt5	Strongyloides ratti	U81581
	StrRobu2	Strongyloides robustus	AB272232
	StrRobus	Strongyloides robustus	AB272233
	StrSpec2	Strongyloides sp. Yufuin-2004	AB453312
	StrSter5	Strongyloides stercoralis	AB453315
	StrSter6	Strongyloides stercoralis	AF279916
	AnmXenur	Anomyctus xenurus	FJ040413
	AphBesse	Aphelenchoides besseyi	AY508035
	AphBicau	Aphelenchoides bicaudatus	AY284643
	AphBlast	Aphelenchoides blastophtorus	AY284644
	AphelCf4	Aphelenchoides cf. bicaudatus MHMH-2008	FJ040407
	AphFrag2	Aphelenchoides fragariae	AB067755
	AphFrag3	Aphelenchoides fragariae	AY284645
	AphFrag4	Aphelenchoides fragariae	AJ966475
	AphRitze	Aphelenchoides ritzemabosi	DQ901554
	AphSpec2	Aphelenchoides sp. JB012	DQ901553
	AphSpec3	Aphelenchoides sp. JB011	DQ901550
	AphSpec4	Aphelenchoides sp. SAS-2006	DQ901552
	AphSpec5	Aphelenchoides sp. 2137	FJ040412
	AphSpec6	Aphelenchoides sp. 2130	FJ040410

	AphSpec8	Aphelenchoides sp. JH-2004	AY284646
	AphSpec9	Aphelenchoides sp. JH-2004	AY284647
	AphStamm	Aphelenchoides stammeri	AB368535
	BurAbru2	Bursaphelenchus abruptus	AY508010
	BurBorea	Bursaphelenchus borealis	AY508012
	BurCocop	Bursaphelenchus cocophilus (red ring nematode)	AY509153
	BurFraud	Bursaphelenchus fraudulentus	AB067758
	BurHylob	Bursaphelenchus hylobianum	AY508019
	BurPolig	Bursaphelenchus poligraphi	AY508028
	BurSexde	Bursaphelenchus sexdentati	AY508031
	EktObtus	Ektaphelenchus obtusus	AB368532
	LmpPena2	Laimaphelenchus penardi	AY593918
	LmpPena3	Laimaphelenchus penardi	EU306346
	LmpPenar	Laimaphelenchus penardi	AY593919
	RueSpeci	Ruehmaphelenchus sp. NK202	AB368534
	SchAureu	Schistonchus aureus	DQ912922
	SchCente	Schistonchus centerae	DQ912923
	SchGuang	Schistonchus guangzhouensis	DQ912924
	SeiSpeci	Seinura sp. JH-2004	AY284651
Panagrolaimidae	BauMirab	Baujardia mirabilis	AF547385
	HlcGingi	Halicephalobus gingivalis	AF202156
	PanagCf0	Panagrolaimus cf. rigidus AF40	DQ285636
	PanDavid	Panagrolaimus davidi	AJ567385
	PanDetri	Panagrolaimus detritophagus	EU543176
	PanPaetz	Panagrolaimus paetzoldi	FJ040414
	PanSpec9	Panagrolaimus sp. PS1159	U81579
	PanSubel	Panagrolaimus subelongatus	AY284681
	PlcSpec2	Plectonchus sp. PDL0025	AF202154

Cephalobidae	PlcSpeci	Plectonchus sp. JH-2004	AY593920
	PnlRedi2	Panagrellus redivivus	AF036599
	PnlRediv	Panagrellus redivivus	AF083007
	PnrStamm	Panagrobelus stammeri	AF202153
	PrcSpec3	Procephalobus sp. 1 WB-2008	EU543179
	TurAceti	Turbatrix aceti	AF202165
	AcbCilia	Acrobeles ciliatus	AF202148
	AcbCompl	Acrobeles complexus	AY284671
	AcbMaxim	Acrobeles maximus	EU196016
	AcbSpec4	Acrobeles sp.	U81576
	AcrApicu	Acrobeloides apiculatus	AY284673
	AcrBode2	Acrobeloides bodenheimeri	AF202162
	AcrBoden	Acrobeloides bodenheimeri	AF202159
	AcrBuets	Acrobeloides buetschlii	EU543174
	AcrMaxi2	Acrobeloides maximus	EU306344
	AcrNanu2	Acrobeloides nanus	AY284672
	AcrNanus	Acrobeloides nanus	DQ102707
	AcrSp135	Acrobeloides sp. PS1146	AF034391
	AcrThorn	Acrobeloides thornei	EU543175
	CepSpec3	Cephalobidae sp. MHMH-2008	FJ040406
	CerAlutu	Cervidellus alutus	AF202152
	CerSpeci	Cervidellus sp. JH-2004	AY284674
	ChiPropi	Chiloplacus propinquus	AY284677
	CphCubae	Cephalobus cubaensis	AF202161
	CphOryza	Cephalobus oryzae	AF034390
	CphPers2	Cephalobus persegnis	AY284662
	CphPerse	Cephalobus persegnis	AY284663
	CphSpec3	Cephalobus sp. PS1143	AF202158

		CphSpec4	Cephalobus sp. PS1196	AF202160
		DriSpec2	Drilocephalobus sp. JH-2004	AY284678
		DriSpec3	Drilocephalobus sp. JH-2004	AY284679
		EcphICf6	Eucephalobus cf. oxyuroides JH-2004	AY284664
		EcpOxyur	Eucephalobus oxyuroides	AY284665
		EcpStri3	Eucephalobus striatus	AY284667
		EcpStri4	Eucephalobus striatus	AY284666
		HtrElon2	Heterocephalobus elongatus	AY284669
		HtrElon3	Heterocephalobus elongatus	AY284668
		HtrElon4	Heterocephalobus elongatus	AY284670
		PscVaria	Pseudacrobeles variabilis	AF202150
		SelCompl	Seleborca complexa	U81577
		ZelPunc2	Zeldia punctata	U61760
		ZelSpec2	Zeldia sp. JH-2004	AY284676
		ZelSpec3	Zeldia sp. JH-2004	AY284675
Tylenchomorpha	Aphelenchoidea	AplAvena	Aphelenchus avenae	AY284640
		AplAven2	Aphelenchus avenae	AY284639
		AplAven3	Aphelenchus avenae	AF036586
		AplAven4	Aphelenchus avenae	EU306347
		AplAven5	Aphelenchus avenae	AB368918
		AplSpec3	Aphelenchus sp. JH-2004	AY284641
		PphSpeci	Paraphelenchus sp. JH-2004	AY284642
Tylenchomorpha	Sphaerulariidae	BraListr	Bradynema listronotum	DQ915805
		DelSiri2	Deladenus siricidicola	FJ004889
		DelSiri3	Deladenus siricidicola	FJ004890
		DelSiri4	Deladenus siricidicola	EU545475
		DelSiric	Deladenus siricidicola	AY633447
		DelSpeci	Deladenus sp. 1 WB-2008	EU306345

FerSpe10	Fergusobia sp. 56	AY589295
FerSpe11	Fergusobia sp. 444	EF011667
FerSpe12	Fergusobia sp. 281	AY589298
FerSpe13	Fergusobia sp. 469	EF011671
FerSpe15	Fergusobia sp. 282	AY589299
FerSpe16	Fergusobia sp. 330	AY589302
FerSpe17	Fergusobia sp. 19	EF029084
FerSpe20	Fergusobia sp. 451	EF011669
FerSpe22	Fergusobia sp. 465	EF011670
FerSpe23	Fergusobia sp. 329	AY589301
FerSpec3	Fergusobia sp. 39	AY589292
FerSpec4	Fergusobia sp. 357	AY633448
FerSpec5	Fergusobia sp. 421	EF011666
FerSpec6	Fergusobia sp. 54	AY589294
FerSpec9	Fergusobia sp. 339	AY589303
HowAoro2	Howardula aoronymphium	AY589304
HowAoron	Howardula aoronymphium	AF519224
HowarCf0	Howardula cf. aoronymphium	AF519225
HowNeoco	Howardula neocosmis	AF519226
HowSpec2	Howardula sp. SP-F	AF519222
HowSpec3	Howardula sp. SP-B	AF519223
HowSpec4	Howardula sp. SP-PS	AF519231
HowSpec5	Howardula sp. SP-MA	AF519233
HowSpec6	Howardula sp. SP-A	AF519232
NotAcris	Nothotylenchus acris	AY593914
SprBomb2	Sphaerularia bombi	AB250212
SprBombi	Sphaerularia bombi	AB250213
SprVespa	Sphaerularia vespae	AB300595

		TnchdCf0	Tylenchida cf. Helionema sp. MHMH-2008	EU669913
		TnhSpeci	Tylenchina sp. WY-433	EU024567
Tylenchomorpha	Anguinidae	AngTrit3	Anguina tritici	AY593913
		DitAdasi	Ditylenchus adasi	EU669909
		DitAngus	Ditylenchus angustus	AJ966483
		DitDes10	Ditylenchus destructor	EU188752
		DitDes26	Ditylenchus destructor	EU188745
		DitDes27	Ditylenchus destructor	EU188729
		DitDes28	Ditylenchus destructor	EU188748
		DitDes29	Ditylenchus destructor	AY593912
		DitDest9	Ditylenchus destructor	EU188744
		DitDips3	Ditylenchus dipsaci	AY284636
		DitDips4	Ditylenchus dipsaci	AY593911
		DitDips5	Ditylenchus dipsaci	EU669931
		DitDips6	Ditylenchus dipsaci	AY593906
		DitDips7	Ditylenchus dipsaci	AY593909
		DitDips8	Ditylenchus dipsaci	AY593908
		DitSpec3	Ditylenchus sp. 1 JH-2003	AY284637
		DitSpec4	Ditylenchus sp. WY-2004	AY589297
		HlnFucic	Halenchus fucicola	EU669912
		PshMinu2	Pseudhalenchus minutus	AY593916
		PshMinut	Pseudhalenchus minutus	AY284638
		SubRadi2	Subanguina radicicola	AF202164
		SubRadic	Subanguina radicicola	EU682392
		TldSpeci	Tylenchidae sp. BHMM-2005	AY854241
		TnhSpec2	Tylenchina sp. WY-460	EU018049
Tylenchomorpha	Pratylenchidae/ Belonolaimidae	Amplcaru	Amplimerlinius icarus	EU306351

Tylenchomorpha	Tylenchoidea	GeoQuadr	Geocenamus quadrifer	AY993977
		MerBrevi	Merlinius brevidens	AY284597
		NagObsc2	Nagelus obscurus	EU306350
		NagObscu	Nagelus obscurus	AY593904
		PtIMagni	Pratylenchoides magnicauda	AF202157
		PtIRitte	Pratylenchoides ritteri	AJ966497
		ScuQuadr	Scutylenchus quadrifer	AY284599
		CpnHexal	Cephalenchus hexalineatus	AY284594
		BitDubiu	Bitylenchus dubius	AY284601
		BlnLong3	Belonolaimus longicaudatus	AY633449
		BlnLongi	Belonolaimus longicaudatus	EU130838
		DolSpeci	Dolichodorus sp. WY-2006	DQ912918
		GloAchil	Globodera achilleae	FJ040399
		GloArte2	Globodera artemisiae	EU855121
		GloArtem	Globodera artemisiae	FJ040400
		GloPalI5	Globodera pallida	AY284620
		GloPalI6	Globodera pallida	AY593875
		GloPalI7	Globodera pallida	EU855119
		GloPalI8	Globodera pallida	AF036592
		GloRost5	Globodera rostochiensis	AY593881
		GloRost9	Globodera rostochiensis	EU855120
		GloTabac	Globodera tabacum	FJ040401
		HelCanad	Helicotylenchus canadensis	AY284605
		HelDihys	Helicotylenchus dihystra	AJ966486
		HelPseu2	Helicotylenchus pseudorobustus	AY284606
		HelVaric	Helicotylenchus varicaudatus	EU306354
		HelVulga	Helicotylenchus vulgaris	AY284607
		HetAven3	Heterodera avenae	FJ040403

HetBetae	Heterodera betae	FJ040404
HeteMani	Heterodera mani	EU669916
HetGly12	Heterodera glycines	ABLA01015961
HetGly13	Heterodera glycines	ABLA01013124
HetGly15	Heterodera glycines	ABLA01017282
HetGly16	Heterodera glycines	ABLA01014545
HetGly18	Heterodera glycines	ABLA01014793
HetGly20	Heterodera glycines	ABLA01016090
HetGlyc5	Heterodera glycines	ABLA01017129
HetGlyc7	Heterodera glycines	ABLA01019319
HetGlyc9	Heterodera glycines	ABLA01020458
HetGoett	Heterodera goettingiana	EU669915
HetHorde	Heterodera hordecalis	FJ040405
HetKore2	Heterodera koreana	EU306357
HetScha2	Heterodera schachtii	AY284617
HetScha3	Heterodera schachtii	EU306355
HetTrifo	Heterodera trifolii	FJ040402
HirGraci	Hirschmanniella gracilis	EU669959
HirLoofi	Hirschmanniella loofi	EU306353
HirPompo	Hirschmanniella pomponiensis	EF029854
HirSanta	Hirschmanniella santarosae	EF029855
HirscCf0	Hirschmanniella cf. belli ITDL-2006	EF029856
HirSpec2	Hirschmanniella sp. Yuma	EF029857
HirSpec3	Hirschmanniella sp. 1 JH-2003	AY284614
HirSpec4	Hirschmanniella sp. 3 JH-2003	AY284616
HirSpeci	Hirschmanniella sp. 2 JH-2003	AY284615
MacArbu2	Macrotrophurus arbusticola	AY284595
MacArbus	Macrotrophurus arbusticola	AY284596

MelChi19	Meloidogyne chitwoodi	EU669934
MelChi20	Meloidogyne chitwoodi	AY593885
MelEthio	Meloidogyne ethiopica	AY942630
MelFall2	Meloidogyne fallax	AY593895
MelHap42	Meloidogyne hapla	ABLG01003285
MelHap43	Meloidogyne hapla	ABLG01000304
MelIchi2	Meloidogyne ichinohei	EU669954
MelInc22	Meloidogyne incognita (southern root-knot nematode)	CABB01002720
MelInc29	Meloidogyne incognita (southern root-knot nematode)	CABB01000342
MelInco7	Meloidogyne incognita (southern root-knot nematode)	AY268120
MelJava5	Meloidogyne javanica (root-knot nematode)	AY942626
MelJava7	Meloidogyne javanica (root-knot nematode)	EU669938
MelJava8	Meloidogyne javanica (root-knot nematode)	AY268121
MelMari3	Meloidogyne maritima	EU669944
MelMicro	Meloidogyne microtyla	AF442198
MelMino2	Meloidogyne minor	EU669937
MelNaas3	Meloidogyne naasi	AY593901
MeloMali	Meloidogyne mali	EU669948
MeloUlmi	Meloidogyne ulmi	EU669947
MelParan	Meloidogyne paranaensis	AY942622
NacAber7	Nacobbus aberrans	AF442190
NacAber8	Nacobbus aberrans	AJ966494
NdlLamel	Neodolichorhynchus lamelliferus	AY284598
NdlMicro	Neodolichorhynchus microphasmis	EU669917
PncStone	Punctodera stonei	EU682391

PriConva	Pratylenchus convallariae	EU669957
PriCren2	Pratylenchus crenatus	EU669920
PriCren4	Pratylenchus crenatus	EU669922
PriGoode	Pratylenchus goodeyi	AJ966498
PriNegl3	Pratylenchus neglectus	EU669923
PriNegl4	Pratylenchus neglectus	EU669924
PriPene7	Pratylenchus penetrans	EU669925
PriPene8	Pratylenchus penetrans	EU669926
PriScri4	Pratylenchus scribneri	EU669958
PriScri5	Pratylenchus scribneri	EU669927
PriTho16	Pratylenchus thornei	EU669928
PriTho17	Pratylenchus thornei	EU669929
PriVuln6	Pratylenchus vulnus	EU669956
PriVuln7	Pratylenchus vulnus	EU669955
RadSimil	Radopholus similis	AJ966502
RadSpeci	Radopholus sp. 1983	FJ040398
RotRen34	Rotylenchulus reniformis	EU306342
RtiGoode	Rotylenchus goodeyi	AY284609
RtiSpeci	Rotylenchus sp. JH-2004	AY284608
RtiUnif2	Rotylenchus uniformis	EU306356
RtiUnifo	Rotylenchus uniformis	AY593882
SauMaxi4	Sauertylechus maximus	AY284604
SauMaxi5	Sauertylechus maximus	AY284602
SauMaxi6	Sauertylechus maximus	AY284603
ScuBrad2	Scutellonema bradys	AY271723
ScuBrady	Scutellonema bradys	AJ966504
TelVentr	Telotylenchus ventralis	AY593905
TlhClayt	Tylenchorhynchus claytoni	EU368587

		TlhDubi2	Tylenchorhynchus dubius	EU306352
		TlhDubiu	Tylenchorhynchus dubius	EU368586
		TlhLevit	Tylenchorhynchus leviterminalis	EU368585
		TlhMaxim	Tylenchorhynchus maximus	AY993979
		ZygGueva	Zygotylenchus guevarae	AF442189
Tylenchomorpha	Tylenchidae	BoIThyl2	Boleodorus thylactus	AY593915
		BoIThyl3	Boleodorus thylactus	AY993976
		MalAndra	Malenchus andrassyi	AY284587
		OttDiscr	Ottolenchus discrepans	AY284590
Tylenchomorpha	Criconematoidea	CriSpec4	Criconema sp. PDL-2005	AJ966480
		HemConi2	Hemicycliophora conida	EU669914
		HemConi3	Hemicycliophora conida	AJ966471
		HemThien	Hemicycliophora thienemanni	EU306341
		HmcPseu2	Hemicriconemoides pseudobrachyurus	AY284622
		HmcPseu3	Hemicriconemoides pseudobrachyurus	AY284624
		HmcPseud	Hemicriconemoides pseudobrachyurus	AY284623
		LooThie2	Loofia thienemanni	AY284629
		LooThien	Loofia thienemanni	AY284628
		MscXeno3	Mesocriconema xenoplax	AY284626
		MscXeno4	Mesocriconema xenoplax	AY284627
		MscXeno5	Mesocriconema xenoplax	AY284625
		OgmCobbi	Ogma cobbi	EU669918
		OgmMenze	Ogma menzeli	EU669919
		PrnchCf2	Paratylenchus cf. neoamblicephalus	AY284634
		PrnDiant	Paratylenchus dianthus	AJ966496
		PrnMicr2	Paratylenchus microdorus	AY284632
		PrnMicro	Paratylenchus microdorus	AY284633
		PrnStra2	Paratylenchus straeleni	AY284630

Tylenchomorpha	Neotylenchoidea	PrnStrae	Paratylenchus straeleni	AY284631
		TlsSemip	Tylenchulus semipenetrans	AJ966511
		DitBrev2	Ditylenchus brevicauda	AY284635
		EchSpe24	Ecphyadophora sp. JH-2004	AY593917
		EchTenu2	Ecphyadophora tenuissima	EU669911
		EchTenui	Ecphyadophora tenuissima	EU669910
		BasGraci	Basiria gracilis	EU130839
Tylenchomorpha	Tylenchidae	PsileCf0	Psilenchus cf. hilarulus	AY284593
		PsiSpec2	Psilenchus sp. CA12	EU130840
		CosCost5	Coslenchus costatus	AY284581
		CosFrank	Coslenchus franklinae	AY284583
		CosleCf0	Coslenchus cf. franklinae	AY284582
		FilFilif	Filenchus filiformis	AY284592
		FilThor3	Filenchus thornei	AY284591
		LelLepto	Lelenchus leptosoma	AY284584
		NpsMagn2	Neopsilenchus magnidens	AY284585
		TlnArcu2	Tylenchus arcuatus	EU306348
		TlnArcua	Tylenchus arcuatus	EU306349
		TlnSpec2	Tylenchus sp. JH-2003	AY284589
Rhabditidae	Steinernema/ Brevibucca	BreSapro	Brevibucca saprophaga	EU196018
		BreSpeci	Brevibucca sp. SB261	AF202163
		CutVivip	Cuticonema vivipara	EU196019
		SteAffin	Steinernema affine	FJ040425
		SteCarp2	Steinernema carpocapsae	FJ040416
		SteCarp3	Steinernema carpocapsae	AF036604
		SteCarpo	Steinernema carpocapsae	FJ040415
		SteFelt2	Steinernema feltiae	FJ040418

	SteFelt3	Steinernema feltiae	FJ040419
	SteFelt4	Steinernema feltiae	FJ040417
	SteGlas2	Steinernema glaseri	AY284682
	SteGlase	Steinernema glaseri	FJ040422
	SteKrau2	Steinernema kraussei	FJ040420
	SteKraus	Steinernema kraussei	FJ040421
	SteMonti	Steinernema monticolum	FJ040423
	SteScara	Steinernema scarabaei	FJ040424
	SteSpeci	Steinernema sp. 1385	FJ040426
Spirurina	AcaVitea	Acanthocheilonema viteae	DQ094171
	AliAmazo	Alinema amazonicum	DQ442672
	AniPegr2	Anisakis pegreffii	EF180082
	AniSpec2	Anisakis sp.	U94365
	AniSpeci	Anisakis sp.	U81575
	AnlCras4	Anguillicola crassus	DQ490223
	AnlCras5	Anguillicola crassus	DQ118535
	AscaSuu2	Ascaris suum (pig roundworm)	U94367
	AscaSuum	Ascaris suum (pig roundworm)	AF036587
	AscLumbr	Ascaris lumbricoides (common roundworm)	U94366
	AsdSpeci	Aspidodera sp. SAN-2007	EF180070
	AshArcti	Ascarophis arctica	DQ094172
	AspTetra	Aspiculuris tetraptera	EF464551
	AsrGalli	Ascaridia galli	EF180058
	BayProcy	Baylisascaris procyonis	U94368
	BayTrans	Baylisascaris transfuga	U94369
	BrmJusti	Brumptaemilius justini	AF036589
	BruMal11	Brugia malayi	AAQA01004941
	BruMal12	Brugia malayi	AAQA01003643

BruMal15	Brugia malayi	AAQA01004529
BruMal16	Brugia malayi	AAQA01004416
BruMal17	Brugia malayi	AAQA01005177
BruMal18	Brugia malayi	AAQA01004588
BruMala3	Brugia malayi	AAQA01010496
BruMala4	Brugia malayi	AAQA01009726
BruMala5	Brugia malayi	AF036588
BruMala7	Brugia malayi	AAQA01003418
CmlCott2	Camallanus cotti	EF180071
CmlCotti	Camallanus cotti	DQ442662
CmlLacus	Camallanus lacustris	DQ442663
CmlOxyce	Camallanus oxycephalus	DQ503463
CmlSpeci	Camallanus sp. MW-2006	DQ442664
ConEudyp	Contracaecum eudypulae	EF180072
ConMicro	Contracaecum microcephalum	AY702702
ConMulti	Contracaecum multipapillatum	U94370
CruAmeri	Cruzia americana	U94371
CyrLepto	Cyrtosia leptoptera	EU004815
CyrMansi	Cyrtosia mansoni	AY702701
CyrSeura	Cyrtosia seurati	EU004816
DenSpeci	Dentiphilometra sp. MW-2006	DQ442673
DipSpe17	Dipetalonema sp. YQ-2006	DQ531723
DirlImmi2	Dirofilaria immitis (dog heartworm nematode)	AF036638
DirlImmit	Dirofilaria immitis (dog heartworm nematode)	AF182647
DntSpeci	Dentostomella sp.	AF036590
DraInsig	Dracunculus insignis	AY947719
DraMedi2	Dracunculus medinensis	AY947720
DraMedin	Dracunculus medinensis	AY852268

DraOesop	Dracunculus oesophageus	AY852269
DraSpeci	Dracunculus sp. V3104	DQ503457
DujWalto	Dujardinascaris waltoni	EF180081
EcnBorea	Echinuria borealis	EF180064
FlrSpeci	Filarioid sp. JK-2007	EF081340
GnaBinuc	Gnathostoma binucleatum	Z96946
GnaNeopr	Gnathostoma neoprocyonis	Z96947
GnaTurgi	Gnathostoma turgidum	Z96948
GoePelag	Goezia pelagia	U94372
HetGalli	Heterakis gallinarum	DQ503462
HetSpec2	Heterakis sp. 14690	AF083003
HtcTunic	Heterocheilus tunicatus	U94373
HysForta	Hysterothylacium fortalezae	U94374
HysPelag	Hysterothylacium pelagicum	U94375
HysReliq	Hysterothylacium reliquens	U94376
IheInqui	Iheringascaris inquires	U94377
LeiPorte	Leidynema portentosa	EF180073
LitSigmo	Litomosoides sigmodontis	AF227233
LoaLoa02	Loa loa	DQ094173
MarBulbo	Margolisianum bulbosum	AB185161
McrAustr	Micropleura australiensis	DQ442678
MctCloac	Microtetrameres cloacitectus	EU004814
MolIntes	Molnaria intestinalis	DQ442668
NemBaker	Nemhelix bakeri	DQ118537
NilSenti	Nilonema senticosum	DQ442671
NscMacro	Neoascarophis macrouri	DQ442660
OncCervi	Onchocerca cervicalis	DQ094174
OnhSpec3	Onchocercidae sp. WB-2005	DQ103704

OxrsEqui	Oxyuris equi	EF180062
PasAmbig	Passalurus ambiguus	EF464552
PasSpeci	Passalurus sp. SAN-2007	EF180061
PhiSangu	Philometroides sanguineus	DQ442676
PhiSerio	Philometroides seriolae	FJ155811
PhiCypri	Philometra cyprinirutili	DQ442675
PhiLateo	Philometra lateolabracis	FJ161972
PhiMadai	Philometra madai	FJ161974
PhiNemip	Philometra nemipteri	FJ161975
PhiObtur	Philometra obturans	AY852267
PhiOvata	Philometra ovata	DQ442677
PhiSciae	Philometra sciaenae	FJ161971
PhiSpec2	Philometra sp. 1 KMAQ-2008	FJ161973
PhiSpec3	Philometra sp. MW-2006	DQ442674
PhnOncor	Philonema oncorhynchi	DQ442670
PhnSpeci	Philonema sp.	U81574
PhyAlata	Physaloptera alata	AY702703
PhyApivo	Physaloptera apivori	EU004817
PhySpeci	Physaloptera sp. SAN-2007	EF180065
PhyTurg2	Physaloptera turgida	DQ503459
PorAngus	Porrocaecum angusticolle	EU004820
PorDepre	Porrocaecum depressum	U94379
PorStrep	Porrocaecum streperae	EF180074
ProObesa	Protozoophaga obesa	EF180075
ProPacif	Procamallanus pacificus	DQ442665
ProPinto	Procamallanus pinto	DQ442666
ProRebec	Procamallanus rebecae	DQ442667
PrpSpeci	Paraspidodera sp. 21303	AF083005

PseDeci2	Pseudoterranova decipiens (codworm)	U94380
PsrEquor	Parascaris equorum	U94378
RaiSpeci	Raillietnema sp. V3060	DQ503461
RaphAcus	Raphidascaris acus	DQ503460
RhaDenud	Rhabdochona denudata	DQ442659
RhiThysa	Rhigonema thysanophora	EF180067
RonRondo	Rondonia rondoni	DQ442679
SeaDigit	Setaria digitata	DQ094175
SeaTundr	Setaria tundra	EF081341
SerTendo	Serratospiculum tendo	AY702704
SkbSpeci	Skrjabinema sp. SAN-2007	EF180060
SkjScard	Skrjabillanus scardinii	DQ442669
SnhHamat	Synhimantus hamatus	EU004819
SnhLatic	Synhimantus laticeps	EU004818
SpcrLupi	Spirocerca lupi	AY751497
SpcSpeci	Spirocerca sp. SAN-2004	AY751498
SpmIstib	Spirocamallanus istiblenni	EF180076
SpmRarus	Spirocamallanus rarus	DQ494195
SpnCarol	Spinitectus carolini	DQ503464
SulSulca	Sulcascaris sulcata	EF180080
SypMuris	Syphacia muris	EF464553
SypObvel	Syphacia obvelata	EF464554
TgdTorre	Turgida torresi	EF180069
TheKraus	Thelastoma krausi	EF180068
ThlLacry	Thelazia lacrymalis	DQ503458
ToxCani2	Toxocara canis	AF036608
ToxCanis	Toxocara canis	U94382
ToxLeoni	Toxascaris leonina	U94383

		ToxoCati	Toxocara cati	EF180059
		ToxVitul	Toxocara vitulorum	EF180078
		TrrCabal	Terranova caballeroi	U94381
		TrrScoli	Terranova scoliodontis	DQ442661
		TruTrutt	Truttaedacnitis truttae	EF180063
		TtrFissi	Tetrameres fissipina	EF180077
		WelSiame	Wellcomia siamensis	EF180079
		WelSpeci	Wellcomia sp. SAN-2007	EF180066
		WucBanc3	Wuchereria bancrofti	AF227234
		WucBanc4	Wuchereria bancrofti	AY843438
Odontopharyngidae/Myolaimidae		MyoSpeci	Myolaimus sp.	U81585
		OdtLongi	Odontopharynx longicaudata	FJ040449
Rhabditidae	Poikilolaimus/ Cuticularia	CutSpec2	Cuticularia sp.	U81583
		CutSpeci	Cuticularia sp. PS-2006	DQ385848
		PoiOxyc2	Poikilolaimus oxycercus	AF083023
		PoiOxyce	Poikilolaimus oxycercus	FJ040436
		PoiRegen	Poikilolaimus regenfussi	AF083022
		PoiSpeci	Poikilolaimus sp. RGD617	AB370214
		RhtSpec2	rhabditoid sp. PDL15	EU196015
Bunonematidae	Bunonema	BunFranz	Bunonema franzi	AJ966477
		BunReti2	Bunonema reticulatum	AY284661
		BunReti3	Bunonema reticulatum	FJ040450
		BunReti4	Bunonema reticulatum	AY593925
		BunRetic	Bunonema reticulatum	EU196017
		BunRich2	Bunonema richtersi	FJ040452
		BunRicht	Bunonema richtersi	FJ040451

Diplogasteroidea	BunSpeci	Bunonema sp.	U81582
	AduHalic	Aduncospiculum halicti	U61759
	DemSpeci	Demaniella sp. 2007	FJ040438
	DpsSpeci	Diplogasterid sp. JH-2004	AY284689
	DptMagnu	Diplogasteroides magnus	FJ040448
	FicSpeci	Fictor sp. 2011	FJ040437
	KoeSpec2	Koerneria sp. SB110	EU196025
	MnnStria	Mononchoides striatus	AY593924
	MyctUlmi	Myctolaimus ulmi	EU196024
	PrsAeri2	Pristionchus aerivorus	FJ040440
	PrsAmer2	Pristionchus americanus	FJ040445
	PrsEnto2	Pristionchus entomophagus	FJ040441
	PrsLhe10	Pristionchus Iheritieri	AY593923
	PrsLhe11	Pristionchus Iheritieri	AY284690
	PrsLhe12	Pristionchus Iheritieri	AF036640
	PrsLher9	Pristionchus Iheritieri	FJ040439
	PrsMari2	Pristionchus marianneae	FJ040442
	PrsMaup3	Pristionchus maupasi	FJ040443
	PrsPaci3	Pristionchus pacificus	AF083010
	PrsPaci4	Pristionchus pacificus	U81584
	PrsPaul2	Pristionchus pauli	FJ040446
	PrsPseu2	Pristionchus pseud aerivorus	FJ040447
	PrsUnif2	Pristionchus uniformis	FJ040444
	TylFoeti	Tylopharynx foetidus	EU306343
Strongyloidea	AelAbstr	Aelurostrongylus abstrusus	AJ920366
	AmiCygni	Amidostomum cygni	AJ920353
	AncCanin	Ancylostoma caninum (dog hookworm)	AJ920347
	AncDuode	Ancylostoma duodenale	EU344798

AnsCanto	Angiostrongylus cantonensis	AY295804
AnsCost2	Angiostrongylus costaricensis	DQ116748
AnsCosta	Angiostrongylus costaricensis	EF514913
AnsDuja2	Angiostrongylus dujardini	EF514915
AnsMalay	Angiostrongylus malaysiensis	EF514914
AnsVaso2	Angiostrongylus vasorum	EF514916
AnsVaso3	Angiostrongylus vasorum	AJ920365
ChaOvina	Chabertia ovina	AJ920341
ClcInsig	Cylicocyclus insignis	AJ920342
CreMephi	Crenosoma mephitidis	AY295805
CreVulpi	Crenosoma vulpis	AJ920367
CycPurvi	Cyclodontostomum purvisi	AJ920340
DctCapr2	Dictyocaulus capreolus	AY168862
DctEcke4	Dictyocaulus eckerti	AY168857
DctFila2	Dictyocaulus filaria	AJ920362
DctFilar	Dictyocaulus filaria	AY168861
DctSpeci	Dictyocaulus sp. P6A1	AY168860
DctVivi2	Dictyocaulus viviparus (bovine lungworm)	AJ920361
DctVivip	Dictyocaulus viviparus (bovine lungworm)	AY168856
DidHayes	Didelphostrongylus hayesi	AY295806
DltDimid	Deletrocephalus dimidiatus	AJ920346
FldMarti	Filaroides martis	AY295807
FlnFlagr	Filarinema flagrifer	AJ920354
HaeCont2	Haemonchus contortus	EU086375
HaeCont3	Haemonchus contortus	L04153
HaeConto	Haemonchus contortus	EU086374
HaeSpeci	Haemonchus sp. V3091	DQ503465
HallInvag	Halocercus invaginatus	AY295808

HerPytho	Herpetostrongylus pythonis	AJ920358
HlgPoly2	Heligmosomoides polygyrus	AJ920355
HlgPolyg	Heligmosomoides polygyrus	AY542283
HovVarie	Hovorkonema variegatum	AY702705
HthBact2	Heterorhabditis bacteriophora	FJ040429
HthBact3	Heterorhabditis bacteriophora	FJ040430
HthBact4	Heterorhabditis bacteriophora	AF036593
HthBacte	Heterorhabditis bacteriophora	FJ040428
HthHepia	Heterorhabditis hepialus	AF083004
HthMarel	Heterorhabditis marelatus	FJ040431
HthMegi2	Heterorhabditis megidis	FJ040433
HthMegi3	Heterorhabditis megidis	FJ040434
HthMegid	Heterorhabditis megidis	FJ040432
HthSpeci	Heterorhabditis sp. 1395	FJ040435
HthZeala	Heterorhabditis zealandica	AJ920368
HypMacro	Hypodontus macropi	AJ920339
KalCrist	Kalicephalus cristatus	AJ920349
LbsBipap	Labiostrongylus bipapillosus	AJ920337
MtsElong	Metastrongylus elongatus	AJ920363
MtsSalmi	Metastrongylus salmi	AY295809
MueCapil	Muellerius capillaris	AY295810
NecAmer2	Necator americanus	AJ920348
NecAmeri	Necator americanus	AY295811
NemBatt2	Nematodirus battus	U01230
NemBattu	Nematodirus battus	AJ920360
NicCamer	Nicollina cameroni	AJ920357
NipBras2	Nippostrongylus brasiliensis	AJ920356
NipBrasi	Nippostrongylus brasiliensis	AF036597

	OsOsler	Oslerus osleri	AY295812
	OstLepto	Ostertagia leptospicularis	AJ920351
	OstOste2	Ostertagia ostertagi	AJ920352
	OstOster	Ostertagia ostertagi	AF036598
	OtoCircu	Otostrongylus circumlitus	AY295813
	OtoSpeci	Otostrongylus sp.	U81589
	PetPocul	Petrovinema poculatum	AJ920343
	PlpOdoco	Parelaphostrongylus odocoilei	AY295815
	PrfDecor	Parafilaroides decorus	AY295814
	PrfSpeci	Parafilaroides sp.	U81590
	PsdInfle	Pseudalius inflexus	AY295816
	PtsRufes	Protostrongylus rufescens	AJ920364
	SkrChitw	Skrjabinstrongylus chitwoodorum	AY295819
	SngTrac2	Syngamus trachea	AJ920344
	SngTrach	Syngamus trachea	AF036606
	StgEquin	Strongylus equinus	DQ094176
	StnMinor	Stenurus minor	AY295817
	StpDenta	Stephanurus dentatus	AJ920345
	TetMacke	Tetrabothriostrongylus mackerrasae	AJ920359
	TorConvo	Torynurus convolutus	AY295818
	TrgWilso	Troglostrongylus wilsoni	AY295820
	TrsColub	Trichostrongylus colubriformis	AJ920350
	ZonMawso	Zoniolaimus mawsonae	AJ920338
Rhabditidae	CaeBrenn	Caenorhabditis brenneri	U13930
	CaeBrig5	Caenorhabditis briggsae	U13929
	CaeBrig6	Caenorhabditis briggsae	FJ380929
	CaeDroso	Caenorhabditis drosophilae	AF083025
	CaeEleg2	Caenorhabditis elegans	EU196001

CaeEleg5	Caenorhabditis elegans	Z92784
CaeEleg6	Caenorhabditis elegans	Z92784
CaeJapon	Caenorhabditis japonica	AY602182
CaePlica	Caenorhabditis plicata	AY602178
CaeReman	Caenorhabditis remanei	U13931
CaeSpec2	Caenorhabditis sp. DF5070	AY602181
CaeSpec3	Caenorhabditis sp. JU727	EU196000
ChhCrist	Choriorhabditis cristata	EU196013
ChhDudic	Choriorhabditis dudichi	AF083012
Cplbdcf0	Cephaloboides cf. armata SB363	EU196005
CplNidro	Cephaloboides nidrosiensis	EU196020
CplSpeci	Cephaloboides sp. SB227	AF083027
CrzSpec2	Cruznema sp. JH-2004	AY284658
CrzSpec3	Cruznema sp. JH-2004	AY284657
CrzSpec4	Cruznema sp. JH-2004	AY284656
CrzSpeci	Cruznema sp. JH-2004	AY284655
CrzTrip2	Cruznema tripartitum	EU196012
CrzTripa	Cruznema tripartitum	U73449
DpcCoron	Diploscapter coronatus	AY593921
DpcSpec2	Diploscapter sp.	U81586
DpcSpec3	Diploscapter sp. PS1897	AF083009
DpcSpeci	Diploscapter sp. JU359	EU196003
HtbChong	Heterorhabditidoides chongmingensis	EF503692
OscDoli2	Oscheius dolichuroides	AF082998
OscDolic	Oscheius dolichura	EU196010
OscGuent	Oscheius guentheri	EU196022
OscInsec	Oscheius insectivora	AF083019
OscSpec2	Oscheius sp. BW282	AF082994

	OscTipu2	Oscheius tipulae	EU196009
	OscTipu3	Oscheius tipulae	AF036591
	PdnWirth	Prodontorhabditis wirthi	AY602179
	PelMarin	Pellioditis marina	AF083021
	PelMedit	Pellioditis mediterranea	AF083020
	PelSpe28	Pellioditis sp. JU274	EU196011
	PelTypic	Pellioditis typica	U13933
	PhaHerm2	Phasmarhabditis hermaphrodita	DQ639981
	PhaHerma	Phasmarhabditis hermaphrodita	DQ639980
	PhaSpeci	Phasmarhabditis sp. EM434	EU196008
	PrbSpec2	Protorhabditis sp. JB122	EU196002
	PrbSpec3	Protorhabditis sp. SB208	AF083024
	PrbSpeci	Protorhabditis sp. DF5055	AF083001
	RhbBlumi	Rhabditis blumi	U13935
	RhbBrass	Rhabditis brassicae	EU196006
	RhbColom	Rhabditis colombiana	AY751546
	RhbdtCf5	Rhabditis cf. terricola JH-2004	AY284653
	RhbMyri2	Rhabditis myriophila	U13936
	RhbMyrio	Rhabditis myriophila	U81588
	RhbRaina	Rhabditis rainai	AF083008
	RhbSpec2	Rhabditis sp. Tumian-2007	EU273597
	RhbSpec3	Rhabditis sp. SB347	EU196004
	RhbSpeci	Rhabditis sp. DF5059	EU196007
	RhIIAxe2	Rhabditella axei	U13934
	RhIIAxei	Rhabditella axei	AY284654
	RhISpeci	Rhabditella sp. DF5044	AF083000
Rhabditidae	CruScan2	Crustorhabditis scanica	AF083014
	DstVeec2	Distolabrellus veechi	AF082999

DstVeech	Distolabrellus veechi	AF083011
MsrAniso	Mesorhabditis anisomorpha	AF083013
MsrLong2	Mesorhabditis longespiculosa	EU543178
MsrLonge	Mesorhabditis longespiculosa	EU196014
MsrMiotk	Mesorhabditis miotki	EU543177
MsrSpec6	Mesorhabditis sp. JH-2004	AY284660
MsrSpec7	Mesorhabditis sp.	U73452
MsrSpec8	Mesorhabditis sp. JH-2004	AY593922
MsrSpicu	Mesorhabditis spiculigera	AF083016
PelPseud	Pelodera pseudoteres	EU196023
PelTeres	Pelodera teres	AF083002
PstObtus	Parasitorhabditis obtusa	EU003189
PstSpeci	Parasitorhabditis sp. SB281	AF083028
RhaRegin	Rhabditoides regina	AF082997
TrtPalma	Teratorhabditis palmarum	U13937
TrtSynp2	Teratorhabditis synpapillata	AF083015
TrtSynpa	Teratorhabditis synpapillata	AB269816

Table A2.3: List of all LSU nematode sequences utilised in this study, including accession numbers, taxonomic information from EMBL, and ARB alphanumeric code used in phylogenetic trees.

ARB Code	Taxonomic ID (EMBL)	Accession Number
AcbComp2	Acrobeles complexus	DQ145620
AcbMaene	Acrobeles maeneeneus	DQ145621
AcbMaxi2	Acrobeles maximus	EU195987
AcbSingu	Acrobeles singulus	DQ145622
AcbSpec5	Acrobeles sp. JB-132	DQ145623
AcmlldAff	Acromoldavicus aff. mojavicus SAN-2001	AY027534
AcmMojav	Acromoldavicus mojavicus	DQ145626
AcrBode3	Acrobeloides bodenheimeri	AF147065
AcrBode4	Acrobeloides bodenheimeri	AF147064
AcrBode5	Acrobeloides bodenheimeri	DQ145625
AcrBuet2	Acrobeloides buetschlii	DQ903104
AcrBuet3	Acrobeloides buetschlii	DQ903081
AcrCamb2	Acrobeloides camberenensis	DQ903088
AcrCambe	Acrobeloides camberenensis	AF147069
AcrElles	Acrobeloides ellesmerensis	DQ145624
AcrMaxi3	Acrobeloides maximus	AF147066
AcrMaxi4	Acrobeloides maximus	AF147067
AcrMaxi5	Acrobeloides maximus	DQ903097
AcrMaxi6	Acrobeloides maximus	EF417138
AcrMaxi7	Acrobeloides maximus	DQ903078
AcrNanu3	Acrobeloides nanus	EF417139
AcrNanu4	Acrobeloides nanus	DQ903075
AcrNanu5	Acrobeloides nanus	DQ903076
AcrNanu6	Acrobeloides nanus	DQ903103
AcrSp136	Acrobeloides sp. PP2	DQ077788
AcrSp137	Acrobeloides sp. JB-68	DQ903091
AcrSp138	Acrobeloides sp. JB-80	DQ903096
AcrSp139	Acrobeloides sp. DWF-1106	DQ903080
AcrSp140	Acrobeloides sp. JB-77	DQ903093
AcrSp141	Acrobeloides sp. PS-1146	DQ903101
AcrSp142	Acrobeloides sp. DWF-1108	DQ903082
AcrSp143	Acrobeloides sp. IZ-001	DQ903085
AcrSp144	Acrobeloides sp. JB-14	DQ903086
AcrSp145	Acrobeloides sp. PDL-33	DQ903099
AcrSp146	Acrobeloides sp. DWF-1105	DQ903079
AcrThor2	Acrobeloides thornei	AF147068
AcrThor3	Acrobeloides thornei	DQ903083
AcrUberr	Acrobeloides uberrinus	DQ903087
AcsHalic	Acrostichus halicti	EU195983
AelAbst2	Aelurostrongylus abstrusus	AM039759
AlaSpec3	Alaimus sp. PDL-2005	DQ077791
AldAndr2	Allodorylaimus andrassyi	AY593016

AldAndr3	Allodorylaimus andrassyi	AY593015
AmiCygn2	Amidostomum cygni	AM039745
Amplcar2	Amplimerlinius icarus	DQ328714
AnaTrid3	Anatonchus tridentatus	AY593065
AncCani2	Ancylostoma caninum (dog hookworm)	AM039739
AngTrit4	Anguina tritici	DQ328723
AniSimp5	Anisakis simplex 'C' SAN-2004	AY821754
AniSpec9	Anisakis sp. SAN-2004	AY821759
AnsCant2	Angiostrongylus cantonensis	AY292792
AnsVaso4	Angiostrongylus vasorum	AM039758
AnsVaso5	Angiostrongylus vasorum	AM039758
AphBess2	Aphelenchoides besseyi	DQ328684
AphBess3	Aphelenchoides besseyi	AY508109
AphFrag5	Aphelenchoides fragaria	DQ328683
AphFrag6	Aphelenchoides fragariae	AB368540
AphSpe11	Aphelenchoides sp. TG102006	EU084037
AphSpe12	Aphelenchoides sp. CA22	DQ328682
AphStam2	Aphelenchoides stammeri	AM396582
AplAven6	Aphelenchus avenae	AB368536
AplSpec4	Aphelenchus sp. SAN-2005	DQ145664
ApoObtu3	Aporcelaimellus obtusicaudatus	AY593018
ApoObtu4	Aporcelaimellus obtusicaudatus	AY593019
AporcC10	Aporcelaimellus cf. paraobtusicaudatus JH-2004	AY593020
AporcC11	Aporcelaimellus cf obtusicaudatus JH-2004	AY593017
ApoSpec5	Aporcelaimellus sp. JH-2004	AY593021
AscaSuu4	Ascaris suum (pig roundworm)	AY821773
AscLumb6	Ascaris lumbricoides (common roundworm)	AY210806
AscSpec2	Ascolaimus sp. 1P6K2	DQ077749
AtaCrass	Atalodera crassicrustata	DQ328704
AUhYyyy2	AUK_35_Oncholaimus_D2D3	(Present Study)
AUhYyyy3	AUK_36_Oncholaimus_D2D3	(Present Study)
AUhYyyy	AUK_23_Oncholaimus_D2D3	(Present Study)
AUpYyyy	AUK_13_Calyptronema_D2D3	(Present Study)
AUrYyyy	AUK_45_Tripyloides_D2D3	(Present Study)
AUVYyyy	AUK_10_Viscosia_D2D3	(Present Study)
AUxYyyy	AUK_14_Oxystomina_D2D3	(Present Study)
AxnProp2	Axonchium propinquum	AY593022
BAHYyyy2	BCA_16_Halalaimus_D2D3	(Present Study)
BAHYyyy3	BCA_17_Halalaimus_D2D3	(Present Study)
BAHYyyy4	BCA_25_Halalaimus_D2D3	(Present Study)
BAHYyyy5	BCA_38_Halalaimus_D2D3	(Present Study)
BAHYyyy	BCA_12_Halalaimus_D2D3	(Present Study)
BAKYyyy	BAUK_9_Oxystomina_D2D3	(Present Study)
BALYyyy	BCA_37_Phanodermatidae_D2D3	(Present Study)
BAmYyyy	BCA_3_Pareurystomina_D2D3	(Present Study)
BAnYyyy	BCA_32_Phanodermatidae_D2D3	(Present Study)
BAOYyyy	BCA_35_Oxystomina_D2D3	(Present Study)
BAPYyyy	BCA_20_Phanodermatidae_D2D3	(Present Study)

BArnYyyg	BCA_47_Syringolaimus_D2D3	(Present Study)
BArYyyy2	BCA_2_Syringolaimus_D2D3	(Present Study)
BArYyyy3	BCA_31_Syringolaimus_D2D3	(Present Study)
BArYyyy4	BCA_41_Syringolaimus_D2D3	(Present Study)
BArYyyy5	BCA_5_Syringolaimus_D2D3	(Present Study)
BArYyyy6	BCA_6_Syringolaimus_D2D3	(Present Study)
BArYyyyy	BCA_1_Syringolaimus_D2D3	(Present Study)
BasGrac2	Basiria gracilis	DQ328717
BasSpeci	Basiria sp. SAN-2005	DQ145619
BayProc2	Baylisascaris procyonis	AY821774
BCcYyyy2	BCA_19_Mesacanthion_Paramesacanthion_D2D3	(Present Study)
BCcYyyyy	BCA_14_Mesacanthion_Paramesacanthion_D2D3	(Present Study)
BCfYyyyy	BCA_10_Trefusia_D2D3	(Present Study)
BCxsYyyf	BCA_42_Oxystomina_D2D3	(Present Study)
BCxYyyy2	BCA_22_Oxystomina_D2D3	(Present Study)
BCxYyyy3	BCA_23_Oxystomina_D2D3	(Present Study)
BCxYyyy4	BCA_21_Oxystomina_D2D3	(Present Study)
BCxYyyyy	BCA_15_Oxystomina_D2D3	(Present Study)
BlnEuth2	Belonolaimus euthychilus	DQ672359
BlnEuth3	Belonolaimus euthychilus	DQ672360
BlnEuthy	Belonolaimus euthychilus	DQ672361
BlnGrac2	Belonolaimus gracilis	DQ672362
BlnGraci	Belonolaimus gracilis	DQ672363
BlnLon10	Belonolaimus longicaudatus	DQ672354
BlnLon11	Belonolaimus longicaudatus	DQ672345
BlnLon12	Belonolaimus longicaudatus	DQ672356
BlnLon13	Belonolaimus longicaudatus	DQ672347
BlnLon14	Belonolaimus longicaudatus	DQ672358
BlnLon15	Belonolaimus longicaudatus	DQ672343
BlnLon16	Belonolaimus longicaudatus	DQ672355
BlnLon17	Belonolaimus longicaudatus	DQ672349
BlnLon18	Belonolaimus longicaudatus	DQ672353
BlnLon19	Belonolaimus longicaudatus	DQ672352
BlnLon20	Belonolaimus longicaudatus	DQ672346
BlnLon21	Belonolaimus longicaudatus	DQ672348
BlnLong5	Belonolaimus longicaudatus	DQ672350
BlnLong6	Belonolaimus longicaudatus	DQ915803
BlnLong7	Belonolaimus longicaudatus	DQ672344
BlnLong8	Belonolaimus longicaudatus	DQ672357
BlnLong9	Belonolaimus longicaudatus	DQ672351
BoISpeci	Boleodorus sp. Germany 709	DQ328718
BraList2	Bradynema listronotum	DQ915804
BraRigid	Bradynema rigidum	DQ328730
BrePunct	Brevibucca punctata	DQ077787
BreSapr2	Brevibucca saprophaga	DQ077786
BreSapr3	Brevibucca saprophaga	EU195990
BreSpec2	Brevibucca sp. SB-261	DQ145627
BrsSpec2	Bursilla sp. PS1179	EF990722

BrsSpeci	Bursilla sp. PS1179	EF990722
BUcYyyy2	BUS_2_Oncholaimus_D2D3	(Present Study)
BUcYyyy3	BUS_3_Oncholaimus_D2D3	(Present Study)
BUcYyyy4	BUS_4_Oncholaimus_D2D3	(Present Study)
BUcYyyy5	BUS_5_Oncholaimus_D2D3	(Present Study)
BUcYyyy6	BUS_7_Oncholaimus_D2D3	(Present Study)
BUcYyyy	BUS_1_Oncholaimus_D2D3	(Present Study)
BUIYyyy	BUS_21_Anoplostoma_D2D3	(Present Study)
BunReti5	Bunonema reticulatum	EU195989
BunSpec2	Bunonema sp. PDL-2005	DQ077789
BUpYyyy	BUS_15_Tripyloides_D2D3	(Present Study)
BurAbie2	Bursaphelenchus abietinus	AY508074
BurArthu	Bursaphelenchus arthuri	AM396564
BurHylo2	Bursaphelenchus hylobianum	AY508085
BurMuc10	Bursaphelenchus mucronatus	EU295500
BurMuc11	Bursaphelenchus mucronatus	EU295493
BurParv2	Bursaphelenchus parvispicularis	AB368537
BurRain4	Bursaphelenchus rainulfi	AM396575
BursDou5	Bursaphelenchus doui	AB299226
BurSexd5	Bursaphelenchus sexdentati	AY508100
BurSexd6	Bursaphelenchus sexdentati	AY508103
BurSine3	Bursaphelenchus sinensis	EU752257
BurSpec7	Bursaphelenchus sp. 169	AY508092
BurSpec8	Bursaphelenchus sp. P4193	EU159108
BurTusc2	Bursaphelenchus tusciae	AY508104
BurXyl15	Bursaphelenchus xylophilus	EU295491
CacCacti	Cactodera cacti	DQ328702
CaeBren3	Caenorhabditis brenneri	DQ059062
CaeBren4	Caenorhabditis brenneri	AY602175
CaeBrig7	Caenorhabditis briggsae	EF417140
CaeBrig8	Caenorhabditis briggsae	AY604481
CaeBrig9	Caenorhabditis briggsae	AY604481
CaeDros2	Caenorhabditis drosophilae	AY602172
CaeEleg7	Caenorhabditis elegans	EF417141
CaeEleg8	Caenorhabditis elegans	X03680
CaeJapo2	Caenorhabditis japonica	AY602173
CaePlic2	Caenorhabditis plicata	AY602167
CaeRema5	Caenorhabditis remanei	AY602174
CaeSpe10	Caenorhabditis sp. SB341	AY602170
CaeSpe11	Caenorhabditis sp. JU727	EU195957
CaeSpec5	Caenorhabditis sp. SB341	AY602170
CaeSpec6	Caenorhabditis sp. DF5070	AY602171
CaeSpec7	Caenorhabditis sp. JU727	EU195957
CaeSpec8	Caenorhabditis sp. PS1010	AY604482
CaeSpec9	Caenorhabditis sp. DF5070	AY602171
CAnYyyy	Cr_38_Anticomidae_D2D3	(Present Study)
CarBana2	Carcharodiscus banaticus	AY593023
CarBana3	Carcharodiscus banaticus	AY593024

CbDYyyy2	Cr_21b_Comesomatidae_D2D3	(Present Study)
CbDYyyy3	Cr_74b_Halalaimus_D2D3	(Present Study)
CbDYyyy4	Cr_75b_Halalaimus_D2D3	(Present Study)
CbDYyyy5	Cr_77b_Halalaimus_D2D3	(Present Study)
CbDYyyy6	Cr_85b_Halalaimus_D2D3	(Present Study)
CbDYyyyy	Cr_20b_Halalaimus_D2D3	(Present Study)
CbEYyyy	Cr_71b_Phanodermopsis_D2D3	(Present Study)
CbMYyyy	Cr_18b_Mesacanthion_Paramesacanthion_D2D3	(Present Study)
CbnYyyy	Cr_19b_Phanodermopsis_D2D3	(Present Study)
CbRYyyy	Cr_82b_Thoracostomopsidae_D2D3R_F09	(Present Study)
CbxYyyy	Cr_76b_Oxystomina_D2D3	(Present Study)
CCDYyyy	Cr_83b_Halalaimus_D2D3	(Present Study)
CClYyyy	Cr_83a_Chaetonema_D2D3	(Present Study)
CCOYyyy	Cr_76a_Chaetonema_D2D3	(Present Study)
CdrBrink	Cryphodera brinkmani	DQ328705
CepSpec4	Cephalobidae sp. PS1146	EF417142
CerAlut2	Cervidellus alutus	DQ145629
CerAlut3	Cervidellus alutus	AF331911
CerDoors	Cervidellus doorsselaeri	DQ145630
CerNefta	Cervidellus neftasiensis	DQ145631
CerSpec2	Cervidellus sp. JB-138	DQ145632
ChaOvin4	Chabertia ovina	AM039733
CHCYyyy	Cr_73a_Chaetonema_D2D3	(Present Study)
ChhCris2	Choriorhabditis cristata	EU195976
ChhDudi2	Choriorhabditis dudichi	EU195975
ChiSpec2	Chiloplacus sp. JB-81	DQ145634
ChmSpec3	Chromadorina sp. 1M21G4	DQ077776
ChoSpec3	Choanolaimus sp. 8M21G4	DQ077777
ChsAtte4	Chrysonema attenuatum	AY593029
CHtYyyy	Cr_73b_Halalaimus_D2D3	(Present Study)
ClaClav2	Clavicaudoides clavicaudatus	EF207234
ClaClav3	Clavicaudoides clavicaudatus	EF207235
ClaTrop4	Clavicaudoides trophurus	EF207237
ClaTrop5	Clavicaudoides trophurus	EF207236
ClcInsi2	Cylicocyclus insignis	AM039734
CIIYyy10	Cr_62_Halalaimus_D2D3	(Present Study)
CIIYyy11	Cr_63_Halalaimus_D2D3	(Present Study)
CIIYyy12	Cr_64_Halalaimus_D2D3	(Present Study)
CIIYyy13	Cr_86_Halalaimus_D2D3	(Present Study)
CIIYyy2	Cr_9_Halalaimus_D2D3	(Present Study)
CIIYyy3	Cr_11_Halalaimus_D2D3	(Present Study)
CIIYyy4	Cr_13_Halalaimus_D2D3	(Present Study)
CIIYyy5	Cr_35_Halalaimus_D2D3	(Present Study)
CIIYyy6	Cr_55_Halalaimus_D2D3	(Present Study)
CIIYyy7	Cr_59_Halalaimus_D2D3	(Present Study)
CIIYyy8	Cr_60_Halalaimus_D2D3	(Present Study)
CIIYyy9	Cr_61_Halalaimus_D2D3	(Present Study)
CIIYyyy	Cr_7_Halalaimus_D2D3	(Present Study)

ClSYYYY2	Cr_77a_Oxystomina_D2D3	(Present Study)
ClSYYYY3	Cr_85a_Halalaimus_D2D3	(Present Study)
ClSYYYY	Cr_74a_Halalaimus_D2D3	(Present Study)
CmdSpec2	Chromadorida sp. 9P8K2	DQ077765
CmdSpec3	Chromadorida sp. 1I11K2	DQ077757
CmdSpeci	Chromadorida sp. 5I9K2	DQ077755
CmnSpeci	Ceramonematidae sp. 8I12K2	DQ077773
CMsYYYY	Cr_34_Mesacanthion_Paramesacanthion_D2D3	(Present Study)
CnDYYYYY	Cr_78a_Bathyeurystomina_D2D3	(Present Study)
CnfCrani	Cranifera cranifera	EU365632
COCYYYY	Cr_84b_Chaetonema_D2D3	(Present Study)
COhYYYY	Cr_80b_Bathyeurystomina_D2D3	(Present Study)
COmYYYY	Cr_87_Oxystomina_D2D3	(Present Study)
ConEudy2	Contracaecum eudyptulae	AF226586
ConMicr2	Contracaecum micropapillatum	AF226587
ConMicr3	Contracaecum microcephalum	AF226573
ConMirou	Contracaecum mirounga	AF226581
ConMult4	Contracaecum multipapillatum	AF226574
ConOgmor	Contracaecum ogmorhini	AF226582
ConOscu3	Contracaecum osculatum baicalensis	AF226589
ConOscu4	Contracaecum osculatum	AF226583
ConOscu5	Contracaecum osculatum	AF226576
ConOscu6	Contracaecum osculatum	AF226580
ConRadia	Contracaecum radiatum	AF226577
ConRudo2	Contracaecum rudolphii	AF226579
ConRudo3	Contracaecum rudolphii	AF226585
ConSepte	Contracaecum septentrionale	AF226588
ConSpec3	Contracaecum sp. SAN-2004	AY821768
ConSpec4	Contracaecum sp. SAN-2004	AY821770
ConSpec5	Contracaecum sp. SAN-2004	AY821769
CosCost6	Coslenchus costatus	DQ328719
COTYYYY	Cr_80a_Oxystomina_D2D3	(Present Study)
CPdYyyy2	Cr_33_Phanodermopsis_D2D3	(Present Study)
CPdYyyy3	Cr_54_Phanodermopsis_D2D3	(Present Study)
CPdYyyy4	Cr_56_Phanodermopsis_D2D3	(Present Study)
CPdYyyy5	Cr_66_Phanodermopsis_D2D3	(Present Study)
CPdYyyy6	Cr_68_Phanodermopsis_D2D3	(Present Study)
CPdYyyy	Cr_3_Phanodermopsis_D2D3	(Present Study)
CphCuba2	Cephalobus cubaensis	DQ903102
CphPers3	Cephalobus persegnis	DQ903077
CphSpe10	Cephalobus sp. JB-65	DQ903090
CphSpe11	Cephalobus sp. JB-63	DQ903089
CphSpe12	Cephalobus sp. DWF-1301	DQ903084
CphSpe13	Cephalobus sp. JB-78	DQ903094
CphSpec5	Cephalobus sp. JB-117	DQ903098
CphSpec6	Cephalobus sp. JB-67	DQ145628
CphSpec7	Cephalobus sp. JB-70	DQ903092
CphSpec8	Cephalobus sp. JB-79	DQ903095

CphSpec9	Cephalobus sp. PS-1143	DQ903100
CplbdCf2	Cephaloboides cf. armata SB363	EU195961
CplNidr2	Cephaloboides nidrosiensis	EU195992
CPrYyyy	Cr_26_Phanodermatidae_D2D3	(Present Study)
CreMeph2	Crenosoma mephitidis	AY292793
CreVulp2	Crenosoma vulpis	AM039760
CreVulp3	Crenosoma vulpis	AM039760
CrFYyyy	Cr_24b_Metaparoncholaimus_Meyer_D2D3F_E10	(Present Study)
CruTrans	Crustorhabditis transita	EU195995
CrzTrip3	Cruznema tripartitum	EU195974
CSHYyyy	Cr_72a_Halalaimus_D2D3	(Present Study)
CSLYyyy	Cr_72b_Phanodermatidae_D2D3	(Present Study)
CstAtrac	Cystoopsis atractostei	DQ060331
CtDYyyy	Cr_82a_Halalaimus_D2D3	(Present Study)
CTrYyyy	Cr_1_Thoracostomopsidae_D2D3	(Present Study)
CutVivi2	Cuticonema vivipara	EU195991
CyaSpec3	Cyatholaimidae sp. 2I12K3	DQ077782
CycPurv2	Cyclodontostomum purvisi	AM039732
DBcYyyy	DBA_4_Oncholaimus_D2D3	(Present Study)
DBdsYyyh	DBA_7_Enoploides_D2D3	(Present Study)
DBdYyyy2	DBA_2_Enoploides_D2D3	(Present Study)
DBdYyyy3	DBA_3_Enoploides_D2D3	(Present Study)
DBdYyyy4	DBA_5_Enoploides_D2D3	(Present Study)
DBdYyyy	DBA_1_Enoploides_D2D3	(Present Study)
DBFYyyy	DBA6_Enoploides_D2D3F_G10	(Present Study)
DBsYyyy	_DBA_21_Enoplus_D2D3	(Present Study)
DctFila3	Dictyocaulus filaria	AM039754
DctFila4	Dictyocaulus filaria	AM039754
DctVivi3	Dictyocaulus viviparus (bovine lungworm)	AM039753
DeISiri5	Deladenus siricidicola	AY633444
DicLova2	Dicelis lovatiana	AY967868
DicRubi2	Dicelis rubidi	AY967866
DicSpec9	Dicelis sp. 'Aberdeen'	AY967867
DidHaye3	Didelphostrongylus hayesi	AY292794
DiscoCf2	Discolaimus cf. major HHBM-2007a	EF207239
DisMajo2	Discolaimus major	AY593025
DisMajo3	Discolaimus major	AY593026
DlcSpeci	Dolichodera sp. New Zealand 576	DQ328701
DltDimi2	Deletrocephalus dimidiatus	AM039738
DoIMedit	Dolichodorus mediterraneus	DQ838803
DpcSpec4	Diploscapter sp. JU359	EU195959
DpgIneri	Diplogaster inerti	EF417143
DphSpeci	Diphtherophora sp. PDL-2005	DQ077790
DrmLimn3	Dorylaimoides limnophilus	AY593003
DrmMico2	Dorylaimoides micoletzkyi	AY593004
DrsStag3	Dorylaimus stagnalis	AY592995
DrsStag4	Dorylaimus stagnalis	AY592994
DscSymme	Discolaimoides symmetricus	EF207238

DstVeec3	Distolabrellus veechi	EF990725
EcpSpec4	Eucephalobus sp. JB-55	DQ145635
EcuMono5	Ecumenicus monohystera	AY593013
EcuSpec3	Ecumenicus sp. JH-2004	AY593014
EkhCompa	Ektaphelenchoides compasi	DQ257625
EkhIPini	Ektaphelenchoides pini	DQ257623
EktObtu2	Ektaphelenchus obtusus	AB368533
EncMacr2	Enchodelus macrodorus	AY593054
EncSpec5	Enchodelus sp. HHBM-2007a	EF207240
EnISpec2	Enoplolaimus sp. 2P6K2	DQ077750
EnoSpec6	Enoploides sp. 3I11K2	DQ077759
EnoSpec7	Enoploides sp. 1P11K2	DQ077760
EnoSpec8	Enoploides sp. 2P9K2	DQ077764
EpiLugd6	Epidorylaimus lugdunensis	AY593036
EpiLugd7	Epidorylaimus lugdunensis	AY593035
EudCentr	Eudorylaimus centrocerus	AY593007
EudSpec6	Eudorylaimus sp. JH-2004	AY593037
EumFili3	Eumonhystera filiformis	DQ086658
FesGross	Fescia grossa	DQ145636
FldMart2	Filaroides martis	AY292795
FlnFlag2	Filarinema flagrifer	AM039746
GloArte3	Globodera artemisiae	EU855121
GloMille	Globodera millefolii	DQ328700
GloPal10	Globodera pallida	AY592991
GloPal11	Globodera pallida	AY592992
GloPal13	Globodera pallida	EU855119
GloRos12	Globodera rostochiensis	AY592988
GloRos13	Globodera rostochiensis	AY592987
GloRos14	Globodera rostochiensis	AY592993
GloRos15	Globodera rostochiensis	EU855120
HaeCont5	Haemonchus contortus	AM039742
HaeSpec2	Haemonchus sp. 92619	AY292796
HalSpec2	Haliplectus sp. 7I16G4	DQ077774
HamCrist	Hammerschmidtella cristata	EU365629
HCDYyyk	HCL_24_Viscosia_D2D3	(Present Study)
HCDYyyy2	HCL_11_Viscosia_D2D3	(Present Study)
HCDYyyyi	HCL_15_Viscosia_D2D3	(Present Study)
HCDYyyyl	HCL_27_Viscosia_D2D3	(Present Study)
HCDYyyyo	HCL_9_Viscosia_D2D3	(Present Study)
HCDYyyyy	HCL_10_Viscosia_D2D3	(Present Study)
HelMult2	Helicotylenchus multicinctus	DQ328746
HelMulti	Helicotylenchus multicinctus	DQ328745
HelPseu3	Helicotylenchus pseudorobustus	DQ328750
HelPseu4	Helicotylenchus pseudorobustus	DQ328751
HelPseu5	Helicotylenchus pseudorobustus	DQ328747
HelPseu6	Helicotylenchus pseudorobustus	DQ328748
HelPseu7	Helicotylenchus pseudorobustus	DQ328749
HemSpeci	Hemicyclophora sp. Vovlas-IPP	AY780974

HerPyth2	Herpetostrongylus pythonis	AM039750
HetAuckl	Heterodera aucklandica	DQ328688
HetCajan	Heterodera cajani	DQ328693
HetCynod	Heterodera cynodontis	DQ328698
HeteZae	Heterodera zae	DQ328695
HetGly22	Heterodera glycines	DQ328692
HetGoet2	Heterodera goettingiana	DQ328697
HetKore3	Heterodera koreana	EU284032
HetLati3	Heterodera latipons	DQ328687
HetLitor	Heterodera litoralis	DQ328691
HetOrien	Heterodera orientalis	EU284033
HetOryzi	Heterodera oryzicola	DQ328694
HetSalix	Heterodera salixophila	DQ328690
HetSorgh	Heterodera sorghi	DQ328689
HetSpec3	Heterodera sp. SAS-2008	EU284031
HetUrtic	Heterodera urticae	DQ328696
HirPomp2	Hirschmanniella pomponiensis	DQ077795
HirSant2	Hirschmanniella santarosae	EF029859
HirscCf2	Hirschmanniella cf. belli ITDL-2006	EF029860
HirSpec5	Hirschmanniella sp. VietNam Chau	DQ328686
HirSpec6	Hirschmanniella sp. Yuma	EF029861
HlcGin10	Halicephalobus gingivalis	AB289346
HlcGin11	Halicephalobus gingivalis	AY294178
HlcGing3	Halicephalobus gingivalis	AY294181
HlcGing4	Halicephalobus gingivalis	AY294177
HlcGing5	Halicephalobus gingivalis	AB288935
HlcGing6	Halicephalobus gingivalis	AY294182
HlcGing7	Halicephalobus gingivalis	AY294179
HlcGing8	Halicephalobus gingivalis	AB289345
HlcGing9	Halicephalobus gingivalis	AY294180
HlgPoly5	Heligmosomoides polygyrus	AM039747
HLOnYyyyn	HCL_5_Oncholaimidae_D2D3	(Present Study)
HLOYyyy2	HCL_7_Oncholaimidae_D2D3	(Present Study)
HLOYyyyj	HCL_2_Oncholaimidae_D2D3	(Present Study)
HLOYyyyy	HCL_12_Oncholaimidae_D2D3	(Present Study)
HLVYyyyy	HCL_23_Oncholaimidae_D2D3	(Present Study)
HLxsYyym	HCL_32_Oxystomina_D2D3	(Present Study)
HLxYyyy2	HCL_21_Oxystomina_D2D3	(Present Study)
HLxYyyyy	HCL_20_Oxystomina_D2D3	(Present Study)
HopCol10	Hoplolaimus columbus	EU554668
HopCol14	Hoplolaimus columbus	EU554674
HopColu3	Hoplolaimus columbus	EU554669
HopColu6	Hoplolaimus columbus	EU554670
HopConca	Hoplolaimus concaudajuvencus	EU626792
HopGale6	Hoplolaimus galeatus	EU626785
HopGale7	Hoplolaimus galeatus	EU626784
HopMagn2	Hoplolaimus magnistylus	EU626789
HopSein2	Hoplolaimus seinhorsti	EU626791

HopSpec3	Hoplolaimus sp. 1 CB-2008	EU626793
HopSpec4	Hoplolaimus sp. 2 CB-2008	EU626795
HopSpeci	Hoplolaimus sp. 3 CB-2008	EU586797
HowPhyll	Howardula phyllotretae	DQ328728
HtbChon2	Heterorhabditoides chongmingensis	EF503691
HtcTuni3	Heterocheilus tunicatus	AF226592
HthAmazo	Heterorhabditis amazonensis	EU099036
HthBact6	Heterorhabditis bacteriophora	EU313541
HthBact7	Heterorhabditis bacteriophora	EU099037
HthFlori	Heterorhabditis floridensis	EU099034
HthGeorg	Heterorhabditis georgiana	EU099033
HthIndic	Heterorhabditis indica	EU100415
HthMare2	Heterorhabditis marelatus	DQ145665
HthMare3	Heterorhabditis marelatus	EU100412
HthMegi4	Heterorhabditis megidis	EU100413
HthMexic	Heterorhabditis mexicana	EU100414
HthSafri	Heterorhabditis safricana	EU100416
HthSpec7	Heterorhabditis sp. DHAF-2007a	EU195993
HthZeal2	Heterorhabditis zealandica	EU099035
HthZeal6	Heterorhabditis zealandica	AM039761
HthZeal7	Heterorhabditis zealandica	AM039761
HtnGrami	Heteroanguina graminophila	DQ328720
HtpSpeci	Heterocephalobellus sp. JB-8	DQ145638
HUOYyyy	HUK_1_Oncholaimidae_D2D3	(Present Study)
HypMacr2	Hypodontus macropi	AM039731
HysAuctu	Hysterothylacium auctum	AF226591
HysPela3	Hysterothylacium pelagicum	AF226590
JCdYyyy2	JCC_89_Phanodermopsis_D2D3	(Present Study)
JCdYyyy	JCC_59_Phanodermopsis_D2D3	(Present Study)
JCIYyyy	JCC_52_Phanodermatidae_D2D3	(Present Study)
JCnYyyy	JCC_23_Phanodermatidae_D2D3	(Present Study)
JCrYyyy	JCC_29_Anticomidae_D2D3	(Present Study)
KalCris2	Kalicephalus cristatus	AM039741
KoeSpec3	Koerneria sp. 228	AY840563
KoeSpec4	Koerneria sp. SB110	EU195999
LatSpec2	Latronema sp. 2P15K2	DQ077784
LatSpeci	Latronema sp. 1P10K3	DQ077780
LbrVulv2	Labronema vulvapapillatum	AY592996
LbrVulv3	Labronema vulvapapillatum	AY592997
LbsBipa2	Labiostrogylus bipapillosus	AJ512837
LCDYyyy2	LCL_5_Bathylaimus_D2D3	(Present Study)
LCDYyyy3	LCL_7_Trefusia_D2D3	(Present Study)
LCDYyyyp	LCL_2_Trefusia_D2D3	(Present Study)
LCDYyyyr	LCL_3_Trefusia_D2D3	(Present Study)
LCDYyyys	LCL_4_Trefusia_D2D3	(Present Study)
LCDYyyyt	LCL_8_Trefusia_D2D3	(Present Study)
LCDYyyyy	LCL_1_Trefusia_D2D3	(Present Study)
LChYyyyy	LCL_19_Bathylaimus_D2D3	(Present Study)

LCnYyyyq	LCL_20_Oncholaimidae_D2D3	(Present Study)
LeiAppen	Leidynema appendiculata	EU365630
LLTYyyy2	LCL_9_Bathylaimus_D2D3	(Present Study)
LLTYyyyy	LCL_21_Bathylaimus_D2D3	(Present Study)
LmpSpeci	Laimaphelenchus sp. RGD636L	AB368539
LonAmeri	Longidorus americanum	AY494715
LonCaes2	Longidorus caespiticola	AF480080
LonCaes3	Longidorus caespiticola	AF480079
LonCaesp	Longidorus caespiticola	AF480081
LonCarpa	Longidorus carpathicus	AF480072
LonElon3	Longidorus elongatus	AF480077
LonElon4	Longidorus elongatus	AF480075
LonElon5	Longidorus elongatus	AF480076
LongiCf2	Longidorella cf macramphis JH-2004	AY593042
LonInter	Longidorus intermedius	AF480074
LonMacr3	Longidorus macrosoma	AF480082
LonProf2	Longidorus profundorum	AF480073
LonSpe12	Longidorella sp. 1 JH-2004	AY593045
LonSpe13	Longidorella sp. 3 JH-2004	AY593044
LonSpe14	Longidorella sp. 2 JH-2004	AY593043
LonSturh	Longidorus sturhanii	AF480071
LonUros2	Longidorus uroshis	EF538754
LUmYyyyy	LUK_6_Halalaimus_D2D3	(Present Study)
LUpYyyyy	LUK_12_Calyptronema_D2D3	(Present Study)
LUsYyyyy	LUK_7_Calyptronema_D2D3	(Present Study)
LUVYyyy2	LUK_3_Viscosia_D2D3	(Present Study)
LUVYyyyy	LUK_1_Viscosia_D2D3	(Present Study)
MacArbu3	Macrotrophurus arbusticola	DQ328708
MclSpeci	Macrolaimellus sp. SAN-2005	DQ145640
McmSpeci	Macrolaimus sp. SAN-2005	DQ145639
MelAren7	Meloidogyne arenaria	U42339
MelAren8	Meloidogyne arenaria	AF435803
MelAren9	Meloidogyne arenaria	EU364889
MelArti3	Meloidogyne artiellia	AY150369
MelBaeti	Meloidogyne baetica	AY150367
MelChi27	Meloidogyne chitwoodi	AF435802
MelDune2	Meloidogyne dunensis	EF612712
MelExig3	Meloidogyne exigua	AF435804
MelExig4	Meloidogyne exigua	AF435796
MelExig5	Meloidogyne exigua	AF435795
MelGram6	Meloidogyne graminicola	AF435793
MelHap49	Meloidogyne hapla	DQ328685
MelHisp4	Meloidogyne hispanica	EU443608
MelHisp5	Meloidogyne hispanica	EU443607
MelHisp6	Meloidogyne hispanica	EU443606
MelIchi4	Meloidogyne ichinohei	EF029862
MelInc35	Meloidogyne incognita (southern root-knot nematode)	AF435794
MelKonae	Meloidogyne konaensis	AF435797

MelPara2	Meloidogyne paranaensis	AF435800
MelPara3	Meloidogyne paranaensis	AF435799
MelPara4	Meloidogyne paranaensis	AF435798
MelThail	Meloidogyne thailandica	EU364890
MelTrifo	Meloidogyne trifoliophila	AF435801
MetSpec6	Metachromadora sp. 2114K2	DQ077783
MetSpec7	Metachromadora sp. 4P6K2	DQ077752
MicMise5	Microdorylaimus miser	AY593046
MicMode3	Microdorylaimus modestus	AY593049
MldKirja	Meloidoderita kirjanovae	DQ768428
MlrAlni0	Meloidoderaalni	DQ328706
MnsSpeci	Monhysterida sp. 3P12K2	DQ077767
MonTrun3	Mononchus truncatus	AY593064
MonTunb3	Mononchus tunbridgensis	AY593063
MsdSpec3	Mesodorylaimus sp. JH-2004	AY593006
MsdSpec4	Mesodorylaimus sp. JH-2004	AY593005
MsgMille	Mesoanguina millefolii	DQ328722
MsrAnis2	Mesorhabditis anisomorpha	EF990723
MsrLong3	Mesorhabditis longespiculosa	EU195980
MtcAmbly	Metacrobeles amblyurus	DQ145642
MtsElon2	Metastrongylus elongatus	AM039755
MtsSalm3	Metastrongylus salmi	AY292797
MueCapi3	Muellerius capillaris	AY292798
MyctUlm2	Myctolaimus ulmi	EU195998
MyctUlm3	Myctolaimus ulmi	EU195998
MyoSpec2	Myolaimus sp. RGD233	DQ145643
NADYyyy	NAR_6_Chaetonema_D2D3	(Present Study)
NAEYyyy2	NAR_2_Enoplolaimus_D2D3	(Present Study)
NAEYyyy3	NAR_5_Enoplolaimus_D2D3	(Present Study)
NAEYyyy4	NAR_8_Enoplolaimus_D2D3	(Present Study)
NAEYyyy5	NAR_9_Enoplolaimus_D2D3	(Present Study)
NAEYyyy	NAR_1_Enoplolaimus_D2D3	(Present Study)
NagLept2	Nagelus leptus	DQ328715
NAsYyyy2	NAR_4_Oncholaimus_D2D3	(Present Study)
NAsYyyy3	NAR_7_Oncholaimus_D2D3	(Present Study)
NAsYyyy	NAR_16_Oncholaimus_D2D3	(Present Study)
NAtYyyy2	NAR_14_Bathylaimus_D2D3	(Present Study)
NAtYyyy3	NAR_15_Bathylaimus_D2D3	(Present Study)
NAtYyyy4	NAR_20_Bathylaimus_D2D3	(Present Study)
NAtYyyy	NAR_11_Bathylaimus_D2D3	(Present Study)
NecAmer3	Necator americanus	AF217868
NecAmer4	Necator americanus	AM039740
NemBatt3	Nematodirus battus	AY292799
NemBatt5	Nematodirus battus	AM039752
NemBatt6	Nematodirus battus	AM039752
NeoCren2	Neodiplogaster crenatae	AB326309
NicCame2	Nicollina cameroni	AM039749
NipBras3	Nippostrongylus brasiliensis	AM039748

NSAYyyy	NUS_40_Anoplostoma_D2D3	(Present Study)
NSOnYyya	NUS_5_Oncholaimus_D2D3	(Present Study)
NSOYyyy2	NUS_4_Oncholaimus_D2D3	(Present Study)
NSOYyyy3	NUS_6_Oncholaimus_D2D3	(Present Study)
NSOYyyy4	NUS_7_Oncholaimus_D2D3	(Present Study)
NSOYyyyy	NUS_2_Oncholaimus_D2D3	(Present Study)
NthBorre	Nothacrobeles borregi	DQ145645
NthSpat2	Nothacrobeles spatulatus	DQ145644
NthSpatu	Nothacrobeles spatulatus	AY027532
NthTrini	Nothacrobeles trinigliarus	DQ145646
NtlSpeci	Neotylenchus sp. SAS-2006	DQ328725
NUmYyyyy	NUS_11_Bathylaimus_D2D3	(Present Study)
NUPYyyyy	NUS_1_Pareurystomina_D2D3	(Present Study)
NUrYyyy2	NUS_41_Tripyloides_D2D3	(Present Study)
NUrYyyyy	NUS_14_Tripyloides_D2D3	(Present Study)
NUxYyyy2	NUS_3_Oxystomina_D2D3	(Present Study)
NUxYyyyy	NUS_21_Oxystomina_D2D3	(Present Study)
NygoICf5	Nygolaimus cf. brachyuris JH-2004	AY593061
OdnSpec2	Odontophora sp. 5P9K2	DQ077756
OdnSpec3	Odontophora sp. 2I11K2	DQ077758
OdtLong2	Odontopharynx longicaudata	DQ077775
OnhSpec4	Oncholaimidae sp. 2I6K2	DQ077753
OpiSylp3	Opisthodorylaimus sylphoides	AY593008
OpiSylp4	Opisthodorylaimus sylphoides	AY593009
OpiSylp5	Opisthodorylaimus sylphoides	AY593010
OscDoli3	Oscheius dolichuroides	EU195970
OscDoli4	Oscheius dolichura	EU195971
OscGuen2	Oscheius guentheri	EU195996
OscInse2	Oscheius insectivora	EU195968
OscMyrio	Oscheius myriophila	AY602176
OscTipu4	Oscheius tipulae	DQ059063
OscTipu5	Oscheius tipulae	EU195969
OsIOsle3	Oslerus osleri	AY292800
OstLept3	Ostertagia leptospicularis	AM039744
OtoCirc4	Otostrongylus circumlitus	AY292801
OU DYyyy2	OUS_4_Halalaimus_D2D3	(Present Study)
OU DYyyyy	OUS_22_Halalaimus_D2D3	(Present Study)
OU EYyyyy	OUS_10_Enoploides_D2D3	(Present Study)
OU mYyyy2	OUS_14_Oncholaimidae_D2D3	(Present Study)
OU mYyyy3	OUS_2_Oncholaimus_D2D3	(Present Study)
OU mYyyy4	OUS_21_Oncholaimidae_D2D3	(Present Study)
OU mYyyyy	OUS_1_Oncholaimidae_D2D3	(Present Study)
OU tmYyyb	OUS_6_Anoplostoma_D2D3	(Present Study)
OU tmYyyC	OUS_7_Anoplostoma_D2D3	(Present Study)
OU tmYyyd	OUS_8_Anoplostoma_D2D3	(Present Study)
OU tYyyy2	OUS_5_Anoplostoma_D2D3	(Present Study)
OU tYyyyy	OUS_3_Anoplostoma_D2D3	(Present Study)
OU VYyyyy	OUS_9_Oncholaimidae_D2D3	(Present Study)

OxdNeth4	Oxydirus nethus	AY593011
OxdOxyc4	Oxydirus oxycephalus	AY593012
PanSpe16	Panagrolaimus sp. 2 PS1159	DQ059061
PanSpe17	Panagrolaimus sp. RS-2007a	EF417144
PanSpe18	Panagrolaimus sp. R18	EF417146
PanSpe19	Panagrolaimus sp. RS-2007b	EF417145
PanSpe20	Panagrolaimus sp. JB115	AY294183
PanSpe21	Panagrolaimus sp. SAN-15	DQ145651
ParHart7	Paravulvus hartingii	AY593062
PasAmbi2	Passalurus ambiguus	EF464552
PctMacr3	Paractinolaimus macrolaimus	AY593000
PctMacr4	Paractinolaimus macrolaimus	AY592999
PctMacr5	Paractinolaimus macrolaimus	AY592998
PdnWirt2	Prodontorhabditis wirthi	AY602169
PdrSpec2	Prodorylaimus sp. HHBM-2007a	EF207241
PdrUlig2	Prodorylaimus uliginosus	AY593034
PelCyli2	Pelodera cylindrica	EU195994
PelMar16	Pellioditis marina	AM937040
PelMar17	Pellioditis marina	AM399044
PelMar20	Pellioditis marina	AM399038
PelMar22	Pellioditis marina	AM399055
PelMar23	Pellioditis marina	AM399063
PelMar24	Pellioditis marina	AM937034
PelMar25	Pellioditis marina	AM399043
PelMar32	Pellioditis marina	AM937038
PelMar35	Pellioditis marina	AM399062
PelMari2	Pellioditis marina	AM399039
PelMari9	Pellioditis marina	AM399050
PelPseu2	Pelodera pseudoteres	EU195997
PelPunc2	Pelodera punctata	EU195978
PelStro2	Pelodera strongyloides	EU195977
PelTere2	Pelodera teres	EU195979
PetPocu2	Petrovinema poculatum	AM039735
PhaSpec2	Phasmarhabditis sp. EM434	EU195967
PhdSpec2	Phanoderma sp. 3I23B4	DQ077781
PhdSpeci	Phanoderma sp. 5I23B4	DQ077769
PhoCysto	Phocascaris cystophorae	AF226578
PhoPhoca	Phocascaris phocae	AF226584
PhoSpeci	Phocascaris sp. 112000	AF226575
PlcHunti	Plectonchus hunti	DQ145652
PlcSpec5	Plectidae sp. SAS-2004	AY652779
PleAqua3	Plectus aquatilis	EF417147
PleMinim	Plectus minimus	EF417148
PlnMaxi2	Paralongidorus maximus	AF480083
PlnPara2	Paralongidorus paramaximus	EU026156
PlpOdoc2	Parelaphostrongylus odocoilei	AY292803
PltPersc	Peltamigratus perscitus	DQ328744
PncPunct	Punctodera punctata	DQ328699

PnlCeylo	<i>Panagrellus ceylonensis</i>	DQ408251
PnlDubi2	<i>Panagrellus dubius</i>	DQ408258
PnlDubi3	<i>Panagrellus dubius</i>	DQ408253
PnlDubi4	<i>Panagrellus dubius</i>	DQ408257
PnlDubi5	<i>Panagrellus dubius</i>	DQ408256
PnlDubi6	<i>Panagrellus dubius</i>	DQ408254
PnlDubi7	<i>Panagrellus dubius</i>	DQ408255
PnlDubi8	<i>Panagrellus dubius</i>	DQ408252
PnlRedi3	<i>Panagrellus redivivus</i>	DQ145647
PnlRedi4	<i>Panagrellus redivivus</i>	DQ408249
PnlRedi5	<i>Panagrellus redivivus</i>	AF331910
PnlRedi6	<i>Panagrellus redivivus</i>	DQ408250
PnlRedi8	<i>Panagrellus redivivus</i>	EU195986
PnrStam2	<i>Panagrobelus stammeri</i>	DQ145649
PoiErns2	<i>Poikilolaimus ernstmayri</i>	DQ059058
PoiOxyc3	<i>Poikilolaimus oxycercus</i>	DQ059059
PoiOxyc4	<i>Poikilolaimus oxycercus</i>	EU195984
PoiRege2	<i>Poikilolaimus regenfussi</i>	DQ059057
PoiSpec2	<i>Poikilolaimus</i> sp. RGD617	AB370213
PomSpeci	<i>Pomponema</i> sp. 2P12K2	DQ077763
PonSpec2	<i>Pontonema</i> sp. 6I23B4	DQ077771
PonSpeci	<i>Pontonema</i> sp. 3I24B4	DQ077768
PPEYyyyy	PPA_7_Enoplus_D2D3	(Present Study)
PrbSpec4	<i>Protorhabditis</i> sp. DF5055	AY602168
PrbSpec5	<i>Protorhabditis</i> sp. JB122	EU195958
PrcSpec4	<i>Paracanthochus</i> sp. 4I6K2	DQ077754
PrfDeco3	<i>Parafilaroides decorus</i>	AY292802
PrfDeco4	<i>Parafilaroides decorus</i>	AM039757
PrhSpeci	<i>Prionchulus</i> sp. DGW_GPhi	DQ077802
PrIBrz10	<i>Pratylenchus brzeskii</i>	AM231927
PrIBrz17	<i>Pratylenchus brzeskii</i>	AM231912
PrIBrz18	<i>Pratylenchus brzeskii</i>	AM231920
PrICof13	<i>Pratylenchus coffeae</i>	EU130850
PrICoff6	<i>Pratylenchus coffeae</i>	AF170429
PrIDun16	<i>Pratylenchus dunensis</i>	AM231946
PrIDune5	<i>Pratylenchus dunensis</i>	AM231939
PrIDune9	<i>Pratylenchus dunensis</i>	AM231948
PrIGuti2	<i>Pratylenchus gutierrezi</i>	AF170442
PrILOo10	<i>Pratylenchus loosi</i>	EF446994
PrILOos4	<i>Pratylenchus loosi</i>	EF446992
PrInZea7	<i>Pratylenchus zeae</i>	EU130896
PrInZea9	<i>Pratylenchus zeae</i>	EU130894
PrIPen10	<i>Pratylenchus penetrans</i>	EU130859
PrIPen12	<i>Pratylenchus penetrans</i>	EU130860
PrIPrat3	<i>Pratylenchus pratensis</i>	AM231934
PrITho33	<i>Pratylenchus thornei</i>	EU130880
PrIVul14	<i>Pratylenchus vulnus</i>	EU130887
PrIVuln9	<i>Pratylenchus vulnus</i>	EU130882

PrsLhe13	Pristionchus lheritieri	DQ059066
PrsMaup4	Pristionchus maupasi	DQ059065
PrsPaci6	Pristionchus pacificus	DQ059064
PrsPaci7	Pristionchus pacificus	EU195982
PrsSpec9	Pristionchus sp. RS141	AF549407
PrtAnem4	Paratrichodorus anemones	AJ781505
PrtPach6	Paratrichodorus pachydermus	AM180727
PrtPoro4	Paratrichodorus porosus	EU827614
PrtRenif	Paratrichodorus renifer	EU827615
PrxLaet4	Paraxonchium laetificans	AY593001
PscSpec2	Pseudacrobeles sp. JB-85	DQ145654
PscSpeci	Pseudacrobeles sp. JB-56	DQ145653
PscVari2	Pseudacrobeles variabilis	AF143368
PsdInfl3	Pseudalius inflexus	AY292804
PseDec10	Pseudoterranova decipiens (codworm)	AY821761
PseDec11	Pseudoterranova decipiens (codworm)	AY821760
PseDec12	Pseudoterranova decipiens (codworm)	AY821762
PseDec13	Pseudoterranova decipiens (codworm)	AY821763
PsiSpec3	Psilenchus sp. USA CA9	DQ328716
PsnSpeci	Parasitylenchus sp. SAS-2006	DQ328729
PspCitri	Parasitodiplogaster citrinema	AY840555
PspLaev2	Parasitodiplogaster laevigata	AY840558
PspLaev3	Parasitodiplogaster laevigata	AY840557
PspLaevi	Parasitodiplogaster laevigata	AY840556
PspMaxin	Parasitodiplogaster maxinema	AY840559
PspPopen	Parasitodiplogaster popenema	AY840560
PspSpec2	Parasitodiplogaster sp. WY-579p	EU018054
PspSpec3	Parasitodiplogaster sp. WY-463p	EU018051
PspSpeci	Parasitodiplogaster sp. 239	AY840561
PspTrigo	Parasitodiplogaster trigonema	AY840562
PsrEquo3	Parascaris equorum	AY821775
PstObtu2	Parasitorhabditis obtusa	EF990724
PtnSpec2	Pratylenchidae sp. Trinh 104108	EF645137
PtnSpeci	Pratylenchidae sp. Trinh 104107	EF645138
PtsRufe2	Protostrongylus rufescens	AM039756
PunEngad	Pungentus engadinensis	AY593050
PunSilv2	Pungentus silvestris	AY593053
PunSilv3	Pungentus silvestris	AY593052
RadSpec2	Radopholus sp. 7B VietNam	DQ328712
RaphAcu2	Raphidascaris acus	AY821772
RchSpec2	Richtersia sp. 4P11K2	DQ077762
RchSpeci	Richtersia sp. 5P12K2	DQ077770
RhaIner4	Rhabditoides inermis	EU195981
RhaIner5	Rhabditoides inermiformis	EF990727
RhaRegi2	Rhabditoides regina	EF990726
RhbBras2	Rhabditis brassicae	EU195963
RhbDolic	Rhabditis dolichura	EF417150
RhbRain2	Rhabditis rainai	EU195966

RhbSpec4	Rhabditis sp. BC7735	EU303298
RhbSpec6	Rhabditis sp. SB347	EU195960
RhbSpec7	Rhabditis sp. DF5059	EU195964
RhcSpeci	Rhabdocoma sp. 1112K3	DQ077778
RhdBak10	Rhabdias bakeri	EU360836
RhdBak11	Rhabdias bakeri	EU360833
RhdBake3	Rhabdias bakeri	DQ264774
RhdBake5	Rhabdias bakeri	DQ264773
RhdBake6	Rhabdias bakeri	EU360835
RhdPseu3	Rhabdias pseudosphaerocephala	DQ845736
RhdPseu6	Rhabdias pseudosphaerocephala	DQ845737
RhdPseu7	Rhabdias pseudosphaerocephala	DQ845735
RhdRana2	Rhabdias ranae	DQ264768
RhdRana3	Rhabdias ranae	DQ264769
RhdRana5	Rhabdias ranae	EU360844
RhdRana7	Rhabdias ranae	EU360842
RhdRana8	Rhabdias ranae	EU360843
RhdsCf03	Rhabdias cf. hylae SD-2008	EU836866
RhdsCf06	Rhabdias cf. hylae SD-2008	EU836874
RhdSpec2	Rhabdias sp. SD-2008	EU836870
RhdSpha2	Rhabdias sphaerocephala	DQ845739
RhdSpha3	Rhabdias sphaerocephala	DQ845741
RhIIAxe3	Rhabditella axei	AY602177
RhpSpec2	Rhabditophanes sp. KR3021	AY294185
RhpSpec3	Rhabditophanes sp. KR3021	DQ145655
RhtSpec3	rhabditoid sp. PDL15	EU195985
RhzSequo	Rhizonema sequoiae	DQ328703
RomCuli3	Romanomermis culicivorax	EF417153
RotMacro	Rotylenchulus macrodoratus	DQ328711
RotRen35	Rotylenchulus reniformis	DQ328713
RtICazo2	Rotylenchus cazorlaensis	EU280792
RtICazor	Rotylenchus cazorlaensis	EU280793
RtIExim2	Rotylenchus eximius	EU280794
RtIEximi	Rotylenchus eximius	DQ328741
RtIGood2	Rotylenchus goodeyi	DQ328756
RtIIncu2	Rotylenchus incultus	EU280797
RtIIncul	Rotylenchus incultus	EU280796
RtIJaeni	Rotylenchus jaeni	EU280791
RtILaur2	Rotylenchus laurentinus	EU280798
RtILAure	Rotylenchus laurentinus	DQ328757
RtIMagn2	Rotylenchus magnus	EU280790
RtIMagnu	Rotylenchus magnus	EU280789
RtIRobu2	Rotylenchus robustus	EU280788
RtIUnif3	Rotylenchus uniformis	DQ328737
RtIUnif4	Rotylenchus uniformis	DQ328738
RtIUnif5	Rotylenchus uniformis	DQ328735
RtIUnif6	Rotylenchus uniformis	DQ328740
RtIUnif7	Rotylenchus uniformis	DQ328736

RtlUnif8	Rotylenchus uniformis	DQ328739
RtlUnise	Rotylenchus unisexus	EU280799
RueAsiat	Ruehmaphelenchus asiaticus	AM269475
SBHYyyyu	SBA_10_Halalaimus_D2D3	(Present Study)
SBHYyyyv	SBA_12_Halalaimus_D2D3	(Present Study)
SBHYyyyy	SBA_1_Halalaimus_D2D3	(Present Study)
SBIYyyw	SBA_3_Oncholaimus_D2D3	(Present Study)
SBIYyyx	SBA_5_Oncholaimus_D2D3	(Present Study)
SBIYyyyy	SBA_2_Oncholaimus_D2D3	(Present Study)
SBrYyyyy	SBA_13_Thoracostompsidae_D2D3	(Present Study)
SBSYyyyy	SBN_3_Oxystomina_D2D3	(Present Study)
SBVYyy2	SBN_4_Viscosia_D2D3	(Present Study)
SBVYyyyy	SBN_2_Viscosia_D2D3	(Present Study)
SchAure2	Schistonchus aureus	DQ912925
SchCent2	Schistonchus centerae	DQ912928
SchGuan2	Schistonchus guangzhouensis	DQ912927
SchLaev3	Schistonchus laevigatus	DQ912926
SchSpec3	Schistonchus sp. WY-463s	EU018052
SecBarb2	Sectonema barbatoides	AY593032
SecBarb3	Sectonema barbatoides	AY593031
SecBarb4	Sectonema barbatoides	AY593030
SecSpec2	Sectonema sp. JH-2004	AY593033
SevSpeci	Severianoia sp. 1 SS-2008	EU365631
SkrChit2	Skrjabinylus chitwoodorum	AY292805
SngTrac3	Syngamus trachea	AM039736
SprBomb3	Sphaerularia bombi	DQ328726
SteAbba2	Steinernema abbasi	AF331890
SteArena	Steinernema arenarium	AF331892
SteCerat	Steinernema ceratophorum	AF331888
SteCuban	Steinernema cubanum	AF331889
SteInter	Steinernema intermedium	AF331909
SteKhois	Steinernema khoisanae	DQ314289
SteKrau3	Steinernema kraussei	AF331896
SteKushi	Steinernema kushidai	AF331897
SteLong2	Steinernema longicaudum	AF331901
SteRarum	Steinernema rarum	DQ221118
SteScar2	Steinernema scarabaei	AY172023
SteSpec6	Steinernema sp. SS-2007a	EU177771
SteSpec7	Steinernema sp. 1 'Costa Rica'	EF187017
SteWeise	Steinernema weiseri	DQ400854
SteVirga	Steinernema yirgalemense	AY748451
StlSimil	Stegelletina similis	AY027533
StlSpec2	Stegelletina sp. JB-139	DQ145659
StlSpec3	Stegelletina sp. JB-64	DQ145658
StlSpeci	Stegelletina sp. SAN-2005	DQ145657
StpDent2	Stephanurus dentatus	AM039737
StpDent3	Stephanurus dentatus	AM039737
StrCall5	Strongyloides collosciureus	AB272229

StrCall6	Strongyloides callosciureus	AB272230
StrCall7	Strongyloides callosciureus	AB272231
StrFue10	Strongyloides fuelleborni	U42595
StrFue11	Strongyloides fuelleborni fuelleborni	AB272235
StrProc3	Strongyloides procyonis	AB205054
StrRatt7	Strongyloides ratti	U39490
StrRobu3	Strongyloides robustus	AB272232
StrSte11	Strongyloides stercoralis	U38855
StrSte12	Strongyloides stercoralis	U39489
StrSter8	Strongyloides stercoralis	DQ145661
StrSter9	Strongyloides stercoralis	AY294186
SttSpeci	Stegelleta sp. JB-75	DQ145656
SubChile	Subanguina chilensis	DQ328724
SubRadi3	Subanguina radicola	DQ328721
SUCYyyy	SUS_27_Oncholaimidae_D2D3	(Present Study)
SUDDYyye	SUS_15_Enoplolaimus_D2D3	(Present Study)
SUDYyyy2	SUS_10_Enoplolaimus_D2D3	(Present Study)
SUDYyyy3	SUS_2_Enoplolaimus_D2D3	(Present Study)
SUDYyyy4	SUS_21_Enoplolaimus_D2D3	(Present Study)
SUDYyyy5	SUS_6_Enoplolaimus_D2D3	(Present Study)
SUDYyyyy	SUS_1_Enoplolaimus_D2D3	(Present Study)
SypObve2	Syphacia obvelata	EF464554
TbHYyyy	TCR_87_Bathylaimus_D2D3	(Present Study)
TbtYyyy2	TCR_109_Bathyeurystomina_D2D3	(Present Study)
TbtYyyy3	TCR_81_Bathyeurystomina_D2D3	(Present Study)
TbtYyyy4	TCR_128_Bathyeurystomina_D2D3	(Present Study)
TbtYyyyy	TCR_106_Bathyeurystomina_D2D3	(Present Study)
TCgYyyy	TCR_145_Syringolaimus_D2D3	(Present Study)
TDIYyyy	TCR_114_Dolicholaimus_D2D3	(Present Study)
TEEYyyy	TCR_184_Epicanthion_D2D3	(Present Study)
TEMYyyy	TCR_143_Enoplolaimus_Mesacanthion_D2D3	(Present Study)
TEnYyyy	TCR_74_Thoracostomopsidae_D2D3	(Present Study)
TetMack2	Tetrabothriostrogylus mackerrasae	AM039751
ThdYyyy2	TCR_130_Rhabdocoma_D2D3	(Present Study)
ThdYyyy3	TCR_139_Rhabdocoma_D2D3	(Present Study)
ThdYyyy	TCR_125_Rhabdocoma_D2D3	(Present Study)
THmYyyy2	TCR_3_Halalaimus_D2D3	(Present Study)
THmYyyy3	TCR_1_Halalaimus_D2D3	(Present Study)
THmYyyy4	TCR_112_Halalaimus_D2D3	(Present Study)
THmYyyy5	TCR_13_Halalaimus_D2D3	(Present Study)
THmYyyy6	TCR_131_Halalaimus_D2D3	(Present Study)
THmYyyy7	TCR_93_Halalaimus_D2D3	(Present Study)
THmYyyy8	TCR_97_Cricohalalaimus_D2D3	(Present Study)
THmYyyy	TCR_26_Halalaimus_D2D3	(Present Study)
ThoCirc2	Thonus circulifer	AY593038
ThoCirc3	Thonus circulifer	AY593039
ThoMinu2	Thonus minutus	AY593047
ThoMinu3	Thonus minutus	AY593048

ThoSpec4	Thonus sp. JH-2004	AY593040
ThoSpec5	Thonus sp. JH-2004	AY593041
THxYyyyy	TCR_68_Oxystomina_D2D3	(Present Study)
TicSpeci	Tricoma sp. 3P15K2	DQ077785
TlchICf3	Tylencholaimus cf. teres HHBM-2007a	EF207243
TlcMira4	Tylencholaimus mirabilis	AY593059
TlcMira5	Tylencholaimus mirabilis	AY593027
TlcMira6	Tylencholaimus mirabilis	EF207242
TlcSpec3	Tylencholaimus sp. JH-2004	AY593060
TlcSpec4	Tylencholaimus sp. JH-2004	AY593028
TlhClay2	Tylenchorhynchus claytoni	EU368588
TlhClay3	Tylenchorhynchus claytoni	EU368589
TlhDubi3	Tylenchorhynchus dubius	EU368590
TlhDubi4	Tylenchorhynchus dubius	DQ328707
TlhLevi2	Tylenchorhynchus leviterminalis	EU368591
TlISpeci	Tylencholaimellus sp. JH-2004	AY593055
TLRYyyyy	TCR_230_Thalassoalaimus_D2D3R_G11	(Present Study)
TLtYyyyy	TCR_192_Leptosomatides_D2D3	(Present Study)
TMPYyyy2	TCR_94_Mesacanthion_Paramesacanthion_D2D3	(Present Study)
TMPYyyyy	TCR_158_Mesacanthion_Paramesacanthion_D2D3	(Present Study)
TnhSpec3	Tylenchina sp. WY-460	EU018047
TOnYyyy2	TCR_17_Oncholaimidae_D2D3	(Present Study)
TOnYyyy3	TCR_69_Oncholaimidae_D2D3	(Present Study)
TOnYyyyy	TCR_12_Oncholaimidae_D2D3	(Present Study)
TorConv3	Torynurus convolutus	AY292806
TPhYyyy2	TCR_148_Phanodermopsis_D2D3	(Present Study)
TPhYyyy3	TCR_152_Phanodermopsis_D2D3	(Present Study)
TPhYyyy4	TCR_188_Phanodermopsis_D2D3	(Present Study)
TPhYyyy5	TCR_190_Phanodermopsis_D2D3	(Present Study)
TPhYyyy6	TCR_216_Phanodermopsis_D2D3	(Present Study)
TPhYyyy7	TCR_78_Phanodermopsis_D2D3	(Present Study)
TPhYyyy8	TCR_80_Phanodermopsis_D2D3	(Present Study)
TPhYyyyy	TCR_108_Phanodermopsis_D2D3	(Present Study)
TpmArena	Trophonema arenarium	AY780971
TPnYyyy2	TCR_173_Phanodermatidae_D2D3	(Present Study)
TPnYyyy3	TCR_70_Phanodermatidae_D2D3	(Present Study)
TPnYyyy4	TCR_75_Phanodermatidae_D2D3	(Present Study)
TPnYyyyy	TCR_153_Phanodermatidae_D2D3	(Present Study)
TpsYyyyy	TCR_197_Anticoma_D2D3	(Present Study)
TPtYyyy2	TCR_149_Anticomidae_D2D3	(Present Study)
TPtYyyyy	TCR_141_Cephalanticoma_D2D3	(Present Study)
TRAYyyyy	TCR_44_Anticoma_D2D3	(Present Study)
TrcCyli3	Trichodorus cylindricus	AM180728
TrcPrim6	Trichodorus primitivus	AM180729
TrcSimi5	Trichodorus similis	DQ832183
TrcSimi6	Trichodorus similis	AM180730
TREYyyyy	TCR_102_Thoracostomopsidae_D2D3	(Present Study)
TrgWils3	Troglostrongylus wilsoni	AY292807

TrhSpir3	Trichinella spiralis	AF342803
TroSculp	Trophurus sculptus	DQ328709
TrsColu2	Trichostrongylus colubriformis	AM039743
TrtPalm2	Teratorhabditis palmarum	EF990717
TrtSynp3	Teratorhabditis synpapillata	AB269817
TRVYyyyy	TCR_42_Oncholaimidae_D2D3	(Present Study)
TRxYyyy2	TCR_180_Oxystomina_D2D3	(Present Study)
TRxYyyy3	TCR_202_Oxystomina_D2D3	(Present Study)
TRxYyyy4	TCR_212_Oxystomina_D2D3	(Present Study)
TRxYyyy5	TCR_91_Oxystomina_D2D3	(Present Study)
TRxYyyyy	TCR_21_Oxystomina_D2D3	(Present Study)
TSnYyyyy	TCR_206_Synonchus_D2D3	(Present Study)
TTLYyyyy	TCR_82_Comesomatidae_D2D3	(Present Study)
TtnYyyy2	TCR_89_Litinium_D2D3	(Present Study)
TtnYyyy3	TCR_90_Litinium_D2D3_	(Present Study)
TtnYyyyy	TCR_205_Litinium_D2D3	(Present Study)
TurAcet2	Turbatrix aceti	AY294184
UncAphan	uncultured Aphanolaimus sp.	DQ086654
UnnSpe12	Uncinaria sp. 3677	AF217874
UnnSpe13	Uncinaria sp. 3675	AF217882
UnnSpe15	Uncinaria sp. 3679	AF217881
UnnSpe17	Uncinaria sp. 3671	AF217880
UnnSpe18	Uncinaria sp. 3672	AF217888
UnnSpe20	Uncinaria sp. 3681	AF217883
UnnSpec6	Uncinaria sp. 3688	AF217887
UnnSpec8	Uncinaria sp. 3682	AF217884
UnnSpec9	Uncinaria sp. 3676	AF217869
UnnSpeci	Uncinaria sp. 3685	AF217870
UnnSteno	Uncinaria stenocephala	AF217867
VisSpec4	Viscosia sp. 3P6K2	DQ077751
VisSpec5	Viscosia sp. 1114K2	DQ077779
WUMYyyy2	WUS_6_Enoplolaimus_Mesacanthion_D2D3	(Present Study)
WUMYyyyy	WUS_3_Enoplolaimus_Mesacanthion_D2D3	(Present Study)
WUpYyyy2	WUS_2_Enoplolaimus_D2D3	(Present Study)
WUpYyyy3	WUS_4_Enoplolaimus_D2D3	(Present Study)
WUpYyyy4	WUS_5_Enoplolaimus_D2D3	(Present Study)
WUpYyyy5	WUS_7_Enoplolaimus_D2D3	(Present Study)
WUpYyyyy	WUS_1_Enoplolaimus_D2D3	(Present Study)
XipCitr2	Xiphinema citricolum	DQ299491
XipCitr3	Xiphinema citricolum	DQ299492
XipCitr4	Xiphinema citricolum	DQ285668
XipCitr5	Xiphinema citricolum	DQ299494
XipCitr6	Xiphinema citricolum	DQ299490
XipCitr7	Xiphinema citricolum	DQ299493
XipFlor2	Xiphinema floridae	DQ299508
XipFlor3	Xiphinema floridae	DQ299509
XipFlor4	Xiphinema floridae	DQ299507
XipFlor5	Xiphinema floridae	DQ299510

XipGeor2	Xiphinema georgianum	DQ299502
XipGeor3	Xiphinema georgianum	DQ299498
XipGeor4	Xiphinema georgianum	DQ299495
XipGeor5	Xiphinema georgianum	DQ299500
XipGeor6	Xiphinema georgianum	DQ299497
XipGeor7	Xiphinema georgianum	DQ299501
XipGeor8	Xiphinema georgianum	DQ299499
XipGeor9	Xiphinema georgianum	DQ299496
XipLaev2	Xiphinema laevistriatum	DQ299506
XipLaev3	Xiphinema laevistriatum	DQ299503
XipLaev4	Xiphinema laevistriatum	DQ299505
XipLaevi	Xiphinema laevistriatum	DQ299504
XipTarja	Xiphinema tarjanense	DQ299511
XyaSpeci	Xyala sp. 3P11K2	DQ077761
ZelPunc3	Zeldia punctata	AF147070
ZelPunc4	Zeldia punctata	DQ145662
ZelPunc6	Zeldia punctata	EU195988
ZelSpec4	Zeldia sp. JB-118	DQ145633
ZelSpec5	Zeldia sp. JB-140	DQ145663
ZonMaws2	Zoniolaimus mawsonae	AM039730

Appendix III: Published Manuscripts

Appendix IV: Recipe for DESS preservative

*Don Personal Protective Equipment – laboratory coat, gloves & goggles.

<u>D.E.S.S. ingredients:</u>	<u>Equipment:</u>
DMSO soln.	Heat & stir device with magnet
EDTA disodium salt	1 & 2 litre glass beaker
20% NaOH soln.	250 & 50ml measuring cylinders
25% HCl soln.	pH meter
NaCl crystals	Balance (to 2 decimal points)
Distilled water	Funnel
	Squeeze bottle
	Pipette
	Large dessert spoon (for adding NaCl)

D.E.S.S. recipe (for 1 litre):

- Measure out 93.06g of EDTA disodium salt (Formula weight 372.24g) – for a 0.25Mol soln. Place a magnet in the glass beaker and place on the heat & stir device. Add 200ml of distilled water to the beaker, set the temperature for 30°C and the magnet to stir. Add the EDTA salt to the beaker. **N.B. for EDTA salt with a different FW you will need to recalculate.**
- The EDTA salt solution will be in the region of 3-4pH. Quickly add 60ml of NaOH; the alkalinity will peak at over 13 but steady off at a pH of about 9 as the EDTA dissolves. **Raising the alkalinity quickly will assist in dissolving of the EDTA salt as does heating to 30°C.**
- Once the EDTA salt is dissolved, reduce the pH to 7.5 using about 20ml of HCl (adjust with pipette near the end) and top the volume up to 800ml with distilled water.
- Make up 20% DMSO by adding 40ml of DMSO to 160ml of distilled water (*note that the measuring cylinder will warm due to a chemical reaction), add to the beaker and continue stirring.
- Transfer the solution to a 1 litre measuring cylinder and top up if necessary and transfer to a 2 litre beaker back on the heat and stir.
- Add NaCl crystals till saturation is achieved; at least a centimetre of undissolved salt should be sitting on the bottom of the beaker to ensure this. Pour the solution into a container through a 45 micron sieve leaving most of the un-dissolved salt crystals in the beaker.
- Rinse all equipment into the D.E.S.S. waste bottle and rinse/wash thoroughly.

References

- Abebe, E., I. Andr ssy and W. Traunspurger (2006). Freshwater nematodes: ecology and taxonomy. Wallingford, UK, CABI Publishing, 576 pp.
- Aleshin, V. V., O. S. Kedrova, I. A. Milyutina, N. S. Vladychenskaya and N. B. Petrov (1998). "Relationships among nematodes based on the analysis of 18S rRNA gene sequences: molecular evidence for monophyly of chromadorian and secernentian nematodes." Russian Journal of Nematology **6**: 175-184.
- Alve, E. and S. T. Goldstein (2003). "Propagule transport as a key method of dispersal in benthic foraminifera (Protista)." Limnology and Oceanography **48**: 2163-2170.
- Andr ssy, I. (1976). Evolution as a Basis for the Systematization of Nematodes. London, San Francisco, Melbourne, Pitman Publishing, 288 pp.
- Armonies, W. (1989). "Occurrence of meiofauna in *Phaeocystis* seafoam." Marine Ecology Progress Series **53**: 305-309.
- Armstrong, M. R., V. C. Blok and M. S. Phillips (2000). "A multipartite mitochondrial genome in the potato cyst nematode *Globodera pallida*." Genetics **154**: 181-192.
- Arntz, W. E., J. Gutt and M. Klages (1997). Antarctic marine biodiversity: An overview. Antarctic communities: species, structure and survival. B. Battaglia, J. Valencia and D. W. H. Wallon. Cambridge, UK, Cambridge University Press, pp. 3-14.
- Arroyo, N. L., K. Aarnio and E. Bonsdorff (2006). "Drifting algae as a means of re-colonizing defaunated sediments in the Baltic Sea. A short-term microcosm study." Hydrobiologia **554**: 83-95.
- Baas-Becking, L. G. M. (1934). Geobiologie of inleiding tot de milieukunde. The Hague, The Netherlands, W.P. van Stockum and Zoon, 263 pp.
- Baccetti, B., R. Dallai, S. G. Dezio and A. Marinaria (1983). "The evolution of the nematode spermatozoon." Gamete Research **8**: 309-323.
- Bakker, J. and L. Bouwman-Smits (1988). "Contrasting rates of protein and morphological evolution in cyst nematode species." Phytopathology **78**: 900-904.
- Ban, N., P. Nissen, J. Hansen, M. Capel, P. B. Moore and T. A. Steitz (1999). "Placement of protein and RNA structures into a 5  -resolution map of the 50S ribosomal subunit." Nature **400**(841-847).
- Barnes, D. K. A. and P. Milner (2005). "Drifting plastic and its consequences for sessile organism dispersal in the Atlantic Ocean." Marine Biology **146**: 815-825.
- Beebe, T. J. C. and G. Rowe (2003). Phylogeography. An Introduction to Molecular Ecology. Oxford, UK, Oxford University Press, pp. 165-197.

- Bhadury, P., M. C. Austen, D. T. Bilton, P. J. D. Lamshead, A. Rogers and G. R. Smerdon (2007). "Exploitation of archived marine nematodes--a hot lysis DNA extraction protocol for molecular studies." Zoologica Scripta **36**(1): 93-98.
- Bhadury, P., M. C. Austen, D. T. Bilton, P. J. D. Lamshead, A. D. Rogers and G. R. Smerdon (2006). "Development and evaluation of a DNA-barcoding approach for the rapid identification of nematodes." Marine Ecology Progress Series **320**: 1-9.
- Bhadury, P., M. C. Austen, D. T. Bilton, P. J. D. Lamshead, A. D. Rogers and G. R. Smerdon (2006). "Molecular detection of marine nematodes from environmental samples: overcoming eukaryotic interference." Aquatic Microbial Ecology **44**: 97-103.
- Bhadury, P., M. C. Austen, D. T. Bilton, P. J. D. Lamshead, A. D. Rogers and G. R. Smerdon (2008). "Evaluation of combined morphological and molecular techniques for marine nematode (*Terschellingia* spp.) identification." Marine Biology **154**: 509-518.
- Bhadury, P., H. Bik, A. D. Rogers, P. J. D. Lamshead, M. C. Austen, D. T. Bilton and G. R. Smerdon (In preparation). "Molecular diversity of fungi co-amplified alongside nematode 18S rRNA amplicons from coastal and deep-sea marine environments."
- Bickley, J. and D. Hopkins (1999). Inhibitors and Enhancers of PCR. Analytical Molecular Biology. G. C. Saunders, H. C. Parkes and S. B. Primrose. Cambridge, Royal Society of Chemistry, pp. 81-102.
- Blair, J. E., P. Shah and S. B. Hedges (2005). "Evolutionary sequence analysis of complete eukaryote genomes." BMC Bioinformatics **6**: 53.
- Blaxter, M., J. Mann, T. Chapman, F. Thomas, C. Whitton, R. Floyd and A. Eyalalem (2005). "Defining operational taxonomic units using DNA barcode data." Philosophical Transactions of the Royal Society B **360**: 1935-1943.
- Blaxter, M. L. (2004). "The promise of a DNA taxonomy." Philosophical Transactions of the Royal Society of London B **359**(1444): 669-679.
- Blaxter, M. L., P. De Ley, J. R. Garey, L. X. Liu, P. Scheldeman, A. Vierstraete, J. R. Vanfleteren, L. Mackey, M. Dorris, L. M. Frisse, J. T. Vida and W. K. Thomas (1998). "A molecular evolutionary framework for the phylum Nematoda." Nature **392**: 71-75.
- Boore, J. L. and W. M. Brown (2000). "Mitochondrial genomes of *Galathealinum*, *Helobdella*, and *Platynereis*: sequence and gene arrangement comparisons indicate that pogonophora is not a phylum and annelida and arthropoda are not sister taxa." Molecular Biology and Evolution **17**: 87-106.
- Brandt, A., A. J. Gooday, S. N. Brandao, S. Brix, W. Brokeland, T. Cedhagen, M. Choudhury, N. Cornelius, B. Danis, I. De Mesel, R. J. Diaz, D. Gillan, B. Ebbe, J. A. Howe, D. Janussen, S. Kaiser, K. Linse, M. Malyutina, J. Pawlowski, M. Raupach and A. Vanreusel (2007). "First insights into the biodiversity and biogeography of the Southern Ocean deep sea." Nature **447**: 307-311.

- Bremer, B., R. K. Jansen, b. Oxelman, M. Backlund, H. Lantz and K.-J. Kim (1999). "More characters or more taxa for a robust phylogeny: case study from the coffee family (Rubiaceae)." Systematic Biology **48**: 413-435.
- Brey, T., C. Dahm, M. Gorny, M. Klages, M. Stiller and W. E. Arntz (1996). "Do Antarctic benthic invertebrates show an extended level of eurybathy?" Antarctic Science **8**(1): 3-6.
- Brinkmann, H. and H. Philippe (2008). "Animal phylogeny and large-scale sequencing: progress and pitfalls." Journal of Systematics and Evolution **46**(3): 274-286.
- Burki, F., Y. Inagaki, J. Bråte, J. M. Archibald, P. J. Keeling, T. Cavalier-Smith, M. Sakaguchi, T. Hashimoto, A. Horak, S. Kumar, D. Klaveness, K. S. Jakobsen, J. Pawlowski and K. Shalchian-Tabrizi (2009). "Large-scale phylogenomic analyses reveal that two enigmatic protist lineages, Theloniella and Centroheliozoa, are related to photosynthetic chromalveolates." Genome Biology and Evolution **1**(1): 231-238.
- Bussau, C. (1993). Taxonomische und ökologische untersuchungen an Nematoden des Peru-Beckens. Mathematisch-Naturwissenschaftlichen Fakultät. Kiel, Christian-Albrechts-Universität. **PhD Thesis**: 625.
- Butler, M. H., S. M. Wall, K. R. Luehrsen, G. E. Fox and R. M. Hecht (1981). "Molecular relationships between closely related strains and species of nematodes." Journal of Molecular Evolution **18**: 18-23.
- Cáceres, C. E. (1997). "Dormancy in invertebrates." Invertebrate Biology **116**(4): 371-383.
- Cannon, J. T., A. L. Rychel, H. Eccleston, K. M. Halanych and B. J. Swalla (2009). "Molecular phylogeny of hemichordata, with updated status of deep-sea enteropneusts." Molecular Phylogenetics and Evolution **52**(1): 17-24.
- Castresana, J. (2000). "Selection of conserved blocks for their use in phylogenetic analysis." Molecular Biology and Evolution **17**: 540-552.
- Cate, J. H., M. M. Yusupov, G. Z. Yusupova, T. N. Earnest and H. F. Noller (1999). "X-ray crystal structures of 70S ribosome functional complexes." Science **285**: 2095-2104.
- Chilton, N. B., L. A. Newton, I. Beveridge and R. B. Gasser (2001). "Evolutionary relationships of trichostrongyloid nematodes (Strongylida) inferred from ribosomal DNA sequence data." Molecular Phylogenetics and Evolution **19**: 367-386.
- Chitwood, B. G. (1937). A revised classification of the Nematoda. Papers in Helminthology, 30 Year Jubileum K.J. Skryabin. R.-E. S. Schulz and M. P. Gnyedina. Moscow, All-Union Lenin Academy of Agricultural Sciences, pp. 67-80.
- Chitwood, B. G. and M. B. Chitwood (1950). An Introduction to Nematology, second edition. Baltimore, MD, Monumental Printing Company, 372 pp.
- Churchill, G. A., A. von Haeseler and W. C. Navidi (1992). "Sample size for a phylogenetic inference " Molecular Biology and Evolution **9**: 753-769.

- Clark, W. C. (1961). "A revised classification of the Enoplida (Nematoda) " New Zealand Journal of Science **4**: 123-150.
- Clark, W. C. (1962). "The systematic position of the Alaimidae and the Diphtherophoroidea (Enoplida, Nematoda)." Nematologica **7**: 119-121.
- Clemons, W. M., J. L. C. May, B. T. Wimberly, J. P. McCutcheon, M. S. Capel and V. Ramakrishnan (1999). "Structure of a bacterial 30S ribosomal subunit at 5.5 Å resolution." Nature **400**: 833-840.
- Cook, A. A., P. Bhadury, N. J. Debenham, B. H. M. Meldal, M. Blaxter, G. R. Smerdon, M. C. Austen, P. J. D. Lamshead and A. Rogers (2005). "Denaturing gradient gel electrophoresis (DGGE) as a tool for identification of marine nematodes." Marine Ecology Progress Series **291**: 103-113.
- Coomans, A. (2002). "Present status and future of nematode systematics." Nematology **4**(5): 573-582.
- Coomans, A. V. and D. J. Raski (1988). "Two new species of *Prismatolaimus* De Man, 1880 (Nemata, Prismatolaimidae) in Southern Chile." Journal of Nematology **20**: 288-303.
- Crame, J. A. (1993). "Bipolar molluscs and their evolutionary implications." Journal of Biogeography **20**: 145-161.
- Creer, S., V. G. Fonseca, D. L. Porazinska, G. Giblin-Davidson, W. Sung, D. M. Power, M. Packer, G. R. Carvalho, M. Blaxter, P. J. D. Lamshead and W. K. Thomas (In press). "Ultra sequencing of the meiofaunal biosphere: Practice, pitfalls and promises." Molecular Ecology.
- Da Conceição, I. L. P. M., M. C. V. Dos Santos, I. M. De Oliveira Abrantes and M. S. N. De Almeida Santos (2003). "Using RAPD markers to analyse genetic diversity in Portuguese potato cyst nematode populations." Nematology **5**(1): 137-143.
- Da Fonsêca-Genevois, V., P. J. Somerfield, M. H. Baeta Neves, R. Coutinho and M. Moens (2006). "Colonization and early succession on artificial hard substrata by meiofauna." Marine Biology **148**(1039-1050).
- Dalevi, D., P. Hugenholtz and L. L. Blackall (2001). "A multiple-outgroup approach to resolving division-level phylogenetic relationships using 16S rDNA data." International Journal of Systematic and Evolutionary Microbiology **51**: 385-91.
- Darling, K. F., C. M. Wade, I. A. Stewart, D. Kroon, R. Dingle and A. J. L. Brown (2000). "Molecular evidence for genetic mixing of Arctic and Antarctic subpolar populations of planktonic foraminifers." Nature **405**: 43-47.
- Dayrat, B. (2005). "Towards integrative taxonomy." Biological Journal of the Linnean Society **85**: 407-415.
- De Broyer, C. and K. Jazdzewski (1996). "Biodiversity of the Southern Ocean: towards a new synthesis for the Amphipoda (Crustacea)." Bolletino del Museo Civico di Storia Naturale **20**: 547-568.

De Coninck, L. A. P. (1965). Systématique des Nématodes. Traite de Zoologie. P.-P. Grassé. **4**, pp. 1-731.

De Ley, P. (2000). "Lost in worm space: phylogeny and morphology as road maps to nematode diversity." Nematology **2**(1): 9-16.

De Ley, P. and W. Bert (2002). "Video capture and editing as a tool for the storage, distribution, and illustration of morphological characters of nematodes." Journal of Nematology **34**(4): 296-302.

De Ley, P. and M. Blaxter (2002). Systematic position and phylogeny. (Chapter 1). The Biology of Nematodes. D. Lee. Reading, Harwood Academic Publishers, pp. 1-30.

De Ley, P. and M. L. Blaxter (2004). A new system for Nematoda: combining morphological characters with molecular trees, and translating clades into ranks and taxa. Proceedings of the Fourth International Congress of Nematology, 8-13 June 2002, Tenerife, Spain. R. Cook and D. J. Hunt, Nematology Monographs and Perspectives, pp. 633-653.

De Ley, P., M. A. Félix, L. M. Frisse, S. A. Nadler, P. W. Sternberg and W. K. Thomas (1999). "Molecular and morphological characterisation of two reproductively isolated species with mirror-image anatomy (Nematoda: Cephalobidae)." Nematology **1**(6): 591-612.

De Ley, P., I. Tandingan De Ley, K. Morris, A. Eyualem, M. Mundo-Ocampo, M. Yoder, J. Heras, D. Waumann, A. Rocha-Olivares, A. H. J. Burr, J. G. Baldwin and W. K. Thomas (2005). "An integrated approach to fast and informative morphological vouchers of nematodes for applications in molecular barcoding." Philosophical Transactions of the Royal Society B **360**: 1945-1958.

De Mesel, I., H. J. Lee, S. Vanhove, M. Vincx and A. Vanreusel (2006). "Species diversity and distribution within the deep-sea nematode genus *Acantholaimus* on the continental shelf and slope in Antarctica." Polar Biology **29**: 860-871.

Debry, R. W. and R. G. Olmstead (2000). "A simulation study of reduced tree-search effort in bootstrap resampling analysis." Systematic Biology **49**: 171-179.

Derycke, S., T. Backeljau, C. Vlaeminck, A. Vierstraete, J. Vanfleteren, M. Vincx and T. Moens (2007). "Spatiotemporal analysis of population genetic structure in *Geomonhystera disjuncta* (Nematoda, Monhysteridae) reveals high levels of molecular diversity." Marine Biology **151**(5): 1799-1812.

Derycke, S., T. Remerie, T. Backeljau, A. Vierstraete, J. Vanfleteren, M. Vincx and M. Moens (2008). "Phylogeography of the *Rhabditis (Pellioditis) marina* species complex: evidence for long-distance dispersal, and for range expansions and restricted gene flow in the northeast Atlantic." Molecular Ecology **17**: 3306-3322.

Derycke, S., T. Remerie, A. Vierstraete, T. Backeljau, J. Vanfleteren, M. Vincx and T. Moens (2005). "Mitochondrial DNA variation and cryptic speciation within the free-living marine nematode *Pellioditis marina*." Marine Ecology Progress Series **300**: 91-103.

Dunn, C. W., A. Hejnal, D. Q. Matus, K. Pang, W. E. Browne, S. A. Smith, E. Seaver, G. W. Rouse, M. Obst, G. D. Edgecombe, M. V. Sørensen, Haddock, S.H.D., A. Schmidt-Rhaesa, A. Okusu, R. Møbjerg Kristensen, W. C. Wheeler, M. Q. Martindale and G. Giribet (2008). "Broad phylogenomic sampling improves resolution of the animal tree of life." Nature: doi:10.1038/nature06614.

Edwards, R. A., B. Rodriguez-Brito, L. Wegley, M. Haynes, M. Breitbart, D. M. Peterson, M. O. Saar, S. Alexander, E. C. Alexander Jr and F. Rohwer (2006). "Using pyrosequencing to shed light on deep mine microbial ecology." BMC Genomics **7**.

Elbadri, G. A. A., P. De Ley, L. Waeyenberge, A. Vierstraete, M. Moens and J. Vanfleteren (2002). "Intraspecific variation in *Radopholus similis* isolates assessed with restriction length polymorphism and DNA sequencing of the internal transcribed spacer region of the ribosomal RNA cistron." International Journal for Parasitology **32**: 199-205.

Ellis, R. E., J. E. Sulston and A. R. Coulson (1986). "The rDNA of *C. elegans*: sequence and structure." Nucleic Acids Research **14**: 2345-2364.

Esbenshade, P. R. and A. C. Triantaphyllou (1987). "Enzymatic relationships and evolution in the genus *Meloidogyne* (Nematoda: Tylenchida)." Journal of Nematology **19**: 8-18.

Eyuaem, A. and M. Blaxter (2003). "Comparison of biological, molecular, and morphological methods of species identification in a set of cultured *Panagrolaimus* isolates." Journal of Nematology **35**(1): 119-128.

Faust, M. A. and R. A. Gulledge (1996). "Associations of microalgae and meiofauna in floating detritus at a mangrove island, Twin Cays, Belize." Journal of Experimental Marine Biology and Ecology **197**: 159-175.

Felix, M. A., A. Verstraete and J. Vanfleteren (2001). "Three biological species closely related to *Rhabditis* (*Oscheius*) *pseudodolichura* Körner in Osche, 1952." Journal of Nematology **33**: 104-109.

Felsenstein, J. (1978). "Case in which parsimony and compatibility methods will be positively misleading." Systematic Zoology **27**: 401-410.

Felsenstein, J. (1985). "Confidence limits on phylogenies: an approach using the bootstrap." Evolution **39**: 783-791.

Felsenstein, J. and H. Kishino (1993). "Is there something wrong with the bootstrap on phylogenies? A reply to Hillis and Bull." Systematic Biology **42**(2): 193-200.

Fenchel, T. (2005). "Cosmopolitan microbes and their 'cryptic' species." Aquatic Microbial Ecology **41**: 49-54.

Fenchel, T. and B. J. Finlay (2004). "The ubiquity of small species: patterns of local and global diversity." BioScience **54**: 777-784.

Filipjev, I. N. (1918). "Nématodes libres marins des environs de Sébastopol. Partie I." Trudy Osoboï Zoologicheskoi Laboratorii I Sevastopol'skoi Biologicheskii Stantsii **4**: 1-362

(English Translation by Raveh, M. (1968) Free-living marine nematodes in the vicinity of Sevastopol. Part I. Israel Program for Scientific Translations, Jerusalem, 255 pp.).

Filipjev, I. N. (1929). "Les nématodes libres de la baie de la Neva et de l'extrémité orientale du Golfe de Finlande. Première partie." Archiv für Hydrobiologie **20**: 637-699.

Filipjev, I. N. (1934). "The classification of the free-living nematodes and their relation to the parasitic nematodes." Smithsonian Miscellaneous Collections **89**: 1-64.

Finlay, B. J. (2002). "Global diversity of free-living microbial eukaryote species." Science **296**: 1061-1063.

Floyd, R., E. Abebe, A. Papert and M. Blaxter (2002). "Molecular barcodes for soil nematode identification." Molecular Ecology **11**: 839-850.

Floyd, R., A. Rogers, P. J. D. Lamshead and C. R. Smith (2005). "Nematode-specific PCR primers for the 18S small subunit rRNA gene." Molecular Ecology Notes **5**: 611-612.

Folkertsma, R. T., J. N. Rouppe van der Voort, K. E. de Groot, P. M. van Zandvoort, A. Schots, F. J. Gommers, J. Helder and J. Bakker (1996). "Gene pool similarities of potato cyst nematode populations assessed by AFLP analysis." Molecular Plant-Microbe Interactions **9**(1): 47-54.

Fonseca, G., W. Decraemer and A. Vanreusel (2006). "Taxonomy and species distribution of the genus *Manganonema* Bussau, 1993 (Nematoda: Monhysterida)." Cahiers de Biologie Marine **47**: 189-203.

Fonseca, G., S. Derycke and T. Moens (2008). "Integrative taxonomy in two free-living nematode species complexes." Biological Journal of the Linnean Society **94**(4): 737-753.

Fonseca, V. G., G. R. Carvalho, W. Sung, H. F. Johnson, D. M. Power, S. P. Neill, M. Packer, M. Blaxter, P. J. D. Lamshead, W. K. Thomas and S. Creer (Submitted). "How much do we know about marine metazoan biodiversity? Results from second generation sequencing."

Fontaneto, D., T. G. Barraclough, K. Chen, C. Ricci and E. A. Herniou (2008). "Molecular evidence for broad-scale distributions in bdelloid rotifers: everything is not everywhere but most things are widespread." Molecular Ecology **17**: 3136-3146.

Fontaneto, D., G. F. Ficetola, R. Ambrosini and C. Ricci (2006). "Patterns of diversity in microscopic animals: are they comparable to those in protists or larger animals?" Global Ecology and Biogeography **15**: 153-162.

Foucher, A. L. J. L., T. Bongers, L. R. Noble and M. J. Wilson (2004). "Assessment of nematode biodiversity using DGGE of 18S rDNA following extraction of nematodes from soil." Soil Biology & Biochemistry **36**: 2027-2032.

Gerlach, S. A. and F. Riemann (1973). "The Bremerhaven checklist of aquatic nematodes. A catalogue of nNematoda Adenophorea excluding the Dorylaimida. Part I." Veröffentlichungen des Institutes für Meeresforschung Bremerhaven, Sonderdruck **4**: 1-404.

Gibbons, L. M. (2001). General Organisation. The Biology of Nematodes. D. L. Lee. London, Taylor & Francis.

Giere, O. (2008). Meiobenthology: The microscopic motile fauna of aquataic sediments, 2nd Edition. Berlin, Springer, 528 pp.

Giere, O. (2009). Meiobenthology: The microscopic motile fauna of aquataic sediments, 2nd Edition. Berlin, Springerpp.

Giribet, G., C. W. Dunn, G. D. Edgecombe and G. W. Rouse (2007). "A modern look at the Animal Tree of Life." Zootaxa **1668**: 61-79.

Glennner, H., A. J. Hansen, M. V. Sorensen, F. Ronquist, J. P. Huelsenbeck and E. Willerslev (2004). "Bayesian inference of the metazoan phylogeny: A combined molecular and morphological approach." Current Biology **14**: 1644-1649.

Gómez, A., P. J. Wright, D. H. Lunt, J. M. Cancino, G. R. Carvalho and R. N. Hughes (2007). "Mating trials validate the use of DNA barcoding to reveal cryptic speciation of a marine bryozoan taxon." Proceedings of the Royal Society B **274**(1607): 199-207.

Graur, D. and W.-H. Li (1991). "Neutral mutation hypothesis test." Nature **354**: 114-115.

Graybeal, A. (1998). "Is it better to add taxa or characters to a difficult phylogenetic problem?" Systematic Biology **47**(1): 9-17.

Griffiths, B. S., S. Donn, R. Neilson and T. J. Daniell (2006). "Molecular sequencing and morphological analysis of a nematode community." Applied Soil Ecology **32**: 325-337.

Gu, X., Y.-X. Fu and W.-H. Li (1995). "Maximum likelihood estimation of the heterogeneity of substitution rate among nucleotide sites." Molecular Biology and Evolution **12**: 546-557.

Guil, N., S. Sánchez-Moreno and A. Machordom (2009). "Local biodiversity patterns in micrometazoans: Are tardigrades everywhere?" Systematics and Biodiversity **7**(3): 259-268.

Hackett, S. J., R. T. Kimball, S. Reddy, R. C. K. Bowie, E. L. Braun, M. J. Braun, J. L. Chojnowski, W. A. Cox, K.-L. Han, J. Harshman, C. J. Huddleston, B. D. Marks, K. J. Miglia, W. S. Moore, F. H. Sheldon, D. W. Steadman, C. C. Witt and T. Yuri (2008). "A phylogenomic study of birds reveals their evolutionary history." Science **320**(5884): 1763-1768.

Hagerman, G. M. and R. M. Rieger (1981). "Dispersal of benthic meiofauna by wave and current action in Bogue Sound, North Carolina, USA." Marine Ecology **2**(3): 245-270.

Hajibabaei, M., D. H. Janzen, J. M. Burns, W. Hallwachs and P. D. N. Hebert (2006). "DNA barcodes distinguish species of tropical Lepidoptera." Proceedings of the National Academy of Science USA **103**(4): 968-971.

Halanych, K. M. (2004). "The new view of animal phylogeny." Annual Review of Ecology and Systematics **35**: 229-256.

Hall, B. G. (2005). "Comparison of the accuracies of several phylogenetic methods using protein and DNA sequences." Molecular Biology and Evolution **22**: 792-802.

Hall, B. G. (2008). Phylogenetic trees made easy: A how-to manual, 3rd edition. Sunderland, MA, Sinauer Associates, Inc., 233 pp.

Harris, T. S., L. J. Sandall and T. O. Powers (1990). "Identification of single *Meloidogyne* juveniles by polymerase chain reaction amplification of mitochondrial DNA." Journal of Nematology **22**(4): 518-524.

Hasegawa, M., H. Kishino and T. Yano (1985). "Dating of the human-ape splitting by a molecular clock of mitochondrial DNA." Journal of Molecular Evolution **22**: 160-174.

Heath, T. A., S. M. Hedtke and D. M. Hillis (2008). "Taxon sampling and the accuracy of phylogenetic analyses." Journal of Systematics and Evolution **46**(3): 239-257.

Hebert, P. D., S. Ratnasingham and J. R. deWaard (2003). "Barcoding animal life: cytochrome c oxidase subunit 1 divergences among closely related species." Proceedings of the Royal Society of London B **270**: S96-S99.

Hebert, P. D. N., A. Cywinska, S. L. Ball and J. R. deWaard (2003). "Biological identifications through DNA barcodes." Proceedings of the Royal Society of London B **270**: 313-321.

Hebert, P. D. N., E. H. Penton, J. M. Burns, D. H. Janzen and W. Hallwachs (2004). "Ten species in one: DNA barcoding reveals cryptic species in the neotropical skipper butterfly *Astraptes fulgerator*." Proceedings of the National Academy of Science USA **101**(41): 14812-14817.

Hendy, M. D. and D. Penny (1989). "A framework for the quantitative study of evolutionary trees." Systematic Biology **34**(4): 297-309.

Hessler, R. R. and D. Thistle (1975). "On the place of origin of deep-sea isopods." Marine Biology **32**: 155-165.

Hessler, R. R., G. D. Wilson and D. Thistle (1979). "The deep-sea isopods: a biogeographic and phylogenetic overview." Sarsia **64**: 67-75.

Hickson, R. E., C. Simon, A. Cooper, G. S. Spicer, J. Sullivan and D. Penny (1996). "Conserved sequence motifs, alignment, and secondary structure for the third domain of animal 12S rRNA." Molecular Biology and Evolution **13**(1): 150-169.

Hillis, D. M. (1996). "Inferring complex phylogenies." Nature **383**: 130-131.

Hillis, D. M. and J. J. Bull (1993). "An empirical test of bootstrapping as a method for assessing confidence in phylogenetic analysis." Systematic Biology **42**(2): 182-192.

Hillis, D. M., J. J. Bull, M. E. White, M. R. Badgett and I. J. Molineux (1992). "Experimental phylogenetics: generation of a known phylogeny." Science **255**: 589-592.

- Hillis, D. M. and M. T. Dixon (1991). "Ribosomal DNA: molecular evolution and phylogenetic inference." Quarterly Review of Biology **66**: 411-436.
- Hillis, D. M., J. P. Huelsenbeck and D. L. Swofford (1994). "Hobgoblin of phylogenetics?" Nature **369**: 363-364.
- Hillis, D. M., C. Moritz and B. K. Mable (1996). Applications of molecular systematics. Molecular Systematics, Second Edition. D. M. Hillis, C. Moritz and B. K. Mable. Sunderland, MA, Sinauer Associates, Inc., pp. 515-543.
- Hillis, D. M., D. D. Pollock, J. A. McGuire and D. J. Zwickl (2003). "Is sparse taxon sampling a problem for phylogenetic inference?" Systematic Biology **52**(1): 124-126.
- Hines, H. M., J. H. Hunt, T. K. O'Connor, J. J. Gillespie and S. A. Cameron (2007). "Multigene phylogeny reveals eusociality evolved twice in vespid wasps." Proceedings of the National Academy of Science USA **104**(9): 3295-3299.
- Holterman, M., O. Holovachov, S. Van den Elsen, H. van Megen, T. Bongers, J. Bakker and J. Helder (2008). "Small subunit ribosomal DNA-based phylogeny of basal Chromadorea (Nematoda) suggests that transitions from marine to terrestrial habitats (and *vice versa*) require relatively simple adaptations." Molecular Phylogenetics and Evolution **48**: 758-763.
- Holterman, M., A. van der Wurff, S. van den Elsen, H. van Megen, T. Bongers, O. Holovachov, J. Bakker and J. Helder (2006). "Phylum-wide analysis of SSU rDNA reveals deep phylogenetic relationships among nematodes and accelerated evolution toward crown clades." Molecular Biology and Evolution **23**(9): 1792-1800.
- Hope, W. D. and D. G. Murphy (1972). "A taxonomic hierarchy and checklist of the genera and higher taxa of marine nematodes." Smithsonian Contributions to Zoology **137**: 1-101.
- Hu, M., A. R. Jex, B. E. Campbell and R. B. Gasser (2007). "Long PCR amplification of the entire mitochondrial genome from individual helminths for direct sequencing." Nature Protocols **2**(10): 2339-2344.
- Huang, C. G., S. T. Lamitina, P. Agre and K. Strange (2007). "Functional analysis of the aquaporin gene family in *Caenorhabditis elegans*." American Journal of Physiology--Cell Physiology **292**: C1867-C1873.
- Huelsenbeck, J. P. and D. M. Hillis (1993). "Success of phylogenetic method in the four-taxon case." Systematic Biology **42**: 247-264.
- Huelsenbeck, J. P., D. M. Hillis and R. Jones (1996). Parametric bootstrapping in molecular phylogenetics: applications and performance. Molecular Zoology: Advances, Strategies, and Protocols. J. D. Ferraris and S. R. Palumbi. New York, Wiley-Liss, pp. 19-45.
- Huelsenbeck, J. P. and F. Ronquist (2001). "MRBAYES: Bayesian inference of phylogenetic trees." Bioinformatics **17**(8): 754-755.

- Hugall, A., J. Stanton and C. Moritz (1999). "Reticulate evolution and the origins of ribosomal internal transcribed spacer diversity in apomictic *Meloidogyne*." Molecular Biology and Evolution **16**(2): 157-164.
- Hugot, J. P., P. Baujard and S. Morand (2001). "Biodiversity in helminths and nematodes as a field of study: an overview." Nematology **3**(3): 199-208.
- Hung, G.-C., N. B. Chilton, I. Beveridge, X. Q. Zhu, J. R. Lichtenfels and R. B. Gasser (1999). "Molecular evidence for cryptic species within *Cylicostephanus minutus* (Nematoda: Strongylidae)." International Journal for Parasitology **29**: 285-291.
- Hunt, T. and A. P. Vogler (2008). "A protocol for large-scale rRNA sequence analysis: Towards a detailed phylogeny of Coleoptera." Molecular Phylogenetics and Evolution **47**: 289-301.
- Hutcheon, J. M., J. A. W. Kirsch and J. D. Pettigrew (1998). "Base-compositional biases and the bat problem. III. The question of microchiropteran monophyly." Philosophical Transactions of the Royal Society B **353**: 607-617.
- Hyde, K. D., E. B. G. Jones, E. Leañó, S. B. Pointing, A. D. Poonyth and L. L. P. Vrijmoed (1998). "Role of fungi in marine ecosystems." Biodiversity and Conservation **7**(9): 1147-1161.
- Hyman, B. C. and T. M. Slater (1990). "Recent appearance and molecular characterization of mitochondrial DNA deletions within a defined nematode pedigree." Genetics **124**: 845-853.
- Inglis, W. G. (1983). "An outline classification of the phylum Nematoda." Australian Journal of Zoology **31**: 243-255.
- Jablonski, D. and D. J. Bottjer (1988). Onshore-offshore evolutionary patterns in post-Paleozoic echinoderms. Echinoderm Biology, Proceedings of the 6th International Echinoderm Conference. R. D. Burke. Rotterdam, Balkema, pp. 81-90.
- Jairajpuri, M. S. and W. Ahmad (1992). Dorylaimida, Free living, Predacious and Plant-Parasitic Nematodes. New Delhi, Oxford & IBH Publishing Co. Pvt. Ltd., 458 pp.
- Janecek, L. L., R. L. Honeycutt, R. M. Adkins and S. K. Davis (1996). "Mitochondrial gene sequences and the molecular systematics of the artiodactyl subfamily Bovinae." Molecular Phylogenetics and Evolution **6**: 107-119.
- Jensen, P. (1988). "Nematode assemblages in the deep-sea benthos of the Norwegian Sea." Deep-Sea Research I **35**(7): 1173-1184.
- Johnson, K. P. (2001). "Taxon sampling and the phylogenetic position of Passeriformes: evidence from 916 avian cytochrome b sequences." Systematic Biology **50**: 128-136.
- Jones, C. J., K. J. Edwards, S. Castaglione, M. O. Winfield, F. Sala, C. van de Wiel, G. Bredemeijer, B. Vosman, M. Matthes, A. Daly, R. Brettschneider, P. Bettini, M. Buiatti, E. Maestri, A. Malcevski, N. Marmioli, R. Aert, G. Volckaert, J. Rueda, R. Linacero, A.

Vazquez and A. Karp (1997). "Reproducibility testing of RAPD, AFLP and SSR markers in plants by a network of European laboratories." Molecular Breeding **3**: 381-390.

Justine, J.-L. (2002). Male and female gametes and fertilisation. The biology of nematodes. D. L. Lee. London, Taylor & Francis, pp. 73-119.

Kanzaki, N. and K. Futai (2002). "A PCR primer set for determination of phylogenetic relationships of *Bursaphelenchus* species within the *xylophilus* group." Nematology **4**(1): 35-41.

Kaplan, D. T., W. K. Thomas, L. M. Frisse, J.-L. Sarah, J. M. Stanton, P. R. Speijer, D. H. Marin and C. H. Opperman (2000). "Phylogenetic analysis of geographically diverse *Radopholus similis* via rDNA sequence reveals a monomorphic motif." Journal of Nematology **32**: 134-142.

Kenny, R. and L. P. Knauth (2001). "Stable isotope variations in the Neoproterozoic Beck Spring Dolomite and Mesoproterozoic Mescal Limestone paleokarst: Implications for life on land in the Precambrian." Geological Society of America Bulletin **113**(5): 650-658.

Kjer, K. M. (1995). "Use of rRNA secondary structure in phylogenetic studies to identify homologous positions: An example of alignment and data presentation from the frogs." Molecular Phylogenetics and Evolution **4**(3): 314-330.

Knauth, L. P. (1998). "Salinity history of the Earth's early ocean." Nature **395**: 554-555.

Knowlton, N. (2000). "Molecular genetic analyses of species boundaries in the sea." Hydrobiologia **420**: 73-90.

Kumar, S. and A. Filipski (2007). "Multiple sequence alignment: In pursuit of homologous DNA positions." Genome Research **17**: 127-135.

Labandeira, C. C. (2005). "Invasion of the continents: cyanobacterial crusts to tree-inhabiting arthropods." Trends in Ecology and Evolution **20**: 253-262.

Lamshead, P. J. D. (1986). "Sub-catastrophic sewage and industrial waste contamination as revealed by marine nematode faunal analysis." Marine Ecology Progress Series **29**: 247-260.

Lamshead, P. J. D. (1993). "Recent developments in marine benthic biodiversity research." Océanis **19**(6): 5-24.

Lamshead, P. J. D. (2004). Marine Nematode Biodiversity. Nematology: Advances and Perspectives. Z. X. Chen, Chen, S.Y., and Dickson, D.W. Wallingford, CABI Publishing. **1**, pp. 439-468.

Lamshead, P. J. D. and G. Boucher (2003). "Marine nematode deep-sea biodiversity--hyperdiverse or hype?" Journal of Biogeography **30**: 475-485.

Lamshead, P. J. D., C. J. Brown, T. Ferrero, L. E. Hawkins, C. R. Smith and N. J. Mitchell (2003). "Biodiversity of nematode assemblages from the region of the Clarion-Clipperton Fracture Zone, and area of commercial mining interest." BMC Ecology **3**(1): 1-12.

Lambshead, P. J. D. and P. Schalk (2001). Overview of Marine Invertebrate Biodiversity. Encyclopedia of Biodiversity, Volume 3. S. Levin. New York, Academic Press, pp. 543-559.

Lamitina, S. T., R. Morrison, G. W. Moeckel and K. Strange (2004). "Adaptation of the nematode *Caenorhabditis elegans* to extreme osmotic stress." American Journal of Physiology--Cell Physiology **286**: C785-C791.

Lecointre, G., H. Philippe, H. L. Van Le and H. Le Guyader (1993). "Species sampling has a major impact on phylogenetic inference." Molecular Phylogenetics and Evolution **2**(3): 205-224.

Lee, D. L. (1961). "Two new species of cryptobiotic (anabiotic) freshwater nematodes, *Actinolaimus hintoni* sp. nov. and *Dorylaimus keilini* sp. nov. (Dorylaimidae)." Parasitology **51**: 237-240.

Lee, M. S. Y. (2001). "Unalignable sequences and molecular evolution." Trends in Ecology and Evolution **16**(12): 681-685.

Lerat, E., V. Daubin and N. A. Moran (2003). "From gene trees to organismal phylogeny in prokaryotes: The case of the γ -proteobacteria." Plos Biology **1**(1): 101-109.

Lindbergh, D. R. (1991). "Marine biotic interchange between the northern and southern hemispheres." Paleobiology **17**: 308-324.

Lindner, A., S. D. Cairns and C. W. Cunningham (2008). "From offshore to onshore: Multiple origins of shallow-water corals from deep-sea ancestors." PLoS One **3**(6): e2429.

Liò, P. and N. Goldman (1998). "Models of molecular evolution and phylogeny." Genome Research **8**: 1233-1244.

Lockhard, P. J., M. A. Steel, M. D. Hendy and D. Penny (1994). "Recovering evolutionary trees under a more realistic model of sequence evolution." Molecular Biology and Evolution **11**(4): 605-612.

Lorenzen, S. (1981). Entwurf eines phylogenetischen Systems der freilebenden Nematoden. Veröffentlichungen des Instituts für Meeresforschung in Bremerhaven (Supplement), pp. 1-472. (English Translation: Lorenzen, S., 1994. The Phylogenetic Systematics of Freelifving Nematodes. The Ray Society, London, 383 pp). .

Lorenzen, S., M. Prein and C. Valentin (1987). "Mass aggregations of the free-living marine nematode *Pontonema vulgare* (Oncholaimidae) in organically polluted fjords." Marine Ecology Progress Series **37**: 27-34.

Ludwig, W., O. Strunk, R. Westram, L. Richter, H. Meier, Y. Kumar, A. Buchner, T. Lai, S. Steppi, G. Jobb, W. Förster, I. Brettske, S. Gerber, A. W. Ginhart, O. Gross, S. Grumann, S. Hermann, R. Jost, A. König, T. Liss, R. Lüßmann, M. May, B. Nonhoff, B. Reichel, R. Strehlow, A. Stamatakis, N. Stuckmann, A. Vilbig, M. Lenke, T. Ludwig, A. Bode and K. H. Schleifer (2004). "ARB: a software environment for sequence data." Nucleic Acids Research **32**(4): 1363-1371.

Lyons-Weiler, J., G. A. Hoelzer and R. J. Tausch (1998). "Optimal outgroup analysis." Biological Journal of the Linnean Society **64**: 493-511.

Maddison, D. R., M. Ruvolo and D. L. Swofford (1992). "Geographic origins of human mitochondrial DNA phylogenetic evidence from control region sequences." Systematic Biology **41**: 111-124.

Maddison, W. P. (1989). "Reconstructing character evolution on polytomous cladograms." Cladistics **5**: 365-377.

Maddison, W. P., M. J. Donoghue and D. R. Maddison (1984). "Outgroup analysis and parsimony." Systematic Zoology **33**: 83-103.

Maggenti, A. R. (1963). Comparative morphology on nemic phylogeny. The Lower Metazoa, comparative biology and phylogeny. E. C. Dougherty, Z. N. Brown, E. D. Hanson and W. D. Hartmann. Berkeley, University of California Press, pp. 273-282.

Maggenti, A. R. (1982). Nematoda. Synopsis and classification of living organisms. S. P. Parker. New York, McGraw-Hill Book Co. **1**, pp. 879-929.

Maggenti, A. R. (1983). Nematode higher classification as influenced by species and family concepts. Concepts in Nematode Systematics. A. R. Stone, H. M. Platt and L. F. Khalil. London, Academic Press, pp. 25-40.

Malakhov, V. V. (1994). Nematodes: structure, development, classification, and phylogeny. Washington, WA, Smithsonian Institution Press, 286 pp.

Mayden, R. L. and E. O. Wiley (1992). The fundamentals of phylogenetic systematics. Stanford, CA, Stanford University Press, 977 pp.

Meldal, B. H. M. (2004). Phylogenetic systematics of the phylum Nematoda: evidence from molecules and morphology. PhD Thesis. Southampton, UK, University of Southampton.

Meldal, B. H. M., N. J. Debenham, P. De Ley, I. Tandingan De Ley, J. R. Vanfleteren, A. R. Vierstraete, W. Bert, G. Borgonie, T. Moens, P. Tyler, M. C. Austen, M. Blaxter, A. D. Rogers and P. J. D. Lamshead (2007). "An improved molecular phylogeny of the Nematoda with special emphasis on marine taxa." Molecular Phylogenetics and Evolution **42**(3): 622-636.

Meudt, H. M. and A. C. Clarke (2007). "Almost Forgotten or Latest Practise? AFLP applications, analyses and advances." Trends in Plant Science **12**(3): 106-117.

Milinkovitch, M. C. and J. Lyons-Weiler (1998). "Finding optimal ingroup topologies and convexities when the choice of outgroups is not obvious." Molecular Phylogenetics and Evolution **9**: 348-57.

Miyamoto, M. M. and W. M. Fitch (1995). "Testing species phylogenies and phylogenetic methods with congruence." Systematic Biology **44**(1): 64-76.

Moens, T., D. Van Gansbeke and M. Vincx (1999). "Linking Estuarine nematodes to their suspected food. A case study from the Westerschelde Estuary (south-west Netherlands)." Journal of the Marine Biological Association of the UK **79**: 1017-1027.

Mort, M. E., P. S. Soltis and M. L. Mabry (2000). "Comparison of three methods for estimating internal support on phylogenetic trees." Systematic Biology **49**: 160-171.

Mullin, P. G., T. S. Harris and T. O. Powers (2003). "Systematic status of *Campydora* Cobb, 1920 (Nematoda: Campydorina)." Nematology **5**(5): 699-711.

Munn, E. A. and P. D. Munn (2002). Feeding and Digestion. The Biology of Nematodes. D. L. Lee. London, Taylor & Francis, pp. 211-232.

Muthumbi, A., K. Soetaert and M. Vincx (1997). "Deep-sea nematodes from the Indian Ocean: new and known species of the family Comesomatidae." Hydrobiologia **346**: 25-57.

Nei, M. (1987). Molecular Evolutionary Genetics. New York, Columbia University Press, 512 pp.

Nichols, R. (2001). "Gene trees and species trees are not the same." Trends in Ecology and Evolution **16**: 358-364.

Nixon, K. C. and J. M. Carpenter (1994). "On outgroups." Cladistics **9**: 413-26.

Nóbrega, R., A. M. Solé-Cava and C. A. M. Russo (2004). "High genetic homogeneity of an intertidal invertebrate along 8000km of the Atlantic coast of the Americas." Journal of Experimental Marine Biology and Ecology **303**: 173-181.

Noller, H. F. (1984). "Structure of ribosomal RNA." Annual Review of Biochemistry **53**: 119-162.

Ogden, T. H. and M. S. Rosenberg (2006). "Multiple sequence alignment accuracy and phylogenetic inference." Systematic Biology **55**(2): 314-328.

Okimoto, R., H. M. Chamberlin, J. MacFarlane and D. R. Wolstenholme (1991). "Repeated sequence sets in mitochondrial DNA molecules of root knot nematodes (*Meloidogyne*): nucleotide sequences, genome location and potential for host-race identification." Nucleic Acids Research **19**(7): 1619-1626.

Omland, K. E., S. M. Lanyon and S. J. Fritz (1999). "A molecular phylogeny of the New World orioles (*Icterus*): the importance of dense taxon sampling." Molecular Phylogenetics and Evolution **12**: 224-239.

Page, R. D. M. and E. C. Holmes (1998). Molecular evolution: a phylogenetic approach. Oxford, UK, Blackwell Publishing, 346 pp.

Palmer, M. A. (1988). "Dispersal of marine meiofauna: a review and conceptual model explaining passive transport and active emergence with implications for recruitment." Marine Ecology Progress Series **48**: 81-91.

- Palumbi, S. (1989). "Rates of molecular evolution and the fraction of nucleotide positions free to vary." Journal of Molecular Evolution **29**: 180-187.
- Palumbi, S., A. Martin, S. Romano, W. O. McMillan, L. Stice and G. Grabowski (1991). The Simple Fool's Guide to PCR, Version 2.0. Honolulu, Department of Zoology, University of Hawaii, 20 pp.
- Pawlowski, J., J. Fahrni, B. Lecroq, D. Longet, N. Cornelius, L. Excoffier, T. Cedhagen and A. J. Gooday (2007). "Bipolar gene flow in deep-sea benthic foraminifera." Molecular Ecology **16**: 4089-4096.
- Pearse, A. S. (1942). An Introduction to Parasitology. Springfield, Illinois, Charles C. Thomas, 375 pp.
- Philippe, H., R. Derelle, P. Lopez, K. Pick, C. Borchellini, N. Boury-Esnault, J. Vacelet, E. Renard, E. Houlston, E. Quéinnec, C. Da Silva, P. Wincker, H. Le Guyader, S. Leys, D. J. Jackson, F. Schreiber, D. Erpenbeck, B. Morgenstern and G. Wörheide (2009). "Phylogenomics revives traditional views on deep animal relationships." Current Biology **19**: 706-712.
- Philippe, H. and M. J. Telford (2006). "Large-scale sequencing and the new animal phylogeny." Trends in Ecology and Evolution **21**(11): 614-620.
- Phillips, A., D. Janies and W. Wheeler (2000). "Multiple sequence alignment in phylogenetic analysis." Molecular Phylogenetics and Evolution **16**(3): 317-330.
- Platonova, T. A. and V. V. Gal'tsova (1985). Nematodes and their role in the marine benthos. New Delhi, Amerind Publishing Co. Pvt. Ltd., 366 pp.
- Platt, H. M. and R. M. Warwick (1983). Free-Living Marine Nematodes, Part I: British Enoplids. Cambridge, Cambridge University Press, 307 pp.
- Platt, H. M. and Z. N. Zhang (1982). "New species of marine nematodes from Loch Ewe, Scotland." Bulletin of the British Museum of Natural History (Zoology) **42**: 227-246.
- Poinar Jr., G., H. Kerp and H. Hass (2008). "*Palaeonema phyticum* gen. n., sp. n. (Nematoda: Palaeonematidae fam. n), a Devonian nematode associated with early land plants." Nematology **10**(1): 9-14.
- Poinar Jr., G. O. (1991). Nematoda and Nematomorpha. Ecology and classification of North American freshwater invertebrates. J. H. Thorp and A. P. Covich. San Diego, CA, Academic Press, Inc.
- Porazinska, D. L., R. M. Giblin-Davis, L. Faller, W. Farmerie, N. Kanzaki, K. Morris, T. O. Powers, A. E. Tucker, W. Sung and W. K. Thomas (2009). "Evaluating high-throughput sequencing as a method for metagenomic analysis of nematode diversity." Molecular Ecology Resources **9**(6): 1439-1450.
- Posada, D. and K. A. Crandall (1998). "MODELTEST: testing the model of DNA substitution." Bioinformatics **14**(9): 817-818.

Powers, T. (2004). "Nematode molecular diagnostics: from bands to barcodes." Annual Review of Phytopathology **42**: 367-383.

Powers, T. O., T. C. Todd, A. M. Burnell, P. C. B. Murray, C. C. Fleming, A. L. Szalanski, B. A. Adams and T. S. Harris (1997). "The rDNA Internal Transcribed Spacer region as a taxonomic marker for nematodes." Journal of Nematology **29**(4): 441-450.

Prien, M. (1988). "Evidence for a scavenging lifestyle in the free-living nematode *Pontonema vulgare*." Kieler Meeresforsch **6**: 389-394.

Pruesse, E., C. Quast, K. Knittel, B. M. Fuchs, W. Ludwig, J. Peplies and F. O. Glöckner (2007). "SILVA: a comprehensive online resource for quality checked and aligned ribosomal RNA sequence data compatible with ARB." Nucleic Acids Research **35**(21): 7188-7196.

Razouls, S., C. Razouls and F. De Bovee (2000). "Biodiversity and biogeography of Antarctic copepods." Antarctic Science **3**: 343-362.

Reeves, J. H. (1992). "Heterogeneity in the substitution process of amino acid sites of proteins coded for by mitochondrial DNA." Journal of Molecular Evolution **35**: 17-35.

Rex, M. A., C. R. McClain, N. A. Johnson, R. J. Etter, J. A. Allen, P. Bouchet and A. Warén (2005). "A Source-sink hypothesis for abyssal biodiversity." The American Naturalist **165**(2): 163-178.

Riley, I. T., T. B. Reardon and A. C. McKay (1988). "Electrophoretic resolution of species boundaries in seed-gall nematodes, *Anguina* spp. (Nematoda, Anguinidae), from some graminaceous hosts in Australia and New Zealand." Nematologica **34**: 401-411.

Ripplinger, J. and J. Sullivan (2008). "Does choice in model selection affect maximum likelihood analysis?" Systematic Biology **57**(1): 76-85.

Robertson, C., J. K. Harris, J. R. Spear and N. R. Pace (2005). "Phylogenetic diversity and ecology of environmental Archaea." Current Opinion in Microbiology **8**: 638-642.

Rodriguez-Ezpeleta, N., H. Brinkmann, B. Roure, N. Lartillot, B. F. Lang and H. Philippe (2007). "Detecting and overcoming systematic errors in genome-scale phylogenies." Systematic Biology **56**: 389-399.

Rodríguez, F., J. L. Oliver, A. Marín and J. R. Medina (1990). "The general stochastic model of nucleotide substitution." Journal of Theoretical Biology **142**: 485-501.

Rogers, A. D. (2000). "The role of the oceanic oxygen minima in generating biodiversity in the deep sea." Deep-Sea Research II **47**(1-2): 119-148.

Rosenberg, M. S. (2005). "Evolutionary distance estimation and fidelity of pair wise sequence alignment." BMC Bioinformatics **6**: 102.

Rubtsova, T. V., M. Moens and S. A. Subbotin (2005). "PCR amplification of a rRNA gene fragment from formalin-fixed and glycerine-embedded nematodes from permanent slides." Russian Journal of Nematology **13**(2): 137-140.

- Rundle, S. D., D. T. Bilton and D. K. Shiozawa (2000). "Global and regional patterns in lotic meiofauna." Freshwater Biology **44**: 123-134.
- Runnagar, B. (2000). "Loophole for snowball earth." Nature **405**: 403-404.
- Rusin, L. Y., V. V. Aleshin, N. S. Vladychenskaya, I. A. Milyutina, O. S. Kedrova and N. B. Petrov (2001). "Trefusiidae are a subtaxon of marine Enoplida (Nematoda): evidence from primary structure of hairpin 35 and 48 loops of SSU rRNA gene." Molecular Biology **35**: 778-784.
- Saccone, C., C. De Giorgi, C. Gissi, G. Pesole and A. Reyes (1999). "Evolutionary genomics in Metazoa: the mitochondrial DNA as a model system." Gene **238**: 195-209.
- Sanderson, M. J. (1989). "Confidence limits on phylogenies: the bootstrap revisited." Cladistics **5**: 113-129.
- Sanderson, M. J. and H. B. Shaffer (2002). "Troubleshooting Molecular Phylogenetic Analyses." Annual Review of Ecology, Evolution and Systematics **33**: 49-72.
- Sanderson, M. J., M. F. Wojciechowski, J. M. Hu, T. S. Khan and S. G. Brady (2000). "Error, bias, and long-branch attraction in data for two chloroplast photosystem genes in seed plants." Molecular Biology and Evolution **17**: 782-797.
- Saunders, G. C. and H. C. Parkes (1999). Analytical Molecular Biology. Cambridge, Royal Society of Chemistry, 200 pp.
- Savolainen, V., M. W. Chase, S. B. Hoot, C. M. Morton, D. E. Soltis, C. Bayer, M. F. Fay, A. Y. De Bruijn, S. Sullivan and Y.-L. Qiu (2000). "Phylogenetics of flowering plants based on combined analysis of plastid atpB and rbcL gene sequences." Systematic Biology **49**: 306-362.
- Scheltema, R. S. and I. P. Williams (2009). "Reproduction among protobranch bivalves of the family Nuculidae from sublittoral, bathyal, and abyssal depths off the New England coast of North America." Deep-sea Research II **56**: 1835-1846.
- Schierenberg, E. (2005). "Unusual cleavage and gastrulation in a freshwater nematode: developmental and phylogenetic implications." Development genes and evolution **215**: 103-108.
- Sebastian, S., M. Raes, I. De Mesel and A. Vanreusel (2007). "Comparison of the nematode fauna from the Weddell Sea Abyssal Plain with two North Atlantic abyssal sites." Deep-sea Research II **54**: 1727-1736.
- Semblat, J. P., E. Wajnberg, A. Dalmasso, P. Abad and P. Castagnone-Sereno (1998). "High-resolution DNA fingerprinting of parthenogenetic root-knot nematodes using AFLP analysis." Molecular Ecology **7**: 119-125.
- Sepkoski, J. J., Jr. (1991). "A Model of Onshore-Offshore Change in Faunal Diversity." Paleobiology **17**(1): 58-77.

Shalchian-Tabrizi, K., M. A. Minge, M. Espelund, R. Orr, T. Ruden, K. S. Jakobsen and T. Cavalier-Smith (2008). "Multigene phylogeny of Choanozoa and the origin of animals." PLoS ONE **3**(5): e2098.

Shanks, A. L. and E. W. Edmondson (1990). "The vertical flux of metazoans (holoplankton, meiofauna, and larval invertebrates) due to their association with marine snow." Limnology and Oceanography **35**(2): 455-463.

Shannon, A. J., J. A. Browne, J. Boyd, D. A. Fitzpatrick and A. M. Burnell (2005). "The anhydrobiotic potential and molecular phylogenies of species and strains of *Panagrolaimus* (Nematoda, Panagrolaimidae)." Journal of Experimental Biology **208**(12): 2433-2445.

Shaw, A. K., A. L. Halpern and K. Beeson (2008). "It's all relative: ranking the diversity of aquatic bacterial communities." Environmental Microbiology **10**: 2200-2210.

Siddiqi, M. R. (1983). "Phylogenetic relationships of the soil nematode orders Dorylaimida, Mononchida, Triplonchida and Alaimida, with a revised classification of the subclass Enoplia." Pakistan Journal of Nematology **1**(2): 79-110.

Sidow, A. T., T. Nguyen and T. P. Speed (1992). "Estimating the fraction of invariable codons with a capture-recapture method." Journal of Molecular Evolution **35**: 253-260.

Skantar, A. M. and L. K. Carta (2004). "Molecular characterization and phylogenetic evaluation of the Hsp90 gene from selected nematodes." Journal of Nematology **36**(4): 466-480.

Smith, A. B. (1994). "Rooting molecular trees: Problems and strategies." Biological Journal of the Linnean Society **51**: 279-292.

Smith, M. A., B. L. Fisher and P. D. Hebert (2005). "DNA barcoding for effective biodiversity assessment of a hyperdiverse arthropod group: the ants of Madagascar." Philosophical Transactions of the Royal Society B **360**: 1825-1834.

Snelgrove, P. V. R., T. M. Blackburn, P. Hutchings, D. Alongi, J. F. Grassle, H. Hummel, G. King, I. Koike, P. J. D. Lamshead, N. B. Ramsing, v. Solis-Weiss and D. W. Freckman (1997). "The importance of marine sediment biodiversity in ecosystem processes." Ambio **26**: 578-583.

Sogin, M. L., H. G. Morrison, J. A. Huber, D. M. Welch, S. M. Huse, P. R. Neal, J. M. Arrieta and G. J. Herndl (2006). "Microbial diversity in the deep sea and the unexplored "rare biosphere"." Proceedings of the National Academy of Science USA **103**(32): 12115-12120.

Soltis, D. E., P. S. Soltis, M. E. Mort, M. W. Chase, V. Savolainen, S. B. Hoot and C. M. Morton (1998). "Inferring complex phylogenies using parsimony: an empirical approach using three large DNA data sets for angiosperms." Systematic Biology **47**: 32-42.

Somerfield, P. J., R. M. Warwick and M. Moens (2005). *Meiofauna Techniques. Methods for the Study of Marine Benthos*, 3rd edition. A. Eleftheriou and A. McIntyre. Oxford, Blackwell Science, pp. 229-272.

Sommer, R. J., L. K. Carta, S.-Y. Kim and P. Sternberg (1996). "Morphological, genetic, and molecular description of *Pristionchus pacificus* sp. n. (Nematoda: Neodiplogasteridae)." Fundamental and Applied Nematology **19**: 511-521.

Sorokin, V. A., G. O. Gladchenko, V. A. Valeev, I. V. Sysa, L. G. Petrova and Y. P. Blagoi (1997). "Effect of salt and organic solvents on DNA thermal stability and structure." Journal of Molecular Structure **408/409**: 237-240.

Sperling, F. (2003). "DNA barcoding: Deus ex Machina." Newsletter of the Biological Survey of Canada (Terrestrial Arthropods), Opinion Page **22(1)**: http://www.biology.ualberta.ca/bsc/news22_2/contents.htm.

Stamatakis, A. (2006). Phylogenetic models of rate heterogeneity: a high performance computing perspective. Proceedings of the 20th IEEE/ACM International Parallel and Distributed Processing Symposium (IPDPS 2006), High Performance Computational Biology Workshop. Rhodos, Greece, April 2006, Proceedings on CD.

Stamatakis, A. (2006). "RAxML-VI-HPC: Maximum Likelihood-based phylogenetic analyses with thousands of taxa and mixed models." Bioinformatics **22(21)**: 2688-2690.

Stamatakis, A. (2008). "The RAxML 7.0.4 Manual." <http://www.phylo.org/news/countManual7.0.4.php>.

Stamatakis, A., P. Hoover and J. Rougemont (2008). "A rapid bootstrapping algorithm for the RAxML web-servers." Systematic Biology **75(5)**: 758-771.

Steel, M. A., L. Székely, P. L. Erdős and P. J. Waddell (1993). "A complete family of phylogenetic invariants for any number of taxa under Kimura's 3ST model." New Zealand Journal of Botany **31**: 289-296.

Steel, M. A., L. A. Szikely and M. D. Hendy (1994). "Reconstructing trees when sequence sites evolve at variable rates." Journal of Computational Biology **1**: 153-163.

Stock, S. and S. A. Nadler (2006). "Morphological and molecular characterisation of *Panagrellus* spp. (Cephalobina: Panagrolaimidae): taxonomic status and phylogenetic relationships." Nematology **8(6)**: 921-938.

Subbotin, S. A., A. Vierstraete, P. De Ley, J. Rowe, L. Waeyenberge, M. Moens and J. R. Vanfleteren (2001). "Phylogenetic relationships within the cyst-forming nematodes (Nematoda Heteroderidae) based on analysis of sequences from the ITS regions of ribosomal DNA." Molecular Phylogenetics and Evolution **21**: 1-16.

Sung, W., and others (in preparation). "OCTUPUS: A package for defining operationally clustered taxonomic units from parallel-tagged ultra sequencing."

Sunnucks, P., A. C. C. Wilson, L. B. Beheregaray, K. Zenger, J. French and A. C. Taylor (2000). "SSCP is not so difficult: The application and utility of single-stranded conformational polymorphism in evolutionary biology and molecular ecology." Molecular Ecology **9**: 1699-1710.

Swofford, D. L., G. J. Olsen, P. J. Waddell and D. M. Hillis (1996). Phylogenetic Inference. Molecular Systematics, Second Edition. D. M. Hillis, C. Moritz and B. K. Mable. Sunderland, MA, Sinauer Associates, Inc., pp. 407-514.

Szalanski, A. L., D. D. Sui, T. S. Harris and T. O. Powers (1997). "Identification of cyst nematodes of agronomic and regulatory concern by PCR-RFLP of ITS1." Journal of Nematology **29**.

Tamura, K., J. Dudley, M. Nei and S. Kumar (2007). "MEGA4: Molecular Evolutionary Genetics Analysis (MEGA) software version 4.0." Molecular Biology and Evolution **24**: 1596-1599.

Tarrío, R., F. Rodríguez-Trelles and F. J. Ayala (2000). "Tree rooting with outgroups when they differ in their nucleotide composition from the ingroup: The *Drosophila saltans* and *willistoni* groups, a case study." Molecular Phylogenetics and Evolution **16**(3): 344-349.

Thistle, D., L. Sedlacek, K. R. Carman, J. W. Fleeger and J. P. Barry (2007). "Emergence in the deep sea: Evidence from harpacticoid copepods." Deep-sea Research I **54**(6): 1008-1014.

Thomas, W. K., J. T. Vida, L. M. Frisse, M. Mundo and J. G. Baldwin (1997). "DNA sequences from formalin-fixed Nematodes: Integrating molecular and morphological approaches to taxonomy." Journal of Nematology **29**(3): 250-254.

Thompson, J. D., T. J. Gibson, F. Plewniak, F. Jeanmougin and D. G. Higgins (1997). "The CLUSTAL_X windows interface: flexible strategies for multiple sequence alignment aided by quality analysis tools." Nucleic Acids Research **25**(24): 4876-4882.

Thompson, J. D., F. Plewniak and O. Poch (1999). "A comprehensive comparison of multiple sequence alignment programs." Nucleic Acids Research **27**(13): 2689-2690.

Thorne, G. (1939). "A monograph of the nematodes of the superfamilly Dorylaimoidea." Capita Zoologica **8**(5): 1-261.

Tietjen, J. H. (1984). "Distribution and species diversity of deep-sea nematodes in the Venezuela Basin." Deep-Sea Research I **31**(2): 119-132.

Tsagkogeorga, G., X. Turon, R. R. Hopcroft, M. K. Tilak, T. Feldstein, N. Shenkar, Y. Loya, D. Huchon, E. J. P. Douzery and F. Delsuc (2009). "An updated 18S rRNA phylogeny of tunicates based on mixture and secondary structure models." BMC Evolutionary Biology **9**: 187.

Turner, P. C., A. G. McLennan, A. G. Bates and M. R. H. White (2000). Instant Notes in Molecular Biology, Second edition. London, BIOS Scientific Publishers, 346 pp.

Ullberg, J. and E. Ólafsson (2003). "Free-living marine nematodes actively choose habitat when descending from the water column." Marine Ecology Progress Series **260**: 141-149.

Van Megen, H., S. Van den Elsen, M. Holterman, G. Karssen, P. Mooyman, T. Bongers, O. Holovachov, J. Bakker and J. Helder (2009). "A phylogenetic tree of nematodes based on

about 1200 full-length small subunit ribosomal DNA sequences." Nematology **11**(6): 927-950.

Vanfleteren, J. R. and A. R. Vierstraete (1999). "Insertional RNA editing in metazoan mitochondria: The cytochrome *b* gene in the nematode *Teratocephalus lirellus*." RNA **5**: 622-624.

Vanhove, S., W. Arntz and M. Vincx (1999). "Comparative study of the nematode communities on the southeastern Weddel Sea shelf and slope (Antarctica)." Marine Ecology Progress Series **181**: 237-256.

Venter, J. C., K. Remington, J. F. Heidelberg, D. Rusch, J. A. Eisen, D. Wu, I. Paulsen, K. E. Nelson, W. Nelson, D. E. Fouts, S. Levy, A. H. Knap, M. W. Lomas, K. Neelson, O. White, J. Peterson, J. Hoffman, R. Parsons, H. Baden-Tilson, C. Pfannkoch, Y.-H. Rogers and H. O. Smith (2004). "Environmental genome shotgun sequencing of the Sargasso Sea." Science **304**: 66-74.

Vermeeren, H., A. Vanreusel and S. Vanhove (2004). "Species distribution within the free-living marine nematode genus *Dichromadora* in the Weddell Sea and adjacent areas." Deep-sea Research II **51**: 1643-1664.

Voronov, D. A., Y. V. Panchin and S. E. Spiridonov (1998). "Nematode phylogeny and embryology." Nature **395**: 28.

Waite, I. S., A. G. O'Donnell, A. Harrison, J. T. Davies, S. R. Colvan, K. Eckschmitt, H. Dogan, V. Wolters, T. Bongers, M. Bongers, G. Bakonyi, P. Nagy, E. M. Papatheodorou, G. P. Stamou and S. Boström (2003). "Design and evaluation of nematode 18S rDNA primers for PCR and denaturing gradient gel electrophoresis (DGGE) of soil community DNA." Soil Biology & Biochemistry **35**: 1165-1173.

Westheide, W. and H. Schmidt (2003). "Cosmopolitan versus cryptic meiofaunal polychaete species: an approach to molecular taxonomy." Helgoland Marine Research **57**: 1-6.

Wheeler, W. C. (1990). "Nucleic acid sequence phylogeny and random outgroups." Cladistics **6**: 363-368.

Wieser, W. (1953). "Reports of the Lund University Chile Expedition 1948-49. Free-living marine nematodes. I. Enoploidea." Acta Universitatis Lundensis, n.s. **49** **6**: 1-155.

Wilcox, T. P., L. Hugg, D. W. Zeh and J. A. Zeh (1997). "Mitochondrial DNA sequencing reveals extreme genetic differentiation in a cryptic species complex of neotropical pseudoscorpions." Molecular Phylogenetics and Evolution **7**(2): 208-216.

Wilson, G. D. F. (1998). "Historical influences on deep-sea isopod diversity in the Atlantic Ocean." Deep-sea Research II **45**: 279-301.

Wuyts, J., P. De Rijk, Y. Van de Peer, G. Pison, P. Rousseeuw and R. De Wachter (2000). "Comparative analysis of more than 3000 sequences reveals the existence of two pseudoknots in area V4 of eukaryotic small subunit ribosomal RNA." Nucleic Acids Research **28**(23): 4698-4708.

Wuyts, J., Y. Van de Peer, T. Winkelmans and R. D. De Wachter (2002). "The European database on small subunit ribosomal RNA." Nucleic Acids Research **30**(1): 183-185.

Yang, Z. (1993). "Maximum likelihood estimation of phylogeny from DNA sequences when substitution rates differ over sites." Molecular Biology and Evolution **10**: 1396-1401.

Yang, Z. (1994). "Maximum Likelihood phylogenetic estimation from DNA sequences with variable rates over sites: Approximate methods." Journal of Molecular Evolution **39**: 306-314.

Yang, Z. (1996). "Among-site variation and its impact on phylogenetic analyses." Trends in Ecology and Evolution **11**: 367-371.

Yang, Z. (2006). Computational Molecular Evolution. Oxford, UK, Oxford University Press, 376 pp.

Yang, Z., N. Goldman and A. Friday (1994). "Comparison of models for nucleotide substitution used in maximum likelihood phylogenetic estimation." Molecular Biology and Evolution **11**: 316-324.

Ye, W., A. L. Szalanski and R. T. Robbins (2004). "Phylogenetic relationships and genetic variation in Longidorus and Xiphinema species (Nematoda: Longidoridae) using ITS1 sequences of nuclear ribosomal DNA." Journal of Nematology **36**: 14-19.

Yoder, M., I. Tandingan De Ley, I. W. King, M. Mundo-Ocampo, J. Mann, M. Blaxter, L. Poiras and P. De Ley (2006). "DESS: a versatile solution for preserving morphology and extractable DNA of nematodes." Nematology **8**(3): 367-376.

Yushin, V. V. (2003). "Ultrastructure of spermatogenesis in the free-living marine nematode *Anticoma possjetica* (Enoplida: Anticomidae)." Nematology **5**: 777-788.

Zardus, J. D., R. J. Etter, M. R. Chase, M. A. Rex and E. E. Boyle (2006). "Bathymetric and geographic population structure in the pan-Atlantic deep-sea bivalve *Deminucula atacellana* (Schenck, 1939)." Molecular Ecology **15**: 639-651.

Zwickl, D. J. and D. M. Hillis (2002). "Increased taxon sampling greatly reduces phylogenetic error." Systematic Biology **51**(4): 588-598.